DISSERTATION

LIFE HISTORY AND POPULATION DYNAMICS OF HUMPBACK CHUB IN THE GRAND CANYON

Submitted by

Maria C. Dzul

Department of Fish, Wildlife, and Conservation Biology

In partial fulfillment of the requirements

For the Degree of Doctor of Philosophy

Colorado State University

Fort Collins, Colorado

Summer 2021

Doctoral committee:

Advisor: William Kendall

Charles Yackulic
Dana Winkelman
LeRoy Poff

ABSTRACT

LIFE HISTORY AND POPULATION DYNAMICS OF HUMPBACK CHUB IN THE GRAND CANYON

Freshwater ecosystems are in peril worldwide and large rivers have been particularly impacted by anthropogenic disturbances. The Colorado River is no exception as this river has experienced changes to both its physical (e.g., dam construction) and biologic (e.g., invasion by non-native fishes) environment, and these alterations resulted in the near-collapse of its native fish assemblage. The Colorado River stretches over 2,330 kilometers from its source in the Rocky Mountains, through the Sonoran Desert, to empty (historically) into the Gulf of California, but in this dissertation I focus specifically on one segment that runs through the Grand Canyon in northern Arizona.

Once characterized by its highly dynamic hydrologic regime, the Grand Canyon stretch of the Colorado River and its native fish assemblage historically experienced fast flows and seasonal disturbances. Consequently, its fish assemblage, though relatively depauperate with only eight species, was highly unique and exhibited numerous adaptations for swimming in turbulent waters. Following Glen Canyon Dam (GCD) enclosure in 1963, river flows became regulated by dam operations and large floods were eliminated from the river. Also, water temperatures and suspended sediment concentrations decreased and seasonal fluctuations in discharge and water temperatures were dampened. These abiotic changes altered the fish community, which was already home to numerous non-native fishes before GCD construction. Declines in many Colorado River native species, namely Colorado pikeminnow (*Ptychocheilus*

lucius), bonytail chub (*Gila elegans*), roundtail chub (*Gila robusta*), razorback sucker (*Xyrauchen texanus*), and humpback chub (*Gila cypha*), ensued in years following. While Colorado pikeminnow, bonytail chub, roundtail chub, and razorback sucker were all extirpated from this reach (though razorback sucker have since been found in very small numbers, presumably they were extirpated and then recolonized from Lake Mead though it's possible they were never extirpated), one humpback chub population was able to persist due to the presence of a warmwater tributary, the Little Colorado River (LCR), which humpback chub would migrate to each spring to spawn. Other native species, such as flannelmouth sucker (*Catostomus latipinnis*), speckled dace (*Rhinichthys osculus*), and bluehead sucker (*Catostomus discolobus*) also persisted, most likely because they were also spawning in tributaries.

Humpback chub in Grand Canyon currently inhabit an environment very different from that in which they evolved. Today's flows in the Grand Canyon stretch of the Colorado River are highly managed by water releases from the reservoir Lake Powell, and the magnitude, timing, and fluctuations of these flow releases are of interest to a diverse set of stakeholders, including numerous Native American tribes, recreationists, conservationists, and government agencies overseeing power production and water delivery. Stakeholders participate in the Glen Canyon Dam Adaptive Management Program (GCDAMP), which meets regularly to assess the current state of the Colorado River and determine whether or not certain actions are needed to achieve specific goals. Scientists regularly supply the GCDAMP with abundance estimates of humpback chub to monitor population trend. Additionally, scientists are often asked to provide expert opinions about how certain dam operations (e.g., high flows or increased water temperatures) should affect humpback chub population dynamics. Accordingly, a better

understanding of humpback chub life history is needed to identify vulnerabilities, inform management decisions, and forecast population trend.

Studies have illustrated how LCR-spawning humpback chub exhibit alternative life histories (migrant and resident) and partial migration, strategies that may increase resilience of humpback chub and act to buffer against population change. However, the additional complexity associated with alternative life history types and partial migration makes it more difficult to identify environmental drivers of population dynamics, because population growth is determined by different rates of survival and growth for alternate life history types, as well as different year to year probabilities of partial migration. Studies suggest that long term population trends seem to be driven primarily by migrant humpback chub, which exhibit a slow life history with high adult survival. Adult abundance patterns indicate that the population size has experienced gradual fluctuations, where abundance declined in the early 2000s but started increasing sometime in the mid-2000s up until recent years (i.e., 2018), where there is some evidence to suggest adult numbers may be declining once again. Identifying which conditions promote population growth of humpback chub will help forecast how this population may respond to water shortages and drought, which are forecasted for the Southwest region.

This dissertation is comprised of three chapters that describe both ecological investigations of humpback chub population dynamics and model developments. While the ultimate goals were ecological inference, it was often necessary to develop new models in order to leverage data from multiple sources and answer ecological questions. One specific model development goal that is a large focus of Chapters 1 and 2 is how to incorporate autonomous antenna detections of passive integrated transponder (PIT) tags into mark-recapture models. Because autonomous antennas improve detection probabilities of fish marked with PIT tags,

methods for incorporating antenna detections into population models may be broadly useful for fish studies in other systems. In Chapter 3, ecological analysis required a multi-step approach that shared information about abundances and vital rates to estimate outmigration and survival.

In Chapter 1, I evaluate the migration dynamics of adult humpback chub that spawn in the LCR to learn more about energetic tradeoffs associated with migration and spawning. Namely, for migratory adults that move between the Colorado River and LCR in spring, I assess how often adults migrate (e.g., yearly? every other year?) and whether or not there are survival or growth costs associated with migrating between the Colorado River and LCR. Additionally, I test hypotheses suggesting that, if migration is exclusively motivated by spawning, the energetic costs of migration are higher for females than males and higher for small fish compared to large fish. I compare survival and growth rates from migratory humpback chub to resident humpback chub, the latter which reside in the LCR for their entire lives. Chapter 1 also describes the development of a mark-recapture model that combined data from physical captures with detection data from an array of autonomous antennas. I compare estimates of survival and migration probabilities from models with and without the antenna arrays to learn more about the potential value of PIT antennas. I find that adding PIT antennas increases survival estimates for large adults and also increases migration probabilities, suggesting that a subset of adults are relatively invulnerable to capture and that adding antennas may help correct for this sampling bias. Growth and survival of migrants and skipped migrants were similar for all four demographic groups (i.e., small females, large females, small males, large males), showing no evidence for costs associated with migration. In contrast, residents exhibited much lower overwinter survival probabilities compared to migrants, suggesting that winter may be a time of severe food limitation for adults in the LCR. Lastly, there was some indirect evidence for

spawning heterogeneity among large females, because migrants were likely to migrate every year but skipped migrants migrated much less frequently.

In Chapter 2, I describe an approach for using PIT antenna detections to improve abundance estimation. I develop a closed population model, open population model, and robust design model that pair physical sampling methods (e.g., hoop netting, electrofishing, angling) with detections from autonomous antennas. Additionally, I include size uncertainty in the model structure by using a multievent approach, where size is known if fish are physically captured, but unknown when fish are only detected on antennas. I illustrate how including antenna data can reduce uncertainty in abundance, and then apply this approach to three applied examples: estimating abundance of bull trout in Hells Canyon (closed model), estimating adult humpback chub in that spawn in the LCR (open model), and estimating abundance and temporary emigration in western Grand Canyon (robust design model). Simulations showed this approach was unbiased and noticeably improved precision (compared to model without antennas) if the proportion of fish with PIT tags was greater than 10%. Improvements in the precisions of abundance estimates were also noticeable in all applied examples.

Chapter 3 focuses on evaluating the population dynamics of juvenile humpback chub. Mark-recapture of juveniles is challenging because capture probabilities are low for this size class and because fish are too small to be marked with individually identifiable tags. Nevertheless, this size class is characterized by high year to year variability in abundance, which affects recruitment and future adult population trends. Furthermore, there is evidence that the most often the migrant/resident life history trajectory of fish is determined by whether or not individuals migrate from the LCR into the Colorado River within their first year. I develop mark-recapture model to estimate survival and migration probabilities for this size class, and

then use observed relationships to reconstruct age-0 abundance estimates from 2000-2020 and evaluate hypotheses about which environmental factors affect age-0 abundance. The best-supported regression model predicting age-0 abundance included effects of absence of winter floods (-), catfish predation (-), and non-native egg predation (+). Evaluation of outmigration emphasizes the importance of 2011 and 2012, as these were years with high outmigration into the mainstem Colorado River and these cohorts were tractable through lagged increases in subadults and adults. Assessment of survival and outmigration indicates that a higher proportion of age-0 humpback chub remain within the LCR under low densities and absence of floods, providing some indirect evidence of food limitation in the LCR as a driver of migration.

Humpback chub are one of the last remnant species of the wild, pre-dam Colorado River and are a success story of how a native fish was able to survive, and eventually thrive, after its environment was modified by humans. Since 2014, humpback chub have experienced a geographic expansion into the western reaches of Grand Canyon, where the population has grown rapidly and where reproduction is not reliant on the LCR. A better understanding of how humpback chub respond to environmental disturbances, and specifically what role (if any) alternative life history strategies and partial migration play in promoting resilience, will help with species recovery and may also have broader implications for conservation of other fishes.

ACKNOWLEDGEMENTS

Funding was provided by the U.S. Bureau of Reclamation as part of the Glen Canyon Dam Adaptive Management Program. Fieldwork occurred on lands owned and managed by the Navajo Nation and the National Park Service. I thank the U.S. Geological Survey (USGS), specifically the Grand Canyon and Monitoring and Research Center (GCMRC) and the Southwest Biological Science Center (SBSC), for providing me this opportunity and for the amazing network of scientists, managers, and support staff who I have interacted with over the years. Additionally, I thank the Department of Fish, Wildlife, and Conservation Biology at Colorado State University (CSU) for making me feel welcome within the academic community.

I thank Dr. William (Bill) Kendall, my main advisor at CSU, for serving as a mentor and sharing his vast knowledge of mark-recapture models. I have always admired Bill's natural talent and creativity in using mark-recapture to go beyond the basics (e.g., estimate abundance or survival) and instead use them to test more advanced (and interesting) ecological hypotheses. I thank Dr. Dana Winkelman for his insight about fish ecology, population dynamics, and PIT antennas. I extend a very large thanks to Dr. Charles Yackulic. I have worked for Charles for eight years and continue to be amazed by his aptitude for problem solving and his quantitative knowledge. I have learned so much from Charles and would not be building complex models if it weren't for his mentorship. I thank Dr. LeRoy Poff for serving as an outside committee member and for his expertise in life history theory and linkages between hydrology and ecology.

In addition to my PhD committee, I thank others that I have interacted with throughout the course of my PhD work and my time with USGS. Specifically, I thank David R Van Haverbeke (Dawg) from the U.S. Fish and Wildlife Service (USFWS) for sharing his knowledge about humpback chub and for his collaboration on numerous population modeling efforts, and I thank

Dr. Michael Yard for organizing and leading the tremendous field effort involved in sampling the Colorado River. Additionally, I thank Michael Dodrill (USGS), Dr. Josh Korman (Ecometric Research), and Dr. Mary Conner (Utah State University) for their expert advice on computing, modeling, and fish. I also thank Kirk Young for advice on how to tie research into management goals, Dr. Kevin Bestgen (CSU) for sharing his observations of larval fish in the Colorado River drainage, and Dr. Jeff Muehlbauer (USGS) and Dr. Kim Dibble (USGS) for their mentorship on having a science career and parenting. I thank the numerous biologists, field technicians, and volunteers who have helped collect data, as well as the boatmen and science support staff that make fieldwork possible. In particular, I thank Mariah Giardina (USGS), Laura Tennant (USGS), Dave Ward (USGS), Clay Nelson (USGS), Pilar Wolters (USFWS), Dennis Stone (USFWS), Michael Pillow (USFWS), Tim Andrews (USGS), Peter Mackinnon (Biomark/ Utah State University), Mark Mckinstry (Bureau of Reclamation), Glenn Bennet (USGS), Carol Fritzinger (USGS), Ann-Marie Bringhurst (USGS), Dave Foster (USGS), Seth Felder (USGS), Dr. Bill Pine (University of Florida), Tom Gushue (USGS), Gabriele Engler (CSU), and Kim Samsel (CSU). Bull trout data analyzed in Chapter 2 were collected biologists from Idaho Power Company (Rick Wilkison, Brandon Bentz, Phil Bates).

My family has supported me throughout my PhD, and none of this work would have been possible without their help. I am grateful to my husband, Chris Ebert, for his ongoing encouragement, support, and love. I thank my two daughters, Anya and Alina Ebert, who I love more than anything. I thank my mother, Christina Dzul, for watching Anya in Fort Collins so that I could complete my classwork. I also thank my dad, Andrew Dzul, for always being an enthusiastic proponent of my science career.

TABLE OF CONTENTS

ABSTRACT ii
ACKNOWLEDGEMENTS viii
LIST OF TABLES xii
LIST OF FIGURES xiii
CHAPTER 1 PARTIAL MIGRATION AND SPAWNING MOVEMENTS OF HUMPBACK CHUB IN THE LITTLE COLORADO RIVER ARE BETTER UNDERSTOOD USING DATA FROM AUTONOMOUS PIT TAG ANTENNAS 1
1.1. Summary 1
1.2. Introduction 2
1.3. Methods 5
1.3.1. Study species 5
1.3.2. Study site 7
1.3.3. General overview of model and sampling 8
1.3.4. Revisiting common challenges to using PIT antenna data 9
1.3.5. Process model 11
1.3.6. Data model 14
1.3.7. Assessing ecological hypotheses: Skipped migration, permanent residency, and variability in the timing of first migration 23
1.3.8. Running the model 24
1.4. Results 24
1.4.1 Comparing models with and without antenna data: 24
1.4.2. Migration probabilities and tradeoffs 26
1.4.3. Alternative life histories 27
1.5. Discussion 28
CHAPTER 2 INCORPORATING ANTENNA DETECTIONS INTO ABUNDANCE ESTIMATES OF FISH 49
2.1. Summary 49
2.2. Introduction 50
2.3. Methods 52

2.3.1. Closed model simulation and modeling 53
2.3.2. Open model simulation and modeling 57
2.3.3. Closed model – bull trout in Hells Canyon, Snake River 61
2.3.4. Open model – humpback chub that spawn in the Little Colorado River 62
2.3.5. Robust design model -western Grand Canyon 63
2.4. Results 66
2.4.1. Simulation results 66
2.4.2. Closed model – bull trout in the Snake River 67
2.4.3. Open model – Humpback chub that spawn in the Little Colorado River 67
2.4.4. Robust design model -humpback chub in western Grand Canyon 68
2.5. Discussion 69
CHAPTER 3 LIFE HISTORY IMPLICATIONS OF PRODUCTION AND DISPERSAL OF AGE-0 HUMPBACK CHUB 87
3.1.Summary 87
3.2. Introduction 88
3.3. Methods 91
3.3.1. Species background 91
3.3.2. Sampling Methods 92
3.3.3. Overview of modeling approach 94
3.4. Results 108
3.5. Discussion 110
Bibliography 128
Appendix A Field methods for humpback chub sampling 140
Appendix B Bias of using a hidden Markov model for continuous resight data 144
B.1 Methods 144
B.2. Results 147
Appendix C Estimating state-specific abundances (with state uncertainty) 152
Appendix D Stan code for skipped migration model 154
Appendix E. Code for including PIT antenna detections into abundance estimates 191
Appendix F. Closed models to estimate abundance of age-0 humpback chub in summer and fall 243
Appendix G. Time series comparison of juvenile, subadult, and adult humpback chub abundances 252

LIST OF TABLES

1.1. Description of parameters used to model migration dynamics of humpback chub..……..35

1.2. Adult humpback chub survival, migration, and growth probabilities…...……37

2.1. Model parameters for closed and open models……...75

2.2. Event probabilities for three size class model..……...77

2.3. Parameter values for simulations……..……..78

LIST OF FIGURES

1.1 Map depicting the Colorado River (CR) near its confluence with the Little Colorado River (LCR) in northern Arizona…….39

1.2 Diagram explaining skipped migration model for adult humpback chub……40

1.3 Graph showing the number of humpback chub PIT tags detected on a multiplexer array…..41

1.4 Illustration describing the parameterization of the initial state assignment vector……..42

1.5 Availability estimates of migrating adult humpback chub in spring ……..43

1.6 Mean estimates of skipped migration probabilities from models with and without antenna detections….44

1.7 Fall abundance estimates of adult humpback chub……..45

1.8 Mean estimates of annual survival from models with and without antenna detections……...46

1.9 Summer and winter survival rates for residents, migrants, and skipped migrants……..47

1.10 Graphs that probabilistically describe the fate of adult humpback chub that spawn in the Little Colorado River……...……48

2.1 Conceptual diagram that describes calculation of catch……..79

2.2 Relative standard error comparison for closed model……..……...80

2.3 Relative standard error comparison for open model (long-lived scenario)…….81

2.4 Relative standard error comparison for open model (short-lived scenario)……82

2.5 Abundance of bull trout in Hells Canyon from closed models……....83

2.6 Abundance of humpback chub adults that spawn in the Little Colorado River from open models…….....84

2.7 Survival of humpback chub adults that spawn in the Little Colorado River from open models……..85

2.8 Abundance of humpback chub subadults and adults in Fall Canyon from a robust design model ……...86

3.1 Map of the Colorado River and Little Colorado River study sites……117

3.2 Illustration of size and growth differences of juvenile humpback chub in two rivers……...118

3.3 Hypothetical hydrograph to illustrate flow-recruitment hypotheses…….……119

3.4 Diagram representing relationship between abundances and vital rates……...120

3.5 Comparison of age-0 abundance estimates from different modeling steps……...121

3.6 Juvenile humpback chub abundances and immigration in the observed Colorado River.....122

3.7 Environmental effects on juvenile humpback chub vital rates in the Colorado River…....123

3.8 Comparison of resident and migrant survival to becoming a large subadult……124

3.9 Probability of residency for age-0 humpback chub in the Little Colorado River……125

3.10 Relationships between snowmelt floods and age-0 abundance in the LCR……126

3.11 Relationships between snowmelt floods and non-native catch on age-0 abundance…….127

B1. Bias in survival when treating continuous antenna detections as discrete……...150

B2. Bias in state transitions when treating continuous antenna detections as discrete……...151

G1. Abundances of juvenile, subadult, and adult humpback chub from 2009-2020……253

CHAPTER 1

PARTIAL MIGRATION AND SPAWNING MOVEMENTS OF HUMPBACK CHUB IN THE LITTLE COLORADO RIVER ARE BETTER UNDERSTOOD USING DATA FROM AUTONOMOUS PIT TAG ANTENNAS[1]

1.1. Summary

Choosing whether or not to migrate is an important life history decision for many fishes. Here we combine data from physical captures and detections on autonomous passive integrated transponder (PIT) tag antennas to study migration in an endangered fish, the humpback chub (*Gila cypha*). We develop hidden Markov mark-recapture models with and without antenna detections and find that the model fit without antenna detections misses a large proportion of fish and underestimates migration and survival probabilities. We then assess survival and growth differences associated with life history strategy and migration for different demographic groups (small male, small female, large male, large female). We find large differences in survival according to life history strategy, where residents had much lower over-winter survival than migrants. However, within the migratory life history strategy, survival and growth were similar for active migrants and skipped migrants for all demographic groups. We discuss some common

[1] This paper has been accepted for publication by the *Canadian Journal of Fisheries and Aquatic Sciences* (see citation below)

Dzul, M. C., Kendall, W. L., Yackulic, C. B., Winkelman, D. L., Van Haverbeke, D. R., & Yard, M. D. (2021). Partial migration and spawning movements of humpback chub in the Little Colorado River are better understood using data from autonomous PIT tag antennas. *Canadian Journal of Fisheries and Aquatic Sciences*, (ja).

challenges to incorporating detections from autonomous antennas into population models and demonstrate how these data can provide insight about fish movement and life history strategies.

1.2. Introduction

An individual's decision to migrate, or not, is an important life history strategy decision faced by many organisms. The impetus for migration can be better forage (Holdo et al. 2009; Yackulic et al. 2017), lower competition (Grayson et al. 2011; Nilsson et al. 2006), improved reproduction (Hebblewhite and Merrill 2011), or reduced predation (Skov et al. 2013) at the destination. However, there can also be costs associated with the act of migration (Hein et al. 2012), such as increased energetic expenditures, predation risk (Hebblewhite and Merrill 2007), or reduced foraging (Chapman et al. 2013) associated with travel. Often, only a subset of the population migrates, and this is known as partial migration (Chapman et al. 2011). Understanding patterns of partial migration can provide context for interpreting behavior and adaptation (Chapman et al. 2012; Lundberg 1988), thereby helping biologists understand mechanisms of population change (Hebblewhite and Merrill 2011; Nelson et al. 2002; Nilsson et al. 2006).

Assessing partial migration dynamics from capture-recapture data requires a large number of recaptures, and thus low recapture probabilities (which are often observed in fishes) limits the sample sizes needed for analysis. For this reason, capture-recapture studies of fishes have increasingly relied on other detection methods, such as radiotelemetry (Skalski et al. 2002), passive acoustic receivers (Dudgeon et al. 2015), and autonomous PIT tag antennas (Pearson et al. 2015). Compared to radio tags and acoustic tags, PIT tags are small and inexpensive and are thus most advantageous when marking large numbers of individuals in small systems (Cooke et

al. 2013). Autonomous PIT tag antennas are placed in a fixed site within a fish's habitat to continuously record PIT tags of fish that swim by. These continuous data are especially useful for assessing temporal patterns in fish movements (Cathcart et al. 2018a; Kanno et al. 2014), evaluating spawning patterns associated with movement (Haraldstad et al. 2018; Pearson et al. 2015), identifying movement barriers to fish migrating along a riverine corridor (Aarestrup et al. 2003; Cathcart et al. 2018b; Piper et al. 2013), quantifying escapement (Wolter et al. 2013) or emigration of recently translocated fish out of the translocation site (Banet and Hewitt 2019; Spurgeon et al. 2015), or measuring invasion potential (movement) by non-native fishes (Dzul et al. 2017).

Our study uses autonomous PIT antenna data to assess partial migration in adult humpback chub that spawn in the Little Colorado River (Grand Canyon, AZ). Our broad goals were twofold: first, to incorporate antenna data into the mark-recapture model framework, and to assess what benefit (if any) antenna detections provide; second, to use this model to learn more about humpback chub ecology and migration. Numerous studies have evaluated humpback chub population dynamics using mark-recapture methods (Coggins et al. 2006; Van Haverbeke et al. 2013), and found that adult humpback chub move from the cold mainstem Colorado River (hereafter CR) to a warm water tributary (the Little Colorado River -or LCR) in spring and return to the mainstem in late spring, summer, or fall (Ryel and Valdez 1995). However, one limitation of these mark-recapture methods has been the low recapture probabilities of adult humpback chub (>200mm TL) with conventional gear types (i.e., unbaited hoop nets and electrofishing) in the CR. To address this shortcoming, autonomous PIT antennas were added as a supplemental gear type in the LCR (in 2009) and in the CR (in 2016) and continue to operate until present.

The first goal required developing a modeling framework for using PIT antenna detections in the mark-recapture model. Using this new model framework, we compared parameter estimates from models fit with and without antenna data to determine the (potential) benefit of including PIT antenna detections in mark-recapture models. During model development, we encountered three challenges for PIT antenna detection data that we believe are likely common to other study systems: the availability challenge, the continuous time challenge, and the state uncertainty challenge. The first two challenges pertain to using continuously-operating antennas and the third challenge pertains to all PIT antennas. The availability challenge arises because stationary antennas only detect fish within a limited spatial extent so that fish that are located far from antennas and (or) fish that are less mobile are less detectable or undetectable. The continuous time challenge arises because if the window for PIT antenna detections is wide (e.g., fish can be detected over the course of weeks or months), then fish can be detected and die within the same sampling occasion and this can bias survival in discrete-time models (Barbour et al. 2013; Conner et al. 2015). Lastly, the state uncertainty challenge occurs because some physical attributes of fish (e.g., size, sex, ripeness) are not observable on antennas. In particular, size uncertainty of antenna detections may be problematic because size often influences capture probability (Dauwalter and Fisher 2007; Hense et al. 2010; Korman et al. 2009), but fish size is not observable with antenna detections.

The second goal involved characterizing yearly and within-population variability in survival, abundance, and movement rates. More specifically, recent mark-recapture studies have identified three migration patterns in this population, including LCR residents – a group that resides in the LCR year-round, migrants – a group that migrates from the CR into the LCR in spring (presumably to spawn), and skipped migrants – a group that resides in the CR for a given

year (Yackulic et al. 2014). The LCR resident group is fairly distinct and has faster growth and lower survival compared to the migrant and skipped migrant groups (Yackulic et al. 2014), yet it is unknown whether fish in the resident category are a fixed group or if residents can change their migratory life history strategy and move to the CR as adults. The migrant and skipped migrant groups are not fixed, so that migrants can become skipped migrants and vice versa (Pearson et al. 2015). We evaluated yearly variability in the probability of migration in four different demographic groups (small females, large females, small males, and large males) and developed a model to compare survival and growth rates for residents, migrants, and skipped migrants in each demographic group. Insight into the migratory dynamics and life history variability of humpback chub may help illuminate why this species was able to persist in Grand Canyon after construction of Glen Canyon Dam.

1.3. Methods

1.3.1. Study species

There are currently five recognized populations of humpback chub, four of which occur in the upper Colorado River Basin (above Lake Powell) and one that occurs in the lower Colorado River Basin in Grand Canyon. Our study focused on the Grand Canyon population, specifically on the subset of population that spawns in the Little Colorado River (Figure 1.1). Within Grand Canyon, reduction in abundances of humpback chub and other native fishes coincided with construction of Glen Canyon Dam in 1963 and filling of the upstream reservoir, Lake Powell. It is hypothesized that humpback chub persisted in Grand Canyon after construction of Glen Canyon Dam due to the LCR spawning migration (Douglas and Marsh 1996; Kaeding and Zimmerman 1983), because the warmer water temperatures in the LCR are

more favorable for spawning and larval development compared to water temperatures in the CR (Kaeding and Zimmerman 1983).

Most movements between the CR and LCR occur in March-May, coincident with spawning timing in the LCR (Ryel and Valdez 1995). Movement back from the LCR to the CR is more prolonged and can occur May – November (Ryel and Valdez 1995), though there is some evidence that large humpback chub >300mm TL exit the LCR by June (Gorman and Stone 1999). A study of humpback chub ripeness concluded that spawning commenced in late March (when water temperatures were ~14°C), peaked in mid-April (when flow was returning to baseflow conditions), and then decreased substantially by mid-May (Gorman and Stone 1999). While most reproduction for LCR-spawning humpback chub occurs in spring, there is evidence that spawning can occur at lower levels year-round (Brizendine 2016; Robinson et al. 1998). Some proportion of the age-0 humpback chub born in the LCR will outmigrate to the CR during their first year, most commonly between mid-summer and mid-fall during the monsoon season (Yackulic et al. 2014).

Mark-recapture studies have suggested there is variability in migratory strategies within LCR spawning humpback chub. Specifically, Douglas and Marsh (1996) observed that a small proportion of humpback chub did overwinter in the LCR (i.e., were LCR residents), and Yackulic et al. (2014) found evidence that the LCR resident group was comprised of the same individuals from year to year. Furthermore, Pearson et al. (2015) and Yackulic et al. (2014) found evidence for skipped migration within the group of humpback chub that overwintered in the mainstem CR.

1.3.2. Study site

Here we refer to distances in the CR as river kilometers (rkm) downstream of Glen Canyon Dam, AZ and distances in the LCR as rkm upstream of the LCR-CR confluence. The sampling site in the CR (i.e., observable Colorado River site) was located just downstream of the LCR confluence (rkm 127-129.7; Figure 1.1). To exclude fish that did not spawn in the LCR, only humpback chub captured in eastern Grand Canyon or lower Marble Canyon (here defined to be between rkm 105.5- 127.0 and 129.7-145.7; or unobservable Colorado River sites) were included in this study.

The LCR stretches from its headwaters in the White Mountains (eastern AZ) to the Grand Canyon but is ephemeral in its mid-reaches. Humpback chub occur only in the lower portion of the LCR, which is perennial and fed by Blue Spring (rkm 20.7). Unlike the regulated CR, flow in the lower LCR is primarily influenced by precipitation and accordingly it displays a more natural hydrothermal regime (Robinson and Childs 2001), with seasonal floods occurring in winter/spring (from snowmelt) and fall (from rainfall; Dean and Topping 2019b). The lower 13.56 rkm of the LCR (below Lower Atomizer Falls) was sampled by the US Fish and Wildlife Service (USFWS) four times each year as part of long-term monitoring. Antenna detections in the LCR came from an antenna system comprised of two multiplexer arrays (MUX), which spanned the entire width of the LCR and was located approximately 1.8 kilometers upstream of the LCR-CR confluence. Fish that moved from the CR into the LCR passed over the MUX and accordingly the MUX provided additional detection information about migrants. All migrants must move into the LCR and thus most are susceptible to MUX detection, the exception being fish that only move into in the lower 1.8 km of the LCR and thereby do not swim up to the

MUX. For this reason, migrants that do not swim past rkm 1.8 were confounded with skipped migrants.

1.3.3. General overview of model and sampling

Data generated during this study are available from the USGS ScienceBase-Catalog (Dzul 2021). Data used to fit the model came from spring and fall mark-recapture sampling events in the CR and LCR for spring 2009 - spring 2019. Here we describe sampling methods briefly, but more details about sampling protocols are included in Appendix A. Spring and fall LCR sampling included two spring and two fall trips each year, which were roughly timed to occur in April and May (spring trips) and September and October (fall trips). During LCR sampling trips, each unbaited hoop net was set for ~72 hours and checked every ~24 hours so that each hoop net was checked three times (i.e., had three passes). However, in some years only two passes occurred due to logistical complications. Spring and fall sampling trips to the CR each included only one trip per year and occurred in April/May (spring) or September/ October (fall). Unbaited hoop nets in the CR where also set for 24 hour intervals and checked either 6 or 10 times (depending on the trip type). Additionally, CR sampling included three passes of electrofishing. In some years in the CR (i.e., 2016 and 2018), we used PIT antenna detection data from baited submersible antennas (Biomark, Inc.) that were deployed for 6-10 day periods in conjunction with electrofishing and hoop netting.

We developed and fit an hidden Markov model (HMM; MacDonald and Zucchini 1997) with 20 states to estimate migration and survival probabilities. These 20 states represented every combination of five migration strategy categories (which correspond with spawning or location status) and four demographic categories (which correspond with sex and size). We refer to the

five migration categories as: LCR resident, observable Colorado River (hereafter oCR) migrant, unobservable Colorado River (hereafter uCR) migrant, oCR skipped migrant, and uCR skipped migrant. While residents and skipped migrants were assumed to remain year-round in the LCR and CR, respectively, migrants were assumed to move into the LCR in spring and could be found in either the CR or the LCR in fall. Therefore, only migrant categories were detectable on the MUX (after filtering out fish that lingered over the array and were detected more than once over the course of 2-13 days).

Additionally, following Yackulic et al. (2014), there were two different categories that corresponded to sampled (oCR) and nonsampled (uCR) segments of the Colorado River, for both the migrant and skipped migrant categories. Note that uCR migrants were only unobservable in the CR and could be detected on the MUX or captured while in the LCR, whereas uCR skipped migrants were completely unobservable. The four demographic categories included small (200-249mm TL) and large (250+mm TL) males and females. The size of fish was known when a fish was live captured but was unknown when fish were detected on PIT antennas or completely undetected. The sex of a fish was known only if it was captured as a ripe individual that expressed gametes, otherwise fish were classified as unknown sex. Restrictions were placed on the transition matrix to help with parameter estimation (see below).

1.3.4. Revisiting common challenges to using PIT antenna data

The availability challenge presented in our study included two components. The first component refers to availability for detection on the MUX. The MUX can only detect fish that are actively moving between the CR and LCR and over the array, it cannot detect fish once they move upstream or downstream of the array. Therefore, the temporal window for MUX

detections must be wide enough to ensure all migrants move into the LCR (and hence are detectable on the MUX) during this interval. Initial analysis suggested that February through June was a reasonable time frame. This wide temporal window required some additional considerations (discussed as part of the continuous time challenge). The second component refers to availability for physical capture because we were concerned that some migrants were not in the LCR during spring sampling trips due to the wide temporal movement window (Pearson et al. 2016). To address this concern, we include parameters to account for the lack of geographic closure within spring sampling events (see Data model description).

The continuous-time challenge pertained to using a wide temporal window for MUX detections, as studies have illustrated that treating continuous resight detections as occurring in discrete time can produce bias in survival estimates (Barbour et al. 2013; Conner et al. 2015). To address this issue, our first approach was to incorporate MUX detections as continuous auxiliary data within the discrete-time mark-recapture model (sensu Barker 1997, Kendall et al., in review). Our first approach, combined with the complex multistate structure, and state uncertainty, proved to be prohibitively slow (i.e., required >1 week to run with only 100 posterior draws) and did not converge. Instead, we used a HMM model structure that allows for state uncertainty (Pradel 2005), with MUX detections incorporated into an open robust design (Kendall et al. 2019) structure for spring sampling. We expect minimal bias in survival estimates because survival probabilities are high (Barbour et al. 2013; Conner et al. 2015). Also, although the window for MUX detections is wide (February-June), these detections are not continuous over the entire survival yearly survival, so that annual survival rates should be minimally affected. We nevertheless assess the potential bias of this approach in Appendix B.

The state uncertainty challenge arises because many fish attributes (i.e. size) are not observable with antenna detection and because other attributes (e.g., migratory status and sex) are not reliably assessed with each physical capture. Our study includes many forms of state uncertainty. For example, a fish captured in the LCR can be either a migrant or a resident and a fish captured in the CR can be either a migrant or a skipped migrant. Additional forms of uncertainty include sex (if a fish is not ripe at capture) and size class (if fish observation is an antenna detection). Obtaining state-specific abundance estimates (e.g., estimates of migrants, skipped migrants, residents) required accounting for uncertainty in state assignment, and we describe our approach in Appendix C.

1.3.5. Process model

Model parameters for the process model included survival, growth, migration probabilities (Table 1.1). The model operated on a semi-annual time step with two seasons: over-summer (April to October) and over-winter (October to April; Figure 1.2a). Parameters were allowed to vary by migration strategy (h; where 1 = resident, 2 = oCR migrant, 3 = uCR migrant, 4 = oCR skipped migrant, 5 = uCR skipped migrant), size (w; where 1 = small, 2 = large), sex (n; where 1 = male, 2 = female), year (t ; where 1 = year 1, 2 = year 2, etc.), and(or) season (k; where 1 = spring/summer, 2= fall/winter). Transition probabilities were a function of survival ($S_{w,n,h,k,t}$), growth ($g_{n,h,k}$), and migration ($m_{w,n,h,k,t}$) parameters, where fish survived first, then grew, then migrated. For example, the probability a small migrant from the oCR in the fall became a large skipped migrant from the oCR in the spring was the product of the survival probability for a small migrant, the probability a small migrant grew to become a large migrant, and the probability a large migrant did not move into the LCR, or $S_{1,n,2,2,t}\, g_{n,2,2}(1 -$

$m_{2,n,2,2,t}$). Growth was permitted from fall to spring and from spring to fall, but transitions among migration categories were permitted only from fall to spring. Also, transition probabilities included the probability, τ, that a CR fish is from the oCR reach (i.e., not from the uCR reach). Specifically, an LCR resident that becomes migratory has probability τ of migrating to the oCR reach and probability 1- τ of migrating to the uCR reach. The state transition matrix (**Ψ**) is presented for overwinter transitions (ignoring male/female and temporal/seasonal effects for simplicity) in Eq (1), where rows and columns are indexed by state of origin and destination, respectively: 1 (small LCR resident), 2 (small oCR migrant), 3 (small uCR migrant), 4 (small oCR skipped migrant), 5 (small uCR skipped migrant), 6-10 (equivalents of 1-5 but for large fish), and 11 (dead). Also, we defined *S*' to be (1-*S*), *g*' to be (1-*g*), *m*' to be (1-*m*), and τ' to be (1-τ). Subscripts on parameters denote size first, then migration category. Parameters were equivalent for oCR/uCR counterparts, so that $S_{w,2} = S_{w,3}$, $S_{w,4} = S_{w,5}$, $g_2 = g_3$, $g_4 = g_5$, $m_{w,2} = m_{w,3}$, and $m_{w,4} = m_{w,5}$.

(1.1)

***small* LCRres**	***small* oCRmig**	***small* uCRmig**	***small* oCRskm**	***small* uCRskm**	***large* LCRres**	***large* oCRmig**	***large* uCRmig**	***large* oCRskm**	***large* uCRskm**	**dead**
$S_{1,1}g_1'm_{1,1}'$	$S_{1,1}g_1'm_{1,1}\tau$	$S_{1,1}g_1'm_{1,1}\tau'$	0	0	$S_{1,1}g_1m_{2,1}'$	$S_{1,1}g_1m_{2,1}\tau$	$S_{1,1}g_1m_{2,1}\tau'$	0	0	$S_{1,1}'$
0	$S_{1,2}g_2'm_{1,2}$	0	$S_{1,2}g_2'm_{1,2}'$	0	0	$S_{1,2}g_2m_{2,2}$	0	$S_{1,2}g_2m_{2,2}'$	0	$S_{1,2}'$
0	0	$S_{1,3}g_3'm_{1,3}$	0	$S_{1,3}g_3'm_{1,3}'$	0	0	$S_{1,3}g_3m_{2,3}$	0	$S_{1,3}g_3m_{2,3}'$	$S_{1,3}'$
0	$S_{1,4}g_4'm_{1,4}$	0	$S_{1,4}g_4'm_{1,4}'$	0	0	$S_{1,4}g_4m_{2,4}$	0	$S_{1,4}g_4m_{2,4}'$	0	$S_{1,4}'$
0	0	$S_{1,5}g_5'm_{1,5}$	0	$S_{1,5}g_5'm_{1,5}'$	0	0	$S_{1,5}g_5m_{2,5}$	0	$S_{1,5}g_5m_{2,5}'$	$S_{1,5}'$
0	0	0	0	0	$S_{2,1}m_{2,1}'$	$S_{2,1}m_{2,1}\tau$	$S_{2,1}m_{2,1}\tau'$	0	0	$S_{2,1}'$
0	0	0	0	0	0	$S_{2,2}m_{2,2}$	0	$S_{2,2}m_{2,2}'$	0	$S_{2,2}'$
0	0	0	0	0	0	0	$S_{2,3}m_{2,3}$	0	$S_{2,3}m_{2,3}'$	$S_{2,3}'$
0	0	0	0	0	0	$S_{2,4}m_{2,4}$	0	$S_{2,4}m_{2,4}'$	0	$S_{2,4}'$
0	0	0	0	0	0	0	$S_{2,5}m_{2,5}$	0	$S_{2,5}m_{2,5}'$	$S_{2,5}'$
0	0	0	0	0	0	0	0	0	0	1

The simplified **Ψ** matrix illustrates some key restrictions that were necessary for differentiating among states. We assumed that resident to migrant transition was unidirectional – that is, residents could transition to become oCR/uCR migrants, but not vice versa (i.e., column 1 contains all zeroes after row 1; Figure 1.2). This assumption seemed reasonable because

residents are most often smaller than migrants and skipped migrants (Stone and Gorman 2006), suggesting that once fish are large enough they do not reside in the LCR year-round or that maximum length and(or) survival are lower for LCR residents. Additionally, we assumed that fish could not transition between oCR and uCR states (e.g., matrix elements (2,3) and (3,4) are 0) based on previous studies which suggest that most humpback chub display high site fidelity when not migrating (Ryel and Valdez 1995) and because previous models that allowed for movement between oCR and uCR states did not converge. Lastly, all survival, growth, and migration parameters from the uCR were set equal to that of oCR to mitigate for the unobservable uCR skipped migrant state (Kendall et al. 2019) and uncertainty in state assignment (Kendall et al. 2012). The oversummer state transition matrix was similar in structure to the overwinter matrix above, with the exception that all $m = 0$ because migration does not occur between spring and fall.

Survival, growth, and movement parameters were dependent on demographic category. Survival was modeled with a logit-transformed random effect that was centered on a mean specific to movement category and season. Variances for survival random effects were season-specific and specific to site, with LCR residents having a different standard deviation on survival compared to migrants and skipped migrants. Survival of skipped migrants was modeled as an additive offset from that of migrants to help with data sparseness due to both low CR capture probabilities and the fact that detection of skipped migrants could never definitively place fish in this category. Migration probabilities were Markovian (i.e., probability a migrant became a skipped migrant was not equal to the probability that a skipped migrant stayed a skipped migrant) and could only occur overwinter. Migration parameters were also modeled with logit-transformed yearly random effects with mean specific to breeding category and variance shared

across all demographic categories. The conditional probability that a fish was from the oCR given it was migratory (τ) was modeled as constant.

1.3.6. Data model

Determining state required linking detection types to state, as illustrated in Figure 1.2b. No single detection could completely define a state (i.e., no event is found in only one row of the matrix in Figure 1.2b), and accordingly multiple detections were often required to definitively place fish in one state. We present the data model in four components: spring captures in the LCR (which included open and closed components), fall captures in the LCR and oCR, and state uncertainty at first capture in the LCR, oCR, and uCR. Additionally, the data model included one parameter to represent initial tag loss or mortality from tagging (χ). Specifically, the model included a vector of 0/1 values used to describe whether or not the fish was newly marked at the start of the study. The newly marked vector was multiplied by χ for the first occasion following release.

1.3.6.1 Spring model: closed component

The closed component of the spring data model pertained to spring LCR sampling and was demographically closed so that fish could not die, grow, or change migratory status. Importantly, the closed component of the model was not truly closed in terms of movement, because it allowed migrants to move between the CR and LCR during spring LCR sampling. The decision to not treat the population as geographically closed within the spring was motivated by the observations of Pearson et al. (2016) and the mismatches in movement timing (as observed on the MUX) and LCR sampling (Figure 1.3).

Specifically, spring LCR sampling included two USFWS trips, roughly timed to occur in April and May (though in some years hydrology or logistical issues delayed sampling to later May and June). To allow for movement between the CR and LCR during the spring sampling period, we included four availability probabilities: available for April LCR sampling only ($a_{A0,w,n,t}$), May LCR sampling only ($a_{0M,w,n,t}$), both April and May LCR sampling ($a_{AM,w,n,t}$), and neither April nor May LCR sampling ($a_{00,w,n,t} = 1 - a_{A0,w,n,t} - a_{0M,w,n,t} - a_{AM,w,n,t}$). Availabilities were transformed to sum to one using a multinomial logistic transformation. Availability parameters were estimated independently for each demographic category and varied by year as random effects.

The data used to inform availability included four sampling occasions from USFWS sampling that corresponded to April pass 1 ($p_{A,1,w,t}$), April passes 2&3 ($p_{A,2,w,t}$; pooled), May pass 1 ($p_{M,1,w,t}$), and May passes 2&3 ($p_{M,2,w,t}$; pooled). Importantly, while the model accounted for potential movement in and out of the LCR between April and May trips it did not allow movement within the April or May trip so that all fish captured during pass 1 are available for passes 2&3 of the same trip (i.e., fish in availability category a_{A0} would have non-zero $p_{A,1}$ & $p_{A,2}$). For this reason, we pooled passes 2&3 to help mitigate for violations in the population closure within-trip (Kendall 1999). MUX detection also informed availability, but this information was included in the open model. Pass-specific capture probabilities were formulated to be size-specific and to have additive offsets for turbidity (β_{TURB}; Stone 2010) and size-specific behavioral response (c_w) to capture. The capture probabilities were modeled with temporally-varying random effects, where capture probabilities for newly captured fish in passes 2&3 were set equal to that of pass 1 (but also accounting for the extra pass).

Importantly, all capture probabilities from the closed model were divided by the probability of being captured at least once in spring, effective detection probability p^*; which is akin to Kendall et al. (2019) and Huggins (1991). This p^* calculation was specific to migration category – p^* is zero for skipped migrants, as by definition this group does not enter the LCR. The p^* calculation for migrants (where h can be 2 or 3) includes availability:

(1.2) $$p^*_{w,n,h,t} = 1 - (a_{\mathrm{AM},w,n,t}\left(1 - p_{\mathrm{A},1,w,t}\right)\left(1 - p_{\mathrm{A},2,w,t}\right)\left(1 - p_{\mathrm{M},1,w,t}\right)\left(1 - p_{\mathrm{M},2,w,t}\right) + a_{A0,w,n,t}\left(1 - p_{\mathrm{A},1,w,t}\right)\left(1 - p_{\mathrm{A},2,w,t}\right) + a_{0\mathrm{M},w,n,t}\left(1 - p_{\mathrm{M},1,w,t}\right)\left(1 - p_{\mathrm{M},2,w,t}\right) + (1 - a_{\mathrm{AM},w,n,t} - a_{A0,w,n,t} - a_{0\mathrm{M},w,n,t}))$$

Eq (1.3) is the likelihood for an example of a migrant that was captured on passes 1 & 2 of the April trip, but not observed during the May trip. This capture history could arise under two availability scenarios: 1) the fish could be available for April and May, captured in April only and not captured in May and 2) the fish could have been available for only April and thus the May capture probability does not apply.

(1.3) $$\frac{a_{\mathrm{AM},w,n,t}\, p_{A,1,w,t} p_{A,2,w,t}\left(1-p_{M,1,w,t}\right)\left(1-p_{M,2,w,t}\right)+a_{A0,w,n,t}\, p_{A,1,w,t} p_{A,2,w,t}}{p^*_{w,n,h,t}}$$

We assumed all residents were available for April and May sampling and thus the p^* calculation for this group does not include availability (Equation 1.4).

(1.4) $$p^*_{w,n,h=1,t} = 1 - \left(1 - p_{\mathrm{A},1,w,t}\right)\left(1 - p_{\mathrm{A},2,w,t}\right)\left(1 - p_{\mathrm{M},1,w,t}\right)\left(1 - p_{\mathrm{M},2,w,t}\right)$$

Accordingly the likelihood for the example above (captured on passes 1 & 2 of the April trip, but not observed during the May trip) for a LCR resident is depicted in Equation 1.5.

(1.5) $$\frac{p_{A,1,w,t}p_{A,2,w,t}(1-p_{M,1,w,t})(1-p_{M,2,w,t})}{p^*_{w,n,h=1,t}}$$

1.3.6.2. Spring model: open component

The open component for spring used p^* in its calculation and included additional information about the size and sex (if fish were ripe) at capture. This necessitated including a parameter ($r_{w,n}$) that described the probability that a fish was ripe upon capture, and r was different for each demographic group and temporally constant. There were six possible events based on physical capture: small ripe female, small ripe male, small nonripe (unknown sex), large ripe female, large ripe male, large nonripe. If fish were captured two or more times during the same closed period, then the largest size at capture was used to define the state. Similarly, ripeness overrode non-ripeness to determine sex. So, for example, if a fish was captured once as a small, ripe male and once as a large, non-ripe fish during the same spring, then we classified that fish as a large male. Each capture type had two possible MUX events (either detected or not detected on the MUX), which translated to 12 total events. We included one additional event for fish that were only detected on the MUX and not captured, and one event for fish that were not captured or detected on the MUX for a total of 14 possible events. The detection probability of the MUX (p_{MUX}) was modeled as year-specific but constant across all demographic categories. As an example of the open model, consider a fish that was captured as a large ripe male and detected on the MUX within the same spring. This fish would be a known migrant (due to the

MUX detection) but there would be uncertainty as to its oCR/uCR status, producing the following likelihood (where *h* could be 2 or 3) for a given set of spring detections in year *t*:

(1.6) $$p^{*}_{2,1,h,t}\, r_{2,1} p_{\mathrm{MUX},t}$$

1.3.6.3. Linking open and closed spring models

For each capture occasion, the open model produced a vector of forward-conditional probabilities that fish were in each state (hereafter the 'state assignment vector'). The state assignment vector was multiplied by the conditional capture probabilities for each state in the closed model to produce a vector of joint probabilities. Joint probabilities were summed across all states to produce a marginal probability of the observed capture history as described in Yackulic et al. (2020). This marginal probability was log-transformed and added to the likelihood from the open model.

1.3.6.4. Fall model

Fall sampling included both CR and LCR sampling and did not include MUX detections. Fall LCR sampling included two trips (typically in September and October in each year), whereas the CR sampling varied by year. From 2009-2011, CR sampling occurred in September and October of each year, while from 2012 onward sampling occurred in either September or October. Fall detection probabilities were modeled with annual random effects while accounting for the number of trips (either 1 or 2) that were conducted in each river per year. Unlike spring detections, all fall detections were condensed into a single period and we refer to the LCR and oCR capture probabilities as $f_{\mathrm{LCR},w,h,t}$ and $f_{\mathrm{oCR},w,h,\mathrm{t}}$, respectively. Capture probabilities in the LCR included additive offsets for turbidity (β_{TURB}) and in the oCR capture probabilities included a

temperature covariate (β_{TEMP}). Additionally, in 2016 and 2018, fish in the oCR in fall could be detected on submersible antennas with size-specific detection probability ($f_{SUB,w}$). Because migrants could be located in either the LCR or the CR during fall sampling, we also included a fall availability parameter for migrants that described the probability a migrant was in the LCR during fall LCR sampling ($b_{w,n,t}$). Thus, the probability a migrant was captured in the LCR was the LCR capture probability (assumed to be the same as for residents) multiplied by $b_{w,n,t}$, whereas the capture probability in the CR was the capture probability (assumed to be the same as skipped migrants) multiplied by (1-$b_{w,n,t}$). These fall availability parameters were modeled independently for all demographic groups and included a yearly random effect.

1.3.6.5. Initial state assignment probabilities

Uncertainties in state assignment required a vector ($\boldsymbol{\pi}$) that represented the probability a newly marked fish was in any particular state at first capture (Pradel 2005). The $\boldsymbol{\pi}$ values are specific to season (fall vs spring) and site (CR vs LCR) of the first capture occasion of a fish (Figure 1.4). Regarding uncertainty in migratory category, fish captured in the CR can be either migrants or skipped migrants, whereas fish captured in the LCR can be either migrants or residents. There is further uncertainty in the demographic states regarding sex but not size (since a fish must be physically captured to be marked, its initial size is always known).

Based on the findings of Yackulic et al. (2014), which found little movement between the LCR and CR for subadult fish (i.e., 100-199mm TL), additional information about previous captures was used to help inform the probability an individual fish released in the LCR was resident or migrant. The π for the probability a fish released in the LCR was a migrant was determined using a logit link that included an intercept term ($\beta_{0,w,n,k,t}$), a parameter describing the effect of previous subadult capture in the LCR on the probability of being migrant ($\beta_{1,w,k,t}$), and a

dummy variable (x_i) that took the value of 1 if fish *i* had a previous LCR capture as a subadult or 0 if not (note since the model pertains to adults only the subadult captures used for the covariate are not included in the capture history). There were four values of β_1 that were specific to season (fall or spring) and size (small or large adult). Furthermore, all fish with previous subadult CR captures were assumed to be migrants, as the CR capture provided evidence that these fish do not reside year-round in the LCR. Including information about previous subadult captures helps test the hypothesis that fish that spend their subadult phase in the LCR are more likely to be resident compared to fish that spend this stage in the CR.

For fish first captured in the LCR, $\boldsymbol{\pi}$ included the following: the size- and season-specific probability a fish is female ($j_{\mathrm{LCR},k,w}$), the size- and sex-dependent probability a fish is a migrant (not a resident), and some information about previous capture history (see previous paragraph). Additionally, since all fish captured in the LCR in spring were checked for ripeness, the $\boldsymbol{\pi}$ for spring LCR captures included ripeness. For example, the probability a nonripe fish was female was conditional on the fish being nonripe (i.e., equal to $(1-r_{w,2})\, j_{\mathrm{LCR},w,k} / ((1-r_{w,2})*j_{\mathrm{LCR},w.k} + (1-r_{w,1})*(1-j_{\mathrm{LCR},w,k}))$). For fish first captured in spring or fall in the CR, $\boldsymbol{\pi}$ included the size- and season-specific probability a fish is female ($j_{\mathrm{CR},w,k}$), and the size and sex-dependent probability a fish is a migrant (not a skipped migrant). Because ripe fish in the CR and in the LCR in fall are rare, *r* was not included as a parameter in $\boldsymbol{\pi}$ for LCR fall or CR release occasions, and consequently we assumed all these fish were unknown sex upon release. Fish that were detected on the MUX the current or previous spring before their first capture as adults were assumed to start as migrants, not skipped migrants.

While the nonsystematic and incomplete sampling of the uCR prohibits information about recaptures, the conditional HMM model was able to include information about fish

initially released in the uCR. Specifically, All $\boldsymbol{\pi}$ from the uCR were assumed to be equal to those of the oCR based on Kendall et al. (2012). On a similar note, spring releases in the CR were included via the $\boldsymbol{\pi}$ but not included in capture parameters due to the low capture probability for CR fish in spring.

1.3.6.6. Capture history

An example of this approach is illustrated by the following capture history (ch) for individual *i*: first captured as a large, ripe male in the LCR in spring of year $t = 1$ ($ch_{i,1,1}$), not observed the following fall of year 1 ($ch_{i,1,2}$), and then detected on the MUX in spring $t = 2$ ($ch_{i,2,1}$). The first step is to populate the initial state assignment vector ($\boldsymbol{\pi}$). While there is no demographic uncertainty in this observation (fish is a known large male so $w = 2$ and $n = 1$), there is uncertainty in migratory status in spring of $t = 1$ because the fish could be an LCR resident ($h = 1$), oCR migrant ($h = 2$), or uCR migrant ($h = 3$), thus the π in Equations 1.7-1.9 are nonzero.

(1.7) $$\pi_{i,2,1,1} = \text{logit}^{-1}(\beta_{0,2,1,1,t} + \beta_{1,2,1,1} x_i)$$

(1.8) $$\pi_{i,2,1,2} = \tau \, \text{logit}^{-1} (\beta_{0,2,1,1,t} + \beta_{1,2,1,1} x_i)$$

(1.9) $$\pi_{i,2,1,3} = (1-\tau) \, \text{logit}^{-1} (\beta_{0,2,1,1,t} + \beta_{1,2,1,1} x_i)$$

where logit^{-1} refers to the inverse logit transformation. Note that skipped migrants cannot be in the LCR, thus $\pi_{i,2,1,4} = 0$ and $\pi_{i,2,1,5} = 0$. The next step requires updating the likelihoods for the following fall (where and $k = 2$ and $t = 1$) based on the observed capture history, where $ch_{i,k,t}$ represents the capture history up to season *k* of year *t*:

(1.10) $P(ch_{i,1,2} \mid h_{i,2,1}= 1) = \pi_{i,2,1,1} S_{2,1,1,1,1} (1 - f_{LCR,2,1,1})$

(1.11) $P(ch_{i,1,2} \mid h_{i,2,1}= 2) = \pi_{i,2,2,1} S_{2,1,2,1,1} (b_{2,1,1} (1 - f_{LCR,2,1,1}) + (1 - b_{2,1,1}) (1 - f_{oCR,2,2,1}))$

(1.12) $P(ch_{i,1,2} \mid h_{i,2,1}= 3) = \pi_{i,2,3,1} S_{2,1,3,1,1} (b_{2,1,1} (1 - f_{LCR,2,1,1}) + (1 - b_{2,1,1}))$

(1.13) $P(ch_{i,1,2} \mid h_{i,2,1}= \text{dead}) = \pi_{i,2,1,1} (1-S_{2,1,1,1,1}) + \pi_{i,2,2,1} (1-S_{2,1,2,1,1}) + \pi_{i,2,3,1} (1-S_{2,1,3,1,1})$

The above likelihoods illustrate how residents must be in the LCR in fall but that migrants can be either in the LCR or CR during fall sampling. Furthermore, comparison of likelihoods for $h_{i,2,1}$ = 2 and $h_{i,2,1}$= 3 shows that whereas oCR fish can be captured in the oCR in fall, by definition uCR fish cannot be observed in the CR in fall because they occur outside the sampling reach.

The conditional likelihoods are then updated for the following spring (k = 1, t = 2) based on the conditional likelihoods from the previous occasion, the state transition matrix, and the observed capture history of the current occasion. Note that, in this particular example, the fish must be a migrant during the second spring ($h_{i,1,2}$ = 2 or $h_{i,1,2}$ = 3) due to its MUX detection:

(1.14) $P(ch_{i,1,2} \mid h_{i,1,2} = 1) = 0$

(1.15) $P(ch_{i,1,2} \mid h_{i,1,2} = 2) = \{P(ch_{i,2,1} \mid h_{i,2,1} = 1) S_{2,1,1,2,1} m_{2,1,1,2,1} \tau + P(ch_{i,2,1} \mid h_{i,2,1} = 2) S_{2,1,2,2,1} m_{2,1,2,2,1}\} (1 - p^*_{2,1,2,1,2}) p_{MUX,2}$

(1.16) $P(ch_{i,1,2} \mid h_{i,1,2} = 3) = \{P(ch_{i,2,1} \mid h_{i,2,1} = 1) S_{2,1,1,2,1} m_{2,1,1,2,1} (1 - \tau) + P(ch_{i,2,1} \mid h_{i,2,1} = 3) S_{2,1,3,2,1} m_{2,1,3,2,1} \} (1 - p^*_{2,1,3,1,2}) p_{MUX,2}$

(1.17) $P(ch_{i,1,2} \mid h_{i,1,2} = \text{dead}) = 0$

These steps are repeated for all time steps until the last occasion. The final likelihood for each capture history is the marginal probability at the last occasion T during season K:

(1.18) $$\sum_{h=1}^{5} \mathrm{P}\left(\mathrm{ch}_{i,K,T} \mid h_{i,K,T}\right)$$

In practice, there is also uncertainty in size and sex in addition to migratory status, and thus the above equation must cycle through all possibilities of size and sex as well (not presented here for simplicity). These steps are accomplished using matrix multiplication, which is illustrated in the supplemental Stan code (S4).

1.3.7. Assessing ecological hypotheses: Skipped migration, permanent residency, and variability in the timing of first migration

We used the Watanabe-Akaike Information Criterion, WAIC (Watanabe 2010), to compare three models, a permanent resident model, a premigrant model, and a skipped migrant model. The permanent resident model tests the hypothesis that all residency is determined at earlier life history stages, thus the resident to migrant transition is fixed to zero. If residency is indeed determined at earlier life history stages, this would indicate managers should aim to better understand the drivers of age-0 emigration from the LCR to the CR (Yackulic et al. 2014), as this early decision would have important implications for life history and population dynamics. The premigrant model infers that there is variability in the size or age at first migration, but that once fish decide to migrate they do so every year and do not become skipped migrants. Thus, the transition probability from migrant to skipped migrant is fixed to zero in the premigrant model. The premigrant model would be a good representation of the data if migration is associated with spawning and there is variability in the age or size at first spawning as has been observed in other fishes (Christie et al. 2018; Secor 2007a). The skipped migrant model is the most general model because it does not restrict transitions from resident to migrant or from migrant to skipped migrant. The skipped migrant model therefore emphasizes flexibility in migratory strategy and

suggests that fish can more easily change migratory categories based on individual characteristics and environmental conditions.

1.3.8. Running the model

Models were fit using a marginalization approach (Yackulic et al. 2020) in Stan via R using the package 'rstan'. Models included three chains, each with 500 iterations, and the first 250 iterations of each chain were used as burn-in. This resulted in a total of 750 posterior draws. All models converged with R-hat less than 1.1. Priors were minimally informative. For example, fixed effects such as τ, growth, sex ratios (for π), ripeness, and tag loss were given a uniform prior between 0-1. Means for random effects of logit-transformed parameters, such as mean *S* or mean *b*, were given a normal prior with mean 0 and standard deviation 2. Priors for standard deviations of random effects were uniform with bounds 0-5. Priors for spring availability were normal with mean -0.5 and standard deviation 1. Priors for specific parameters can be found in the Stan code included as part of Appendix D.

1.4. Results

1.4.1 Comparing models with and without antenna data:

The model with antenna data revealed interesting demographic differences in availability. Small males tended to be available for both April and May sampling occasions, whereas small females were more likely to be available for either April or May sampling, but rarely both (Figure 1.5). Also, both large males and large females tended have a high proportion of the population in the 'MUX only' category, suggesting many large fish are not available for hoop net

capture due to either the timing of migration, trap behavior responses, or hoop net characteristics (e.g., openings are too small). This finding sets the stage for comparing models fit with and without antenna data. In the model without antenna data, fish in the 'MUX only' category are not detectable in the LCR and consequently this model assumed that more fish remained in the CR year-round. Therefore, it overestimated skipped migration probabilities for all groups except small males (Figure 1.6). For this reason, estimates of spring abundances in the LCR were lower for the model fit without antennas than the model fit with antennas. Although spring abundance estimates in the LCR differed between models, fall estimates of total abundance (i.e., the total number of fish in both the LCR and CR) and their precisions were similar for both models (Figure 1.7).

In addition, there were differences in models fit with and without antenna data that likely arose from capture heterogeneity and trap-shy behaviors. For example, the model with antenna data estimated a higher probability a migrant was from the oCR reach (τ = 32.5% compared to 22.9%). Also, the model fit without antenna data tended to have lower annual survival estimates for large migrants, though 95% credible intervals did overlap for all groups (Figure 1.8). Lastly, one-time tag loss and mortality ($\hat{\chi}$) for the model fit with antenna data was estimated to be relatively low (1.8%; 95% CI: 0.0-3.7%) and comparable to the 3% tag loss/ mortality rate observed in a laboratory experiment of bonytail chub *Gila elegans* (Ward et al. 2015), whereas $\hat{\chi}$ for the model fit without antenna data was higher (9.3%; 95% CI: 5.8-12.7%). This latter finding led us to fit one additional model without antenna data and fixed χ (2%), to make sure that differences in models with and without antenna were not due to these different estimates of tag loss. Except for some negligible differences in survival rates across models, the results of two models were similar, so we present results from the model with estimated tag loss.

1.4.2. Migration probabilities and tradeoffs

The skipped migration model was supported over the premigration model (ΔWAIC = 29.9) and the permanent resident model (ΔWAIC = 237.3). Skipped migration probabilities were much lower than those reported in previous studies (Pearson et al. 2015; Yackulic et al. 2014); for details see the Discussion. Furthermore, skipped migration probabilities tended to display low variability from year to year. Small females were the most likely group to transition from migrant to skipped migrant (Figure 1.6). Specifically, the average probability a small female migrant transitioned to a skipped-migrant was 14% and ranged from 9-22% each year. For small males, large females, and large males, mean probabilities that migrants became skipped migrants were 5% (from 3-9% per year), 4% (from 2-9% per year), and 6% (from 3-17% per year), respectively. Probabilities of a skipped migrant becoming a migrant were imprecise yet differed for males and females. Whereas large males had a high probability of transitioning from skipped migrant to migrant (57%), the probability of large females transitioning from skipped migrant to migrant was much lower (12%; Table 1.2). Females had a much lower probability of being ripe upon spring capture compared to males, but ripeness of small and large fish was roughly similar. Specifically, 66% of males were ripe for both small and large adults, whereas ripeness of females was 3.9% (small) and 5.0% (large). Large females had higher annual survival than large males, though 95% credible intervals overlapped for both groups (Figure 1.8).

Using methods described in Appendix C and extrapolating initial starting probabilities and spawning transition rates to spring (the time when fish were actually spawning) suggests that the mean across-year proportion of fish from the Colorado River that were skipped migrants was 35% (small males), 29% (small females), 16% (large males), and 24% (large females). The

inability to distinguish between migrants and skipped migrants at first capture may be a limitation in the current study. For example, the 95% credible interval for the across-year mean probability a fish first captured in the CR was a skipped migrant was 27-96% (small males), 7-77% (small females), 2-99% (large males), and 7-57% (large females).

Comparison of migrants and skipped migrants shows that, generally, there is little evidence for differences in growth or survival, though the imprecise estimates of growth and survival of skipped migrants may obscure differences between groups. Comparing annual growth probabilities using the following equation (prob of annual growth = $1 - (1- g_{n,h,2})(1-g_{n,h,1})$) showed that migrant growth probabilities were actually higher than skipped migrant growth probabilities, though 95% credible intervals did overlap. Specifically, female and male migrant growth probabilities were 72% (95% CI: 66-78%) and 61% (95% CI: 56-66%), respectively, whereas skipped migrant growth probabilities were 48% (95% CI: 20-81%) and 43% (95% CI: 19-70%). Likewise, the 95% credible intervals of survival offsets for skipped migrants for all demographic groups overlapped zero, but tended to be negative for large females (-0.56; 95% CI: -1.48 – 0.95) and large males (-0.37; 95% CI: -2.70 - 3.08) and positive for small females (0.07; 95% CI: -2.35 – 3.78) and males (0.82; 95% CI: -1.31 – 3.98).

1.4.3. Alternative life histories

In fall, residents only comprised 28% (95% CI: 6-55%) of small females, 25% (95% CI: 5-53%) of small males, 9.2% (95% CI: 4-19%) of large females, and 8.2% (95% CI: 3-19%) of large males, suggesting this group is a relatively small proportion of the overall humpback chub population (similar to Yackulic et al. 2014) and that residents are on average smaller than migrants (Stone and Gorman 2006). In all models, resident survival was much lower than

migrant survival. Closer examination reveals that the difference in annual survival rates of migrants and residents is mainly due to winter survival probabilities (Figure 1.9; Table 1.2). Also, residents were more likely to die than become migrants (Figure 1.10), suggesting that determination of life history strategy occurs at earlier life history stages. Note that simulations from Appendix B illustrate the potential for overestimation in the resident to migrant transition, thus it is possible that the true resident to migrant is even lower than the 4-11% values reported in this study. Lastly, β_1 was negative for all groups and the 95% CIs did not overlap zero, suggesting that fish with previous subadult captures in the LCR were more likely to be resident compared to fish without previous subadult LCR capture (Yackulic et al. 2014).

1.5. Discussion

Incorporation of antenna detections into mark-recapture models provided valuable insight into migration patterns in humpback chub in the LCR aggregation. Specifically, not only did antennas increase detection probabilities, they also provided detection information about a subset of fish that were not available for LCR hoop net sampling by USFWS. As a result, skipped migration probabilities from this study were substantially lower than those estimated by previous studies that either did not include antenna detections (Yackulic et al. 2014) or used poor quality antenna detections (Pearson et al. 2015). While estimates of skipped migration and survival differed for models with and without antennas, the fall abundance estimates were similar for both models, though models with antennas did produce slightly more precise estimates. Accordingly, because both models accounted for temporary emigration from the LCR in the form of skipped migration, models with and without antennas were similar in many respects but disagreed on the proportion of adults that were migrants.

In a similar study of humpback chub in the LCR aggregation from 2001-2011, Pearson et al. (2015) estimated the mean probability that a migrant remained a migrant the next year was 55%, which is lower than the 83-97% values observed in this study. While Pearson et al. (2015) did include LCR MUX detections in their population model for a subset of years (2009-2011), the detection rates were very low during this time and the LCR MUX was often not functional during early spring months. Unlike Pearson et al. (2015) or the current study, Yackulic et al. (2014) estimated migration probabilities from 2009-2012 as the proportion of CR adults that moved into the LCR each year and reported that 31% small adults and 61% large adults moved from the CR to the LCR each spring from 2009-2012. A telemetry study of humpback chub observed that only 57% (n = 61) of adult humpback chub moved into the LCR or LCR inflow from 1991-1992 (Ryel and Valdez 1995). By comparison, the current model estimates that, on average, 65% of small males, 71% of small females, 84% of large males, and 76% of large females in the CR were migrants in any given year, and that the yearly percentage ranged from 53-73% (small males), 61-85% (small females), 75-90% (large males), and 66-86% (large females) from 2010-2019. The discrepancy between the migration probabilities observed by Ryel and Valdez (1995) and the current study is unknown, but could be due to changes in hydrothermal regime (early 1990s had colder water and more hydropeaking compared to current conditions), individual heterogeneity in migration probabilities, or potential biases or errors in one of the two studies.

Previous studies have assumed that all CR-LCR migration was associated with spawning (Yackulic et al. 2014, Pearson et al. 2015). While spawning is certainly one impetus for migration between the CR and LCR, results from the current study call into question their assumption that migration is exclusively motivated by spawning. Determining whether all

migration is associated with spawning is nearly impossible because direct information about spawning (e.g., deposition of eggs or milt) is difficult to obtain. The LCR may be a favorable environment for adult humpback chub in spring, as evidenced by high summer survival probabilities of residents and the apparently faster (though statistically insignificant) growth rates for migrants compared to skipped migrants during the summer interval. This, in turn, suggests there might be a growth advantage associated with migration. Comparison of subadult humpback chub growth in the two rivers shows that somatic growth in length is generally higher in the LCR compared to the CR, particularly from April – May, when growth in the LCR is 10-20 times higher than in the CR (Dzul et al. 2016).

The paired finding that female migrants were unlikely to become skipped migrants and female skipped migrants were unlikely to become migrants provides some evidence for migration heterogeneity among females. Individual heterogeneity in migration and spawning strategy may be particularly advantageous in large river desert environments, where the timing and magnitude of floods vary across years. Under these conditions, it is unlikely that a one-size-fits-all spawning strategy would be beneficial to population persistence. Heterogeneity in vital rates among individuals is common, and model efforts to incorporate heterogeneity are burgeoning (Gimenez et al. 2018). If the main impetus for migration is spawning, then one hypothesis for heterogeneity is that individual quality is the main driver of spawning and migration (Beauplet et al. 2006). Individual quality may be an inherent characteristic of the population and(or) it may be influenced by age, where first-time breeders and(or) old individuals spawn (and migrate) less frequently than individuals of prime reproductive age (Jørgensen et al. 2006). Alternatively, heterogeneity in migration could occur if a small subset of large females were mainstem spawners or spawned in the lower 1.8 rkm of the LCR (and are thus not

detectable on the MUX). We attempted to more formally assess spawning heterogeneity using mark-recapture models that incorporated migration heterogeneity, but these models were prohibitively slow, required many simplifying modifications to converge, and were difficult to interpret. Developing humpback chub models that incorporate migration heterogeneity may be an area of future research.

Alternative life histories have been documented among numerous fishes, and often these alternative life histories represent a 'slow' and 'fast' track (Nelson et al. 2002). These 'slow' and 'fast' life histories are supported by a previous humpback chub study that found residents had lower survival but faster growth than migrants at earlier life history stages (Yackulic et al. 2014), and this finding was reinforced by results of the current study, which found residents had substantially lower survival than migrants. The low survival probability of residents suggests that individuals in this group may only live through one or two spawning seasons, and that consequently this group may be generally semelparous. The difference in resident and migrant survival was driven mainly by overwinter survival. In a diet study of LCR fishes, Behn and Baxter (2019) found that humpback chub stomachs were typically empty over winter (at baseflow), suggesting this may be a time of severe food limitation. Although other studies have made the distinction between the migrant and resident life history strategies in humpback chub (Douglas and Marsh 1996; Gorman and Stone 1999; Yackulic et al. 2014), this study was the first (to our knowledge) to assess the potential for adult residents to leave the LCR and become migratory. While model results suggest that some residents do move to the CR, residents have a much higher probability of dying than becoming migratory, suggesting that for most individuals these two life histories diverge at earlier stages (e.g., as juveniles or subadults; Yackulic et al. 2014). In addition, the finding that residents only comprise a small proportion of the overall

adult population suggests that the CR can support more large humpback chub than the LCR and thus is probably a better environment for adults (particularly overwinter).

Importantly, since the only detection method for LCR residents is hoop nets, it is possible that residents develop a long-term trap shy behavior that could be masked as low survival in our model. If this issue is prevalent then, as long as the trap-shy component of the population has a non-zero capture probability, we would expect some issues with retrospective negative bias where survival rates would increase as more years of data are added to the model (Kendall et al. 2013; Langtimm 2009; Peñaloza et al. 2014). While we do not see any evidence for retrospective bias in our model, we believe it would be prudent to add submersible antennas to supplement LCR hoop net sampling in order to help assess potential long-term trap shy behavior in LCR residents. This recommendation stems from the broader lesson learned from adding antenna detections of migrants (MUX and CR submersibles) and skipped migrants (CR submersibles), namely that false conclusions can occur when some proportion of the population is not detectable and that even well-thought-out models cannot always solve sampling issues.

While this study illustrates one method for incorporating antenna data into mark-recapture models, other studies have found solutions to the three challenges highlighted in this paper. For the availability challenge, multistate models with unobservable states can be used to describe fish that are not detectable on antennas. For example, if PIT antennas are set up as multiple arrays that are spaced in close proximity to each other, then detection data from individual arrays can be used to construct a capture history and estimate transition probabilities for individuals that permanently (Horton et al. 2011) or temporarily (Dzul et al. 2017) enter an unobservable state where their PIT antenna detection probability is zero. Another option is to use spatial mark-recapture models, which estimate the ‘activity centers’ for individual fish, and then

to model detection probabilities of each fish as a function of the distance between its activity center and PIT antenna locations (Raabe et al. 2013). In reference to the continuous time challenge, some studies have used a Barker model and treated antenna data as temporally continuous resight probabilities to help avoid bias in survival rates (Al-Chokhachy and Budy 2008; Beard et al. 2017). The state uncertainty challenge, to our knowledge, has not been addressed by previous studies of PIT antenna data, but this issue warrants attention. Other mark-recapture studies have developed hidden Markov models for state uncertainty, where the status of an individual is not always observable upon capture (Conn and Cooch 2009; Kendall et al. 2012), and we illustrated how this approach can be used with PIT antenna data.

Our study provides yet another example of how technological advances in mark-recapture can improve population models (Bravington et al. 2016; Conner et al. 2020; Cunjak et al. 2005), as models with PIT antenna detections led to new inferences in humpback chub population dynamics. We illustrate how, with a reasonable mark-recapture model, these new technologies can improve the ability of biologists to explore more complex ecological questions related to life history strategy and variability in vital rates. Assessing partial migration and life history variability may become increasingly important in the near future, as anthropogenic changes (e.g., habitat fragmentation, pollution, climate change) may imperil select individuals that display a particular life history or migration strategy (Nelson et al. 2002; Nilsson et al. 2006). Accordingly, obtaining a better understanding of if(how) alternative life histories promote overall population resiliency is an important question for guiding conservation efforts in an uncertain future (Gillanders et al. 2015).

Funding statement:

This study was funded by the Bureau of Reclamation in support of the Glen Canyon Dam Adaptive Management Program (Agreement #: R19PG00070).

TABLE 1.1. Description of parameters used to model migration dynamics of humpback chub that spawn in the Little Colorado River (LCR). Parameters are grouped according to process: state transition (ST), spring detection – open (STO), spring detection – closed (STC), fall detection (FD), and initial state (IS). Parameters could vary by year, season (spring/summer or fall/winter), size (200-249mm TL or >250mm TL), sex (male or female), and migration category (mig. cat – or LCR resident, migrant, skipped migrant). Parameters could be modeled as random effects (R), constant (C), independent (I), additive offsets (A), or not applicable (-).

Symbol	Description	Process	Year	Season	Size	Sex	Mig. Cat.
S	Survival	ST	R	I	I	I	A / I
g	Growth	ST	C	I	-	I	I
m	Migration	ST	R	-	I	I	I
τ	Proportion of fish in CR that are in oCR	ST	C	C	C	C	C
r	Probability of ripeness in LCR in spring	SDO	C	-	I	I	C
p_{MUX}	Probability of MUX detection (migrants only)	SDO	I	-	C	C	-
p^*	Probability fish is captured at least once during spring USFWS sampling (derived)	SDO	-	-	-	-	-
a_{AM}	Proportion of migrants in LCR for April and May USFWS sampling	SDC	R	-	I	I	-
a_{A0}	Proportion of migrants in LCR for only April USFWS sampling	SDC	R	-	I	I	-
a_{0M}	Proportion of migrants in LCR for only May USFWS sampling	SDC	R	-	I	I	-
a_{00}	Proportion of migrants that are not in LCR for USFWS sampling (derived)	SDC	-	-	-	-	-
$p_{A,1}$	LCR capture probability - April, pass 1	SDC	R	-	I	C	-
$p_{A,2}$	LCR capture probability - April, passes 2&3	SDC	R	-	I	C	-
$p_{M,1}$	LCR capture probability - May, pass 1	SDC	R	-	I	C	-
$p_{M,2}$	LCR capture probability - May, passes 2&3	SDC	R	-	I	C	-
c	Behavioral offset	SDC	C	-	I	C	-
β_{TURB}	Turbidity offset for LCR	SDC	C	C	C	C	C
p^*	probability fish is captured at least once during spring USFWS sampling (derived)	SDC	-	-	-	-	-
f_{CR}	Fall oCR capture probability	FD	R	-	I	C	-
f_{LCR}	Fall LCR capture probability	FD	R	-	I	C	-
f_{SUB}	Probability of antenna detection for fish in oCR	FD	I	-	I	C	-

b	Probability migrant is in the LCR during fall USFWS sampling	FD	R	-	I	I	-
β_{TEMP}	Temperature offset for CR	FD	C	C	C	C	C
β_{TURB}	Turbidity offset for LCR	FD	C	C	C	C	C
j	Probability fish is female at first capture	IS	C	I	I	-	-
χ	Initial tag loss and tag-induced mortality	IS	C	C	C	C	C
r	probability of ripeness in LCR in spring	IS	C	-	I	I	C
τ	proportion of fish in CR that are in oCR	IS	C	C	C	C	C
β_0	Probability migrant if first captured in LCR with no previous subadult LCR captures	IS	R	I	I	I	-
β_1	Effect of previous LCR subadult capture on migrant probability	IS	C	I	I	C	-

TABLE 1.2. Summary of adult humpback chub estimates of parameters (par) for across-year means of survival (S), transition probability (b), and growth (g). Survival and growth estimates varied by two different seasons, summer (Sum: April to October), and winter (Win: October to April). Estimates for survival and transition probabilities varied for small (S: 200-249mm total length) versus large(>250mm total length) and for males (M) versus females (F). Growth, survival, and transition probabilities also varied for breeding/migratory states, specifically for residents (Res), migrants (Mig), and skipped migrants (Skm).

Par	Season	Size	Sex	State	Mean	95% CI
S	Win	S	F	Res	0.46	0.34-0.57
S	Sum	S	F	Res	0.89	0.81-0.96
S	Win	L	F	Res	0.57	0.46-0.68
S	Sum	L	F	Res	0.98	0.93-1
S	Win	S	M	Res	0.63	0.5-0.75
S	Sum	S	M	Res	0.83	0.72-0.93
S	Win	L	M	Res	0.57	0.45-0.7
S	Sum	L	M	Res	0.97	0.91-1
S	Win	S	F	Mig	0.91	0.77-0.99
S	Sum	S	F	Mig	0.96	0.9-1
S	Win	L	F	Mig	0.94	0.9-0.98
S	Sum	L	F	Mig	0.97	0.93-1
S	Win	S	M	Mig	0.87	0.73-0.98
S	Sum	S	M	Mig	0.95	0.87-1
S	Win	L	M	Mig	0.91	0.82-0.99
S	Sum	L	M	Mig	0.93	0.87-0.99
B		S	F	Res to Mig	0.05	0.01-0.12
B		S	F	Mig to Skm	0.14	0.02-0.35
B		S	F	Skm to Mig	0.40	0.03-0.89
B		S	M	Res to Mig	0.08	0.02-0.17
B		S	M	Mig to Skm	0.05	0-0.15
B		S	M	Skm to Mig	0.41	0.1-0.73
B		L	F	Res to Mig	0.11	0.05-0.2
B		L	F	Mig to Skm	0.04	0.01-0.08
B		L	F	Skm to Mig	0.12	0.03-0.3
B		L	M	Res to Mig	0.11	0.04-0.22
B		L	M	Mig to Skm	0.06	0.01-0.16
B		L	M	Skm to Mig	0.57	0.11-0.97
G	Win	S - L	F	Res	0.54	0.53-0.55
G	Win	S - L	F	Mig	0.55	0.52-0.59
G	Win	S - L	F	Skm	0.58	0.5-0.68
g	Win	S - L	M	Res	0.52	0.51-0.53
g	Win	S - L	M	Mig	0.54	0.51-0.57
g	Win	S - L	M	Skm	0.53	0.5-0.59

g	Sum	S - L	F	Res	0.61	0.6-0.62
g	Sum	S - L	F	Mig	0.66	0.64-0.67
g	Sum	S - L	F	Skm	0.55	0.5-0.65
g	Sum	S - L	M	Res	0.60	0.59-0.62
g	Sum	S - L	M	Mig	0.63	0.61-0.65
g	Sum	S - L	M	Skm	0.59	0.51-0.66

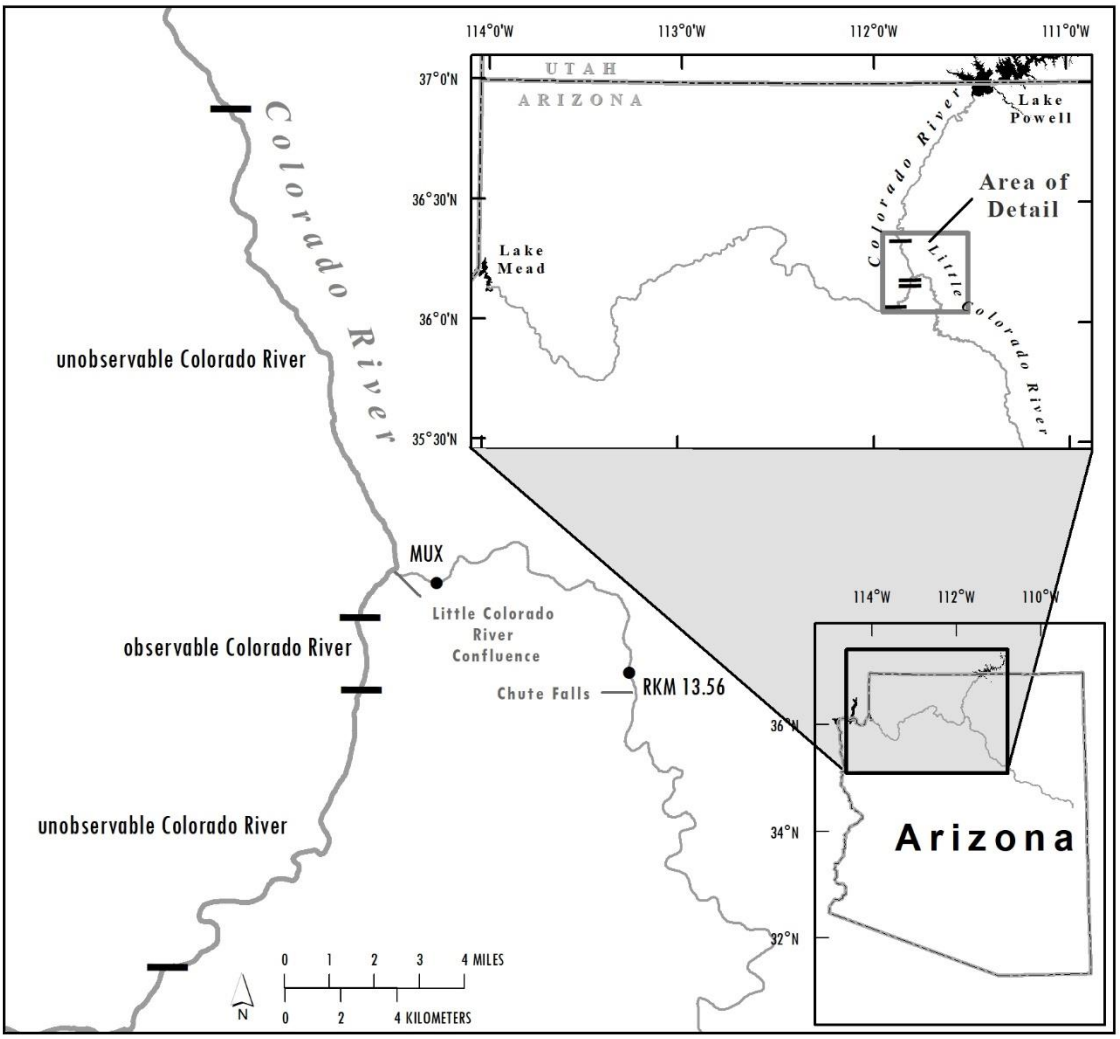

FIGURE 1.1. Map depicting the Colorado River (CR) near its confluence with the Little Colorado River (LCR) in northern Arizona. In the LCR, the multiplexer (MUX) arrays and lower Atomizer Falls (13.56 km) bound the spatial boundaries (in the LCR) for humpback chub that migrate between the LCR and CR. In the CR, bars depict the boundaries of the observable and unobservable CR reaches used in the analysis. The map was created using ESRI ArcGIS desktop software, version 10.7.1, using map features in Gushue (2019).

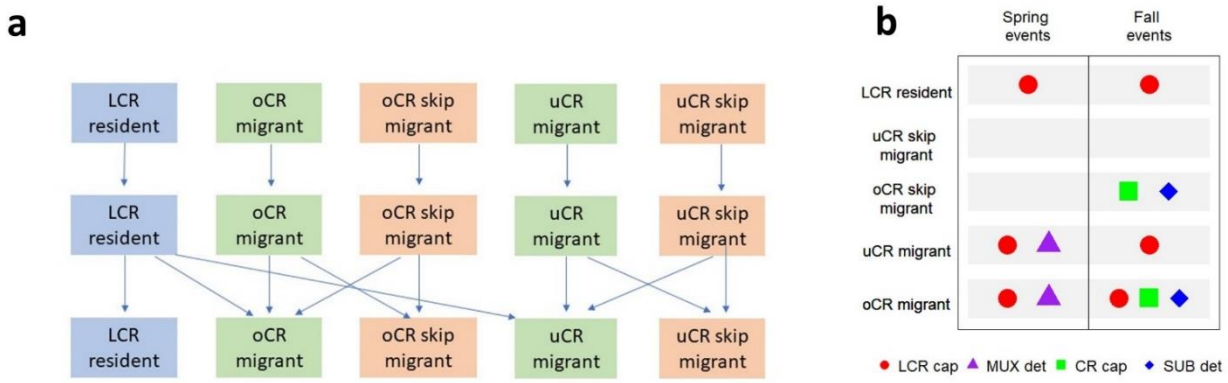

FIGURE 1.2. Schematic of model for adult humpback chub that spawn in the Little Colorado River (LCR), AZ. a) Schematic for the state transitions in the multistate mark-recapture model (ignoring demographic states for simplicity). States correspond to the location and(or) breeding status of individual fish. Fish can remain in the LCR year-round (LCR residents), can move between the Colorado River (CR) and LCR in spring to spawn (migrants), or stay in the CR year-round (skipped migrants). In the CR, fish can either be in the sampling site (observable CR or oCR) or outside the sampling site (unobservable CR or uCR). The model runs on a biannual time step, and the arrows between the boxes illustrate which transitions are allowed in the model. b) Table describing how detections inform state assignment during fall and spring events. For example, LCR residents can be captured in the LCR in spring or fall. However, because LCR residents by definition reside in the LCR year-round, either a MUX detection (indicating movement) or a CR detection (either by capture or on submersible antenna) would preclude assignment to LCR resident state.

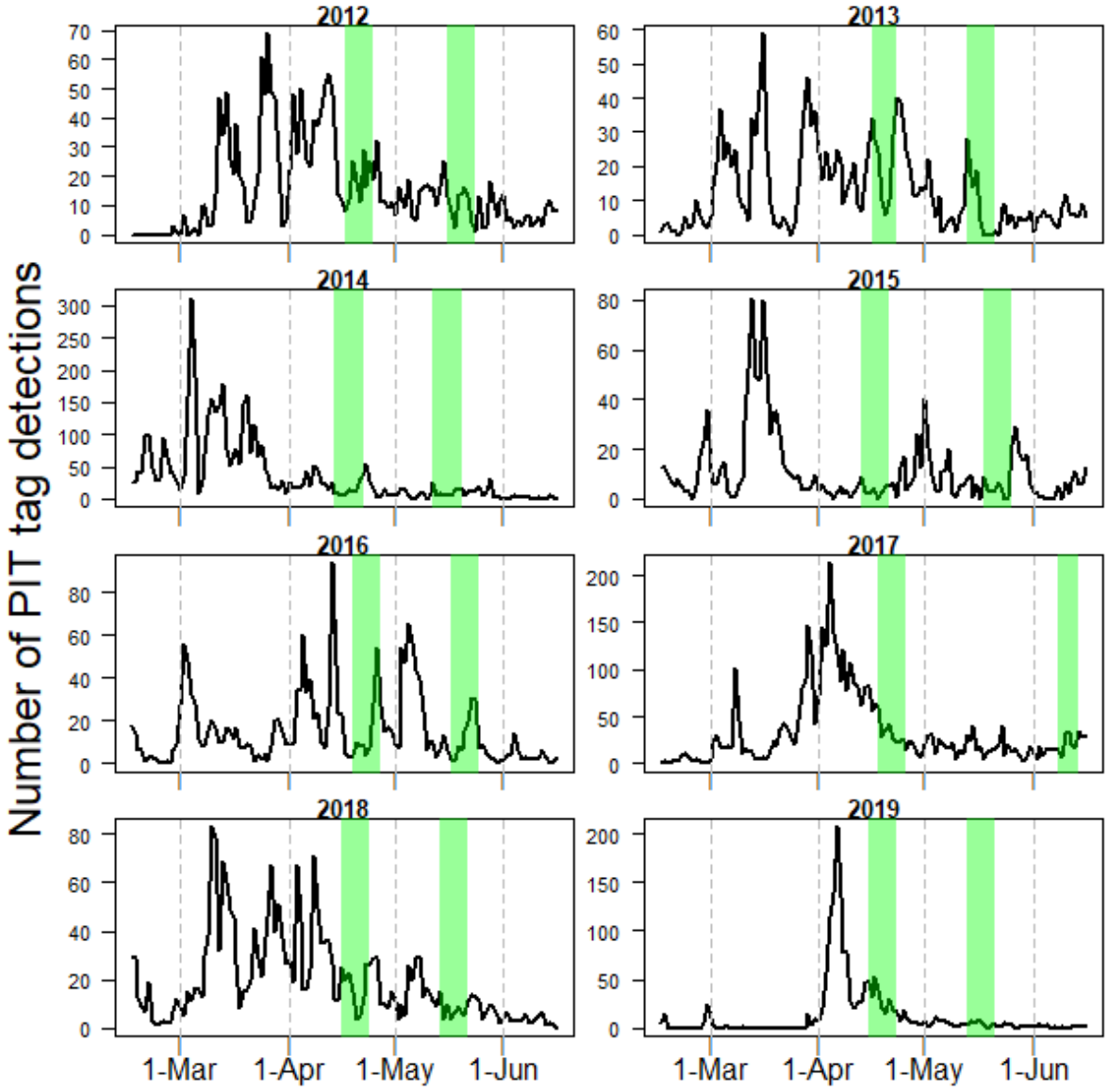

FIGURE 1.3. Graph depicting the number of adult humpback chub (captured previously >199mm TL) detections on the multiplexer (MUX) array from 15-Feb to 15-Jun in years 2012-2019. Detections were filtered to include moving fish, so that PIT tags that had multiple detections within 2-13 consecutive day periods of the same year are not included. The vertical grey rectangles depict the timing of the two USFWS spring sampling trips, which typically occur in mid-April to mid-May; however, in 2017 the second trip occurred later (early June) to issues with helicopter logistics. Note that because LCR residence time is unknown, mismatches in movement timing and LCR sampling do not indicate that migrating humpback chub are not available for LCR sampling.

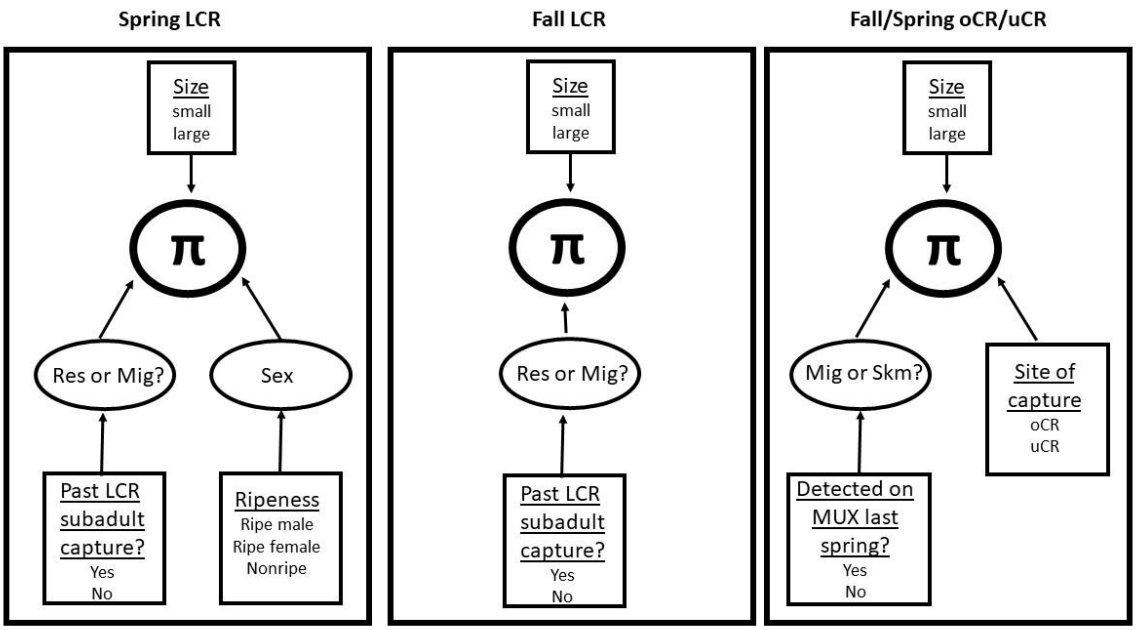

FIGURE 1.4. Illustration describing the parameterization of the initial state assignment vector (π). The three panels indicate the π parameterization for different seasons (fall or spring) and sites (Little Colorado River [LCR], observable Colorado River [oCR], or unobservable Colorado River [uCR]). Rectangles depict nodes associated with data, whereas circle or oval shapes represent unobserved (or partially observed) characteristics that were forms of state uncertainty. For fish first captured in the LCR, migrants could come from the oCR with probability τ and from the uCR with probability $1 - \tau$ (not shown for simplicity).

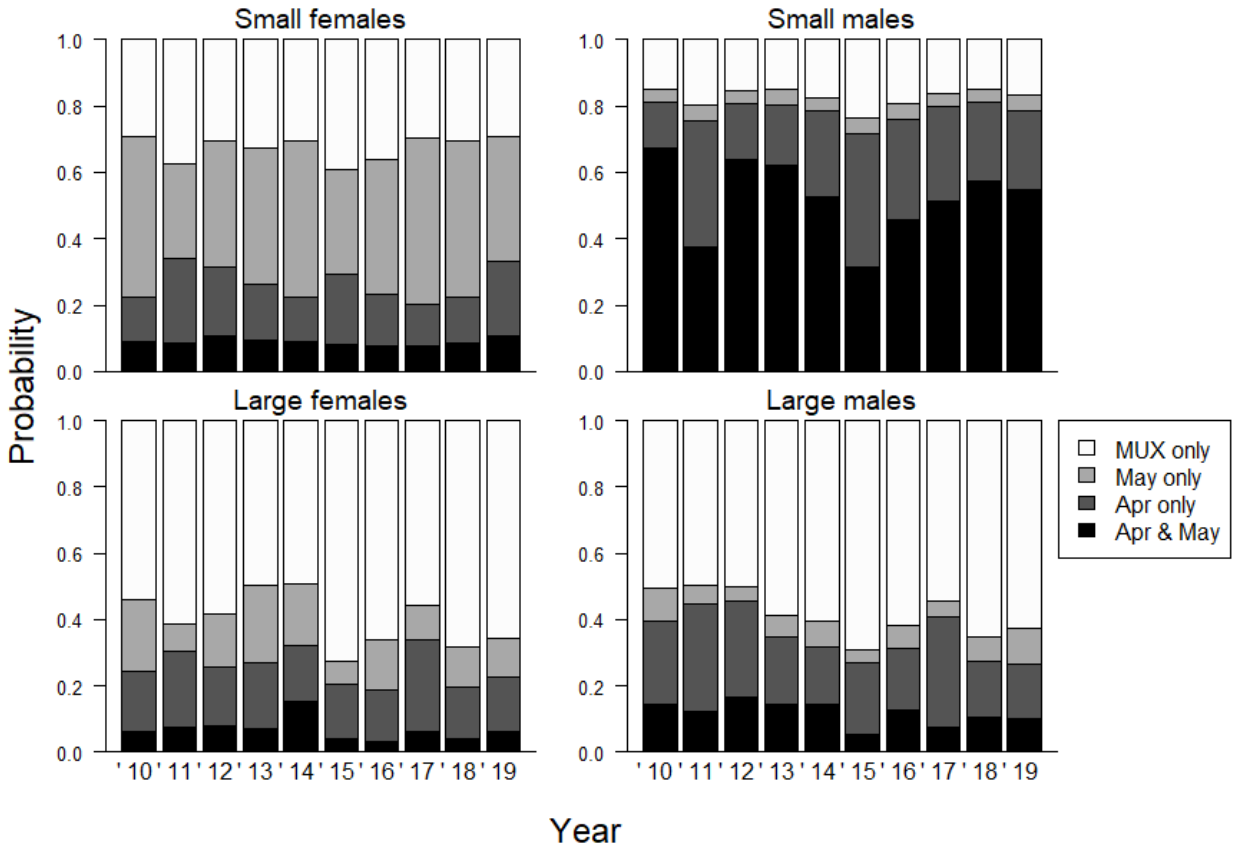

FIGURE 1.5. Availability estimates of migrating adult humpback chub migrants during spring sampling by the U.S. Fish and Wildlife Service (USFWS). All migrants were susceptible to detection on a multiplexer array (MUX) located in the LCR near the LCR-CR confluence, but some availability categories were not susceptible to physical capture by USFWS. The four availability categories were available for April and May sampling, available for April sampling only, available for May sampling only, and not available for April or May sampling (MUX only). Each panel corresponds to a different demographic group : small males (200-249mm total length), small females, large males (250+mm total length), and large females. Each bar corresponds to a specific year (2010-2019).

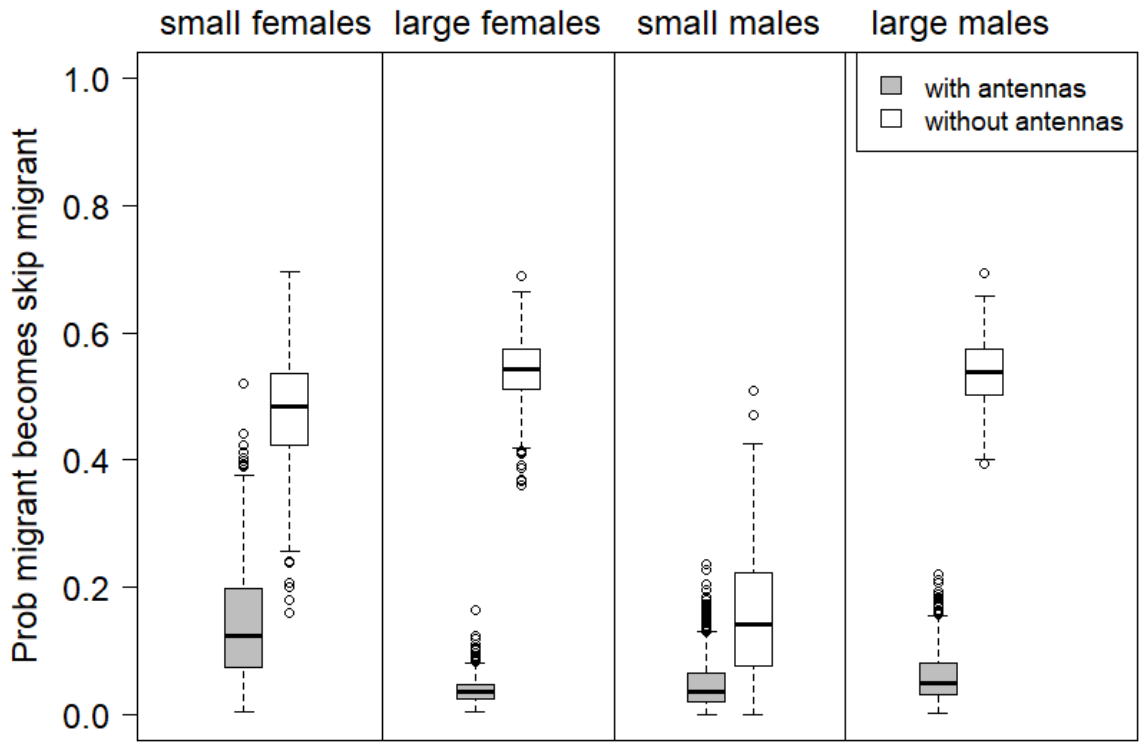

FIGURE 1.6. Mean estimates of skipped migration probabilities (or the probability a migrant does not migrate in the subsequent year) for adult humpback chub in the lower Colorado River. Estimates are shown for four different demographic groups that correspond to size (small : 200-249mm total length, large: 250+mm total length) and sex. Estimates are shown for two different models, one fit with data from autonomous passive integrated transponder (PIT) tag antennas (grey) and one fit without antenna data (white).

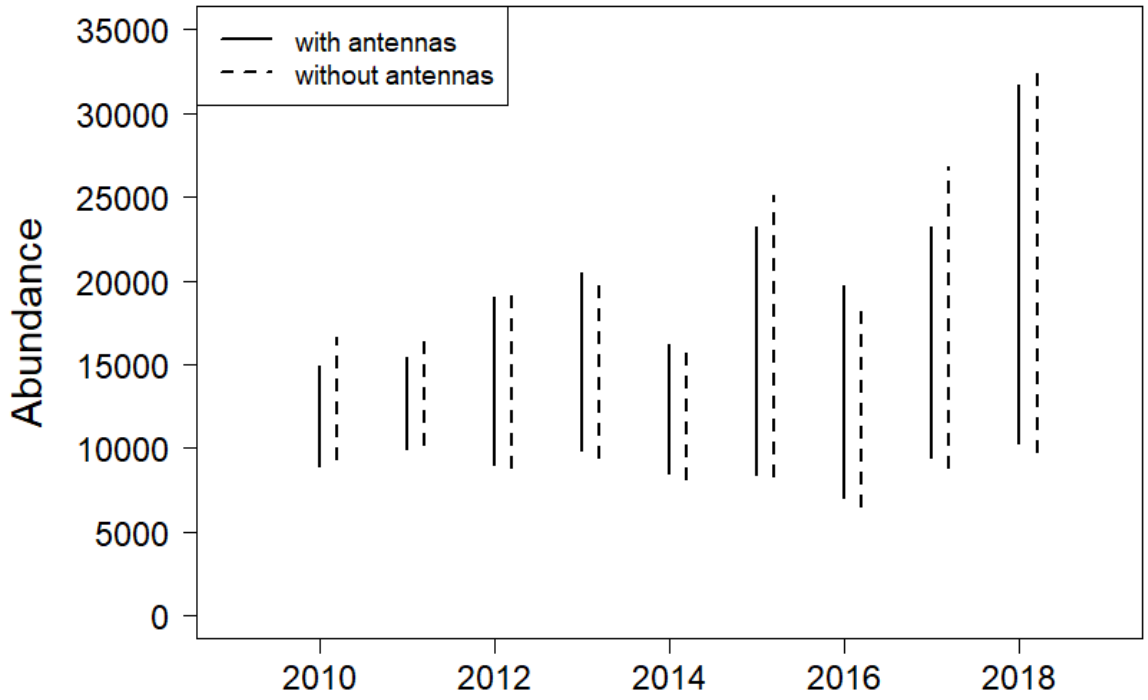

FIGURE 1.7. Comparison of fall abundance estimates of adult humpback chub (>200 mm total length) that spawn in the Little Colorado River. Abundance estimates are obtained from two different models, one fit with data from physical captures and antenna detections and one fit with only data from physical captures.

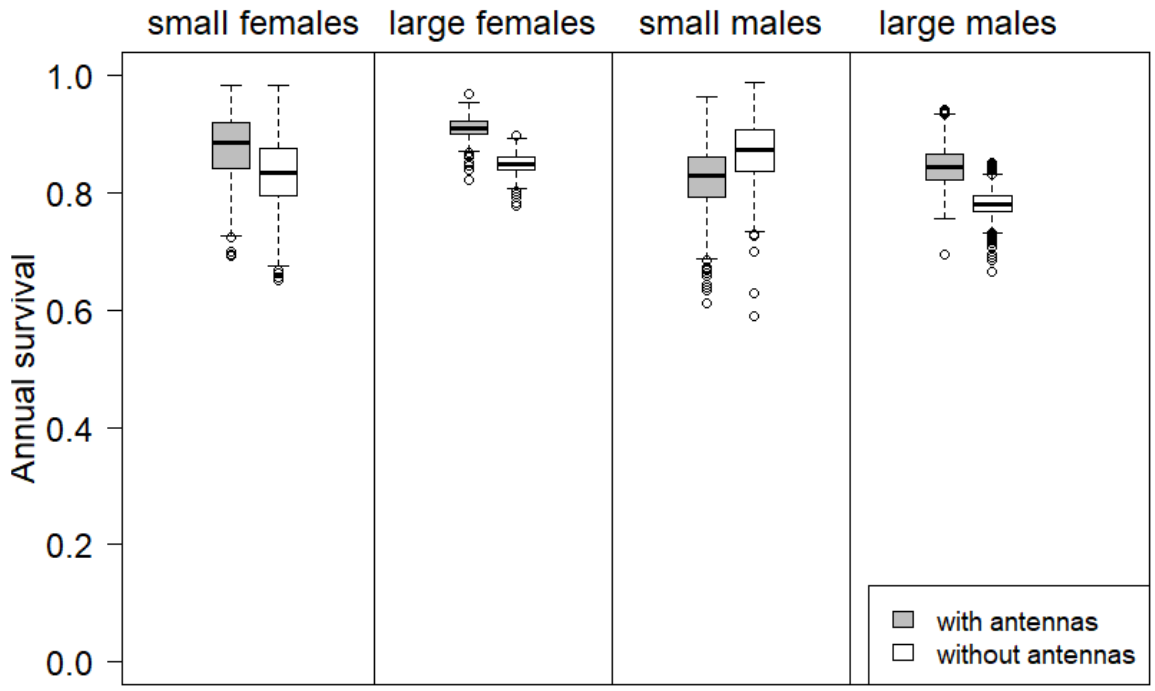

FIGURE 1.8. Mean estimates of annual survival probabilities for adult humpback chub migrants in the lower Colorado River. Estimates are shown for four different demographic groups that correspond to size (small : 200-249mm total length, large: 250+mm total length) and sex. Estimates are shown for two different models, one fit with data from autonomous passive integrated transponder (PIT) tag antennas (grey) and one fit without antenna data (white).

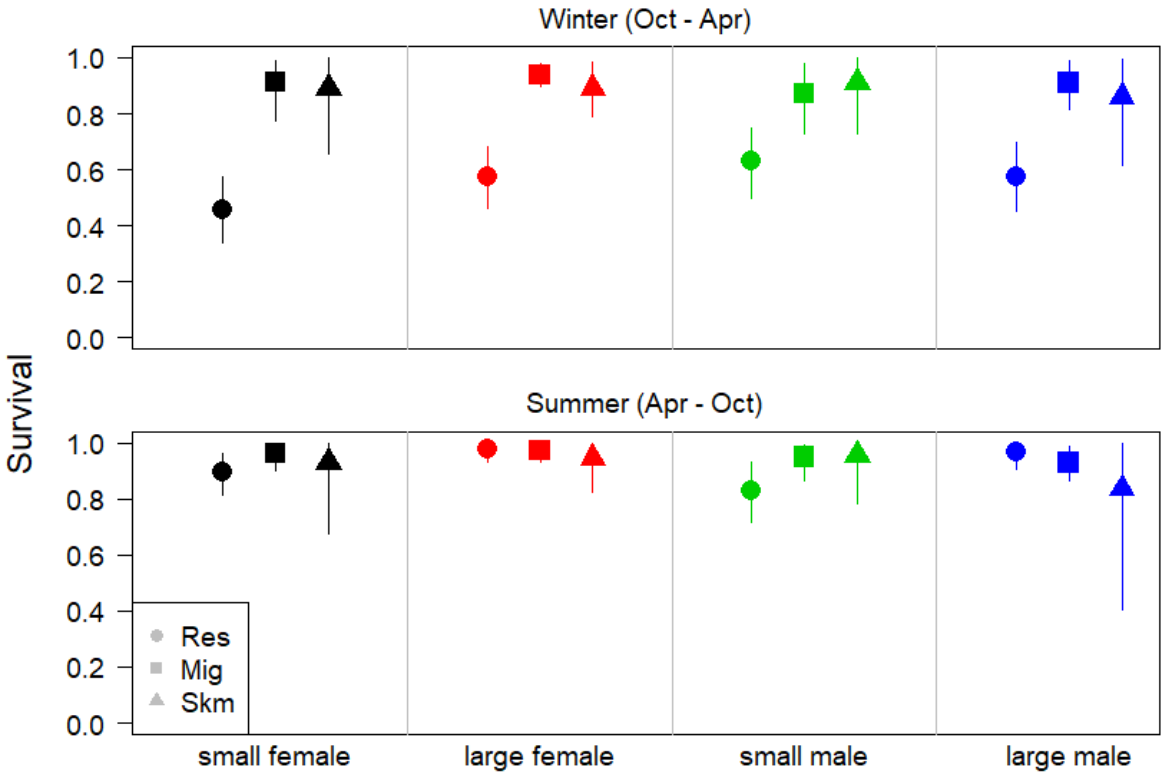

FIGURE 1.9. Comparison of across-year mean overwinter and oversummer survival probabilities for residents (Res), migrants (Mig), and skipped migrants (Skm) for four demographic groups: small females (black), large females (red), small males (green), and large males (blue). Means were estimated on the logit-scale but are presented on the real scale here for better interpretation. Bars represent 95% credible intervals. Note that season-specific estimates of migrants may be prone to slight biases (see Appendix B).

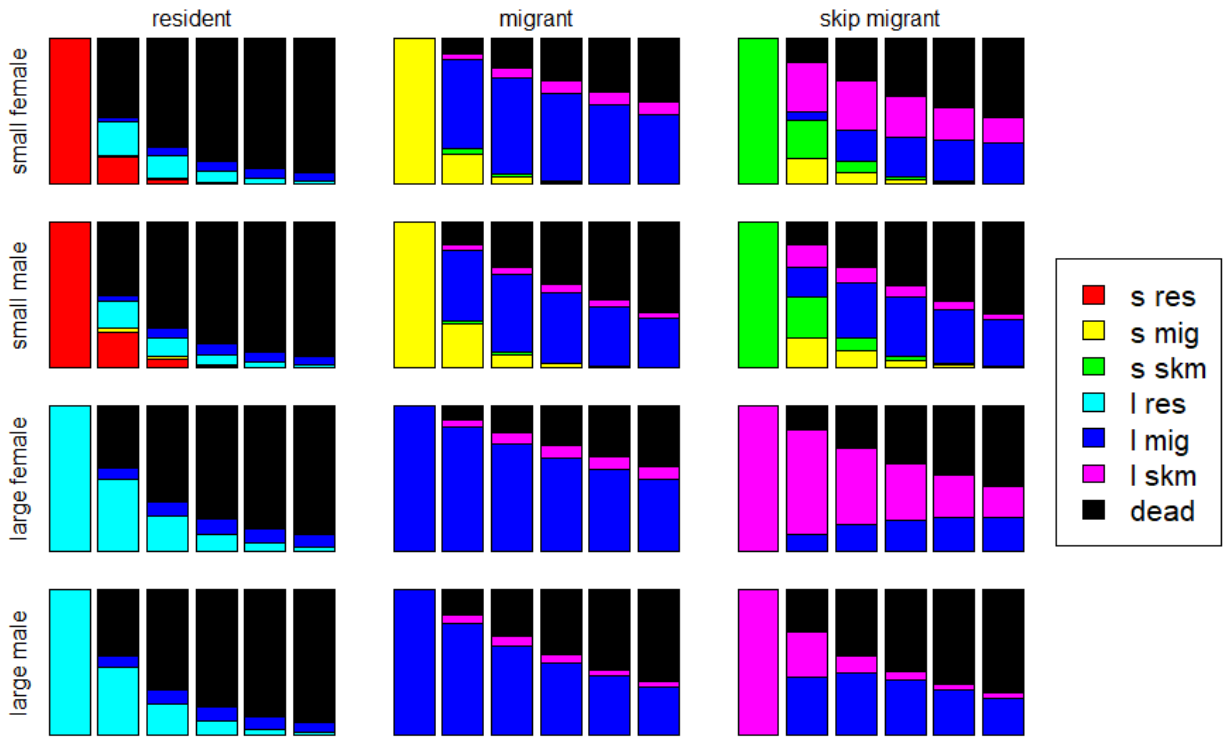

FIGURE 1.10. Graphs that probabilistically describe the fate of adult humpback chub that spawn in the Little Colorado River. Fate differs according to demographic state (rows) and biological state (columns), and the 12 subplots (which each have 6 columns) correspond to one demographic/biological state combination (i.e., group). Within the subplots, the first column shows the starting state in spring of year 1 for each group, and the colors in the 2nd column show the probability fish will be in any other state the next spring. This is continued for 5 years, so that the 6th column represents the fate of a fish in spring of year 5. States in the legend are abbreviated as s (small, 200-249mm total length), l (>250 mm total length), res (resident), mig (migrant), and skm (skipped migrant).

CHAPTER 2

INCORPORATING ANTENNA DETECTIONS INTO ABUNDANCE ESTIMATES OF FISH[2]

2.1. Summary

Autonomous passive integrated transponder (PIT) tag antennas are commonly used to detect fish marked with PIT tags but cannot detect unmarked fish and can introduce state uncertainty to mark-recapture models. Here we describe an approach to estimate abundance from paired physical capture and antenna detection data in closed, open, and robust design mark-recapture models. We illustrate a general method for obtaining state-specific abundance estimates under state uncertainty and use this approach to obtain size-class specific abundance estimates that are informed by antenna detections (where size is unobserved). Simulation studies comparing models with and without antenna detections illustrate that the benefit of our approach increases as a larger proportion of the population is marked. When applied to two field data sets, our approach to incorporating antenna detections reduced uncertainty in abundance substantially. An application to a third data set illustrated how antennas and physical captures can be combined in a robust design model to estimate temporary emigration and abundance. We conclude that PIT antennas hold great potential for improving abundance estimation, despite the challenges they present.

[2] This paper has been submitted to the *Canadian Journal of Fisheries and Aquatic Sciences* where it is currently in review (see citation below).

Dzul, M.C., Yackulic, C.B., Kendall, W.L., Winkelman, D.L., Conner, M., Yard, M. *In Review.* Incorporating antenna detections into abundance estimates of fish. *Canadian Journal of Fisheries and Aquatic Sciences*

2.2. Introduction

Managers regularly require abundance estimates to assess population status and trends (Maxwell and Jennings 2005), inform management decisions (Walters 1986; Williams et al. 2002), trigger management actions (Bair et al. 2018; Donovan et al. 2019), and inform decision to upgrade or downgrade the conservation status of taxa (Haines et al. 2013; Neel et al. 2012). When animals are rare or difficult to capture, abundance estimates can have poor precision and be prone to bias (Pine et al. 2012), which can in turn limit the ability to identify population trends and assess management actions (Maxwell and Jennings 2005; Nuno et al. 2015). New technologies, such as camera traps or genetic mark-recapture techniques, can produce novel detection types that improve detection and abundance estimates, though often these novel detection types differ from conventional detections (e.g., live captures, dead recoveries) and require special considerations for mark-recapture modeling (Augustine et al. 2018; Macbeth et al. 2011). For fishes, autonomous passive integrated transponder (PIT) tag antennas have become a popular detection method, as these antennas are typically placed in aquatic environments to detect PIT tags of fish that swim by (Cooke et al. 2013; Zydlewski et al. 2006). Despite the potential for improved detection (Barbour et al. 2012), studies typically do not utilize antenna detections in abundance estimation because the characteristics of this detection type can make abundance estimation problematic. Here we describe some of the challenges and benefits of including PIT antenna detections in abundance estimation using mark-recapture modeling.

We start by highlighting two main challenges that arise from autonomous antennas. First, antennas produce an extreme form of capture heterogeneity where only fish with PIT tags can be detected. Thus, while it is relatively straight-forward to estimate abundance of the marked population (Fetherman et al. 2014; O'Donnell et al. 2010; Sloat et al. 2011), extending

the abundance estimate to both marked and unmarked fish is more complicated. Second, antenna detections do not provide information about fish attributes commonly observed with physical capture, such as size, weight, disease status, or ripeness. Unknown size can be particularly problematic because size often substantially influences capture probabilities (Dauwalter and Fisher 2007; Hense et al. 2010; Korman et al. 2009; Millar et al. 2016) and antenna detection probabilities (O'Donnell et al. 2010). Unmodelled size effects on capture probabilities in mark-recapture models can be a source of individual heterogeneity and produce negative bias in abundance estimates (Beamesderfer and Rieman 1988; Cubaynes et al. 2010; Otis et al. 1978). These challenges have hindered use of antenna data for abundance estimation (but see Dzul et al. 2017, Conner et al. 2020 for exceptions), even though studies that use autonomous PIT antenna detections to estimate other parameters (namely survival and movement) have burgeoned (Dzul et al. In Review.; Hewitt et al. 2010; Horton et al. 2011; Rudershausen et al. 2014).

To estimate abundance, we develop and apply methods to combine antenna detections with physical captures. These two encounter types are complementary; physical captures sample both marked and unmarked fish (and thereby provide information about the proportion of fish that are marked), and antennas boost detection probabilities for marked fish. We hypothesize that adding antenna data to mark-recapture models will reduce uncertainty in N based on two properties. First, adding antenna detections should reduce uncertainty in physical capture probability estimates, as antennas provide additional information about fish that were present in the study area but not physically captured. Second, antennas can reduce uncertainty in N by increasing detection of marked individuals, since low detection probabilities inherently produce uncertainty (Dixon et al. 2005; MacKenzie et al. 2005), which can cause positive bias in N. In addition to improving detection probabilities, we illustrate that PIT antenna detections can be

used to help inform more complex models, such as models that use robust design to estimate temporary emigration from the study area.

2.3. Methods

In this study, we describe open and closed population models designed to estimate abundance from paired sampling that includes both antenna detections and physical captures. We include code for simulations and applications as part of Appendix E. We use simulation to assess how adding antenna detections impacts abundance estimates under scenarios in which capture probability, antenna detection probability, survival, and proportion of previously marked fish are varied. We then apply closed and open models to applied examples. Applied examples are of varying complexity and include an example where antenna detections are used to inform availability and temporary emigration. The assumptions of each of our approaches include: 1) all fish in the same state in the sampling area have equal physical capture probabilities, 2) all marked fish in the same state in the sampling area have equal antenna detection probabilities, 3) antenna detections occur in discrete time, 4) only live fish are detected with antennas so that ghost tags are absent (Bond et al. 2019; Stout et al. 2020), and 5) antenna detections and physical captures are independent. These approaches are therefore designed for situations where antenna detections and physical captures occur within a short period of closure and where antennas are deployed throughout the study area to ensure all fish have equal detection probability. In practice, this modeling approach would be appropriate for studies where antenna detections most likely come from submersible antennas scattered throughout the sampling area and deployed for short periods (e.g., 1-10 days) or from mobile PIT antenna surveys where biologists actively move antennas through the aquatic habitat to detect PIT tags (O'Donnell et al. 2010; Sloat et al.

2011). These approaches are not developed for situations where antenna detections come from stationary antennas that are deployed continuously, as often these data do not sample the entire study area, but rather only detect fish that move over the antennas.

We apply our modeling approach to estimate abundance of bull trout (*Salvelinus confluentus*) in the Hells Canyon, Snake River, from 2016-2018 (closed model), of humpback chub (*Gila cypha*) that spawn in the LCR (open model), and abundance of humpback chub in western Grand Canyon population (robust design model). The two humpback chub examples differ in terms of movement dynamics. Namely, the model of humpback chub that spawn in the Little Colorado River includes more complex but better understood movement dynamics, as humpback chub regularly move between the LCR and mainstem Colorado River. In this model, antennas are used solely as a supplemental gear type. In contrast, the model for humpback chub in western Grand Canyon is more simplistic in its movement dynamics but uses antenna detections to inform availability based on observations that suggest that these fish are more mobile and may not be present in the sampling reach for all sampling trips. To this end, we use antenna detections and physical captures as two passes in a robust design framework, which allows for estimation of temporary emigration out of the sampling reach.

2.3.1. Closed model simulation and modeling

Our simulated data for the closed model are based on a scenario where three days of sampling occurred. Each day, fish from a fixed population size (N) could be captured either with a physical gear type or detected on antennas. This leads to six passes for the simulated data set, with two passes - one corresponding to physical capture, the other corresponding to antenna detection - occurring each day. Fish that are marked prior to the study are detectable on antennas starting on day 1, but fish that are newly marked during the study cannot be detected on antennas

until the day after marking. For example, consider the following capture history (00 10 01), where 1 and 0 denote detection and non-detection, respectively, and where paired numbers correspond to gear type (physical capture pass first, followed by pass of antenna detection) and spaces between numbers designate days. Thus, fish with the capture history 00 10 01 were physically captured on day 2 and detected on the antenna on day 3. The likelihood of this capture history depends on whether or not the fish was marked prior to day 1 of the study. If the fish had a previous mark, it has a nonzero antenna detection probability on all three days and thus the likelihood would be:

(2.1) $$\frac{p_{cap}(1-p_{cap})^2 \times p_{ant}(1-p_{ant})^2}{p_m^*}$$

(2.2) $$p_m^* = 1 - (1 - p_{cap})^3 (1 - p_{ant})^3$$

where p_{cap} and p_{ant} represent the probability of capture and antenna detection (Table 2.1), respectively, and we assume that p_{cap} and p_{ant} are equal for all three days of sampling. Here p_m^* is the probability that a marked fish was either detected on the antenna and(or) physically captured on at least one pass of the study. If the fish was not marked prior to the sampling occasion, it is first marked on day 2 and only detectable on antennas on day 3, thus its likelihood would be:

(2.3) $$\frac{p_{cap}(1-p_{cap})^2 \times p_{ant}}{p_u^*}$$

(2.4) $$p_u^* = 1 - (1 - p_{cap})^3$$

Parameter estimates were obtained by maximizing the product of these likelihoods across observed capture histories. We fit models without antenna detections to help illustrate the (potential) benefit of antennas. Models were fit in R (R Core Development Team 2012) using

maximum likelihood via the function 'optim' with Broyden-Fletcher-Goldfarb-Shanno method "BFGS".

We calculated abundance ($\widehat{N}$) and SE($\widehat{N}$) using two different methods, hereafter the single group and the separate group approaches. For the single group approach, no antenna detection data were used so $\widehat{N} = \frac{c_{tot}}{p^*_{tot}}$ and SE($\widehat{N}$) was calculated using the Horvitz-Thompson estimator (McDonald and Amstrup 2001), which requires catch of unique individuals encountered by physical capture (here referred to as c_{tot}, which is the same as M_{t+1} in a closed model), as well as estimates of trip capture probability (note that $p^*_{tot} = p^*_u$, but we use p^*_{tot} with the single group approach to illustrate that this form of the equation applies to marked and unmarked individuals) and variance of p^*_{tot} (V) from the closed model:

(2.5) $$SE(\widehat{N}) = c_{tot}\left(\left(1 + \frac{3V}{p^{*2}_{tot}} + \frac{V^2}{p^{*4}_{tot}}\right)\frac{1-p^*_{tot}}{p^{*2}_{tot}} + \frac{c_{tot}V}{p^{*4}_{tot}}\right)$$

Where p^* was the probability a fish was captured at least once during the course of three days: ($p^* = 1-(1-p_{cap})^3$).

For the separate group approach, abundance was calculated separately for previously marked and newly marked fish and then a multivariate version of the HT estimator was used to derive $\widehat{N}$ and SE($\widehat{N}$). In the separate group method, catch and capture probabilities are calculated separately for previously marked and newly marked fish, and thus we replace scalars c_{tot} and p^* above with vectors **c** and $\boldsymbol{p^*}$ and we replace V with the 2 x 2 variance-covariance matrix $\boldsymbol{\Omega}$ which represents the variances and covariances of $\boldsymbol{p^*}$. The **c** vector includes the number of unique individuals that were previously marked and either captured or detected on antennas (c_m) and the of number of unique individuals that were captured as unmarked (c_u). The $\boldsymbol{p^*}$ vector is comprised of the p^*_m for the previously marked group, which is the probability a fish was either

detected by antennas and(or) captured at least once over three days, and the p_u^* for the newly marked group, which is the probability a fish was captured at least once during the study (ignoring antenna detections). Here $\widehat{N} = \frac{c_m}{p_m^*} + \frac{c_u}{p_u^*}$ and the multivariate HT estimator of SE($\widehat{N}$) is the summation of marked and unmarked groups ($J = 2$) accounts for covariance between p^* of marked and unmarked fish (McDonald et al. 2005).

(2.6) $$SE(\widehat{N}) = \sum_{j=1}^{J} c_j \left\{ \frac{(1-p_j^*)}{p_j^{*2}} \left(1 + \frac{3\Omega_{j,j}}{p_j^{*2}} + \frac{\Omega_{j,j}^2}{p_j^{*4}} \right) + \sum_{k=1}^{J} \frac{c_k \Omega_{j,k}}{p_j^{*2} p_k^{*2}} \right\}$$

Simulation scenarios were similar to those used by Conner et al. (2020) and differed by the proportion of marked fish at the start of the study (10%, 20%, 30%, 40%, 50%), by daily capture probabilities (p_{cap} = 10% or 20%), and by daily antenna detection probabilities (p_{det} = 20% or 60%). Results are based on 100 simulated datasets for each scenario. For each simulated data set, we calculated three estimators of ($\widehat{N}$) and SE($\widehat{N}$) and the precision of different estimators is presented using the relative standard error (RSE), here defined as $100 \times \widehat{N}/\mathrm{SE}(\widehat{N})$. We also calculated relative bias, or $100 \times (\widehat{N} - N)/N$, and coverage, or the percent of simulations where N was within the normal-based 95% CI of $\widehat{N}$, for each estimator. The first estimator (E1) uses the single group approach and the model without antennas, the second estimator (E2) uses the single group approach and the model with antennas, and the third estimator (E3) uses the separate group approach and models with antenna data. We hypothesize that, of the three estimators, E1 will have the worst precision because this model does not include antenna detections and thus will likely have the lowest precision on p_{cap} (i.e., highest V). We further hypothesize that E3 will have the best precision because E3 has higher detection probability for marked fish compared to E2. We expect that the relative benefit of E3 over E2 will increase with higher proportions of marked fish.

2.3.2. Open model simulation and modeling

The open model used in our simulation is a conditional multistate population model (Arnason 1973; Schwarz et al. 1993) that includes three size states (small, midsize, and large) in form of size bins. For each size state, there are four possible types of detection for each sampling occasion: captured only, captured and detected on antennas, only detected on antennas, or unobserved (i.e., not captured or detected on antennas). Note that there is state uncertainty for events where fish are only detected on antennas because size is unknown, and this necessitates a model structure that is similar to the multievent model described by Pradel et al. (2005). For our simulation with three size states, there are eight possible events: 1) captured in the small size state but not detected on antennas, 2) captured in the small size state and detected on antennas, 3) captured in the midsize state and not detected on antennas, 4) captured in the midsize state and detected on antennas, 5) captured in the large size state and not detected on antennas, 6) captured in the large size state and detected on antennas, 7) only detected on antennas, and 8) not captured or detected on antennas. The detection probabilities for these eight events are listed in Table 2.2. Importantly, the first capture occasion for each fish corresponds to a physical capture (not an antenna detection), and fish can only be detected on antennas following the first capture. We use a Bayesian approach where states are marginalized (Yackulic et al. 2020) and fit this model in Stan (Stan Development Team 2013).

Deriving abundance estimates from this model using the E3 approach is complicated because the size of many fish detected only on antenna is unknown and thus size-specific "catch" is uncertain. Posterior samples of abundance, $N_{i,t,s}$, are derived for each posterior sample, i, time, t, and state, s, using the steps described below and analyzed across posterior samples to derive

mean and standard error for $\widehat{N}_{t,s}$ (Table 2.1). The first step in deriving abundance for a particular posterior draw, is to derive $\zeta_{i,j,t,s}$ which represents the likelihood that individuals with capture history $Y_{j,t}$ (i.e., jth capture history at time *t*) are in state *s* (out of Z possible states) at time *t,* conditional on the posterior draw *i* of relevant parameters (i.e., survival, size transition, capture, and antenna probabilities). We estimate this likelihood using a forward conditional approach, which we briefly describe here (for a more detailed description and alternatives approaches see Yackulic et al. (2020)). During the interval when a fish is first captured and marked, the size class of a fish is known with certainty, so $\zeta_{i,j,t,s}$ is 1 for the observed size state and zero for all other size classes. So, for example, if a fish was first observed in the midsize state, the vector $\boldsymbol{\zeta}_{i,j,t,1:Z}$ would equal $[0 \quad 1 \quad 0 \quad 0]$. The likelihood values of being in state, *v,* for capture history *j* in subsequent time periods (i.e., $\zeta_{i,j,t+1,v}$) is calculated iteratively based on the vector of likelihoods in the previous time step ($\boldsymbol{\zeta}_{i,j,t,1:Z}$), as well as the array of state transition probabilities $\boldsymbol{\Psi}$ (where element $\Psi_{i,t,s,v}$ represents the probability of transitioning between states *s* and *v* between time *t* and *t* + 1 for posterior draw *i*, based on survival and growth), and the conditional detection probability $p_{i,t+1,v,Y_{j,t+1}}$ which represents the probability of observed event $Y_{j,t+1}$ given state *v*:

$$\zeta_{i,j,t+1,v} = \left(\sum_{s=1}^{Z} \zeta_{i,j,t,s} \cdot \Psi_{i,t,s,v}\right) \cdot p_{i,t+1,v,Y_{j,t+1}} \tag{2.7}$$

Having derived all values of $\zeta_{i,j,t,s}$, the second step of this approach consists of estimating the probability, $\pi_{i,j,t,s}$, of being in state, *s,* for capture history, *j,* at time, *t,* for posterior draw *i* via the following equation:

$$\pi_{i,j,t,s} = \frac{\zeta_{i,j,t,s}}{\sum_{k=1}^{Z} \zeta_{i,j,t,k}} \tag{2.8}$$

Note that whenever $Y_{j,t}$ corresponds to a physical capture, then $\pi_{i,j,t,s}$ will equal 1 for the element that corresponds to the observed size class and will equal 0 for all other elements. Thus, in practice, it is more efficient to import the physical capture data as a separate data matrix and only calculate $\pi_{i,j,t,s}$ when $Y_{j,t}$ corresponds to an antenna detection only (without physical capture). We refer to the subset of $Y_{j,t}$ that corresponds to antenna-only detections as A_t and then estimate catch that corresponds only to these capture histories for time *t*. Thus, given the frequency, f_j, of capture history *j*, we can then estimate the catch of antenna-only detections, c_a, in state, *s,* at time, *t,* for posterior draw *i* according to:

(2.9) $$c_{a,i,s,t} = \sum_{j \in A_t} f_j \, \pi_{i,j,s,t}$$

The last step requires generating random draws from a negative binomial distribution (King et al. 2016), with parameters being equal to the number of successes (i.e., catch) and the probability of success (*i.e.*, capture probability or detection probability). The random draws from the negative binomial distribution represented the expected number of failures (i.e., number of fish in each size state that were not captured), and this vector was added to catch to provide an estimate of $\widehat{N}_{i,t,s}$. Here, we partition catch of all physical captures (c_{tot}) into catch of unmarked fish (c_u) and catch of previously marked fish (c_m; i.e., catch of fish that had a PIT tag and were physically captured before time *t*). Additionally, we represent 'catch' of antenna-only detections as c_a, which is described in the previous paragraph (Figure 2.1). We also define the number of uncaptured fish for the total population (u_{tot}), the number of uncaptured fish for unmarked fish (u_u), and the number of uncaptured and undetected marked fish (u_m). For E1 and E2 the single group approach was used, and thus only estimates of c_{tot} and p_{tot} were used to generate u_{tot} using random draws from a negative binomial distribution:

(2.10) $$u_{tot,i,t,s} \sim NB\ \left(c_{tot,t,s},\ p^*_{tot,i,t,s}\right)$$

Then, the number of uncaptured and captured fish were added to get total abundance for E1 and E2. For E3, the number of uncaptured fish was estimated separately for newly marked and previously marked fish for each posterior draw, time, and state. To get u_u, catch pertained only to catch of unmarked fish (i.e., c_u) and capture probabilities referred only to physical capture (i.e., p_u). To get u_m, catch was the sum of captured fish that were previously marked and antenna-only detections, and detection probability was the probability of being detected on antennas and(or) physically captured:

$$u_{m,i,t,s} \sim NB\ \left(c_{m,t,s} + c_{a,i,t,s},\ p^*_{m,i,t,s}\right) \tag{2.11}$$

Then, for E3 uncaptured fish (from both marked and unmarked groups) was added to catch from both groups to get $\widehat{N}$:

$$\widehat{N}_{i,t,s} = u_{u,i,t,s} + u_{m,i,t,s} + c_{u,t,s} + c_{m,t,s} + c_{a,i,t,s} \tag{2.12}$$

This entire process was repeated for each posterior draw to generate a distribution of abundance estimates for that particular simulation. Then from this distribution, mean $\widehat{N}$, RSE, relative bias, and coverage were calculated and summarized across 100 simulations.

We simulated capture histories for three different size states under two different scenarios: long-lived and short-lived. Simulated data included eight years of mark-recapture data with parameters (i.e., growth, survival, capture, and antenna detection probabilities) that were temporally constant but different among size states. Parameter values differed for long-lived and short-lived scenarios and specific values are listed in Table 2.3. Capture probabilities and antenna detection probabilities in the long-lived scenario were chosen to mimic patterns observed in humpback chub, where capture probabilities decrease but antenna detection probabilities increase as fish grow larger. The short-lived scenario is supposed to represent a

salmonid population were the largest fish have both the highest capture and antenna detection probabilities and where survival is low and population turnover rates are relatively fast.

Starting population size was set to 2 000, 1 000, 2 000 for the three size states (long-lived scenario) or 5 000, 3 000, 750 (short-lived scenario). Each year, either 2 000 (long-lived scenario) or 10 000 (short-lived scenario) were recruited (or released) into the smallest size class of the population. These numbers caused a population trajectory that was more or less stable (no large change in N across years). All models were fit assuming growth and survival differed by size state but were constant across time, and that antenna detections and capture probabilities varied both by time (8 years, 7 intervals) and size state, thus resulting in a total of 47 parameters (2 growth, 3 survival, 21 capture probabilities, and 21 antenna detection probabilities).

2.3.3. Closed model – bull trout in Hells Canyon, Snake River

We estimated abundance of bull trout in a section of the Snake River, from the confluence with the Salmon River to Hells Canyon, from 2016-2018. More detailed sampling methods for this dataset can be found in the supplementary material of Conner et al. (2020). We did not use PIT antenna detections from the Imnaha River reported by Conner et al. (2020) because PIT antenna detections and physical captures did not occur sympatrically as required by our method. Thus, we expect N estimates to be lower than estimates reported in Conner et al. (2020). Briefly, bull trout were physically captured using angling from December to March in 2016-2018. During this same time, submersible antennas (Biomark, Inc., Boise, USA) were distributed throughout the reach to detect bull trout marked with PIT tags. In each year, we divide the sampling effort into four passes of angling and four passes of PIT antenna detections. We then use E1, E2, and E3 to estimate abundance in 2016-2018 using closed models.

2.3.4. Open model – humpback chub that spawn in the Little Colorado River

This model only describes humpback chub that visit the LCR to spawn, and thus it is not pertinent to humpback in western Grand Canyon, which are believed to spawn in the mainstem (Van Haverbeke et al. 2018). Similar to the open model simulations, we include size states (small subadult 100-149mm TL, large subadult 150-199mm TL, small adult 200-249mm TL, and large adult >250mm TL) to account for variability in parameters relating to size. Unlike simulations, we also include location states (LCR, observable CR, unobservable CR) to produce twelve states that correspond to combinations of size and location. Fish sampling occurs in both the observable Colorado River (in the Colorado River study site, located ~127-130 river kilometers downstream of Glen Canyon Dam) and in the LCR, and the unobservable CR (i.e., in the CR outside of the Colorado River study site) is a form of temporary emigration.

This model includes mark-recapture data from sampling trips to the lower 13.56 km of the LCR (typically conducted in April, May, July, September, and October), as well as sampling trips to CR that are roughly timed to occur either in July, August, September, and October (2009-2011) or April/May, July, and September/October (2012-2020). Fish are captured using hoop nets (LCR, CR) or electrofishing (CR only), and all humpback chub >99mm TL are implanted with a PIT tag.

This model is similar in structure to the model described in Yackulic et al. (2014) and we refer readers to this paper for more detailed methods and model description. This model differs from the model described in Yackulic et al. (2014) in the following ways: 1) includes more years of data, 2) does not include fish with visual implant elastomer marks and omits the smallest size class (<100mm TL), 3) implements a Bayesian framework with temporal random effects on

survival, movement, and growth parameters, 4) runs on different time scale with three intervals per year (Apr- Jun, Jul – Sep, and Oct-Mar), 5) includes water temperature covariates for growth transition and capture probabilities in the oCR, and 6) incorporates antenna detections from eight submersible antennas in the fall of 2016 and spring, summer, and fall of 2018-2020. Antennas were suspended in the water column by tying antennas to an anchor on one end and a floating buoy on the other end. No antennas were deployed in 2017 due to complications with the antenna batteries. Models were run for 3 chains (with 1 000 iterations each, with the first 500 discarded for burn-in) in Stan from R using the package rstan (Stan Development Team 2013). We use E1, E2, and E3 to calculate abundance in fall for all adults (small and large adults) that spawn in the LCR.

2.3.5. Robust design model -western Grand Canyon

The western Grand Canyon example illustrates how antenna detections can be used in a robust design (RD) model (Kendall et al. 1997; Pollock 1982) to help estimate temporary emigration. Thus, in this example, comparison of models with and without antennas illustrates how antennas can inform availability, which can help avoid bias and provide spatial boundaries for *N* estimation. We compare three model types: without antennas, with antennas but no temporary emigration (TE), with antennas and TE. Importantly, models without antenna detections only include one pass per trip and do not allow for RD to be used in analysis.

We begin by defining within-trip and between-trip capture probabilities. The following is summarized in Kendall et al. (1997), a study which describes how to use robust design to estimate temporary emigration. Briefly, the between-trip capture probability is the product of availability (i.e., probability the fish is in the sampling reach during the sampling occasion) and

the within-trip capture probability (i.e., probability the fish is captured given it is in the sampling reach during the sampling occasion). If TE is random, the between-trip capture probability can be used to estimate the size of the superpopulation, or the number of fish that visit the sampling reach but may or may not be in the sampling reach at any given time. Note that an understanding of movement and home range size is necessary to help interpret the superpopulation $\widehat{N}^s$. For example, $\widehat{N}^s$ = 300 fish has a different meaning according to whether it is 300 fish per 1 river kilometer or per 10 river kilometers. In contrast to the between-trip capture probability, the within-trip capture probability is used to estimate $\widehat{N}$ in the sampling reach during the sampling occasion. The spatial context for this $\widehat{N}$ is clearly defined, however, often extra information about availability is necessary to help distinguish within-trip and across-trip capture probabilities and thus differentiate $\widehat{N}^s$ from $\widehat{N}$. If no temporary emigration is occurring so that fish are always present in the sampling reach during every sampling occasion, then the between-trip and within-trip capture probabilities will be equal and the $\widehat{N}^s$ is the same as $\widehat{N}$. If fish do move in and out of the sampling reach (i.e., if temporary emigration is occurring), then models will need to include estimates of availability to help estimate *N*.

If TE is present but unmodelled, models with and without antenna data that do not account for TE may produce a temporal bias in survival if temporary emigration is Markovian (Langtimm 2009; Peñaloza et al. 2014). The model without antennas can only estimate between-trip capture probabilities and $\widehat{N}^s$, which will be biased if movement in and out of the sampling reach is Markovian but unbiased if movement is random (Kendall et al. 1997). Furthermore, the $\widehat{N}^s$ will be difficult to interpret because little is known about movement and home range size of humpback chub in western Grand Canyon. The model with antennas but without TE assumes fish never leave the sampling reach and therefore the between and within-trip capture

probabilities are equivalent. In contrast, the model with antenna detections and TE should be able to use the additional 'pass' of antennas to help distinguish between-trip and within-trip capture probabilities and enable estimation of $\widehat{N}$.

Models were fit to hoop net captures and antenna detections in the Fall Canyon reach (located ~362-368 river kilometers downstream of Glen Canyon Dam) for ten occasions from August 2017 – October 2019. All models included five size states: juveniles (80-99mm TL), small subadults (100-149mm TL), large subadults (150-199mm TL), small adults (200-249mm TL), and large adults (>250mm TL). Monthly survival, growth, and physical capture probabilities were modeled as logit-transformed random effects with size-specific means. Growth and physical capture probabilities also included size-specific fixed effects for mean temperature over the interval. The model with TE included movement probabilities (i.e., immigration/emigration), which were estimated for the three largest size classes and modeled as Markovian. Movement probabilities were modeled as logit-transformed random effects with an offset for size class so that the temporal pattern of movement was similar for large subadults and adults. Antenna detection probabilities were size- and time-dependent. Priors for logit-transformed means and coefficients were normal (mu = 0, sd = 2) and standard deviations were uniform (0-5). Priors for antenna detection probabilities were also uniform (0-1). Models were run in Stan using the package rstan in R. The model included three chains, each with 1 000 samples (the first 500 of which were excluded for burn-in) and converged ($\hat{R} < 1.1$ for all parameters). Abundances from the model were estimated using a similar approach to that described for the open model simulations.

2.4. Results

2.4.1. Simulation results

For simulations assessing the closed model, relative bias was negligible (mean ≤ 2% and median < 1%) and coverage was ≥ 95% for all estimators. Comparison of precision illustrates that E3 consistently had the lowest RSE, followed by E2, then E1 (Figure 2.2). With both E2 and E3, RSE improved with higher proportions of marked fish. Also, as the proportion of marked fish increased, the RSE of E3 and E2 diverged, illustrating that E3 is particularly beneficial when a large proportion of fish are marked before the onset of the study. Increasing daily capture probability from 10% to 20% substantially reduced RSE in all scenarios and led to a larger reduction in RSE compared to increasing daily antenna detection probability from 20% to 60%, a finding that was also observed by Conner et al. (2020).

For simulations assessing the open model, all three estimators displayed negligible bias in $\widehat{N}$ for the long-lived scenario, where mean bias was between 0% and 2% and median bias was between -2% and 0% for all three size classes. For the short-lived scenario, bias was low with mean bias between 0% and 2% and median bias between -1% and 1% for the midsize and large size classes, but there was moderate negative bias in abundances of the smallest size class and this bias was consistent across all three estimation methods. Specifically, mean bias was between -8% and -7% and median bias was between -8 and -10 %. Coverage was >95% for all estimators and scenarios. Similar to closed model simulations, comparison of RSE estimates shows that often E3 had the lowest RSE, followed by E2, and then E1. However, the relative benefit of each estimator depended on size state, year, and scenario. For the long-lived scenario, differences in RSEs from the three estimators were similar for small fish and more pronounced for midsize and large fish (Figure 2.3). Also, with midsize and large fish, the benefit of E2 and

E3 tended to increase as more years of data were accumulated (hereafter the 'year effect') so that RSE decreased gradually from year 2 to year 7. The short-lived scenario differed from the long-lived scenario in that the RSE of E1 was lower for midsize and large fish, the benefits of the E2 and E3 were apparent for small fish, and the year effect was more short-lived (Figure 2.4).

2.4.2. Closed model – bull trout in the Snake River

Abundance estimates were relatively similar across years. All three estimators produced similar $\widehat{N}$ in 2016 (367-386), whereas estimators from models with antenna data (i.e., E2 and E3) produced lower $\widehat{N}$ in 2017 and 2018 compared to the E1 estimator from the model without antennas. Specifically, in 2017 $\widehat{N}$ was 294 (E1), 242 (E2), and 237 (E3), and in 2018 $\widehat{N}$ was 388 (E1), 291 (E2), and 280 (E3). Importantly, however, 95% CIs did overlap for all estimators. Furthermore, E2 and E3 both produced more precise $\widehat{N}$ in all years compared to E1, and E3 was slightly more precise than E2 (Figure 2.5). Specifically, compared to E1, use of E2 for $\widehat{N}$ reduced the width of the 95% CI by 37-50% and use of E3 reduced the width by 44-57% depending on the year. The model estimates that the proportion of bull trout marked before the start of the study was 19%, 14%, and 23% in 2016-2018, respectively.

2.4.3. Open model – Humpback chub that spawn in the Little Colorado River

General trends for all three estimators are similar over the 2009-2020 period (Figure 2.6). Abundance estimates were similar across all three estimators prior to 2016, as antennas were not implemented in the sampling design until 2016. We therefore focus on differences between estimators observed in 2016- 2020, after antennas were deployed as an additional gear type. Generally, there was little difference among mean abundance estimates across methods.

Notably, there were differences in the precision of E3 compared to E1 and E2 in 2016, 2018, 2019, and 2020 – the four years antennas were deployed. In these years, $\widehat{N}$ from E3 had much better precision compared to E1 and E2 and displayed a 32-48% reduction in the width of the 95% CI compared to E1 and a 32-44% reduction compared to E2. During the fall sampling trips where antennas were deployed, capture probabilities ranged between 2-5% (small adults) and 1-3% (large adults) and antenna detection probabilities were 9-24% (small) or 19-53% (large). The model estimates that approximately 31-55% of small adults and 56-77% of large adults were marked from 2016-2020, suggesting that a high proportion of individuals are marked. Additionally, models with antenna detections produced higher and more precise annual survival estimates for large adults in the CR compared to models without antenna detections (Figure 2.7).

2.4.4. Robust design model -humpback chub in western Grand Canyon

As expected, for the largest three size classes, $\widehat{N}$ tended to be highest for models fit without antennas (where $\widehat{N}$ estimating the size of the superpopulation N^s), intermediate for models with antennas and no TE, and lowest for models with antennas and TE (where $\widehat{N}$ is abundance in the sampling reach; Figure 2.8). Differences in abundances among models were most pronounced for small and large adults compared to subadults and juveniles. For small adults, $\widehat{N}$ was similar for both antenna models and much higher for models without antennas. Also, small adult p_{cap} was lowest for the no antenna model and higher with wider 95% CIs for models with antenna detections. For large adults, there were large differences in $\widehat{N}$ between methods, where the no antenna method tended to have much wider 95% credible intervals as well as produce higher $\widehat{N}$. Compared to small adults, there were more substantial differences in

the antenna models fit with and without TE, where the model with TE had lower and more precise $\widehat{N}$ estimates compared to the model without TE.

The model with antennas and TE estimated that monthly emigration out of the sampling reach was 26% for large subadults, 19% for small adults, and 35% for large adults. Movement estimates were Markovian and fish always had a higher probability of remaining either inside or outside the sampling reach than of moving. Mean physical capture probabilities were 3% (juveniles), 11% (small subadults), 14% (large subadults), 7% (small adults), and 8% (large adults). Antenna detection estimates were higher for all groups and ranged from 21-43% (juveniles), 10-53% (small subadults), 30-85% (large subadults), 26-66% (small adults), and 31-72% (large adults) between sampling occasions. Detection probabilities were not identifiable for the last sampling occasion. This model estimates that the proportion of marked fish fluctuated during the study. Specifically, the proportions marked for small and large adults were 11% and 8%, resp., during the beginning of the study (September 2017), then grew to 34% and 44% by October 2018. This proportion dropped to 13% and 11% in May 2019 and then grew to 44% and 37% by October 2019. This finding suggests that many unmarked adults immigrated into the sampling reach between October 2018 and May 2019.

2.5. Discussion

Results from closed and open simulations illustrate how including PIT antenna detections in abundance estimation can be advantageous if a substantial proportion of the population is marked. If only a small proportion (e.g., <10%) of fish are marked however, PIT antennas will have little influence on $\widehat{N}$ regardless of whether or not PIT antenna detection probabilities are high. The proportion of marked fish is influenced by p_{cap}, because fish must be first physically

captured to receive a mark, the exception being stocked fish that are released with marks. Accordingly, improving physical capture probabilities will always benefit estimation of *N*, but antennas can still improve precision in $\widehat{N}$ under some circumstances.

For open model simulations, we divided results into three different outcome categories, the best-case, mid-case, and worst-case outcomes, which described the benefit of using PIT antenna detections for *N* estimation. The best-case outcome pertained to large fish in the long-lived scenario. The best-case outcome arises because a large proportion of these fish are already marked and because this group exhibits low capture probability and high antenna detection probability. The high proportion of marks in large fish is due to their relatively high survival rates. Additionally, high capture probabilities for small and mid-size fish allow for marks to accumulate in the population as these fish grow and the proportion marked for large fish increases from 11% (year 2) to 55% (year 7). Under this best case outcome, in year 7 simulations showed a 51% reduction in RSE for E3 compared to E1 (i.e., RSEs for E1 and E3 were 6.7% and 13.6%, respectively). Large fish from the short-lived scenario represent the mid-case outcome. Fish in the mid-case outcome had relatively high capture probabilities and thus better RSE without antennas (E1) so that the room for improvement was narrower for E2 and E3. Nonetheless, large fish under the short-lived scenario saw a 38% reduction in RSE in year 7 for E3 compared to E1 (i.e., RSEs for E1 and E3 were 5.8% and 9.4%, respectively). The proportion marked for this group started at 34% (year 2), grew quickly to 65% (year 4), then grew gradually to 77% (year 7). Small fish in the long-lived and short-lived scenarios represent worst-case outcomes where the benefit of antenna detection was negligible. For this group, the benefit of antennas was low due to the low proportion of marked fish (~10%). Importantly, small fish in the short-lived scenario were problematic as bias was more substantial compared to

other groups. This bias was relatively consistent across E1, E2, and E3 and likely due to small sample sizes (i.e., low numbers of recaptures for fish in the smallest size class), which in turn was likely the result of low survival, high growth, and low capture probabilities for this size class.

Similar to our simulations, all three applied examples illustrated that incorporation of antenna detections into mark-recapture models improved the precision of abundance estimates so that E2 and(or) E3 had higher precision compared to E1. The three examples differed in the proportion of marked fish in the study area and also how antennas were used. In both the bull trout example and the LCR-spawning humpback chub example, antennas were used primarily to boost capture probabilities of marked individuals. In the bull trout example, the proportion of marked individuals was relatively low (14-23%), and there was little difference in the benefit of E2 versus E3. Incorporation of antennas reduced uncertainty in $\widehat{N}$ by improving precision on $\hat{p}_{cap}$(2016, 2017, 2018) and also producing higher values of $\hat{p}_{cap}$ (2017, 2018). In contrast, the benefit of E3 over E2 and E1 was clear in the example of humpback chub that spawn in the LCR, likely because a larger proportion of fish were marked (31-71%). This applied example is similar to the best-case simulation scenario in that adult humpback chub tended to have low capture probabilities and high antenna detection probabilities. Furthermore, antennas improved precision in survival estimates and illustrated that survival was likely higher than estimated in models without antennas.

In the western Grand Canyon example, the main purpose of PIT antennas was not to boost detection probabilities for marked fish, but rather to provide an extra pass of detections for each trip and enable estimation of TE. Antenna detections and TE estimates led to some interesting differences in abundance estimates of small adults and large adults. Namely, for

small adults the two models with antenna data both showed higher $\hat{p}_{cap}$ (and lower $\widehat{N}$) compared to the model without antennas, regardless of whether or not TE was included. For large adults, on the other hand, there was substantial difference in antenna models with and without TE, where generally models with TE tended to have lower $\widehat{N}$ compared to models without TE. It is difficult to understand and assess these observed differences between small and large adults, and we hope additional years of mark-recapture data will clarify these observations. Importantly, the number of small adults and large adults that were physically recaptured was very low, particularly prior to July 2019. Specifically, the number of small adults that were physically captured before July 2019 ranged between 1-9 individuals, though the number of recaptured small adults increased during and after July 2019 and ranged between 20-44 individuals. Similarly, the number of physically recaptured large adults ranged between 3-11 except for August 2019 sampling which had 17 recaptures. Given the low numbers of physical recaptures, it is likely that models without antenna data are too sparse to produce accurate abundance estimates, as abundance estimates are prone to bias when the number of recaptures is low (Chao 1989). Notably, there was a drop in the proportion marked of large adults from October 2018 to May 2019 and initial Jolly-Seber models with immigration suggest that many large adults moved into the sampling reach during this time. One possible reason for the increase in unmarked individuals is that late spring is typically the time when adult humpback chub spawn. Additionally, there is some initial evidence that some adults in this group may be transient, or just moving through the sampling reach on route to a different location. Accordingly, we admit that a better ecological understanding is needed to construct more informed models of humpback chub in western Grand Canyon, and that the results presented here are preliminary but illustrate the potential strength of using antenna detections in estimation of abundance.

While the above-described method improved estimation of *N*, we stress that the independence of PIT antenna detections and physical capture probabilities are necessary for these approaches and achieving this independence must be addressed at the design stage of a study. For instance, minimizing dependence of antennas and other gear types can be achieved by moving submersible antennas frequently so that all fish within the sampling area have equal antenna detection probabilities. In addition, fish captured in hoop nets or trammel nets that are set overnight may have a much lower probability of having an antenna detection because once captured these fish cannot swim freely and encounter antennas. Accordingly, using these gear types in conjunction with antenna detections may be problematic, particularly for closed models. For open models, passive gears, such as hoop nets or trammel nets, could be permittable with certain caveats. In our humpback chub examples, physical capture data and antenna detections were pooled across within-trip passes and days so that for each sampling occasion there was one pass of antennas and one pass of physical capture. For these examples, the main consideration is that the probability of being captured at least once by the physical gear type is independent from the probability of being detected at least once by the autonomous antennas. Accordingly, if physical capture probabilities are generally low and the sampling design includes multiple passes, the bias induced by dependence of sampling gears may be negligible. Another limitation of this method is that it does not address the problem of ghost tags (i.e., tags of dead fish), and further modifications may be necessary to help with this issue.

PIT tags are commonly used to mark fish because they are small in size, provide a unique identifier for each individual tag and are relatively inexpensive (Cooke et al. 2013). Consequently, millions of PIT tags have been implanted in fish in watersheds in the Pacific Northwest (primarily salmonids) and in the Colorado River Basin (Conner et al. 2020). In these

systems, antennas are increasingly being used to monitor fish movement and survival (Cathcart et al. 2018a; Pennock et al. 2018; Sloat et al. 2011). Pairing antenna detections with physical capture methods has the potential to improve monitoring, particularly in situations where marked fish have low probabilities of physical capture but high probabilities of antenna detection. Including PIT antennas in sampling can help managers and biologists develop more efficient sampling designs. For example, in cases where the proportion of marked fish is high, it may make sense to allocate more effort towards deploying antennas in lieu of additional days/nights fishing with the same gear types.

Other studies have used antenna detections to fit spatial mark-recapture models and assess environmental effects on movement (Raabe et al. 2013), to assess movement patterns on multiple spatial scales (Kanno et al. 2020), and to separate permanent emigration from survival (Horton et al. 2011). Importantly, there are numerous mark-recapture applications where antenna detections may be useful, though much of the statistical groundwork for model development in these areas remains unexplored. Specifically, antennas can act as a supplemental gear type that can be used to assess individual heterogeneity in capture probabilities, evaluate potential for trap-happy or trap-shy behaviors (Bunch and Stewart 2020), or inform availability (Dzul et al. In Review). We hope future studies will leverage the potential for antennas to act as a supplemental source of detections to help learn more about fish life history and inform management decisions.

Data availability: Data for both humpback chub applications will be made publicly available as part of the USGS data repository (TBA)

TABLE 2.1. Description of model parameters for closed and open models that include antenna detection and physical capture data. Parameters could be used in abundance estimation for estimators E1 (no antenna model), E2 (model fit with antennas but abundance estimated from physical captures only), and E3 (model fit with antennas and abundance estimated from physical captures and antenna detections).

Closed model

Parameter	*Estimator*	*Description*
p_{cap}	E1,E2,E3	Pass-specific capture probability
p_{ant}	E2,E3	Pass-specific antenna detection probability
c_{tot}	E1,E2	Catch - or total number of unique individuals that were physically captured
V	E1,E2	Variance of capture probability estimate
p_{tot}*	E1,E2	Trip capture probability (equal to p_u*; only includes probability of being captured)
p_m*	E3	Trip capture probability for marked fish (includes probability of being captured and(or) detected on antennas)
p_u*	E3	Trip capture probability for unmarked fish (only includes probability of being captured)
c_m	E3	Number of unique previously marked fish that were captured and(or) detected on antennas
c_u	E3	Number of unique unmarked fish that were captured
C	E3	Vector (c_u and c_m)
p*	E3	Vector (p_u and p_m)
Ω	E3	Variance-covariance matrix for **p***
N	E1,E2,E3	Total abundance

Open model

Parameter	*Estimator*	*Description*
I	-	Subscript indicating posterior draw
T	-	Subscript indicating sampling occasion or interval
S	-	Subscript indicating size state at time *t*
V	-	Subscript indicating size state at time *t*+1
J	-	Subscript indicating row of capture history matrix
Y	E3	Capture history matrix
Z	E3	4-d array of likelihoods for each posterior draw, unique row of **Y**, time, size state
Ψ	E3	3-d array describing the state transition matrix for each posterior draw

$\mathbf{\Pi}$	E3	4-d array of rescaled likelihoods (ζ) or state probability vector for antenna-only detections
A	E3	Vector of indices describing which rows of **Y** are antenna-only detections
F	E3	Vector of frequencies that correspond to the number of individuals observed with particular capture history
$\mathbf{c}_a$	E3	3-d array of 'catch' for antenna-only detections for each posterior draw, time, and size state
$\mathbf{c}_u$	E3	2-d array of physical catch of unmarked fish for each size state and time
$\mathbf{c}_m$	E3	2-d array of physical catch of previously marked fish for each size state and time
$\mathbf{c}_{tot}$	E1,E2	2-d array of the total number of unique individuals that were physically captured
$\mathbf{u}_u$	E3	3-d array of the number of uncaptured fish that are unmarked
$\mathbf{u}_m$	E3	3-d array of the number of uncaptured and undetected fish that are previously marked
$\mathbf{u}_{tot}$	E1,E2	3-d array of the number of uncaptured fish
$\mathbf{p}_{tot}$*	E1, E2	3-d array of capture probability for all fish for each posterior draw, size state, and time (equal to $\mathbf{p}_u$*) Detection probability physical capture probability only
$\mathbf{p}_m$*	E3	3-d array of trip detection probability for previously marked fish for each posterior draw, size state, and time Detection probability includes antenna detection and physical capture probability
$\mathbf{p}_u$*	E3	3-d array of trip detection probability for unmarked fish for each posterior draw, size state, and time Detection probability includes physical capture probability only
N	E1,E2,E3	3-day array describing total abundance for each posterior draw, size state, and time

TABLE 2.2. Probabilities of events for three different size classes in simulations. Events are determined by whether or not a fish was captured and detected on antennas (Y= yes, N = no), as well as the size bin of the fish if the fish was captured. Capture probabilities (p_{cap}) and antenna detection probabilities (p_{ant}) are indexed by subscripts referring to the size state : 1 (small), 2 (midsize), and 3 (large).

Event number	***Size***	***Captured?***	***Detected on antennas?***	***Probability***
1	small	Y	N	$p_{cap,1}\ (1-p_{ant,1})$
2	small	Y	Y	$p_{cap,1}\ p_{ant,1}$
7	small	N	Y	$(1-p_{cap,1})\ p_{ant,1}$
8	small	N	N	$(1-p_{cap,1})\ (1-p_{ant,1})$
3	midsize	Y	N	$p_{cap,2}\ (1-p_{ant,2})$
4	midsize	Y	Y	$p_{cap,2}\ p_{ant,2}$
7	midsize	N	Y	$(1-p_{cap,2})\ p_{ant,2}$
8	midsize	N	N	$(1-p_{cap,2})\ (1-p_{ant,2})$
5	large	Y	N	$p_{cap,3}\ (1-p_{ant,3})$
6	large	Y	Y	$p_{cap,3}\ p_{ant,3}$
7	large	N	Y	$(1-p_{cap,3})\ p_{ant,3}$
8	large	N	N	$(1-p_{cap,3})\ (1-p_{ant,3})$

TABLE 2.3. Parameter values used in simulations of a multi-state model with antenna detections. Parameters were temporally constant but varied by size state (S = small, M = medium, L = large). Parameters for detection probability include p_{cap} – or the probability of physical capture, and p_{ant} - the probability of an antenna detection.

Parameter	***Size state***	***Long-lived***	***Short-lived***
Growth	S to M	50%	70%
Growth	M to L	20%	30%
Survival	S	60%	30%
Survival	M	80%	40%
Survival	L	90%	50%
p_{cap}	S	30%	25%
p_{cap}	M	20%	25%
p_{cap}	L	10%	40%
p_{ant}	S	30%	30%
p_{ant}	M	40%	40%
p_{ant}	L	50%	50%

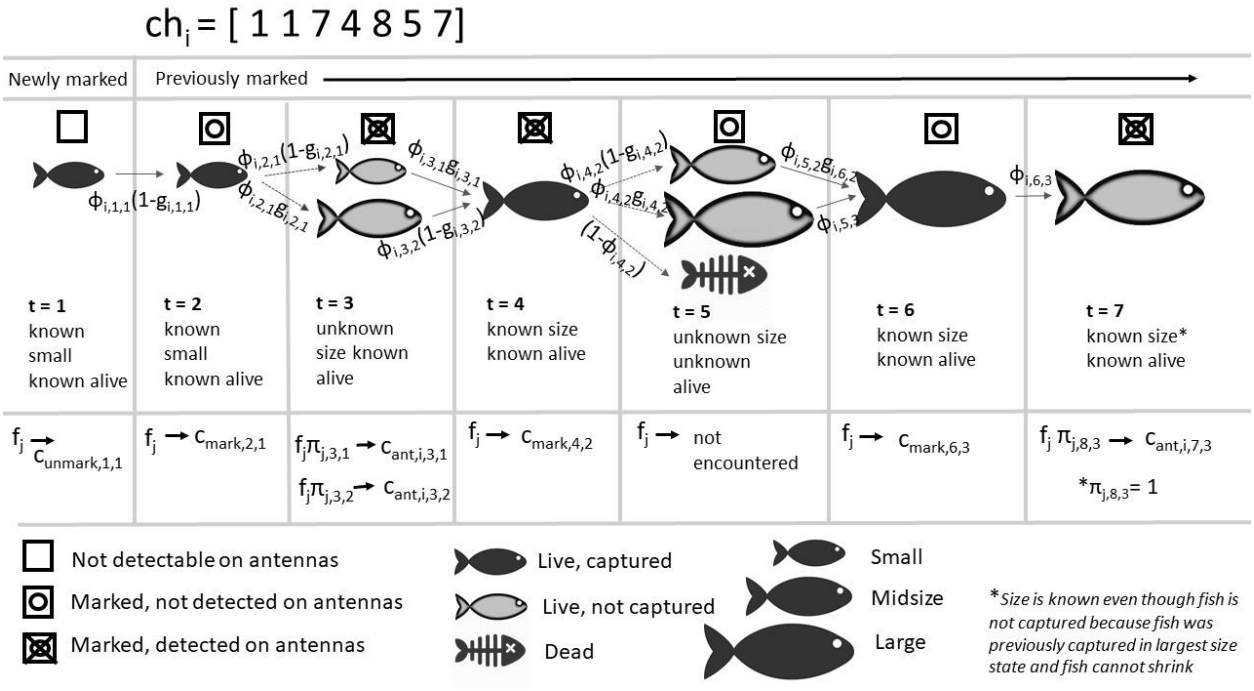

FIGURE 2.1. Conceptual diagram that describes calculation of catch for posterior draw *i*, capture history *j* [1 1 7 5 8 3 7] that was observed with frequency f_j, where 1 = captured as small fish and not detected on antennas, 2 = captured as small fish and detected on antennas, 3 = captured as midsize fish and not detected on antennas, 4 = captured as midsize fish and detected on antennas, 5 = captured as large fish and not detected on antennas, 6 = captured as large fish and detected on antennas, 7 = only detected on antennas (size unknown), and 8 = not captured and not detected on antennas. The probabilities fish transition between states are a function of apparent survival (φ) and growth (g) probabilities. For each sampling occasion (t), illustrations depict whether or not the fish was detected on antennas, whether or not the fish was captured (and at what size), and whether this observation would be included in catch of unmarked fish (c_u), catch of marked fish (c_m), or catch of antenna-only detections (c_a). Here, numeric subscripts refer to time (first index) and state (second index). Note that, for antenna-only detection at t=3, size is unknown and thus c_a must include the probability (π) capture history *j* is in states 1 and 2 at this t = 3, but for the antenna-only detection at t = 7 the fish is known to be large based on previous captures.

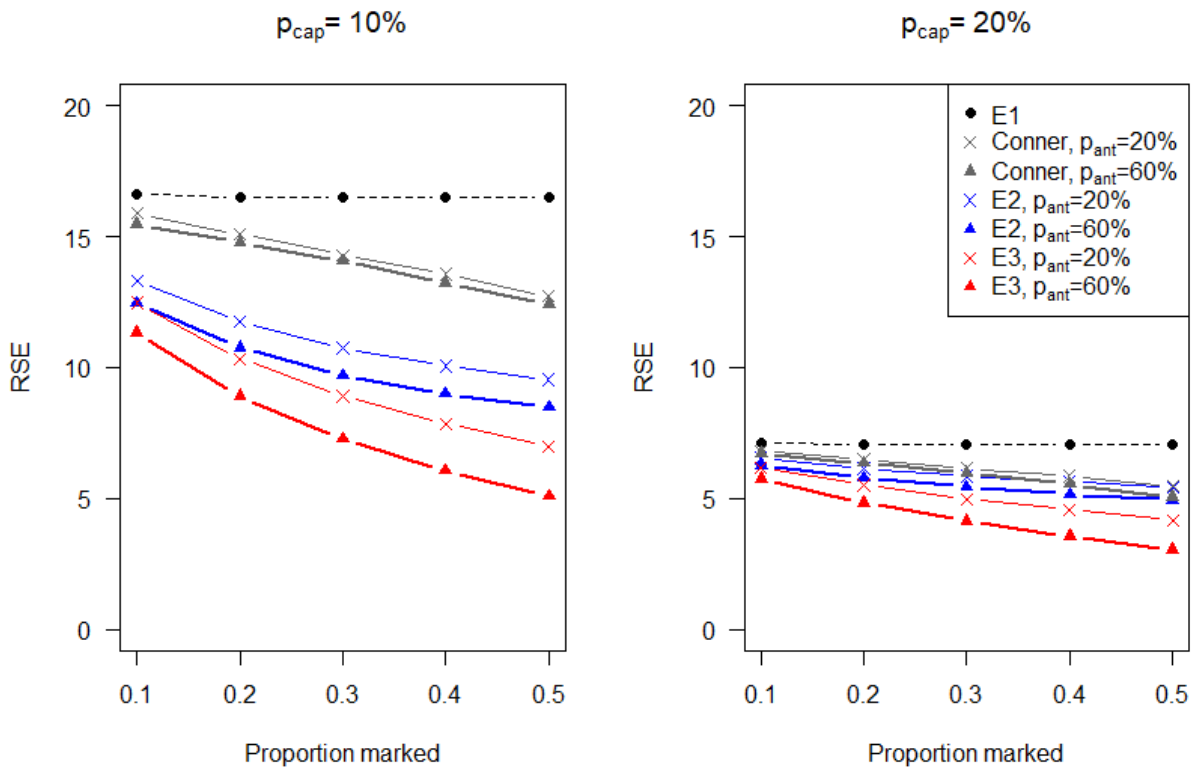

FIGURE 2.2. Comparison of the relative standard error (RSE) for different abundance estimation methods. Estimates of RSE depend on the proportion of fish that are marked with PIT tags (x-axis), as well as the pass-specific probability of physical capture (p_{cap}) and pass-specific antenna detection probability (p_{det}). Results are based on 100 simulations from models with three passes of antenna detections and three passes of physical capture. Abundance estimation methods include the E1 (no antennas), E2 (antennas used in model fitting but not in abundance calculation), E3 (antennas used in both model fitting and abundance calculation), and the RSE from a method described by Conner et al. (2020).

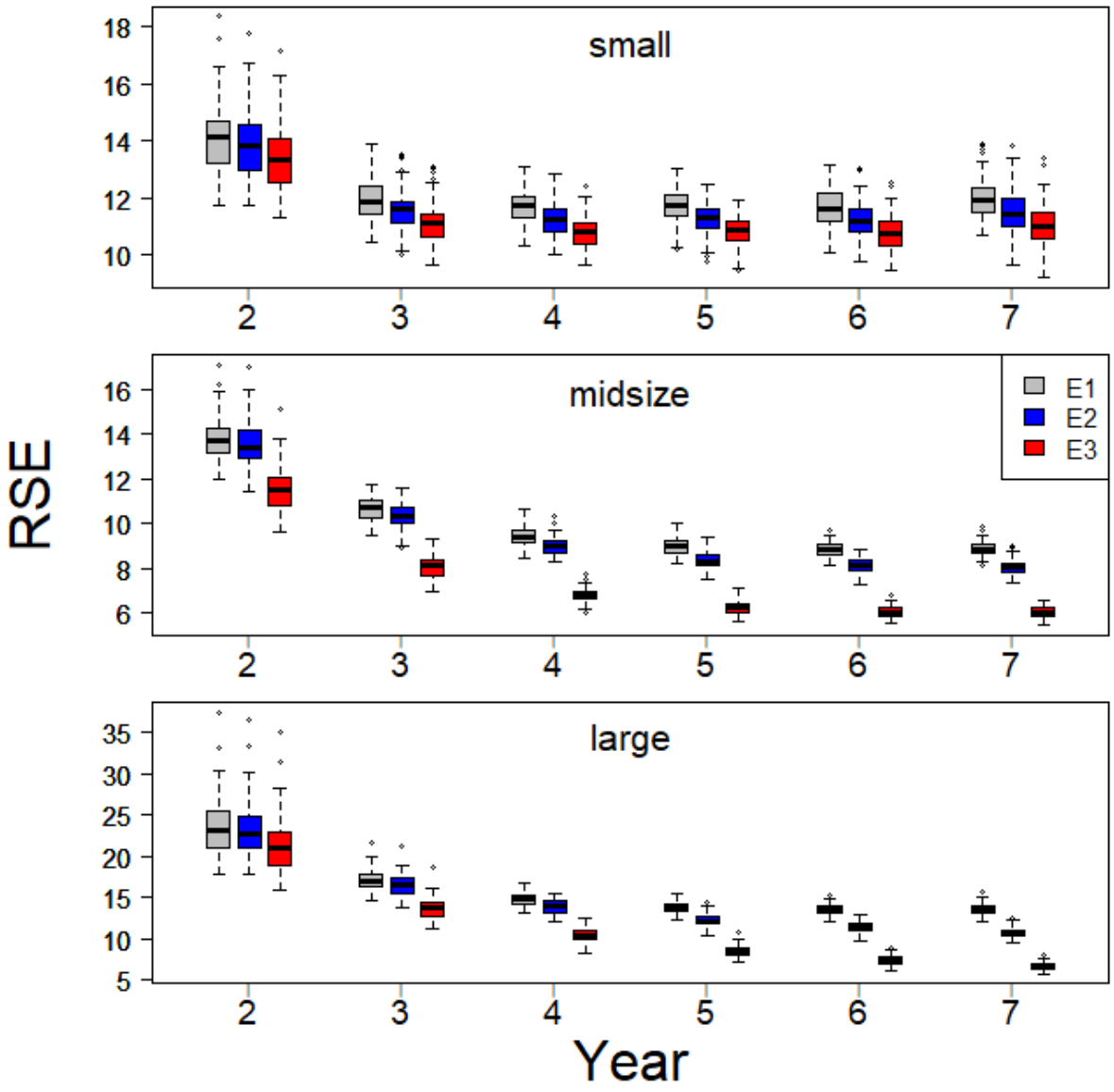

FIGURE 2.3. Relative standard error (RSE) for abundance estimates from the long-lived scenario for three different size classes (small, midsize, and large) by year. Abundance was estimated using three different estimators: E1 (no antennas), E2 (antennas in model but not abundance calculation), and E3 (antennas in model and abundance calculation).

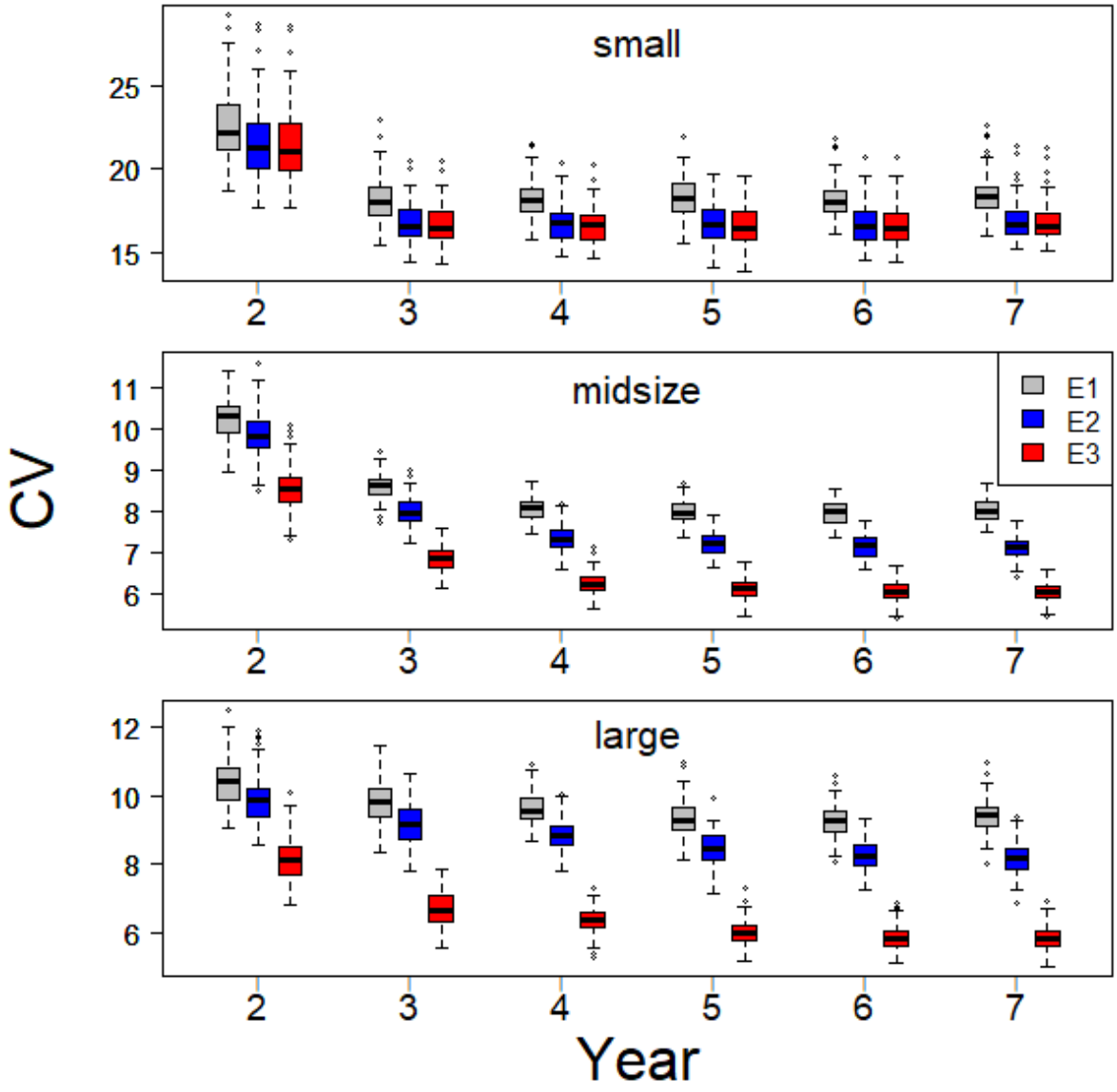

FIGURE 2.4. Relative standard error (RSE) for abundance estimates from the short-lived scenario for three different size classes (small, midsize, and large) by year. Abundance was estimated using three different estimators: E1 (no antennas), E2 (antennas in model but not abundance calculation), and E3 (antennas in model and abundance calculation).

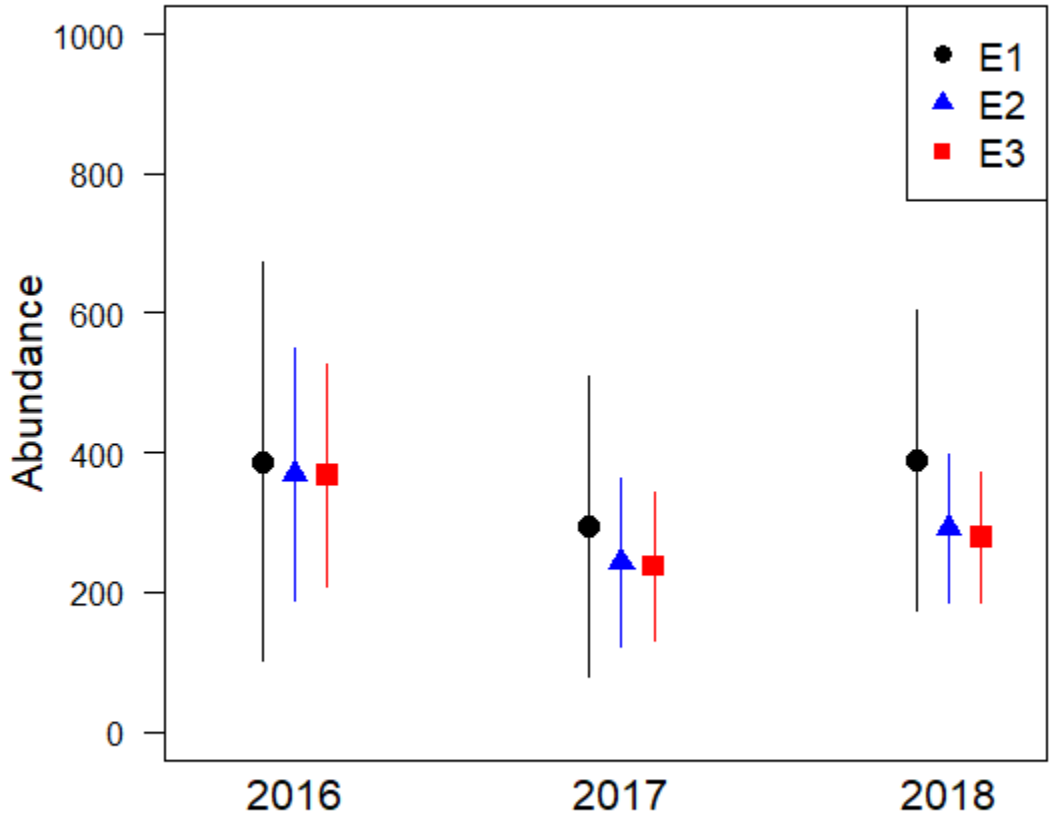

FIGURE 2.5. Population estimates of bull trout in Hells Canyon (Snake River) in the winter of 2016, 2017, and 2018. Error bars represent 95% credible intervals. Abundance estimates come from three different estimators: E1 (no antennas), E2 (antennas used in model but not abundance estimation), and E3 (antennas used in both models and abundance estimation).

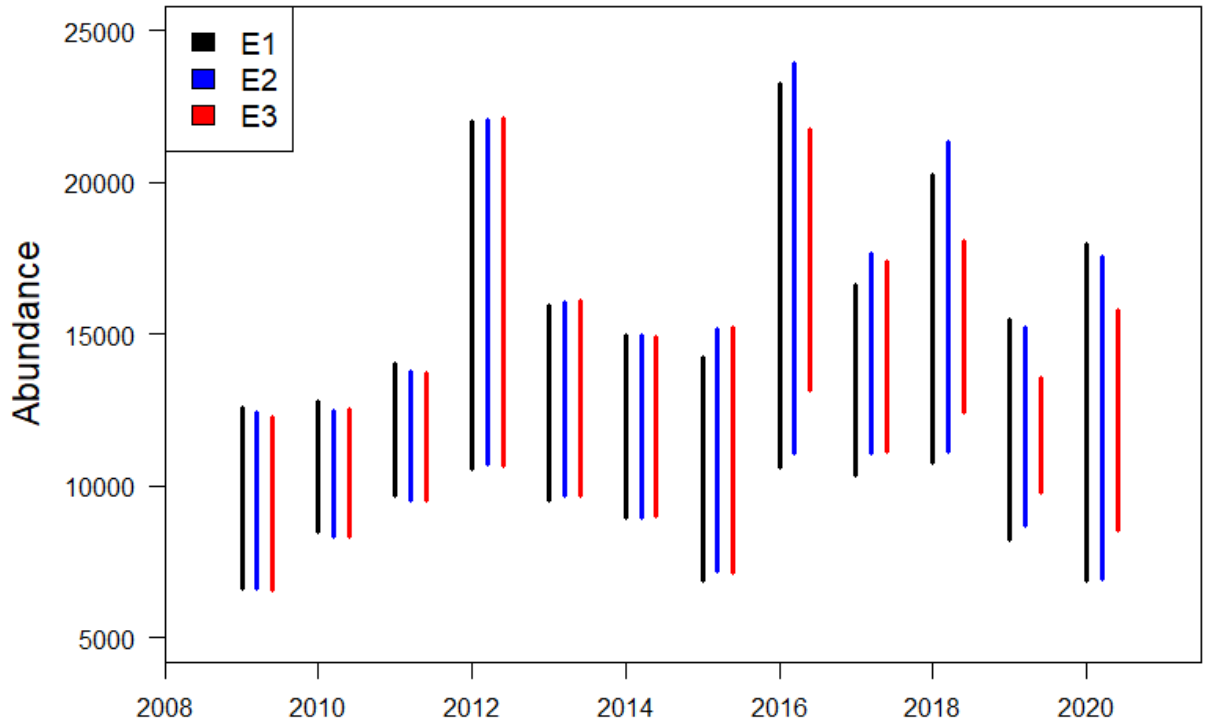

FIGURE 2.6. Abundance estimates (95% CIs) from three different methods for adult humpback chub that spawn in the LCR. Three different estimators were used to estimate abundance: E1 (no antennas), E2 (antennas used in model fitting but not abundance estimation), and E3 (antennas used in both model fitting and abundance estimation).

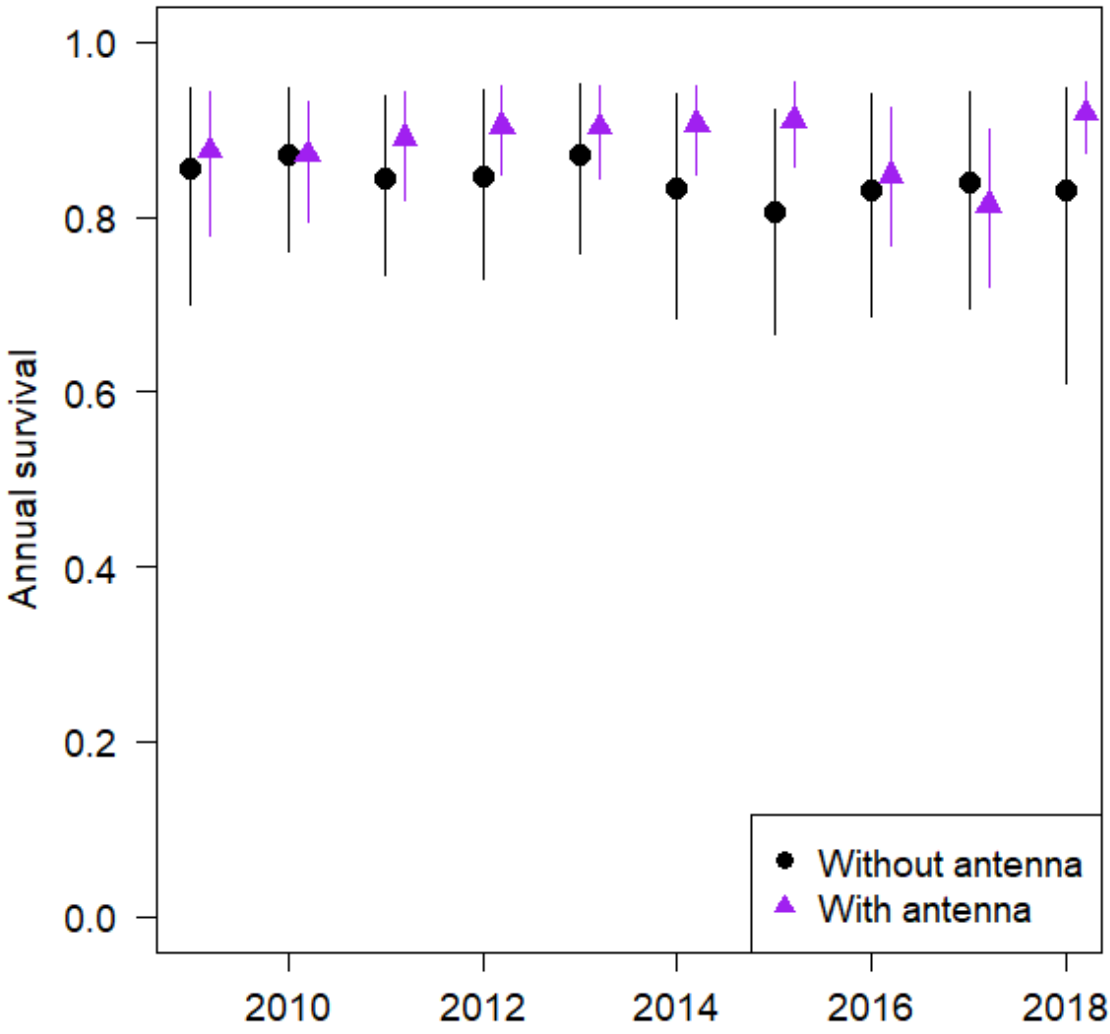

FIGURE 2.7. Comparison of annual survival estimates for large adult humpback chub (≥ 250mm TL) that reside in the Colorado River (CR) and spawn in the Little Colorado River (LCR). The model with antennas utilized mark-recapture data from physical captures in the CR and LCR as well as submersible antenna detections in the CR sampling reach in fall 2016 in spring, summer, and fall of 2018 and 2019. The model without antennas only included data from physical captures.

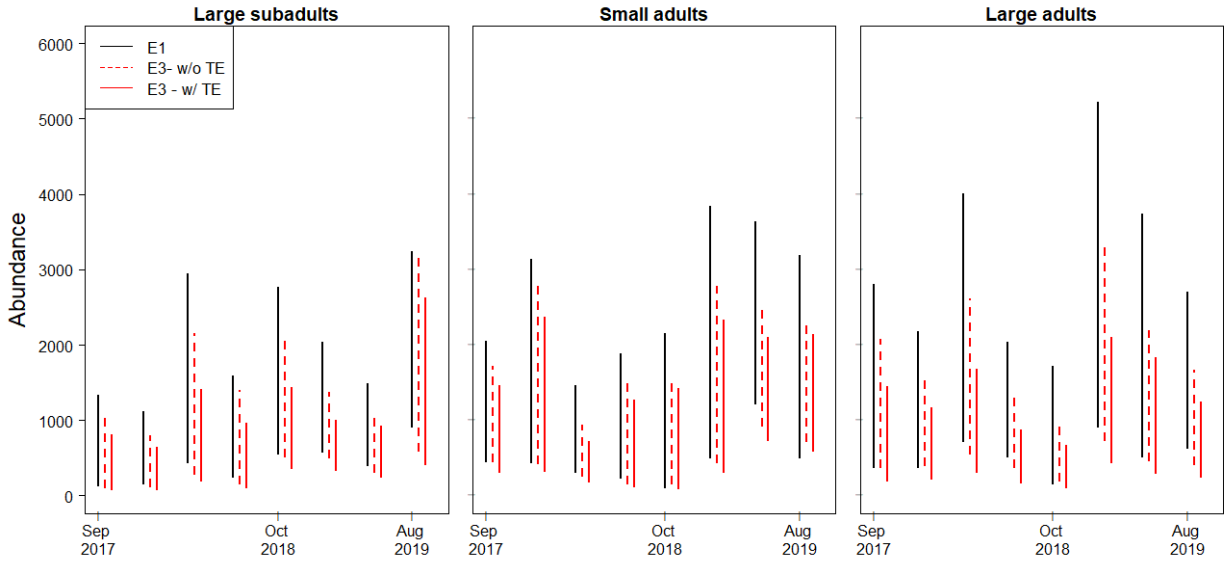

FIGURE 2.8. Comparison of abundance estimates of subadult (150-199mm TL), small adult (200-249mm TL), and large adult (≥250mm TL) humpback chub in western Grand Canyon (about 362-368 river kilometers downstream of Glen Canyon Dam). Abundance estimates come from three different models: a model fit to physical capture data only (E1), a model fit to physical captures and antenna detections but assuming geographic closure (E3 w/o TE), and a model fit to physical captures and antenna detections but allowing for temporary emigration into and out of the sampling reach (E3 w/TE). Abundance estimates are ordered chronologically and pertain to September 2017, May 2018, July 2018, August 2018, October 2018, May 2019, July 2019, and August 2019.

CHAPTER 3

LIFE HISTORY IMPLICATIONS OF PRODUCTION AND DISPERSAL OF AGE-0 HUMPBACK CHUB

3.1.Summary

Life history decisions can be determined at early life history stages, and these decisions can then affect adult population trend in future years. Previous studies of humpback chub in the Little Colorado River (LCR) aggregation have observed large differences in survival, growth, and lifespan based on an individual's life history strategy of either migrating to the mainstem Colorado River (CR) during its first year or remaining a resident in the LCR. Here we evaluate how environmental conditions influence abundance, survival, and migration probabilities of age-0 humpback chub born in the LCR. To estimate age-0 abundances, we evaluate hypotheses related to average and peak snowmelt flows, monsoonal floods, spring flood conditions during egg/larval development, non-native predation, and mainstem food conditions (a proxy of adult fecundity). Furthermore, to explain the fraction of age-0 fish migrating (partial migration), we test hypotheses related to density-dependence and monsoonal floods, the latter which increase turbidity and decrease visibility in the water column. We find that age-0 abundance was low in years lacking snowmelt floods or in years having high spring catch of the non-native predator channel catfish (*Ictalurus punctatus*). Additionally, contrary to expectations, age-0 abundance was high when catch of other non-native egg predators (red shiner (*Cyprinella lutrensis*), fathead minnow (*Pimephales promelas*), common carp (*Cyprinus carpio*), plains killifish (*Fundulus zebrinus*)) was also high, suggesting yearly variability in spring conditions may have widespread effects across numerous species. A model predicting probability of residency (i.e., fish survival

and no migration) found support for negative density-dependence and for a negative response to monsoonal flood duration, though neither density nor flood duration were important when outmigration and survival were treated as separate processes. Consequently, analysis of the life history decision to reside or migrate may be obscured by interannual variability in survival, so that the effective number of age-0 fish that settle in the CR is influenced by survival, floods, and age-0 densities. We relate our age-0 findings to a model of adult dynamics to illustrate how variability in age-0 abundance and migration probabilities leads to recruitment pulses and population growth in CR adults.

3.2. Introduction

Numerous studies have suggested that population growth of fishes is strongly influenced by the population dynamics of age-0 fish (Horst 1977; Lehuta et al. 2010; Morris et al. 2011). Age-0 fish can influence population growth for at least two reasons. First, there is substantial variability in age-0 abundances from year to year (Houde and Hoyt 1987), resulting in variable annual population densities. Second, spatial variability in environmental conditions can lead to partial migration of age-0 fish, where some individuals migrate to a new habitat and others remain resident; these alternative life history trajectories can comprise different vital rates (e.g., survival, growth, fecundity) and rates of turnover for fish populations (Chapman et al. 2012; Jonsson and Jonsson 1993). Often, these two influences interact through density-dependence to cause a type of condition-dependent partial migration, where years with high age-0 density lead to increased competition for food resources and higher rates of migration (Mehner 2015; Morita et al. 2000; Olsson et al. 2006). Condition dependence in migration rates can be beneficial and increase population fitness under low to moderate levels of environmental stochasticity (Vélez-

Espino et al. 2013) because it allows for migrants to minimize competition in high-density years (i.e., the competitive release hypothesis, Chapman et al. 2011) and generally lessens the strength of density-dependence as an inhibitor of population growth (Marco-Rius et al. 2013). Additionally, the growth-survival-breeding asymmetries between migrants and residents that result from partial migration (Gillanders et al. 2015; Skov et al. 2011), can promote population resilience and resistance to ecosystem change (Greene et al. 2010; Schindler et al. 2010).

Density-dependent dispersal may have been an important influence on the population dynamics of large-bodied fish in the Colorado River, where historical seasonal variability in floods and food resources likely shaped life history (Olden et al. 2006; Poff et al. 1997; Winemiller and Rose 1992) and where population dynamics were potentially driven by recruitment pulses that varied spatially within the river network to promote population stability (Terui et al. 2018). Because many large river desert fishes are adapted to seasonal environments and exhibit life history characteristics of periodic strategists (e.g., large body size, long life span, high fecundity, low energetic investment in eggs and parental care; Winemiller and Rose 1992), these fishes often display high year-to-year variability in age-0 abundance, so that recruitment is sporadic and population persistence dependent on a small number of strong year classes (Osmundson and White 2017; Winemiller 2005). Accordingly, under these circumstances a partial migration strategy would be advantageous because increased movement of strong year classes could help offset local competition and promote population growth.

Here we assess environmental influences on abundances and migration probabilities of age-0 humpback chub, *Gila cypha*, that inhabit the Little Colorado River (LCR), a warmwater tributary of the Colorado River in the Grand Canyon. Humpback chub are native to the Colorado River, which historically experienced large seasonal snowmelt floods that likely influenced the

phenology, survival, and movement of age-0 fish (Krabbenhoft et al. 2014). Today's Colorado River differs from historic conditions due to the construction and operation of large dams along its corridor (Carlson and Muth 1989). In the Grand Canyon stretch of the Colorado River, flows are highly regulated by hydroelectric production at Glen Canyon Dam, which has virtually eliminated large annual snowmelt floods and has greatly reduced both average water temperature and its seasonal variation (Topping et al. 2000; Wright et al. 2009). Compared to current conditions in mainstem Colorado River, the LCR exhibits warmer water temperatures and a less altered hydrologic regime due to absence of nearby upstream dams (Robinson and Childs 2001). The LCR near its mouth experiences two periods of flooding each year: late winter/early spring flows coincident with snowmelt from the mountain highlands ~ 200 km upstream, and late summer/early fall flows produced by intense monsoonal rains (monsoonal rains; Dean and Topping 2019b). Here we evaluate environmental drivers of age-0 abundances and explore whether yearly variability in age-0 densities is associated with increased humpback chub emigration from the LCR to the mainstem Colorado River (hereafter outmigration). Additionally, we evaluate the role of floods in influencing age-0 abundance and outmigration. We hypothesize that large snowmelt floods that occur before the onset of humpback chub spawning help restructure substrate and clean interstitial spaces, which has a positive effect on egg survival and food resources (Ortlepp and Mürle 2003; Osmundson et al. 2002). We also assess whether non-native predators and food conditions in the mainstem (a proxy for adult fecundity) are additional drivers. Furthermore, we evaluate if(how) densities affect outmigration probabilities, and hypothesize that outmigration is highest in years with high age-0 abundances, as other studies have observed that, at high densities, the resulting low per capita food availability can motivate migration (Chapman et al. 2012; Olsson et al. 2006).

3.3. Methods

3.3.1. Species background

The humpback chub is a federally endangered cyprinid endemic to the Colorado River. There are currently six recognized populations of humpback chub, though of the original six, one population in the upper Basin is now considered extirpated. The Grand Canyon population is the sole population that occurs in the lower Colorado River basin (USFWS 2002). Within the Grand Canyon population, in recent decades most humpback chub have been born in the LCR, a warmwater tributary, though since 2014 there have been reproduction and population increases documented in western Grand Canyon (Van Haverbeke et al. 2018). In eastern Grand Canyon near the confluence with the LCR, mainstem water temperatures range from 9-12°C in April and May (the main season for humpback chub spawning) and too low for successful spawning and larval development of humpback chub (Hamman 1982; Marsh 1985). Accordingly, near the LCR confluence adult humpback chub spawning occurs from late March to mid-May (Gorman and Stone 1999) so that larval fish are present in April and May (Robinson et al. 1998). During midsummer, a subset of the age-0 cohort migrates to the Colorado River (Yackulic et al. 2014).

The migrant/resident trajectory is primarily determined within the first year (Dzul et al. 2021). For fish that do not outmigrate during their first year, most never leave the LCR and primarily adopt the resident life history strategy. Residents comprise roughly 20-30 % of small adults (200-249mm) and 5-10% of large adults (≥250 mm) and exhibit relatively fast growth rates and low adult survival rates so that this group typically only lives 1-3 years as adults (i.e., fast life history; Dzul et al. 2021). In contrast, age-0 fish that outmigrate to the CR mature to

adulthood in the CR and then as adults migrate between the LCR and CR to spawn and feed. Migrants comprise 70-80% of small adults and 90-95% of large adults and exhibit slow growth. As adults, migrants have a larger maximum body size and higher survival (i.e., live >5 years as adults) compared to residents (Douglas and Marsh 1996), thereby exhibiting a slow life history. The large contrast in survival and growth rates for resident and migrant adults suggests that understanding age-0 outmigration is key to predicting population turnover and forecasting adult abundance trends into the future.

3.3.2. Sampling Methods

This study occurred in the lower Little Colorado River and Colorado River in Grand Canyon, Arizona (Figure 3.1). The methodology and effort for sampling age-0 humpback chub has changed throughout the course of this study period and involved efforts at two spatial locations: the lower 13.56 km of the LCR (2000-2020) and the Colorado River study site (2009-2020). USFWS biologists have visited the LCR four times each year (twice in spring and twice in fall – exceptions being in 2018 when only one fall trip occurred and 2020 when no spring trips occurred) to conduct three passes of hoop net sampling. From 2000-2002, hoop nets were baited but in other years baiting did not occur. Additionally, from 2013-2019, USGS biologists visited the lower 13.56 km of the LCR in late June to sample age-0 humpback chub using seines, dip nets, and unbaited hoop nets. In 2020, the June USGS sampling trip only captured fish in the lower 3.6km of the LCR due to COVID-19 restrictions. More details about LCR sampling can be found in Van Haverbeke et al. (2013) and in Appendix F.

In the Colorado River, sampling occurred at the Colorado River study site, which is located 127-129.7 river kilometers downstream of Glen Canyon Dam, but the size of this study

reach was expanded in 2017 to be between river kilometers 126 -131.2. We refer to the Colorado River study site as the observed Colorado River (oCR) because, unlike the other unsampled stretches of the Colorado River (where we have no mark-recapture information), this is where fish were routinely sampled, marked, and recaptured. Sampling in the oCR included both capture by hoop nets (checked once every 24 hours) and by nighttime electrofishing. Hoop nets were made of 6 mm nylon mesh and were 50–60 cm diameter and 1 m long with a single 10-cm throat. Electrofishing used pulsed DC current, 15–20 amps, 200–300 volts, with an average boat speed of 0.14 m/s. From 2009-2011, sampling occurred in July, August, September, and October as part of the Near Shore Ecology project (Finch et al. 2013) and included 12 passes of hoop nets and 3-5 passes of electrofishing. From 2012-2016, sampling occurred in January (starting 2013), April, July, and September and included 9 passes of hoop nets (80 nets per day) and 5 passes of electrofishing (Yackulic et al. 2018). From 2017 to 2020, sampling has occurred in April (2017) or May (2018-2020), July, and September (2017) or October (2018-2020) and included 6 passes of hoop nets (120 nets per day) and 3 passes of electrofishing.

The marking protocol for humpback chub changed throughout the course of the study and differed by river. In the LCR, the minimum length for PIT tags was 100mm (2000-2002), 150mm (2003-2008), 100mm (2009-2014), and between 65-100mm (2015-2020). Humpback chub that were larger than 39mm but less than the minimum PIT tag length (above) were issued visual implant elastomer (VIE; Northwest Marine Technology) marks during summer (2013-2020) and fall sampling trips (2010-2020) but no VIE marks were issued in spring. In the oCR, the minimum length for PIT tags was 100mm (2009-2016) and 80mm (2016-2020). Similar to the LCR, fish that were larger than 39mm TL and smaller than the minimum PIT tag length were issued VIE marks. For all trips, VIE marks are batch marks that are specific to the trip, and

marks vary in color (red, orange, blue, or green) and body location (dorsal, lip, pelvic, pectoral, caudal, anal). The current protocol has VIE marks varying over a four year cycle, so the same VIE mark can be used after four years. Our multistate model (described below in step 2) accounts for differences in VIE/PIT tag loss by having different transition matrices for juveniles that are VIE marked (in which case they are subject to both initial tag loss and continuous tag loss) and those marked with a PIT tag (where there is only an initial tag loss).

3.3.3. Overview of modeling approach

Before describing our modeling approach below, we define the following terms: age-0 abundance, age-0 fish, outmigration, and juveniles. We note that there is individual-level heterogeneity in growth and movement so that not all individuals fit the pattern described below. Age-0 fish are born into the LCR in spring but are too small to mark until they are 30-60mm TL in July, when they are just large enough to be sampled and marked with VIE. Because July sampling produces the first index of abundance for an age-0 cohort, we refer to July abundances of age-0 fish as age-0 abundance. Outmigration, or movement of age-0 fish from the LCR to the CR, occurs between July-October and (in most years) subsides by winter and spring. For fish that outmigrate, CR growth is slow so that these migrant fish remain less than 100mm TL for multiple (i.e.,~2-4) years (Yackulic et al. 2014). This slow growth, coupled with individual heterogeneity in size at outmigration, causes cohorts in the CR to all overlap in size so that an individual's age cannot be determined based on its size. For fish that do not outmigrate, LCR growth is fast so that by September/October fish are typically 60-100mm TL and by the following April are 90-140mm TL. For this reason, we refer to humpback chub in the LCR that

are less than 100mmTL as age-0 fish because we can be fairly confident of age but in the CR we refer to fish less than 100mm TL as juveniles because their age is unknown (Figure 3.2).

We use modeling approaches to identify influences on both age-0 abundance and outmigration, where floods are of particular interest (Figure 3.3). For age-0 abundance, we are interested in the effects of both monsoon floods and snowmelt floods that precede egg-laying in April and hypothesize that, because monsoon floods have higher sediment concentrations than snowmelt floods, monsoon floods preceding egg-laying will be negatively correlated with age-0 abundance whereas preceding snowmelt floods will have a positive relationship. Floods during the larval development phase (i.e., typically in April) usually decrease water temperatures and may create difficult foraging conditions for larvae, both of which suggest that floods during this short window would have a negative effect on age-0 abundance. For outmigration, we evaluate monsoon floods that occur in the subsequent fall (after hatch), and hypothesize that during monsoon floods, age-0 fish venture out from the cover and become more mobile, thus increasing outmigration probabilities.

Our method is comprised of five steps in which uncertainty in parameters estimated in each step is carried forward through subsequent steps. The modeling methodology works backwards from the true phenology, so that we first evaluate drivers of outmigration and then age-0 abundance (this backwards order is necessary because we first need to understand outmigration to reconstruct age-0 abundances). The five steps are as follows: 1) fit closed models to estimate abundances of age-0 fish in the LCR in July and September, 2) fit an open multistate model to estimate outmigration, 3) fit a type II functional response model to assess density-flood-outmigration relationships, 4) fit a model to reconstruct age-0 abundance over a longer time period (i.e., including 2000-2012 when no July LCR sampling occurred), and 5) fit a

model to predict age-0 abundance from environmental variables. We had to separate steps 1 and 2 into two models because the Stan modeling program (Stan Development Team 2020)does not allow parameters to be discrete, as was necessary for step 1. We kept other steps separate to help with computational efficiency and to help evaluate if(how) age-0 abundance estimates changed during each step, and to this end we plot yearly age-0 abundance estimates (and 95% credible intervals) from steps 1-4.

In step 1, we fit two closed capture-recapture models to estimate age-0 abundances in the LCR in July (2013-2020) and in September (2000-2020). We do not describe methods for step 1 here but refer interested readers to Appendix F. Then, in step 2, we use abundance estimates from step 1 (with associated uncertainty) and mark-recapture data from 2009-2020 to estimate outmigration and survival. Step 3 involves modeling the relationship between age-0 abundance, monsoon floods, outmigration, and survival probabilities from 2009-2020 (where outmigration and survival come from step 2). The relationships from step 3 are used with September abundances from step 1 to reconstruct age-0 abundance from 2000-2020 as part of step 4. Then, in step 5 we use the reconstructed abundances estimates from step 4 to identify environmental drivers of age-0 abundance. All models described in steps 2, 3, and 5 were Bayesian models fit in the program Stan by using the program rstan (Stan Development Team 2020) and R (R Core Development Team 2020) and included three chains, each with 1000 iterations (500 burn-in, 500 for posterior), for a total of 1500 posterior draws.

3.3.3.1. Step 2: Estimating outmigration and survival using a multistate model

Modeling marked individuals to estimate survival, growth, and movement probabilities

For step 2, we fit a multistate mark-recapture model with six states that corresponded to site and size categories as follows: 1) juvenile (<100mm TL) in the oCR, 2) small subadult (100-149mm TL) in the oCR, 3) large subadult or adult (>150mm TL) in the oCR, 4) age-0 fish in the lower LCR, 5) small subadult in the lower LCR, and 6) large subadult or adult in the lower LCR. Because the focus is on juveniles and small subadults, the largest size class (>150mm TL) is not of interest, but rather included so that parameters for smaller size states are not biased. Accordingly, fish must be first captured at ≤ 150mm TL to be included in the model. Also, fish that are recaptured 150-175mm TL are included in the largest size class and released, but fish recaptured >175mm TL are in the largest size class but are censored from further consideration in the likelihood after survival to that size is noted.

Our model operates on a monthly time scale and includes survival (S), growth (g), and movement (m) probabilities. Growth parameters refer to the probability of transitioning to the next size state and movement parameters describe movement from the LCR to the CR and from the CR to the LCR. Accordingly, state transition probabilities are defined as the product of movement and growth transition probabilities where fish first survive, then grow, then move. For example, the probability that a juvenile fish grows to be a small subadult and remains in the LCR is the product of the juvenile survival probability in the LCR, the growth transition probability from juvenile to small subadult in the LCR, and one minus the movement probability for small subadults in the LCR. Because fish may move from the LCR to the CR and settle outside the oCR (where they cannot be sampled), movement from the LCR to CR must be multiplied by the probability that outmigrants settle in the oCR (hereafter $\boldsymbol{\tau}$ – this can also be interpreted as the proportion of CR juveniles that reside in the oCR). Note that $\boldsymbol{\tau}$ is a vector of length 2, where τ_1 is the value from 2009-2016 and τ_2 is the value from 2017-2020 after the

boundaries of the Colorado River study site were expanded. In this model, the proportion of outmigrants that settle outside the oCR (i.e., 1- τ) and survival (S) are confounded (Figure 3.4), which necessitated using information about the means and standard errors of $\boldsymbol{\tau}$ from models of adult humpback chub. Accordingly, the multistate model includes a logit-transformed bivariate normal prior for $\boldsymbol{\tau}$ that is informed by posterior distributions of $\boldsymbol{\tau}$ from the model described in Appendix G (τ_1 = 0.33; 95% CI: 0.29-0.38, τ_2 = 0.40; 95% CI: 0.35-0.45).

One complication in the model is the use of VIE marks, which do not allow for individual identification and are shed at different rates in the LCR and oCR. Accordingly, fish with VIE marks are treated differently in the oCR and LCR. In the oCR, juvenile growth is slow and individuals accumulate multiple VIE marks through time. Fish that are recaptured with VIE marks are treated as removals that are re-released, so that only the most recent VIE recap is included in the capture history. For example, a fish with the following 'true' capture history (0101010) that was tagged with a new VIE mark each time it was captured would have its capture history be recorded as such: 1) .101…, 2) …101., 3) …..10, where '.' is used to signify capture occasions that are not included in the likelihood for that particular fish. For the first capture history segment (.101…) the fish was captured on occasion 2 and given a VIE mark then recaptured on occasion 4. On occasion 4 it was given a new VIE mark then recaptured on occasion 6 (…101.). Lastly, it was released on occasion 6 with another VIE mark and not observed on occasion 7 (…..10). We assume a 0.5% monthly tag loss rate for VIE marks in the oCR based on a linear model evaluating loss of secondary marks. In the LCR, growth is much faster, and fish are only issued VIE marks in July, September, and October. There is some evidence to suggest that tag loss is higher in the LCR than the oCR as preliminary attempts to include July VIE capture-recapture data into step 2 produced unrealistically high abundance

estimates (e.g., >100000), due to the very low number of recaptured fish with VIE marks from the July LCR trip. For this reason, we did not use across-trip information about juveniles in the LCR in July but instead used information about July juvenile abundance obtained from a closed model (step 1; Appendix F) with associated uncertainty (described later). Accordingly, this model only uses VIE marks from September to October, and all individuals with VIE marks are removed from the likelihood in October. Furthermore, in the LCR we assume a 3% monthly tag loss rate, which is based on a tag loss VIE experiment (Yackulic et al. 2014).

Parameters describing vital rates (i.e., survival, growth, and movement) and capture probabilities were all subject to random effects that were logit-transformed and centered on a mean value that was specific to size and location state with shared variances across all states for the same vital rate. Vital rates were modeled on a monthly scale as functions of month-specific environmental covariates and interval-specific time-varying random effects. In the CR, we included environmental covariates that were found to be important in Yackulic et al. (2018). Specifically, survival was modeled as a function of rainbow trout abundance (>175mm fork length; Korman et al. 2016, Korman et al. unpublished data, Yackulic et al. 2018) and a turbidity indicator (from USGS gauge 09402500 located below the LCR confluence), which describes whether or not turbidity was measured at greater than 50 Formazin Nephelometric Units (FNUs). Growth probabilities were modeled as a function of mean monthly water temperature (from USGS gage 09383100), the turbidity indicator, and rainbow trout densities. Lastly, capture probabilities were modeled as a function of water temperature and rainbow trout densities. Movement from the CR to LCR was expected to be minimal for juveniles and small subadults (and likely under-reported for juveniles due to high tag loss rates in the LCR) and only included temporal random effects.

In the LCR, we did not include environmental covariates but rather centered vital rates on both size class and season (April – June (spring), July-September (summer), October – April (winter)). Movement from the LCR to the CR during the summer season was modeled as a time-varying fixed effect. Similar to vital rates, capture probabilities were also modeled on the logit-scale as a function of size, environmental covariates, and time-varying random effects. Because previous studies have illustrated large differences in catch under blue water (not flooding) and brown water (flooding) conditions (Stone 2010), LCR capture probabilities included a turbidity covariate that corresponded to the proportion of days during each sampling trip which were brown water (cfs >250). To determine the benefit/cost of outmigration for individuals, we use the survival and growth probabilities for juveniles and small subadults to estimate the probability that a fish survives from its first July (as an age-0 fish) to become a large subadult under two different life history decisions: 1) outmigrate to CR during the first July as an age-0 fish, and 2) remain in the LCR.

Modeling unmarked individuals in the observed Colorado River to estimate immigration:

Due to the problem with the loss of VIE marks in the LCR, we do not use VIE marked fish to estimate LCR outmigration but rather use increases in the unmarked population in the oCR to estimate the number of new immigrants to the oCR at each sampling occasion. In so doing, we assume all increases in abundance are not due to local reproduction but immigration (where immigrants originate from the LCR). This assumption is highly unlikely to be violated given that mainstem temperatures in this section of the Colorado River are too cold for egg and larval survival. To estimate immigration into the oCR from unmarked fish, we use a Jolly-Seber approach (Jolly 1965, Seber 1965) where we estimate abundance of 'old' unmarked individuals

(i.e., unmarked individuals present in sampling site before time *t*) and 'new' unmarked individuals (i.e., $B_{est,t}$ or the number of individuals that migrated into the sampling site between *t* and *t*+1). To estimate the expected number of unmarked fish in the oCR, we used the following model:

$$U_{t=1} \sim uniform\ (100{,}100000) \tag{3.1}$$

$$U_{t+1} = (U_t - u_t) \cdot S_{CR,t} \cdot (1 - g_{CR,t}) \cdot (1 - m_{CR,t}) + B_{est,t} \tag{3.2}$$

$$u_t \sim Poisson\ (U_t \cdot p_{CR,t}) \tag{3.3}$$

where U_t is the number of unmarked individuals in the population at time *t*, u_t is the number of unmarked individuals captured (and given a mark) at *t,* and $S_{CR,t}$, $g_{CR,t}$, and $m_{CR,t}$ are probabilities of CR survival, CR growth, and movement from the oCR to the LCR, respectively, between *t* and *t*+1. Here we define 'unmarked' in the oCR to be all fish without a VIE mark or PIT tag, as well as all fish whose most recent mark is from the LCR. For immigration estimates (*B*) at time *t* occurring between July and September/October, we used an informative prior, where the number of new immigrants is a function of survival, movement, and age-0 abundance (see next section). For other intervals, we used a uniform prior for B (0,100000).

Using vital rates and abundances to estimate survival and outmigration

Evaluating dynamics of age-0 fish from July to October required additional considerations, as this is the time when migration rates of age-0 fish are high (Yackulic et al. 2014). Additionally, we have incomplete age-0 abundance data from 2009-2012 as no system-wide LCR sampling occurred in July during these years. For these reasons, we share information

about vital rates (informed by capture-recapture) with information about abundances (from closed models) to improve estimation. The improvement in estimation occurs because changes in abundance are a function of vital rates, so there is a benefit to sharing these two types of information. This step is similar to an integrated population model (Besbeas et al. 2002; Schaub and Abadi 2011) but differs in that we use a two-step process and do not estimate abundances and vital rates simultaneously. In our model, we have three abundance estimates that help inform survival and outmigration: 1) July LCR age-0 abundance (only available 2013-2020), 2) September (or October) LCR age-0 abundance, and 3) abundance of new immigrants that enter the oCR between July and September/October. The relationship between these parameters is described below (note that the model runs on a monthly time step but equations below are illustrated with a bimonthly time step to help with interpretability – when run on the monthly scale, this equation accounts for survival differences for fish that move out July-August versus August-September). Unlike previous equations (3.1-3.3) which pertain to each sampling trip (*t*), the following equations (3.4-3.11) only pertain to the time period from July to early fall so we change the temporal notation to year *y*.

$$(3.4) N_{pred,LCR,Sep,y} = N_{pred,LCR,Jul,y} \cdot S_{LCR,Jul-Sep,y} \cdot (1 - g_{LCR,Jul-Sep,y}) \cdot (1 - m_{LCR,Jul-Sep,y})$$

Equation 3.4 includes the probability that an age-0 fish in the LCR at in July will be in the LCR in September, which is the product of surviving in the LCR, not growing into the next size class, and not outmigrating from July-September. We multiply this product by age-0 abundance in year *y* ($N_{pred,LCR,Jul,y}$) to obtain age-0 LCR abundances in September ($N_{pred,LCR,Sep,y}$).

(3.5) $B_{pred,Sep,y} = N_{pred,LCR,Jul,y} \cdot S_{LCR,Jul-Sep,y,} \cdot (1 - g_{LCR,Jul-Sep,y}) \cdot m_{LCR,Jul-Sep,y} \cdot \tau$

Equation 3.5 illustrates how new immigrants into the oCR between July and September ($B_{pred,Sep,y}$) must survive, not grow, outmigrate, and then settle in the oCR. For age-0 abundance and September age-0 abundances in the LCR, we use abundance estimates and associated uncertainties from closed models (step 1) and a multivariate normal (MVN) distribution, where means correspond to vectors of yearly abundances from July and September, $\mathbf{N}_{obs,LCR,Jul}$ and $\mathbf{N}_{obs,LCR,Sep}$, respectively, and variances correspond to variance-covariance matrices, $\mathbf{\Sigma}_{obs,LCR,Jul}$ and $\mathbf{\Sigma}_{obs,LCR,Sep}$, respectively. We use a MVN distribution because closed models shared information about capture probabilities across years, so that there is positive correlation among most yearly abundance estimates.

(3.6) $$\boldsymbol{N}_{obs,LCR,Jul} \sim MVN(\boldsymbol{N}_{pred,LCR,Jul}, \boldsymbol{\Sigma}_{obs,LCR,Jul})$$

(3.7) $$\boldsymbol{N}_{obs,LCR,Sep} \sim MVN(\boldsymbol{N}_{pred,LCR,Sep}, \boldsymbol{\Sigma}_{obs,LCR,Sep})$$

(3.8) $$B_{est,Sep,y} \sim chisquare(B_{pred,Sep,y})$$

Note that B_{pred} is related to B_{est} from the Jolly-Seber approach described earlier. Comparison of these two values will inform outmigration probabilities (m_{LCR}). Survival is informed by differences in age-0 abundance and the number of fish alive in September.

3.3.3.2. Step 3: Evaluating monsoons and density as drivers of outmigration and survival

We used estimates of movement and survival from the outmigration model and their associated uncertainties as response variables in a logit-linear regression model with two

predictors, age-0 abundance (i.e., density) and monsoon duration, and a random effect to account for process error. Age-0 abundance estimates were obtained from the multistate model (step 2) and included uncertainty estimates. Monsoon duration was estimated from USGS gauge 09402300 (located in the LCR ~1 river kilometer upstream of the CR confluence) as the proportion of days from July 1st to September 15th with discharge greater than 250 cfs. In addition to estimating movement and survival separately, we also estimated the effects of monsoons and age-0 abundance on the probability of residency, here defined as the product of survival probability from July to September and the probability that fish did not outmigrate.

We assessed whether or not predictors were significant based on whether or not the posterior distribution of the coefficient from the logit-linear relationship overlapped zero. If the density effect was considered significant, we then fit a Holling type-II response model (Holling 1965) which is based on a relationship where the number of prey consumed per unit time increases as prey become more abundant up to a critical threshold value, after which the number of prey consumed remains constant. This relationship is analogous to the density-outmigration relationship, where we hypothesize that the probability of residency will not decrease indefinitely (as implied by the logit-linear relationship) but will instead asymptote at a minimum value when densities are high.

We used a Bayesian model to fit the type-II relationship as follows.

(3.9) $$a_y = inv\_logit(\beta_0 + \beta_{monsoon} \cdot monsoon_y)$$

(3.10) $$\gamma_y = \frac{a_y}{1+a_y \cdot \eta_y / M}$$

(3.11) $$\mu_{N_{pred,LCR,Jul,y}} \sim Normal\ (\eta_y, \sigma_{N_{pred,LCR,Jul,y}})$$

The relationship in Eq 3.10 is for the probability of residency (γ), which is a function of parameters a and M as well as age-0 abundance η in year y. The model also requires estimates of means and standard deviations of age-0 abundance ($\mu_{N_{pred,LCR,Jul,y}}$ and $\sigma_{N_{pred,LCRJul,y}}$, respectively) in each year y, estimated from posterior distributions of multistate model in step 2. The a parameter ranges from 0-1 and is a linear function of monsoon duration. The M parameter corresponds to the value of age-0 abundance where the density-outmigration relationship changes from linear to flat – for N below M, γ decreases with increasing N and above M, γ remains constant at a lower threshold. We use minimally informative priors for β_0 and $\beta_{monsoon}$ (Normal~(0,2)), whereas we use an informative prior for M (uniform~(0,30000)). We run the model for 3 chains, each with 1000 iterations (500 for burn-in, 500 for posterior) for a total of 1500 posterior draws.

3.3.3.3. Step 4: Reconstructing age-0 abundance from 2000-2020 using the probability of residency

The density-residency relationship above allowed us to simulate September age-0 abundances in the LCR for a large range of possible values of age-0 abundance that ranged from 100 - 100000. Then, we calculate the probability density of each simulated September age-0 abundance value from a normal distribution with mean and standard deviation equal to the means and standard deviations estimated by the closed models of September abundances (step 1). We then fit a lognormal distribution to the probability density distribution using the package MASS (Venables and Ripley 2002) in R.

3.3.3.4. Step 5: Identifying drivers of age-0 abundance

We used the reconstructed age-0 abundance estimates from 2000-2020 to evaluate which environmental factors influenced age-0 abundance. All models included the log of age-0 abundance as the response variable (and associated uncertainties), which was modeled as a linear function of an intercept term and a year-specific random effect for unmodeled variability. Based on results of Van Haverbeke et al. (2013), we first fit a model with a winter baseflow indicator, which took a value of 1 if the LCR was at baseflow and a value of 0 if there was a winter flood that year. We identified baseflow years as years where mean flow from USGS gauge (09402000) was < 2 cfs from the preceding Nov-1 to Apr-1, which corresponded to years 2000, 2002, 2006, and 2018. The choice of < 2 cfs was based on the observation that, generally, flows of this magnitude did not produce any noticeable effect on flows farther downstream (at gage 09402300, which was not used because it did not include all the years in our analysis). We included this baseflow indicator in all subsequent models and used a forward stepwise regression approach, where we fit all candidate models individually and only carried forward effects that did not overlap zero. The candidate predictors were as follows: 1) spring flow conditions (during egg and larval development), 2a) non-native species predation with egg predators, 2b) non-native species predation of channel catfish, 3) duration of large floods during the previous year (includes both snowmelt and monsoonal floods), 4) CR mainstem food conditions, and 5) differential effects of mean snowmelt and monsoonal flows (i.e., very rough proxy of sediment deposition). The spring flow conditions model used mean flow estimates from April 1-May 15 of each year to assess if(how) flood conditions during the larval development window affect egg or larval survival. We fit two versions of the non-native species predation model. The first included species suspected to predate on eggs and early life history stages of eggs (i.e., red shiner

(*Cyprinella lutrensis*), fathead minnow (*Pimephales promelas*), common carp (*Cyprinus carpio*), plains killifish (*Fundulus zebrinus*)) and was motivated by Bestgen et al. (2006), who found evidence for large impacts of red shiner predation on survival of larval Colorado River pikeminnow. Additionally, we fit a model that evaluated abundance of channel catfish on age-0 abundance, as previous diet work has suggested channel catfish may be predatory on humpback chub (Marsh and Douglas 1997). For both non-native predation models, we used catch of the aforementioned non-native species during USFWS spring sampling trips (excluding 2000 and 2020 which did not have spring sampling) as a proxy of non-native abundance. The large flood model was motivated by Brouder (2001) to specifically look at flood intensity and this model used the proportion of days with flow greater than the 90% quantile for the entire study period (i.e., 2000-2020). The CR mainstem food condition model hypothesized that humpback chub recruitment was limited by fecundity, so that favorable food conditions (as indicated by soluble reactive phosphorous (SRP) concentrations in the CR, see Korman et al. 2021) led to more fecund outmigrant adults and this led to greater age-0 abundance in the LCR. Fecundity was inferred by phosphorous concentrations from the preceding fall and this model included measurement error for phosphorous. The sediment deposition model was motivated by the observation that the suspended sediment concentration (turbidity) during monsoon floods are roughly ten times greater than that of winter flood (Dean and Topping 2019b) and that eggs/larvae could be negatively impacted by lack of clean gravels. The sediment deposition model did not include sediment concentrations directly, and instead inferred this effect by considering flows over the snowmelt and monsoon periods as separate processes in an additive model, where snowmelt floods corresponded to the preceding 1-Nov to 1-Apr and mean monsoon flows corresponded to the preceding 1-Jul to 1-Nov.

3.4. Results

Comparison of age-0 abundance estimates from steps 1-4 (i.e., the closed models, the outmigration model, the type-II response model, and the reconstructed abundance models) suggested that there was high agreement between all models (Figure 3.5). Importantly, this agreement is not an independent (i.e., out-of-sample) assessment of model fit because models were constructed from shared information; however, this agreement does help illustrate that abundance estimates were consistent among models fit with and without functional relationships with density and monsoon floods. The two main discrepancies were the back-casted estimate from 2011 (which was low) and estimates from 2020.

The multistate model (step 2) illustrated that age-0 abundance and outmigration were highly variable across the timeframe of our study (Figure 3.6). Specifically, age-0 abundance varied between 2299-38345 and monthly outmigration probability varied between 5-32%, which translated to 9.8-53.8% of fish outmigrating between July and September. Two years (2011 & 2012) stood out from the rest as being exceptionally high for both production and outmigration. In contrast, the 2016-2017 period showed low age-0 abundance and a low outmigration probability. In other years, outmigration probabilities were more uncertain (e.g., 2009, 2013, 2014, 2018). Monthly survival estimates in the LCR before and during outmigration (i.e., July-September) were usually ~90% but were notably lower in 2015 (71%). Interestingly, the model predicted substantial outmigration that occurred between October 2011 and July 2012, outside the outmigration timeframe (July – September) assessed by our model. Posterior draws of outmigration probabilities and τ_1 exhibited a weak negative correlation ($R^2 = 0.11$) so that lower estimates of τ_1 led to higher estimates of outmigration.

Environmental drivers of vital rates in the CR are consistent with those estimated by Yackulic et al. (2018), where capture probabilities were highest under warmer water temperatures with low numbers of rainbow trout, survival was highest in clear waters with low numbers of rainbow trout (though both survival effects barely overlapped zero), and growth was highest in warmer, turbid conditions with low numbers of trout (Figure 3.7). However, compared to Yackulic et al. 2018 which found support for rainbow trout having a stronger negative impact on survival compared to growth, this study found the magnitude of the rainbow trout effect on growth was greater than that on survival.

Age-0 fish that remained resident were more likely to survive to become a large subadult (i.e., grow to over 150mm TL) compared to age-0 fish that outmigrated during their first summer (Figure 3.8). For individual years, survival to >150mm TL was always higher for age-0 fish that remained resident, presumably because resident fish grow faster, but the high interannual variability in and within-year model uncertainty caused error bars for the two life history strategies to overlap.

The logit-linear model predicting the probability of residency indicated significant negative relationships with both density (mean: -0.35; 95% CI: -0.72 to -0.02) and monsoonal flood duration (mean: -1.14; 95% CI: -2.14 to -0.09) so that the predicted probability of residency was highest when monsoons were absent and densities were low (Figure 3.8). In contrast, both density and survival were not significant in logit-linear models of outmigration (95% CI for density: -0.10 to 0.93; 95% CI for flood duration: -1.51 to 1.66) and in logit-linear models of survival (95% CI for density: -1.07 to 0.57; 95% CI for monsoon flood duration: -3.91 to 0.47).

Using the observed type-II relationship between density, monsoon floods, and the probability of residency, we were able to reconstruct estimates of age-0 abundance from 2000-2020 (step 4). These reconstructed estimates emphasize that in years with low September abundances (e.g., 2000, 2002, 2006, 2018), the probability of residency was high so that a low number of fish in the LCR in September was indicative of low age-0 abundance (Figure 3.5). In contrast, years with higher September LCR abundances indicate age-0 abundance (e.g. 2001, 2003-2005, 2007, 2012) was higher and more uncertain.

Results from the age-0 abundance prediction models (step 5) indicated that years without winter snowmelt floods led to poor age-0 abundance and this effect was strong in all models (Figure 3.10). Additionally, the catfish predation model indicated a moderate negative effect of catfish on age-0 abundance (Figure 3.11, top panels), though the range of values for catfish catch (0-52) was narrow. Contrary to our hypothesis, catch of non-native egg predators had a positive, moderate effect on age-0 abundance (Figure 3.11, bottom panels). Models of sediment deposition, spring flood conditions, and mainstem food conditions (adult fecundity) were not well supported (i.e., all coefficients overlapped zero), so we present the results of the model with absence of winter floods, catfish catch, and the catch of non-native egg predators as the best model: the mean coefficient for absence of winter floods was -2.24 (95% CI: -3.05 to -1.48), the mean coefficient for catfish predation was -0.32 (95% CI: -0.59 to -0.07), and the mean coefficient for the ratio of non-native predators was 0.32 (95% CI: 0.06 to 0.60).

3.5. Discussion

Our results emphasize there is high year-to-year variability in both age-0 abundances (correlated with the absence of floods, channel catfish catch, and catch of non-native egg

predators) and outmigration (correlated with age-0 abundance and monsoon flood duration). Importantly, years with high age-0 abundances experience either increased mortality or increased outmigration (or both) relative to years with low age-0 abundances. The high variability among age-0 cohorts is common among fishes (Hjort 1914; Houde 2016; Jackson and Noble 2000) and contrasts with adult humpback chub dynamics, which are relatively constant through time (Coggins et al. 2006; Dzul et al. 2021). Strong recruitment years occur when both age-0 abundances and outmigration probabilities are high, leading to pulses in recruitment in the CR and (lagged) population growth of adults. Improved understanding of age-0 population dynamics should help focus conservation efforts and help forecast population trend.

While we were unable to confidently identify factors that led to good years of age-0 abundance, our model results reinforce the findings of Van Haverbeke et al. (2013) by emphasizing that absence of winter floods leads to poor age-0 abundance as indicated by the years 2002, 2006, and 2018 (Figure 3.10; Note: 2000 also had no winter flood and very low age-0 abundance but is excluded because no spring sampling occurred in this year). However, the mechanism driving the relationship between poor age-0 abundance and absence of winter floods remains unknown and is difficult to specify because winter floods influence both the physical and biological environment. In regards to physical changes, spring runoff in the LCR restructures substrate material, cleanses interstitial space for eggs (Gorman and Stone 1999; Kaeding and Zimmerman 1983; Van Haverbeke et al. 2013), and increases habitat variability and biodiversity (Ward and Stanford 1995; Yarnell et al. 2010), so in the absence of winter floods in the LCR, fine sediments deposited in streambed interstitial spaces may facilitate generation of anoxic conditions that impede development of humpback chub eggs and hatched larvae (Kemp et al. 2011). Absence of winter floods may also reduce food availability because, by removing fine

sediments from interstitial spaces, floods can improve habitat conditions (i.e., dissolved oxygen levels) for benthic microinvertebrates and macroinvertebrates that are primary food resources for young fishes (Osmundson et al. 2002).

Notably, while age-0 abundance was low in years without winter floods, even a small amount of flooding over winter was enough to produce very high age-0 abundance (Figure 3.10). For example, of all the years where winter floods did occur (i.e., all years except 2000, 2002, 2006, and 2018), 2012 had the smallest flood but had the second-highest age-0 abundance estimate. Relationships between flow and biota are often nonlinear (Poff et al. 1997; Rosenfeld 2017) and thus difficult to uncover. We expect that more years of data will allow us to better evaluate age-0 abundance under a wide spectrum of flow conditions to help assess interactions and nonlinear relationships between variables.

Our results also indicated that channel catfish may be another driver of age-0 abundance, though we caution that USFWS catfish catch is a very rough measure of total catfish abundance because catfish are good at avoiding capture by hoop nets. The relationship between catfish catch and age-0 abundance was largely driven by three years (2009, 2016, and 2017) with high catch of catfish and low age-0 abundance (Figure 3.11, upper right panel). In these years, most catfish were small (e.g., 80-140mm total length), which was contrary to our expectations that most predation would be by larger individuals. Generally, diet studies of juvenile catfish have found a large variety of food items in diets and very low rates of piscivory (Marsh and Douglas 1997). However, juvenile channel catfish will consume eggs and larvae in a laboratory setting, even in presence of other food items (Carpenter and Mueller 2008). Notably, the absence of humpback chub eggs and larvae from channel catfish stomachs does not necessarily indicate that predation is not occurring, because once ingested, larval fish are quickly digested and often not

identifiable in stomach contents (Schooley et al. 2008), so more follow-up on diet is needed, perhaps using DNA methods (e.g., Ehlo et al. 2017). It is also possible that juvenile catfish limit age-0 abundances through competition, or that the relationship is purely correlative (i.e., there are certain environmental conditions that are good for channel catfish and bad for age-0 humpback chub).

Unlike catfish, catch of non-native egg predators (i.e., fathead minnow, red shiner, plains killifish, and common carp) was positively correlated with age-0 abundance, a finding that was contrary to our hypothesis. Environmental conditions that are favorable for age-0 abundance of humpback chub may be generally favorable to other species. Specifically, the four highest years of non-native catches also had relatively small winter floods, which may have been strong enough to clean substrates and boost productivity, but not so strong as to disadvantage non-natives (Minckley and Meffe 1987; Propst and Gido 2004). It is possible that these conditions may benefit humpback chub larvae as well because years with the highest age-0 abundance estimates usually occurred in years with modest flooding, though this relationship is highly uncertain based on the available data. Other hypotheses that were tested were not significant, which is perhaps unsurprising as the proxies of egg/larval disturbance, adult fecundity, and sediment deposition are very coarse and may not accurately reflect these measures. Sediment deposition is particularly difficult to quantify, as floods can deposit and(or) scour sediment and the amount of sediment deposited during a flood is a function of flood intensity, duration, and sediment source.

Although we were unable to find evidence for our hypothesis that years with high age-0 abundance increased outmigration probability, we did find some support that age-0 density affects both survival and outmigration probabilities conjointly via the probability of residency.

High densities may increase outmigration and decrease survival if food resources are limiting. Growth/survival studies in the LCR indicate spring is the most productive season (Dzul et al 2016, Dzul et al. 2021), so that larvae are born at a time conducive for feeding and rapid growth. By June, age-0 fish are larger and water temperatures are warmer, so that age-0 fish have higher metabolic demands. Furthermore, adult insect emergence is declining from its peak in spring, suggesting lower food availability (Muehlbauer, unpublished data). Conditions of resource limitation, particularly in high density years, may increase mortality in midsummer and motivate outmigration. Little is known about survival of outmigrants, but movement into the CR exposes them to predation risk (Beamesderfer et al. 1990; Jepsen et al. 1998; Wood 1987) by both larger humpback chub conspecifics and non-native fishes such as channel catfish in the LCR (Marsh and Douglas 1996) and by rainbow trout in the CR (Yackulic et al. 2018; Yard et al. 2011). Our model was unable to evaluate the survival cost of outmigration because fish were not observed throughout the course of their migration, as this requires active telemetry or a large network of PIT tag arrays or acoustic receivers (Buchanan and Skalski 2010; Cordoleani et al. 2018; Michel et al. 2015).

Assessment of outmigration underscored the importance of 2011 and 2012 for recruitment into the Colorado River, and analysis of adults has identified these cohorts as having contributed to recent increases in adult abundances (Appendix G). Evidence suggests that these pulses in recruitment and outmigration to the CR help drive population growth, because large adult migrants in the CR have a life expectancy 2.9-5.0 times greater than their LCR resident counterparts (Dzul et al. 2021) and this high survival produces strong age structure which allows fish to persist through long periods of low recruitment until conditions are favorable for producing another strong year class (i.e., the storage effect – Warner and Chesson 1981, Secor

2007). Although outmigration may ultimately benefit population growth, outmigration is not necessarily advantageous for individuals (under the assumption that all individuals are equal), as evidenced by the lower probability of outmigrants surviving to be a large subadult compared to residents. However, it is likely that age-0 outmigrants may have characteristics (e.g., poor condition, slow growth) that would make them relatively more vulnerable to starvation or predation compared to age-0 residents remaining in the LCR.

Quantifying age-0 dynamics can be challenging due to the difficulties associated with handling and marking small fish. The predominant challenge is tagging this size class, because generally body sizes are too small to use individually-identifiable tags (e.g., PIT tags). Instead of individual identifiable tags, this study used VIE tags as a batch mark (specific to trip and river) for long-term mark-recapture, and we acknowledge that VIE tags are not ideal for long-term mark-recapture because they are subject to confusion in terms of color or location misassignment (Curtis 2006). A better understanding of tag loss rates and their relationship to fish growth rates and body location will improve population models. For example, biologists suspect high tag loss rates for ventral tags compared to dorsal tags, though one experiment comparing these tags did not find support in a laboratory setting (Yackulic et al. 2014). Despite these challenges, large across-year differences can facilitate identification of key environmental drivers. For example, in the current study we have high confidence in distinguishing good versus bad years of age-0 abundance and outmigration (e.g., 2012 vs. 2018), but less confidence in distinguishing the relative differences in moderate years. We therefore rely on the strong between-year contrasts to identify environmental relationships with enough explanatory power to gain precision in years where uncertainty is higher.

One last source of error is the probability that fish settle in the oCR (τ). Movement estimates were sensitive to τ, suggesting better information is needed about τ to better understand absolute survival and outmigration probabilities. Furthermore, we had to make the simplifying assumption that τ was constant across years. Because emigration outside the oCR is non-distinguishable from mortality, any yearly variability in the proportion that settle in the oCR would be attributed to survival variability.

We show that outmigration can help counteract the negative effects of density and resource limitation in the LCR to promote population growth. This result underscores the importance of years with both high age-0 abundance and high outmigration (e.g., 2012), as it is abundance of migrant humpback chub that predominantly affects overall adult abundance trends. While our study identified absence of winter floods and catfish predation as two processes associated with low age-0 abundance, we were unable to identify which environmental conditions led to good years. The inability to predict good years represents a major shortcoming, because population persistence may be dependent on these infrequent good years. We expect that bad years will become more frequent in the future, given that climate change models of the southwest predict drought (Ault et al. 2016; Cayan et al. 2010) and reductions in stream flow (Udall and Overpeck 2017). Whether good years can counteract the expected increase in frequency of bad years is a critical consideration for forecasting humpback chub dynamics and population persistence into the future.

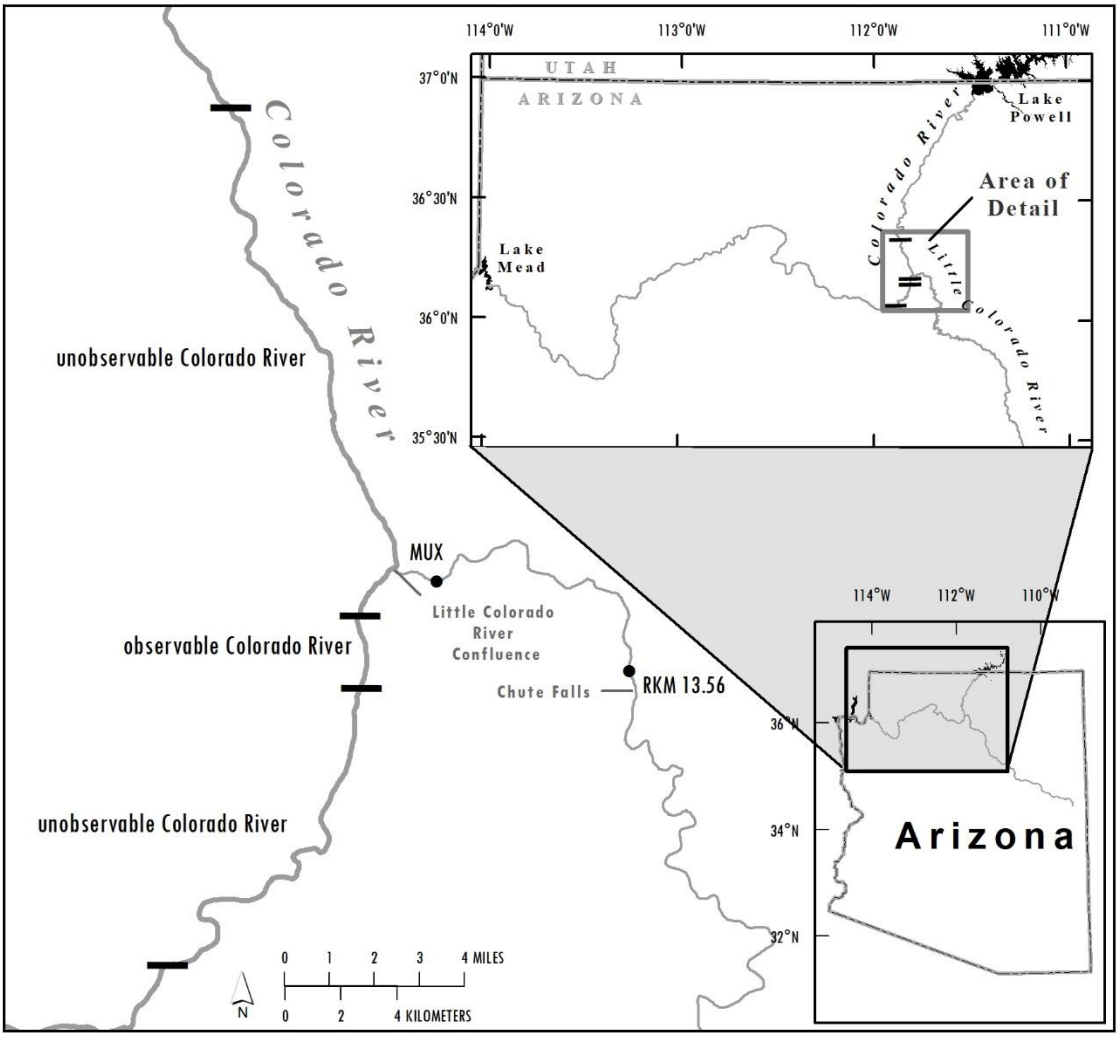

FIGURE 3.1. Map depicting the Colorado River (CR) near its confluence with the Little Colorado River (LCR) in northern Arizona. This study includes capture-recapture data of humpback chub from the lower 13.56 river kilometers of the LCR as well as from the observable CR reaches (127-129.7 river kilometers downstream of Glen Canyon Dam). The map was created using ESRI ArcGIS desktop software, version 10.7.1, using map features in Gushue (2019).

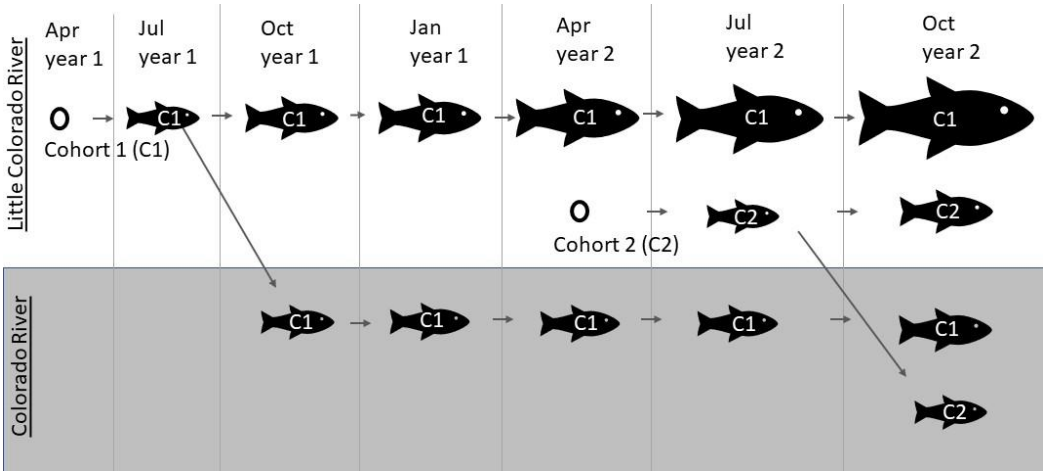

FIGURE 3.2. Illustration demonstrating size and growth differences of juvenile humpback chub for two different cohorts (C1 and C2) in the Little Colorado River (upper white rectangle) and Colorado River (lower grey rectangle). Humpback chub are born in the LCR in spring (egg in April), then some individuals migrate into the Colorado River during summer and fall. Growth in the LCR is fast and there are large size differences across age classes. In contrast, in the Colorado River growth is slow and so age classes overlap in size.

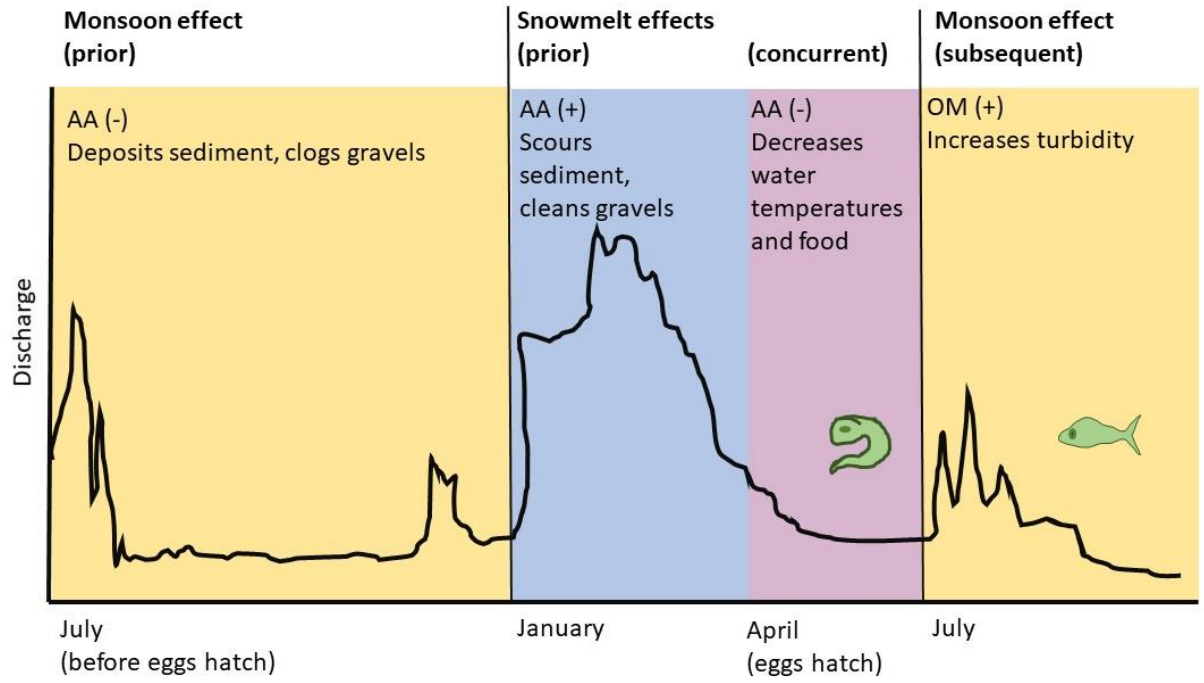

FIGURE 3.3. Conceptual figure illustrating a hypothetical hydrograph and hypotheses about how flows affect population dynamics of age-0 humpback chub. The hydrograph depicts two periods of flooding during each year, monsoonal floods that occur in midsummer/early fall and snowmelt floods that occur in late winter and early spring. For the cohort depicted, this hydrograph starts the summer before eggs hatch, extend through the egg-laying and larval development phases in mid- to late-spring, and ends during the fall when fish are ~1/2 year old. In each of the colored rectangles, there is text describing whether the flood affects age-0 abundance (AA) or outmigration (OM) of the cohort, as well as the hypothesized directionality in parentheses.

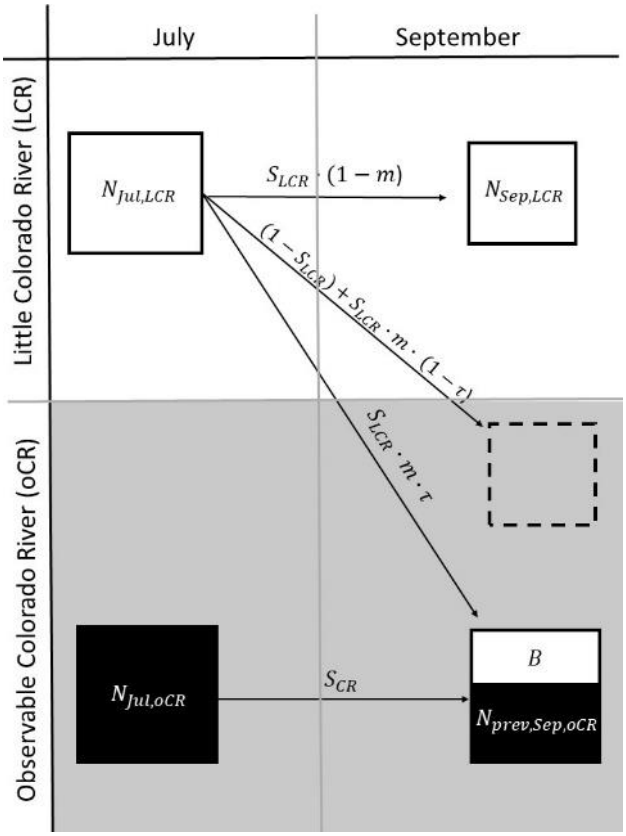

FIGURE 3.4. Diagram representing the integrated population model for estimating age-0 outmigration and production. The upper two quadrants represent the Little Colorado River (LCR) and the lower two represent the observed Colorado River (oCR). Additionally, the two left quadrants represent July (which we assume is the time immediate preceding the outmigration period) and two right quadrants are September (which we assume is the time after most outmigration has occurred). Boxes with solid lines represent abundances that can be estimated from sampling efforts while boxes with dashed lines represent abundances that are unobserved. Abundances are related to each other, and are a function of survival (*S*), movement (*m*), and the probability of settling in the oCR given outmigration (τ). In July, the abundance of age-0 fish ($N_{Jul,LCR}$) represents individuals born in the LCR during the preceding spring. Between July and September, these fish can survive and not move (thus remaining in the LCR – $N_{Sep,LCR}$), survive and outmigrate to settle in the oCR (B), or be unobserved (i.e., fish that either did not survive or survived, outmigrated, and settled outside the oCR). Estimating the number of new immigrants into the oCR required predicting how many of the juveniles present in the oCR in September were from the previous July ($N_{prev,Sep,oCR}$), so that any increase in this number represented recent immigration. The diagram above is simplified from the model used because it does not include temporally-specific subscripts and growth, these were excluded from the diagram for better readability.

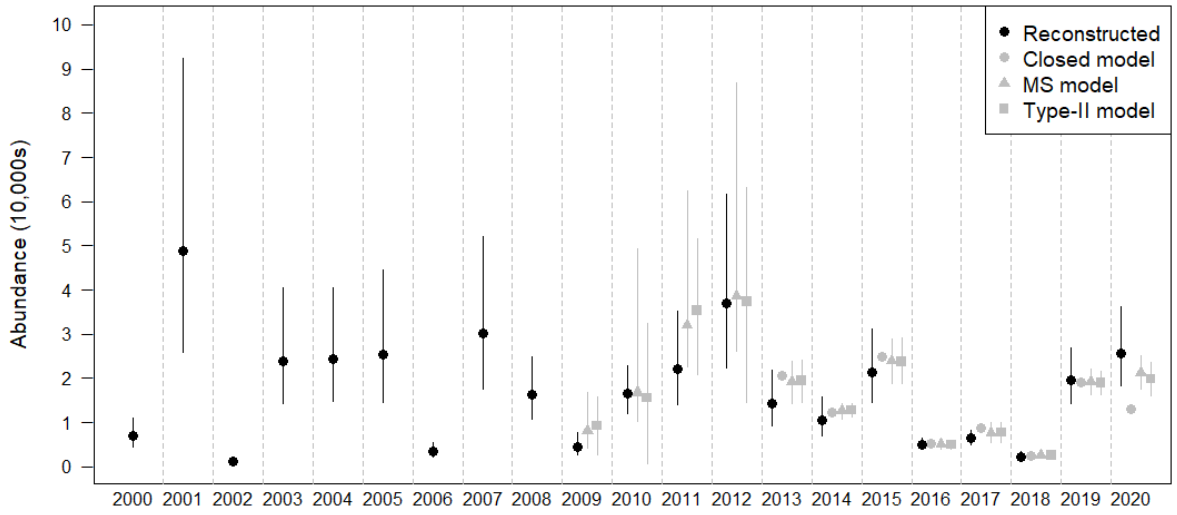

FIGURE 3.5. Estimates of age-0 abundance of humpback chub in the Little Colorado River from 2000-2020. Estimates come from four possible sources: closed models (step 1; 2013-2020 only), a multistate (MS) model (step 2; 2009-2020), a type-II functional response model (step 3; 2009-2020), and a reconstructed abundance model (step 4; 2000-2020). Error bars represent 95% credible intervals.

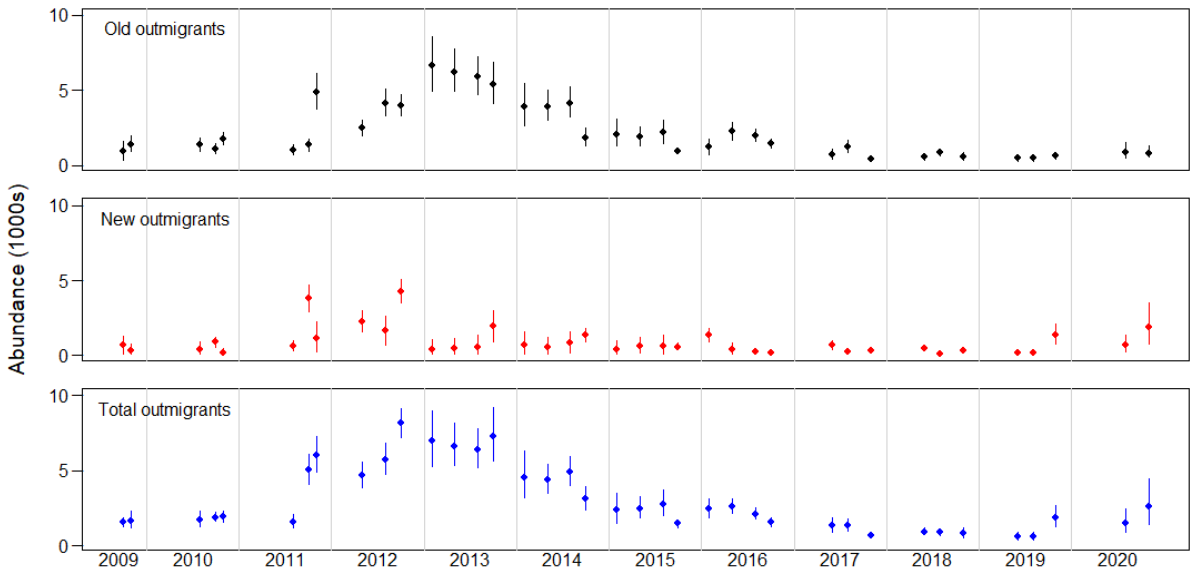

FIGURE 3.6. Time series describing abundances of juvenile (<100mm total length) humpback chub in the observed Colorado River (i.e., the oCR or 127-129.7 river kilometers downstream of Glen Canyon Dam) from 2009-2020. Abundances below are specific to the number of juvenile humpback chub present in the oCR from before the sampling occasion (top panel, old outmigrants), the number of fish that immigrated into the oCR since the previous sampling occasion (middle panel, new outmigrants), and the sum of old and new outmigrants (lower panel, total outmigrants). Estimates are presented based on the timing of sampling trips and refer to Sep & Oct (2009), Jul & Sep & Oct (2010-2011), Apr & Jul & Sep (2012), Jan & Apr & Jul & Sep (2013-2016), Apr & Jul & Sep (2017), May & Jul & Oct (2018-2019), or Jul & Oct (2020). Error bars represent 95% credible intervals.

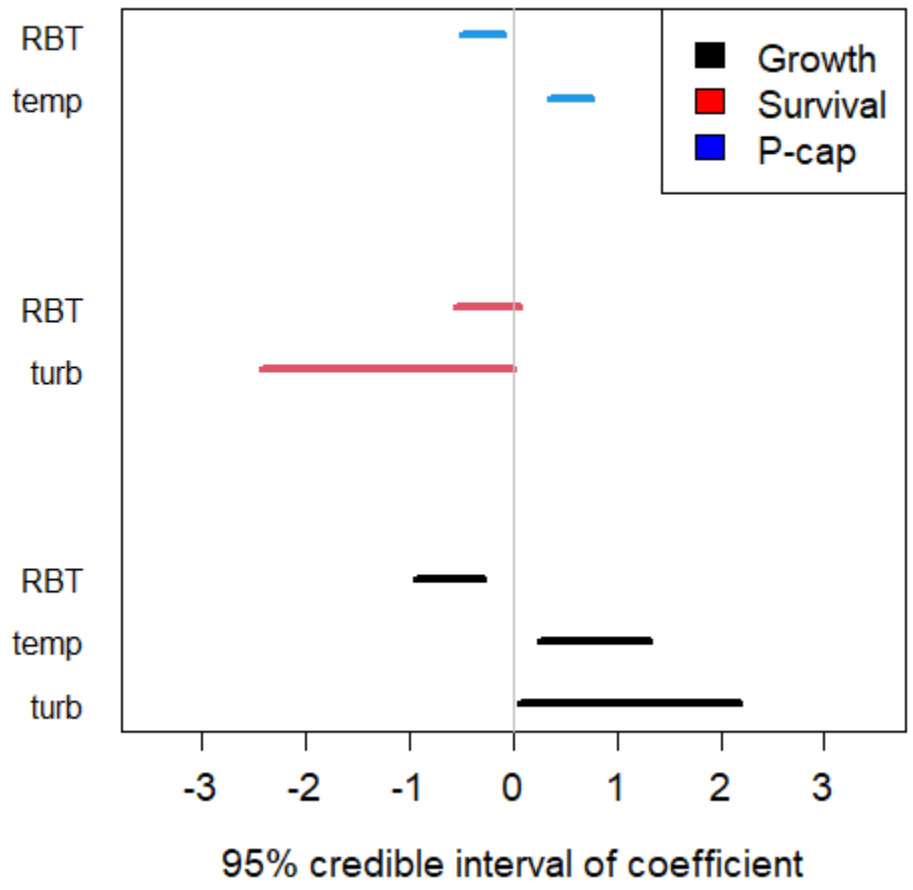

FIGURE 3.7. Ninety-five percent credible intervals for coefficients of growth, survival, and capture probabilities (p-cap) for juvenile (<100 mm total length) humpback chub in the observed Colorado River (127-129.7 river kilometers downstream of Glen Canyon Dam). Covariates included rainbow trout (RBT) effects for survival, growth, and p-cap, turbidity effects (turb) for survival and growth, and water temperature effects (temp) on growth and p-cap. These covariates were included in the model based on results from Yackulic et al.(2018).

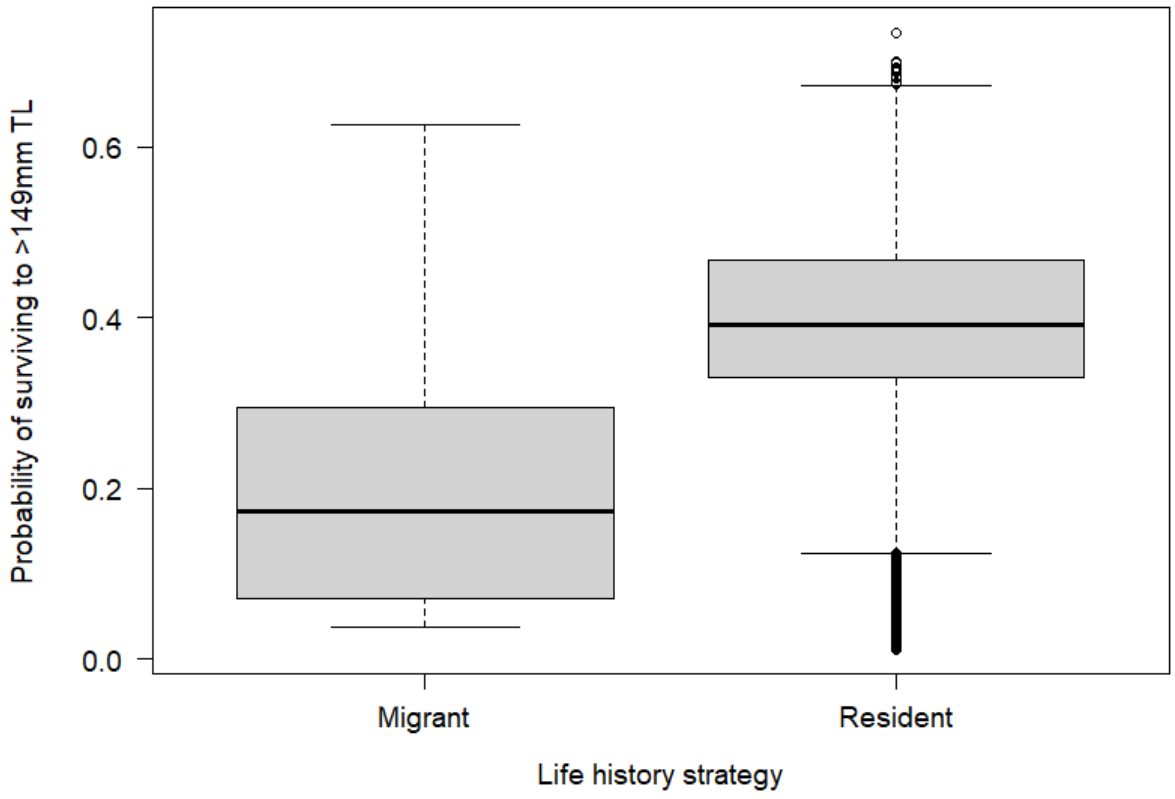

FIGURE 3.8. Box and whisker plot describing the probability that age-0 humpback chub survive from their first July to become large subadults (>149mm total length). The probabilities are illustrated for two different life history strategies, based on whether a fish outmigrates to the Colorado River during its first July (migrant) or remains in the Little Colorado River (resident).

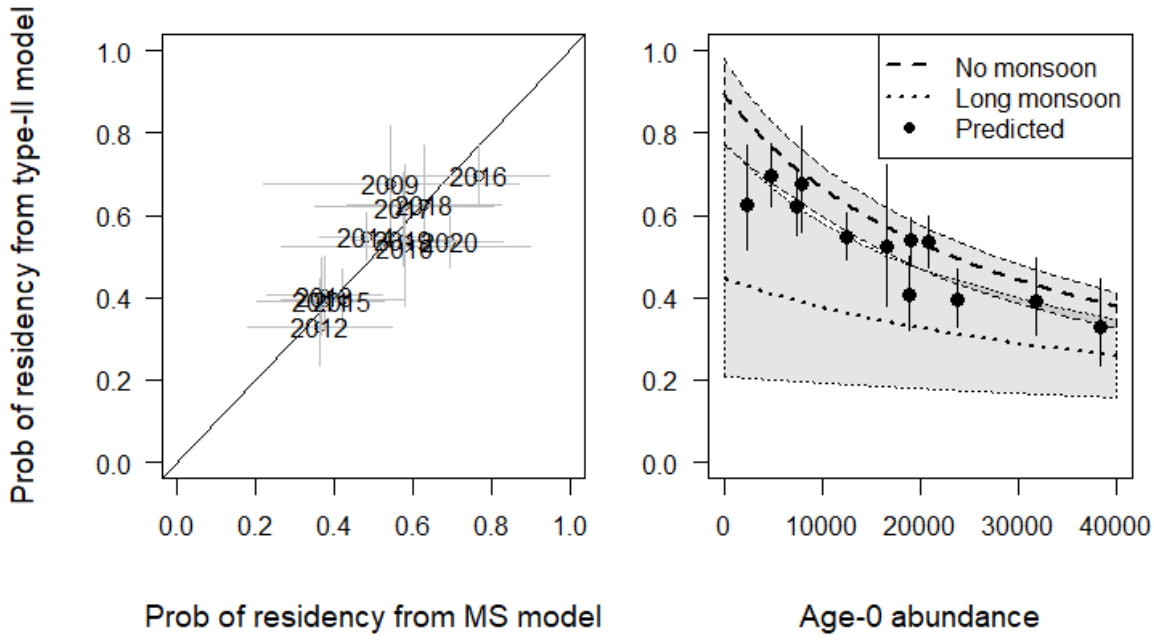

FIGURE 3.9. Graphs illustrating the probability of residency (the product of survival probability and the probability of not outmigrating between July-September) for age-0 humpback chub in the Little Colorado River. The left panel depicts the relationship between 'observed' and fitted values, where 'observed' values were estimated from a multistate (MS) model that did not include any effects on outmigration or survival. In contrast, the fitted model is a type-II functional response model that specifically related the 'observed' probability of residency to a model that included age-0 abundance (i.e., density) and monsoon flood effects. The right panel illustrates how age-0 abundance and monsoon duration are predicted to affect the probability of residency.

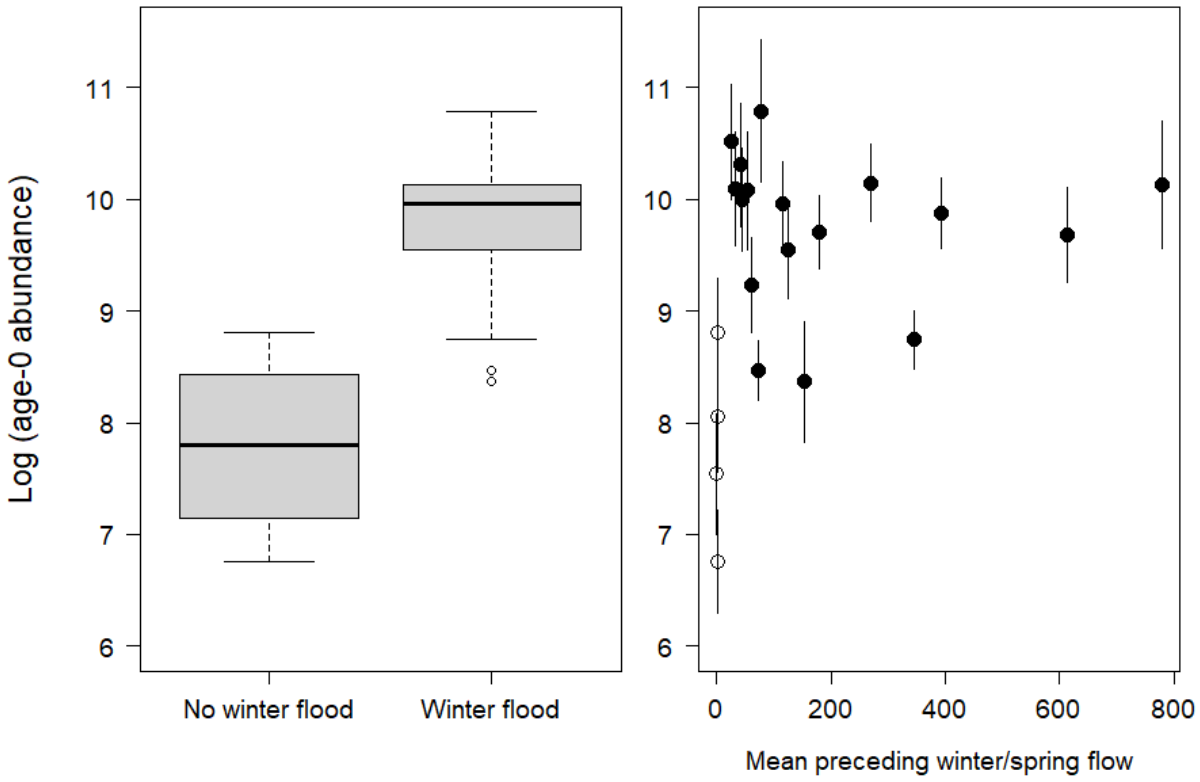

FIGURE 3.10. Graphs illustrating the effects of preceding winter/spring floods on age-0 humpback chub abundances from 2000-2020. The left panel depicts how the log of age-0 abundance is related to presence/absence of winter floods, whereas the right panel depicts how the log of age-0 abundance is related to mean flow from the preceding winter/spring (1-Nov to 1-Apr).

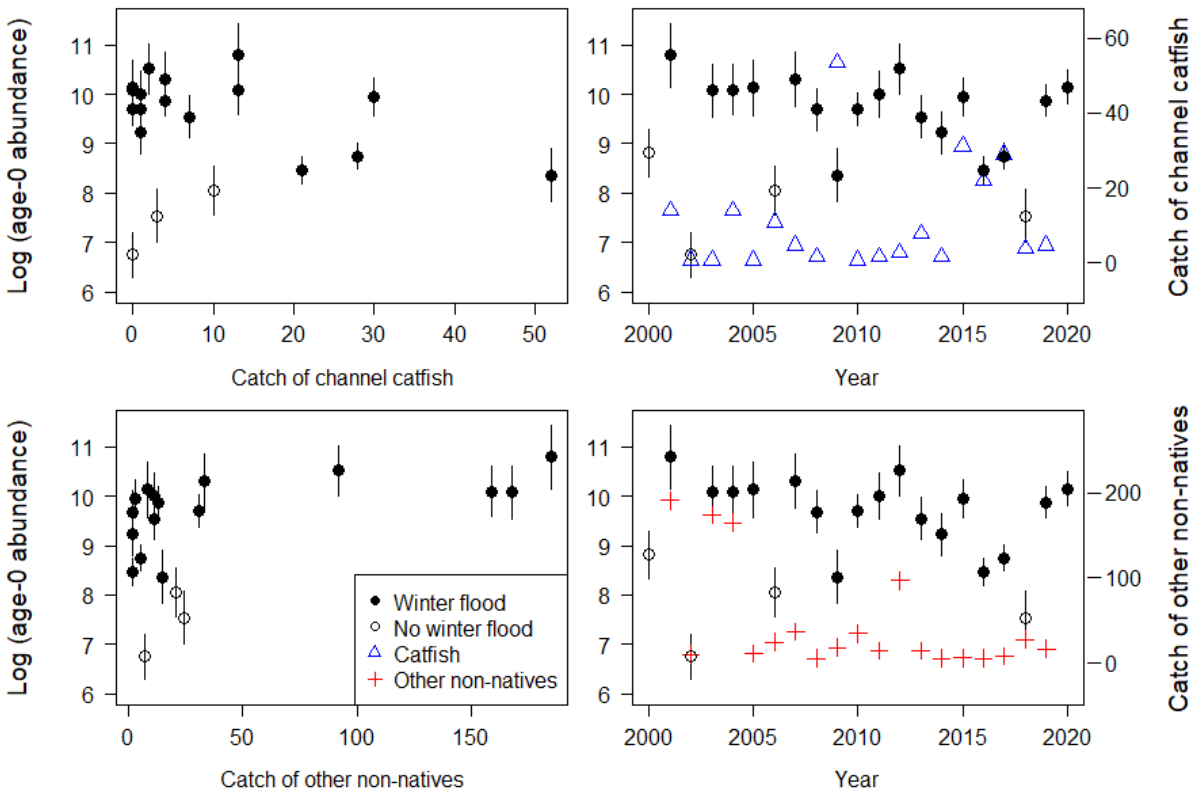

FIGURE 3.11. Graphs depicting the relationship between with channel catfish catch from spring monitoring trips to the Little Colorado River (LCR) and the log of age-0 abundances of humpback chub directly (upper left panel) and year-by-year (upper right panel). Similarly, the relationship between spring LCR catch of other non-native species (i.e., red shiner, fathead minnow, plains killifish, common carp), which are potential egg predators, and age-0 humpback chub abundance is also graphed directly (lower left panel) and year-by-year (lower right panel). For age-0 humpback chub estimates, black points correspond to years where winter floods occurred whereas white points correspond to years without winter floods. Error bars represent 95% credible intervals.

Bibliography

Aarestrup, K., Lucas, M., and Hansen, J. 2003. Efficiency of a nature-like bypass channel for sea trout (Salmo trutta) ascending a small Danish stream studied by PIT telemetry. Ecology of freshwater fish **12**(3): 160-168.

Al-Chokhachy, R., and Budy, P. 2008. Demographic characteristics, population structure, and vital rates of a fluvial population of bull trout in Oregon. Transactions of the American Fisheries Society **137**(6): 1709-1722.

Arnason, A.N. 1973. The estimation of population size, migration rates and survival in a stratified population. Researches on Population Ecology **15**(2): 1-8.

Augustine, B.C., Royle, J.A., Kelly, M.J., Satter, C.B., Alonso, R.S., Boydston, E.E., and Crooks, K.R. 2018. Spatial capture–recapture with partial identity: An application to camera traps. The Annals of Applied Statistics **12**(1): 67-95.

Ault, T.R., Mankin, J.S., Cook, B.I., and Smerdon, J.E. 2016. Relative impacts of mitigation, temperature, and precipitation on 21st-century megadrought risk in the American Southwest. Science Advances **2**(10): e1600873.

Bair, L.S., Yackulic, C.B., Springborn, M.R., Reimer, M.N., Bond, C.A., and Coggins, L.G. 2018. Identifying cost-effective invasive species control to enhance endangered species populations in the Grand Canyon, USA. Biological Conservation **220**: 12-20.

Banet, N.V., and Hewitt, D.A. 2019. Monitoring of endangered Klamath Basin suckers translocated from Lake Ewauna to Upper Klamath Lake, Oregon, 2014− 2017. US Geological Survey 2331-1258.

Barbour, A.B., Ponciano, J.M., and Lorenzen, K. 2013. Apparent survival estimation from continuous mark–recapture/resighting data. Methods in Ecology and Evolution **4**(9): 846-853.

Barbour, A.B., Adams, A.J., Yess, T., Behringer, D.C., and Wolfe, R.K. 2012. Comparison and cost-benefit analysis of PIT tag antennae resighting and seine-net recapture techniques for survival analysis of an estuarine-dependent fish. Fisheries Research **121**: 153-160.

Barker, R.J. 1997. Joint modeling of live-recapture, tag-resight, and tag-recovery data. Biometrics: 666-677.

Beamesderfer, R.C., and Rieman, B.E. 1988. Size selectivity and bias in estimates of population statistics of smallmouth bass, walleye, and northern squawfish in a Columbia River reservoir. North American Journal of Fisheries Management **8**(4): 505-510.

Beamesderfer, R.C., Rieman, B.E., Bledsoe, L.J., and Vigg, S. 1990. Management implications of a model of predation by a resident fish on juvenile salmonids migrating through a Columbia River reservoir. North American Journal of Fisheries Management **10**(3): 290-304.

Beard, Z.S., Quist, M.C., Hardy, R.S., and Ross, T.J. 2017. Survival, Movement, and Distribution of Juvenile Burbot in a Tributary of the Kootenai River. North American Journal of Fisheries Management **37**(6): 1274-1288.

Beauplet, G., Barbraud, C., Dabin, W., Küssener, C., and Guinet, C. 2006. Age-specific survival and reproductive performances in fur seals: evidence of senescence and individual quality. Oikos **112**(2): 430-441.

Behn, K.E., and Baxter, C.V. 2019. The trophic ecology of a desert river fish assemblage: influence of season and hydrologic variability. Ecosphere **10**(1): e02583.

Besbeas, P., Freeman, S.N., Morgan, B.J., and Catchpole, E.A. 2002. Integrating mark–recapture–recovery and census data to estimate animal abundance and demographic parameters. Biometrics **58**(3): 540-547.

Bestgen, K., Beyers, D., Rice, J., and Haines, G. 2006. Factors affecting recruitment of young Colorado pikeminnow: synthesis of predation experiments, field studies, and individual-based modeling. Transactions of the American Fisheries Society **135**(6): 1722-1742.

Bond, R.M., Nicol, C.L., Kiernan, J.D., and Spence, B.C. 2019. Occurrence, fate, and confounding influence of ghost passive integrated transponder tags in an intensively monitored watershed. Canadian Journal of Fisheries and Aquatic Sciences **76**(2): 286-298.

Bravington, M.V., Grewe, P.M., and Davies, C.R. 2016. Absolute abundance of southern bluefin tuna estimated by close-kin mark-recapture. Nature Communications **7**(1): 1-8.

Brizendine, M.E. 2016. Use of Ultrasonic Imaging to Evaluate Egg Maturation of Humpback Chub Gila Cypha. University of Arizona.

Brouder, M.J. 2001. Effects of flooding on recruitment of roundtail chub, Gila robusta, in a southwestern river. The Southwestern Naturalist: 302-310.

Buchanan, R.A., and Skalski, J.R. 2010. Using multistate mark-recapture methods to model adult salmonid migration in an industrialized river. Ecological Modelling **221**(4): 582-589.

Bunch, A.J., and Stewart, W.T. 2020. Integrating PIT technology into gear evaluation in an unregulated desert tributary. Fisheries Research **221**: 105366.

Carlson, C.A., and Muth, R.T. 1989. The Colorado River: lifeline of the American southwest. Canadian Special Publication of Fisheries and Aquatic Sciences **106**: 220-239.

Carpenter, J., and Mueller, G.A. 2008. Small nonnative fishes as predators of larval razorback suckers. The Southwestern Naturalist **53**(2): 236-242.

Cathcart, C.N., Gido, K.B., McKinstry, M.C., and MacKinnon, P.D. 2018a. Patterns of fish movement at a desert river confluence. Ecology of freshwater fish **27**(1): 492-505.

Cathcart, C.N., Pennock, C.A., Cheek, C.A., McKinstry, M.C., MacKinnon, P.D., Conner, M.M., and Gido, K.B. 2018b. Waterfall formation at a desert river–reservoir delta isolates endangered fishes. River Research and Applications **34**(8): 948-956.

Cayan, D.R., Das, T., Pierce, D.W., Barnett, T.P., Tyree, M., and Gershunov, A. 2010. Future dryness in the southwest US and the hydrology of the early 21st century drought. Proceedings of the National Academy of Sciences **107**(50): 21271-21276.

Chao, A. 1989. Estimating population size for sparse data in capture-recapture experiments. Biometrics: 427-438.

Chapman, B., Hulthén, K., Brodersen, J., Nilsson, P.A., Skov, C., Hansson, L.A., and Brönmark, C. 2012. Partial migration in fishes: causes and consequences. Journal of fish biology **81**(2): 456-478.

Chapman, B.B., Brönmark, C., Nilsson, J.Å., and Hansson, L.A. 2011. The ecology and evolution of partial migration. Oikos **120**(12): 1764-1775.

Chapman, B.B., Eriksen, A., Baktoft, H., Brodersen, J., Nilsson, P.A., Hulthen, K., Brönmark, C., Hansson, L.-A., Grønkjær, P., and Skov, C. 2013. A foraging cost of migration for a partially migratory cyprinid fish. PLoS One **8**(5).

Christie, M.R., McNickle, G.G., French, R.A., and Blouin, M.S. 2018. Life history variation is maintained by fitness trade-offs and negative frequency-dependent selection. Proceedings of the National Academy of Sciences **115**(17): 4441-4446.

Coggins, L.G., Pine III, W.E., Walters, C.J., Van Haverbeke, D.R., Ward, D., and Johnstone, H.C. 2006. Abundance trends and status of the Little Colorado River Population of Humpback Chub. North American Journal of Fisheries Management **26**: 233-245.

Conn, P.B., and Cooch, E.G. 2009. Multistate capture–recapture analysis under imperfect state observation: an application to disease models. Journal of Applied Ecology **46**(2): 486-492.

Conner, M.M., Bennett, S.N., Saunders, W.C., and Bouwes, N. 2015. Comparison of Tributary Survival Estimates of Steelhead using Cormack–Jolly–Seber and Barker Models: Implications for Sampling Efforts and Designs. Transactions of the American Fisheries Society **144**(1): 34-47.

Conner, M.M., Budy, P.E., Wilkison, R.A., Mills, M., Speas, D., MacKinnon, P.D., and McKinstry, M.C. 2020. Estimating population abundance with a mixture of physical capture and passive PIT tag antenna detection data. Canadian Journal of Fisheries and Aquatic Sciences(ja).

Cooke, S.J., Midwood, J.D., Thiem, J.D., Klimley, P., Lucas, M.C., Thorstad, E.B., Eiler, J., Holbrook, C., and Ebner, B.C. 2013. Tracking animals in freshwater with electronic tags: past, present and future. Animal Biotelemetry **1**(1): 1.

Cordoleani, F., Notch, J., McHuron, A.S., Ammann, A.J., and Michel, C.J. 2018. Movement and Survival of Wild Chinook Salmon Smolts from Butte Creek During Their Out-Migration to the Ocean: Comparison of a Dry Year versus a Wet Year. Transactions of the American Fisheries Society **147**(1): 171-184.

Cubaynes, S., Pradel, R., Choquet, R., Duchamp, C., GAILLARD, J.M., LEBRETON, J.D., Marboutin, E., Miquel, C., REBOULET, A.M., and Poillot, C. 2010. Importance of accounting for detection heterogeneity when estimating abundance: the case of French wolves. Conservation Biology **24**(2): 621-626.

Cunjak, R., Roussel, J.-M., Gray, M., Dietrich, J., Cartwright, D., Munkittrick, K., and Jardine, T. 2005. Using stable isotope analysis with telemetry or mark-recapture data to identify fish movement and foraging. Oecologia **144**(4): 636-646.

Curtis, J.M. 2006. Visible implant elastomer color determination, tag visibility, and tag loss: potential sources of error for mark–recapture studies. North American Journal of Fisheries Management **26**(2): 327-337.

Dauwalter, D.C., and Fisher, W.L. 2007. Electrofishing capture probability of smallmouth bass in streams. North American Journal of Fisheries Management **27**(1): 162-171.

Dean, D., and Topping, D. 2019. Geomorphic change and biogeomorphic feedbacks in a dryland river: The Little Colorado River, Arizona, USA. Bulletin **131**(11-12): 1920-1942.

Dixon, P.M., Ellison, A.M., and Gotelli, N.J. 2005. Improving the precision of estimates of the frequency of rare events. Ecology **86**(5): 1114-1123.

Donovan, P., Bair, L.S., Yackulic, C.B., and Springborn, M.R. 2019. Safety in numbers: cost-effective endangered species management for viable populations. Land Economics **95**(3): 435-453.

Douglas, M.E., and Marsh, P.C. 1996. Population estimates/population movements of Gila cypha, an endangered cyprinid fish in the Grand Canyon Region of Arizona. Copeia **1996**(1): 15-28.

Dudgeon, C.L., Pollock, K.H., Braccini, J.M., Semmens, J.M., and Barnett, A. 2015. Integrating acoustic telemetry into mark–recapture models to improve the precision of apparent survival and abundance estimates. Oecologia **178**(3): 761-772.

Dzul, M. 2021. Humpback chub spring and fall capture histories in the Little Colorado River, 2009-2019: U.S. Geological Survey data release. https://doi.org/10.5066/P95KA0XI. .

Dzul, M., Yackulic, C.B., Kendall, W.L., Winkelman, D.L., and Yard, M. In Review. Skipped migration of humpback chub in the Little Colorado River: an example of how adding data from autonomous PIT tag antennas can lead to more informed population models.

Dzul, M.C., Yackulic, C.B., and Korman, J. 2017. Estimating animal abundance using continuous detection data from PIT arrays placed near the confluence of two rivers. Canadian Journal of Fisheries and Aquatic Sciences **75**(9): 1393-1404.

Dzul, M.C., Yackulic, C.B., Korman, J., Yard, M.D., and Muehlbauer, J.D. 2016. Incorporating temporal heterogeneity in environmental conditions into a somatic growth model. Canadian Journal of Fisheries and Aquatic Sciences **74**(3): 316-326.

Dzul, M.C., Kendall, W.L., Yackulic, C.B., Winkelman, D.L., Van Haverbeke, D.R., and Yard, M.D. 2021. Partial migration and spawning movements of humpback chub in the Little Colorado River are better understood using data from autonomous PIT tag antennas. Canadian Journal of Fisheries and Aquatic Sciences(ja).

Ehlo, C.A., Saltzgiver, M.J., Dowling, T.E., Marsh, P.C., and Kesner, B.R. 2017. Use of molecular techniques to confirm nonnative fish predation on razorback sucker larvae in Lake Mohave, Arizona and Nevada. Transactions of the American Fisheries Society **146**(2): 201-205.

Fetherman, E.R., Avila, B.W., and Winkelman, D.L. 2014. Raft and floating radio frequency identification (RFID) antenna systems for detecting and estimating abundance of PIT-tagged fish in rivers. North American Journal of Fisheries Management **34**(6): 1065-1077.

Finch, C., Pine, W., and Limburg, K. 2013. Do hydropeaking flows alter juvenile fish growth rates? A test with juvenile humpback chub in the Colorado River. River Research and Applications **2013**.

Gelman, A., Carlin, J.B., Stern, H.S., and Rubin, D.B. 2014. Bayesian data analysis. Taylor & Francis.

Gillanders, B.M., Izzo, C., Doubleday, Z.A., and Ye, Q. 2015. Partial migration: growth varies between resident and migratory fish. Biology letters **11**(3): 20140850.

Gimenez, O., Cam, E., and Gaillard, J.-M. 2018. Individual heterogeneity and capture–recapture models: what, why and how? Oikos **127**(5): 664-686.

Gorman, O.T., and Stone, D.M. 1999. Ecology of spawning humpback chub, Gila cypha, in the Little Colorado River near Grand Canyon, Arizona. . Environmental Biology of Fishes **55**: 115-133.

Grayson, K.L., Bailey, L.L., and Wilbur, H.M. 2011. Life history benefits of residency in a partially migrating pond-breeding amphibian. Ecology **92**(6): 1236-1246.

Greene, C.M., Hall, J.E., Guilbault, K.R., and Quinn, T.P. 2010. Improved viability of populations with diverse life-history portfolios. Biology Letters **6**(3): 382-386.

Haines, A.M., Zak, M., Hammond, K., Scott, J.M., Goble, D.D., and Rachlow, J.L. 2013. Uncertainty in population estimates for endangered animals and improving the recovery process. Animals **3**(3): 745-753.

Hamman, R.L. 1982. Spawning and culture of humpback chub. The Progressive Fish-Culturist **44**(4): 213-216.

Haraldstad, T., Höglund, E., Kroglund, F., Lamberg, A., Olsen, E.M., and Haugen, T.O. 2018. Condition-dependent skipped spawning in anadromous brown trout (Salmo trutta). Canadian Journal of Fisheries and Aquatic Sciences **75**(12): 2313-2319.

Hebblewhite, M., and Merrill, E.H. 2007. Multiscale wolf predation risk for elk: does migration reduce risk? Oecologia **152**(2): 377-387.

Hebblewhite, M., and Merrill, E.H. 2011. Demographic balancing of migrant and resident elk in a partially migratory population through forage–predation tradeoffs. Oikos **120**(12): 1860-1870.

Hein, A.M., Hou, C., and Gillooly, J.F. 2012. Energetic and biomechanical constraints on animal migration distance. Ecology letters **15**(2): 104-110.

Hense, Z., Martin, R.W., and Petty, J.T. 2010. Electrofishing capture efficiencies for common stream fish species to support watershed-scale studies in the central Appalachians. North American Journal of Fisheries Management **30**(4): 1041-1050.

Hewitt, D.A., Janney, E.C., Hayes, B.S., and Shively, R.S. 2010. Improving inferences from fisheries capture-recapture studies through remote detection of PIT tags. Fisheries **35**(5): 217-231.

Hjort, J. Fluctuations in the great fisheries of northern Europe viewed in the light of biological research. *In* 1914. ICES.

Holdo, R.M., Holt, R.D., and Fryxell, J.M. 2009. Opposing rainfall and plant nutritional gradients best explain the wildebeest migration in the Serengeti. The American Naturalist **173**(4): 431-445.

Holling, C.S. 1965. The functional response of predators to prey density and its role in mimicry and population regulation. The Memoirs of the Entomological Society of Canada **97**(S45): 5-60.

Horst, T.J. 1977. Use of the Leslie matrix for assessing environmental impact with an example for a fish population. Transactions of the American Fisheries Society **106**(3): 253-257.

Horton, G.E., Letcher, B.H., and Kendall, W.L. 2011. A multistate capture–recapture modeling strategy to separate true survival from permanent emigration for a passive integrated transponder tagged population of stream fish. Transactions of the American Fisheries Society **140**(2): 320-333.

Houde, E., and Hoyt, R. 1987. Fish early life dynamics and recruitment variability. Trans. Am. Fish. Soc.

Houde, E.D. 2016. Recruitment variability. Fish reproductive biology: 98-187.

Huggins, R. 1991. Some practical aspects of a conditional likelihood approach to capture experiments. Biometrics: 725-732.

Jackson, J.R., and Noble, R.L. 2000. Relationships between annual variations in reservoir conditions and age-0 largemouth bass year-class strength. Transactions of the American Fisheries Society **129**(3): 699-715.

Jepsen, N., Aarestrup, K., Økland, F., and Rasmussen, G. 1998. Survival of radiotagged Atlantic salmon (Salmo salar L.)–and trout (Salmo trutta L.) smolts passing a reservoir during seaward migration. Hydrobiologia **371**: 347-353.

Jonsson, B., and Jonsson, N. 1993. Partial migration: niche shift versus sexual maturation in fishes. Reviews in Fish Biology and Fisheries **3**(4): 348-365.

Jørgensen, C., Ernande, B., Fiksen, Ø., and Dieckmann, U. 2006. The logic of skipped spawning in fish. Canadian Journal of Fisheries and Aquatic Sciences **63**(1): 200-211.

Kaeding, L.R., and Zimmerman, M.A. 1983. Life history and ecology of the humpback chub in the Little Colorado and Colorado Rivers of the Grand Canyon. Transactions of the American Fisheries Society **112**: 577-594. Available from http://dx.doi.org/10.1577/1548-8659(1983)112<577:LHAEOT>2.0.CO;2 [accessed.

Kanno, Y., Letcher, B.H., Coombs, J.A., Nislow, K.H., and Whiteley, A.R. 2014. Linking movement and reproductive history of brook trout to assess habitat connectivity in a heterogeneous stream network. Freshwater Biology **59**(1): 142-154.

Kanno, Y., Yui, N., Mamiya, W., Sakai, R., Yabuhara, Y., Miyazaki, T., Utsumi, S., Kishida, O., and Uno, H. 2020. A multistate mark–recapture approach to characterize stream fish movement at multiple spatial scales. Canadian Journal of Fisheries and Aquatic Sciences **77**(6): 1090-1100.

Kemp, P., Sear, D., Collins, A., Naden, P., and Jones, I. 2011. The impacts of fine sediment on riverine fish. Hydrological Processes **25**(11): 1800-1821.

Kendall, W.L. 1999. Robustness of closed capture–recapture methods to violations of the closure assumption. Ecology **80**(8): 2517-2525.

Kendall, W.L., Nichols, J.D., and Hines, J.E. 1997. Estimating temporary emigration using capture–recapture data with Pollock's robust design. Ecology **78**(2): 563-578.

Kendall, W.L., White, G.C., and Langtimm, C.A. In Review. On improving discrete-time hidden Markov mark-recapture models with the use of continuous-time auxiliary resightings or dead recoveries.

Kendall, W.L., White, G.C., Hines, J.E., Langtimm, C.A., and Yoshizaki, J. 2012. Estimating parameters of hidden Markov models based on marked individuals: use of robust design data. Ecology **93**(4): 913-920.

Kendall, W.L., Barker, R.J., White, G.C., Lindberg, M.S., Langtimm, C.A., and Peñaloza, C.L. 2013. Combining dead recovery, auxiliary observations and robust design data to estimate demographic parameters from marked individuals. Methods in Ecology and Evolution **4**(9): 828-835.

Kendall, W.L., Stapleton, S., White, G.C., Richardson, J.I., Pearson, K.N., and Mason, P. 2019. A multistate open robust design: population dynamics, reproductive effort, and phenology of sea turtles from tagging data. Ecological Monographs **89**(1): e01329.

King, R., McClintock, B.T., Kidney, D., and Borchers, D. 2016. Capture–recapture abundance estimation using a semi-complete data likelihood approach. The Annals of Applied Statistics **10**(1): 264-285.

Korman, J., Yard, M., Walters, C., and Coggins, L.G. 2009. Effects of fish size, habitat, flow, and density on capture probabilities of age-0 rainbow trout estimated from electrofishing at discrete sites in a large river. Transactions of the American Fisheries Society **138**(1): 58-75.

Korman, J., Yard, M.D., Dzul, M.C., Yackulic, C.B., Dodrill, M.J., Deemer, B.R., and Kennedy, T.A. 2021. Changes in prey, turbidity, and competition reduce somatic growth and cause the collapse of a fish population. Ecological Monographs **91**(1): e01427.

Krabbenhoft, T.J., Platania, S.P., and Turner, T.F. 2014. Interannual variation in reproductive phenology in a riverine fish assemblage: implications for predicting the effects of climate change and altered flow regimes. Freshwater Biology **59**(8): 1744-1754.

Langtimm, C.A. 2009. Non-random temporary emigration and the robust design: conditions for bias at the end of a time series. *In* Modeling demographic processes in marked populations. Springer. pp. 745-761.

Lehuta, S., Mahévas, S., Petitgas, P., and Pelletier, D. 2010. Combining sensitivity and uncertainty analysis to evaluate the impact of management measures with ISIS–Fish: marine protected areas for the Bay of Biscay anchovy (Engraulis encrasicolus) fishery. ICES Journal of Marine Science **67**(5): 1063-1075.

Lundberg, P. 1988. The evolution of partial migration in birds. Trends in ecology & evolution **3**(7): 172-175.

Macbeth, G.M., Broderick, D., Ovenden, J.R., and Buckworth, R.C. 2011. Likelihood-based genetic mark–recapture estimates when genotype samples are incomplete and contain typing errors. Theoretical population biology **80**(3): 185-196.

MacDonald, I.L., and Zucchini, W. 1997. Hidden Markov and other models for discrete-valued time series. CRC Press.

MacKenzie, D.I., Nichols, J.D., Sutton, N., Kawanishi, K., and Bailey, L.L. 2005. Improving inferences in population studies of rare species that are detected imperfectly. Ecology **86**(5): 1101-1113.

Marco-Rius, F., Caballero, P., Morán, P., and Garcia de Leaniz, C. 2013. Can migrants escape from density dependence? Ecology and Evolution **3**(8): 2524-2534.

Marsh, P.C. 1985. Effect of incubation temperature on survival of embryos of native Colorado River fishes. The Southwestern Naturalist: 129-140.

Marsh, P.C., and Douglas, M.E. 1997. Predation by introduced fishes on endangered humpback chub and other native species in the Little Colorado River, Arizona. Transactions of the American Fisheries Society **126**: 343-346.

Maxwell, D., and Jennings, S. 2005. Power of monitoring programmes to detect decline and recovery of rare and vulnerable fish. Journal of Applied Ecology **42**(1): 25-37.

McDonald, T.L., and Amstrup, S.C. 2001. Estimation of population size using open capture-recapture models. Journal of Agricultural, Biological, and Environmental Statistics **6**(2): 206.

McDonald, T.L., Amstrup, S.C., Regehr, E.V., and Manly, B.F. 2005. Examples. *In* Handbook of capture-recapture analysis. *Edited by* S.C. Amstrup, T.L McDonald, B.F. Manly. Princeton University Press, Princeton.

Mehner, T. 2015. Partial diel vertical migration of sympatric vendace (Coregonus albula) and Fontane cisco (Coregonus fontanae) is driven by density dependence. Canadian Journal of Fisheries and Aquatic Sciences **72**(1): 116-124.

Michel, C.J., Ammann, A.J., Lindley, S.T., Sandstrom, P.T., Chapman, E.D., Thomas, M.J., Singer, G.P., Klimley, A.P., and MacFarlane, R.B. 2015. Chinook salmon outmigration survival in wet and dry years in California's Sacramento River. Canadian Journal of Fisheries and Aquatic Sciences **72**(11): 1749-1759.

Millar, C.P., Fryer, R.J., Millidine, K.J., and Malcolm, I.A. 2016. Modelling capture probability of Atlantic salmon (Salmo salar) from a diverse national electrofishing dataset: Implications for the estimation of abundance. Fisheries research **177**: 1-12.

Minckley, W.L., and Meffe, G.K. 1987. Differential selection by flooding in stream-fish communities of the arid American Southwest. Community and evolutionary ecology of North American stream fishes. University of Oklahoma Press, Norman: 93-104.

Morita, K., Yamamoto, S., and Hoshino, N. 2000. Extreme life history change of white-spotted char (Salvelinus leucomaenis) after damming. Canadian Journal of Fisheries and Aquatic Sciences **57**(6): 1300-1306.

Morris, J.A., Shertzer, K.W., and Rice, J.A. 2011. A stage-based matrix population model of invasive lionfish with implications for control. Biological Invasions **13**(1): 7-12.
Neel, M.C., Leidner, A.K., Haines, A., Goble, D.D., and Scott, J.M. 2012. By the numbers: How is recovery defined by the US Endangered Species Act? BioScience **62**(7): 646-657.
Nelson, M.L., McMahon, T.E., and Thurow, R.F. 2002. Decline of the migratory form in bull charr, Salvelinus confluentus, and implications for conservation. *In* Ecology, behaviour and conservation of the charrs, genus Salvelinus. Springer. pp. 321-332.
Nilsson, A.L., Lindström, Å., Jonzén, N., Nilsson, S.G., and Karlsson, L. 2006. The effect of climate change on partial migration–the blue tit paradox. Global Change Biology **12**(10): 2014-2022.
Nuno, A., Milner-Gulland, E., and Bunnefeld, N. 2015. Detecting abundance trends under uncertainty: the influence of budget, observation error and environmental change. Animal conservation **18**(4): 331-340.
O'Donnell, M.J., Horton, G.E., and Letcher, B.H. 2010. Use of portable antennas to estimate abundance of PIT-tagged fish in small streams: factors affecting detection probability. North American Journal of Fisheries Management **30**(2): 323-336.
Olden, J.D., Poff, N.L., and Bestgen, K.R. 2006. Life-history strategies predict fish invasions and extirpations in the Colorado River Basin. Ecological Monographs **76**(1): 25-40.
Olsson, I.C., Greenberg, L.A., Bergman, E., and Wysujack, K. 2006. Environmentally induced migration: the importance of food. Ecology letters **9**(6): 645-651.
Ortlepp, J., and Mürle, U. 2003. Effects of experimental flooding on brown trout (Salmo trutta fario L.): The River Spöl, Swiss National Park. Aquatic Sciences **65**(3): 232-238.
Osmundson, D., Ryel, R.J., Lamarra, V., and Pitlick, J. 2002. Flow-sediment-biota relations: implications for river regulation effects on native fish abundance. Ecological Applications **12**(6): 1719-1739.
Osmundson, D.B., and White, G.C. 2017. Long-term mark-recapture monitoring of a Colorado Pikeminnow Ptychocheilus lucius population: assessing recovery progress using demographic trends. Endangered Species Research **34**: 131-147.
Otis, D.L., Burnham, K.P., White, G.C., and Anderson, D.R. 1978. Statistical inference from capture data on closed animal populations. Wildlife Monographs(62): 3-135.
Pearson, K.N., Kendall, W.L., Winkelman, D.L., and Persons, W.R. 2015. Evidence for skipped spawning in a potamodromous cyprinid, humpback chub (Gila cypha), with implications for demographic parameter estimates. Fisheries Research **170**: 50-59.
Pearson, K.N., Kendall, W.L., Winkelman, D.L., and Persons, W.R. 2016. Tradeoffs between physical captures and PIT tag antenna array detections: A case study for the Lower Colorado River Basin population of humpback chub (Gila cypha). Fisheries Research **183**: 263-274.
Peñaloza, C.L., Kendall, W.L., and Langtimm, C.A. 2014. Reducing bias in survival under nonrandom temporary emigration. Ecological Applications **24**(5): 1155-1166.
Pennock, C.A., Cathcart, C.N., Hedden, S.C., Weber, R.E., and Gido, K.B. 2018. Fine-scale movement and habitat use of a prairie stream fish assemblage. Oecologia **186**(3): 831-842.
Pine, W.E., Hightower, J.E., Coggins, L.G., Lauretta, M.V., and Pollock, K.H. 2012. Design and analysis of tagging studies. Fisheries techniques, 3rd edition. American Fisheries Society, Bethesda, Maryland: 521-572.

Piper, A.T., Wright, R.M., Walker, A.M., and Kemp, P.S. 2013. Escapement, route choice, barrier passage and entrainment of seaward migrating European eel, Anguilla anguilla, within a highly regulated lowland river. Ecological Engineering **57**: 88-96.
Plummer, M. JAGS: A program for analysis of Bayesian graphical models using Gibbs sampling. *In* Proceedings of the 3rd international workshop on distributed statistical computing. 2003. Technische Universit at Wien. p. 125.
Plummer, M. 2016. rjags: Bayesian graphical models using MCMC. R package version 4-6. . Available from https://CRAN.R-project.org/package=rjags [accessed.
Poff, N.L., Allan, J.D., Bain, M.B., Karr, J.R., Prestegaard, K.L., Richter, B.D., Sparks, R.E., and Stromberg, J.C. 1997. The natural flow regime. BioScience **47**(11): 769-784.
Pollock, K.H. 1982. A capture-recapture design robust to unequal probability of capture. The Journal of Wildlife Management **46**(3): 752-757.
Pradel, R. 2005. Multievent: an extension of multistate capture–recapture models to uncertain states. Biometrics **61**(2): 442-447.
Propst, D.L., and Gido, K.B. 2004. Responses of native and nonnative fishes to natural flow regime mimicry in the San Juan River. Transactions of the American Fisheries Society **133**(4): 922-931.
R Core Development Team. 2012. R: A language and environment for statistical computing. R Foundation for Statistical Computing, Vienna.
R Core Development Team. 2020. R: A language and environment for statistical computing

R Foundation for Statistical Computing, Vienna.
Raabe, J.K., Gardner, B., and Hightower, J.E. 2013. A spatial capture–recapture model to estimate fish survival and location from linear continuous monitoring arrays. Canadian Journal of Fisheries and Aquatic Sciences **71**(1): 120-130.
Robinson, A.T., and Childs, M.R. 2001. Juvenile growth of native fishes in the Little Colorado River and in a thermally modified portion of the Colorado River. North American Journal of Fisheries Management **21**: 809-815.
Robinson, A.T., Clarkson, R.W., and Forrest, R.E. 1998. Dispersal of larval fishes in a regulated river tributary. Transactions of the American Fisheries Society **127**(5): 772-786.
Rosenfeld, J.S. 2017. Developing flow–ecology relationships: Implications of nonlinear biological responses for water management. Freshwater Biology **62**(8): 1305-1324.
Rudershausen, P.J., Buckel, J.A., Dubreuil, T., Donnell, M.O., Hightower, J.E., Poland, S.J., and Letcher, B.H. 2014. Estimating movement and survival rates of a small saltwater fish using autonomous antenna receiver arrays and passive integrated transponder tags. Marine Ecology Progress Series **499**: 177-192.
Ryel, R., and Valdez, R.A. 1995. Movement of Humpback Chub in the Colorado River, Grand Canyon, Arizona. North American Journal of Fisheries Management.
Schaub, M., and Abadi, F. 2011. Integrated population models: a novel analysis framework for deeper insights into population dynamics. Journal of Ornithology **152**(1): 227-237.
Schindler, D.E., Hilborn, R., Chasco, B., Boatright, C.P., Quinn, T.P., Rogers, L.A., and Webster, M.S. 2010. Population diversity and the portfolio effect in an exploited species. Nature **465**(7298): 609-612.
Schooley, J.D., Karam, A.P., Kesner, B.R., Marsh, P.C., Pacey, C.A., and Thornbrugh, D.J. 2008. Detection of larval remains after consumption by fishes. Transactions of the American Fisheries Society **137**(4): 1044-1049.

Schwarz, C.J., Schweigert, J.F., and Arnason, A.N. 1993. Estimating migration rates using tag-recovery data. Biometrics: 177-193.
Secor, D.H. 2007a. Do some Atlantic bluefin tuna skip spawning. Col Vol Sci Pap ICCAT **60**(4): 1141-1153.
Secor, D.H. 2007b. The year-class phenomenon and the storage effect in marine fishes. Journal of Sea Research **57**(2-3): 91-103.
Skalski, J.R., Townsend, R., Lady, J., Giorgi, A.E., Stevenson, J.R., and McDonald, R.D. 2002. Estimating route-specific passage and survival probabilities at a hydroelectric project from smolt radiotelemetry studies. Canadian Journal of Fisheries and Aquatic Sciences **59**(8): 1385-1393.
Skov, C., Baktoft, H., Brodersen, J., Brönmark, C., Chapman, B.B., Hansson, L.-A., and Nilsson, P.A. 2011. Sizing up your enemy: individual predation vulnerability predicts migratory probability. Proceedings of the Royal Society B: Biological Sciences **278**(1710): 1414-1418.
Skov, C., Chapman, B.B., Baktoft, H., Brodersen, J., Brönmark, C., Hansson, L.-A., Hulthén, K., and Nilsson, P.A. 2013. Migration confers survival benefits against avian predators for partially migratory freshwater fish. Biology letters **9**(2): 20121178.
Sloat, M.R., Baker, P.F., and Ligon, F.K. 2011. Estimating habitat-specific abundances of PIT-tagged juvenile salmonids using mobile antennas: a comparison with standard electrofishing techniques in a small stream. North American Journal of Fisheries Management **31**(5): 986-993.
Spurgeon, J.J., Paukert, C.P., Healy, B.D., Trammell, M., Speas, D., and Omana-Smith, E. 2015. Translocation of Humpback Chub into tributary streams of the Colorado River: implications for conservation of large-river fishes. Transactions of the American Fisheries Society **144**(3): 502-514.
Stan Development Team. 2013. Stan: A C++ library for probability and sampling, Version 2.4.0.
Stan Development Team. 2020. RStan: the R interface to Stan. R package version 2.21.2. http://mc-stan.org/.
Stone, D. 2010. Overriding effects of species-specific turbidity thresholds on hoop-net catch rates of native fishes in the Little Colorado River, Arizona. Transactions of the American Fisheries Society **139**: 1150-1170.
Stone, D.M., and Gorman, O.T. 2006. Ontogenesis of endangered humpback chub (*Gila cypha*) in the Little Colorado River, Arizona. American Midland Naturalist **155**(123-135).
Stout, J.B., Conner, M.M., Budy, P., Mackinnon, P.D., and McKinstry, M.C. 2020. Keeping it classy: Classification of live fish and ghost PIT tags detected with a mobile PIT tag interrogation system using an innovative analytical approach. Canadian Journal of Fisheries and Aquatic Sciences(ja).
Terui, A., Ishiyama, N., Urabe, H., Ono, S., Finlay, J.C., and Nakamura, F. 2018. Metapopulation stability in branching river networks. Proceedings of the National Academy of Sciences **115**(26): E5963-E5969.
Topping, D.J., Rubin, D.M., and Vierra Jr, L. 2000. Colorado River sediment transport: 1. Natural sediment supply limitation and the influence of Glen Canyon Dam. Water Resources Research **36**(2): 515-542.
Udall, B., and Overpeck, J. 2017. The twenty-first century Colorado River hot drought and implications for the future. Water Resources Research **53**(3): 2404-2418.

USFWS. 2002. Humpback chub (*Gila cypha*) Recovery Goals: amendment and supplement to the Humpback Chub Recovery Plan., Denver, Colorado.
Van Haverbeke, D.R., Stone, D.M., Coggins, L.G., and Pillow, M.J. 2013. Long-term monitoring of an endangered desert fish and factors influencing population dynamics. Journal of Fish and Wildlife Management **4**(1).
Van Haverbeke, D.R., Stone, D.M., Dodrill, M.J., Young, K.L., and Pillow, M.J. 2018. Population expansion of humpback chub in western Grand Canyon and hypothesized mechanisms. **Southwest Naturalist.**
Vélez-Espino, L.A., McLaughlin, R.L., and Robillard, M. 2013. Ecological advantages of partial migration as a conditional strategy. Theoretical Population Biology **85**: 1-11.
Venables, W.N., and Ripley, B.D. (eds). 2002. Modern Applied Statistics with S. 4 ed. Springer, New York.
Walters, C.J. 1986. Adaptive management of renewable resources. Macmillan Publishers Ltd.
Ward, D., Childs, M., and Persons, W. 2008. PIT tag retention and tag induced mortality in juvenile bonytail and Gila chub. Fisheries Management and Ecology **15**(2): 159-161.
Ward, D.L., Persons, W.R., Young, K.L., Stone, D.M., Vanhaverbeke, D.R., and Knight, W.K. 2015. A laboratory evaluation of tagging-related mortality and tag loss in juvenile Humpback Chub. North American journal of fisheries management **35**(1): 135-140.
Ward, J.V., and Stanford, J. 1995. Ecological connectivity in alluvial river ecosystems and its disruption by flow regulation. River Research and Applications **11**(1): 105-119.
Warner, R.R., and Chesson, P.L. 1985. Coexistence mediated by recruitment fluctuations: a field guide to the storage effect. The American Naturalist **125**(6): 769-787.
Watanabe, S. 2010. Asymptotic equivalence of Bayes cross validation and widely applicable information criterion in singular learning theory. The Journal of Machine Learning Research **11**: 3571-3594.
Williams, B.K., Nichols, J.D., and Conroy, M.J. 2002. Analysis and management of animal populations. Academic Press.
Winemiller, K.O. 2005. Life history strategies, population regulation, and implications for fisheries management. Canadian Journal of Fisheries and Aquatic Sciences **62**(4): 872-885.
Winemiller, K.O., and Rose, K.A. 1992. Patterns of life-history diversification in North American fishes: implications for population regulation. Canadian Journal of Fisheries and aquatic sciences **49**(10): 2196-2218.
Wolter, M.H., DeBoom, C.S., and Wahl, D.H. 2013. Field and laboratory evaluation of dam escapement of Muskellunge. North American Journal of Fisheries Management **33**(4): 829-838.
Wood, C. 1987. Predation of juvenile Pacific salmon by the common merganser (Mergus merganser) on eastern Vancouver Island. I: Predation during the seaward migration. Canadian Journal of Fisheries and Aquatic Sciences **44**(5): 941-949.
Wright, S.A., Anderson, C.R., and Voichick, N. 2009. A simplified water temperature model for the Colorado River below Glen Canyon Dam. River Research and Applications **25**(6): 675-686.
Yackulic, C.B., Blake, S., and Bastille-Rousseau, G. 2017. Benefits of the destinations, not costs of the journeys, shape partial migration patterns. Journal of Animal Ecology **86**(4): 972-982.

Yackulic, C.B., Yard, M.D., Korman, J., and Haverbeke, D.R. 2014. A quantitative life history of endangered humpback chub that spawn in the Little Colorado River: variation in movement, growth, and survival. Ecology and Evolution.

Yackulic, C.B., Korman, J., Yard, M., and Dzul, M.C. 2018. Inferring species interactions through joint mark-recapture analysis. Ecology.

Yackulic, C.B., Dodrill, M., Dzul, M., Sanderlin, J.S., and Reid, J.A. 2020. A need for speed in Bayesian population models: a practical guide to marginalizing and recovering discrete latent states. Ecological Applications.

Yard, M.D., L.G. Coggins, and C.V. Baxter, G.E.B., J. Korman. 2011. Trout piscivory in the Colorado River, Grand Canyon: Effects of turbidity, temperature, and fish prey availability. Transactions of the American Fisheries Society **140**: 471-486.

Yarnell, S.M., Viers, J.H., and Mount, J.F. 2010. Ecology and management of the spring snowmelt recession. BioScience **60**(2): 114-127.

Zydlewski, G.B., Horton, G., Dubreuil, T., Letcher, B., Casey, S., and Zydlewski, J. 2006. Remote monitoring of fish in small streams: a unified approach using PIT tags. Fisheries **31**(10): 492-502.

Appendix A

Field methods for humpback chub sampling

Sampling of the observable CR included data collected by biologists as part of both the Near Shore Ecology (NSE, 2009–2011) and the Juvenile Chub Monitoring (JCM, 2012– 2019) projects. The sampling design of JCM trips was modified in 2017, so that the spatial extent of sampling and number of trips differed between 2012-2016 and 2017-2019. All projects sampled a reach of the CR located approximately 1 km below the LCR confluence, though the size of the sampling reach in the CR differed across projects as follows and is described as river kilometers (rkm) below Glen Canyon Dam: rkm 127-131 (NSE), rkm 127-129.7 (JCM 2012-2016), and rkm 126-131.2 (JCM 2017-2019). For data analysis, the boundaries of the sampling reach from 2012-2016 were used to define the observable CR reach (Figure 1), and all fish captured outside the original reach boundary in 2009-2011 or 2017-2019 were treated as being from the unobservable CR (i.e., only the original marking occasion was in the data set and no information about recaptures was included in these reaches). Sampling during NSE trips occurred in July, August, September, and October, whereas sampling for JCM trips occurred in January, April, July, and September (except no January 2012 trip; 2012-2016) or April/May, June/July, or September/October (2017-2019). Trips that occurred in January, June/July, or August were not used in the data analysis.

Both the NSE and JCM trips used two gear types: 47–90 unbaited hoop nets (6 mm nylon mesh, 50–60 cm diameter, 1 m long, single 10-cm throat) checked once a day, and nighttime slow-speed boat electrofishing (pulsed DC current, 15–20 amps, 200–300 volts, average boat speed of 0.14 m/s). NSE trips included 12 passes of hoop nets (45-60 hoopnets/day) and 3-5 electrofishing passes. JCM trips included either 9 hoop net passes (80 hoop nets/day) and 3

electrofishing passes (2012-2016) or 6 hoop net passes (120 hoop nets/day) and 3 electrofishing passes (2017-2019). During the 2012-2016 JCM study there were also additional fast boat electrofishing passes (boat speed of 0.33 m/s). During both NSE and JCM studies, all humpback chub were measured for total length (TL), scanned for prior marks, and, if appropriate, marked. The minimum length of marking was either 100mm TL (2009-2016) or 80mm TL (2017-2019). All chub >80mm TL or >100 mm TL that did not already have a 134.2 kHz passive integrated transponder (PIT) tag received a PIT tag with a unique alphanumeric code allowing future identification of individual fish. Juvenile chub >40mm TL that were too small to be PIT tagged received a visible implant elastomer (VIE) mark that identified the current sampling trip. The fish handling protocol is described in more detail in Persons et al. (2015).

In addition to physical captures, fish in the observable CR could also be detected on antennas. Specifically, eight moveable, submersible antennas (Biomark Inc., Boise, ID) were used as an additional gear type in fall of 2016 and 2018. These submersible antennas are deployed broadly throughout the sampled JCM reach (250 m x 32 sites). A set of four antennas were downloaded, moved and redeployed daily along the shoreline to new site locations. The subsequent set of four were moved the following day. Antennas were baited and changed daily using a fish attractant (AquaMax®) with no excess. Each submersible was anchored offshore approximately 10 to 20 m with a float so that it was suspended at 2 to 5 m depths. For each trip, a total of 32 sites were sampled for a 24 to 48 hr deployment period. Submersible antennas were redeployed in new sites (left and right bank) that are at least 250 m apart in distance.

Outside the JCM sampling reach in the unobservable CR (rkm 105.5- 127.0 and 129.7-145.7), certain portions of the CR were sampled in some years, but these data were difficult to include in the model because sites were not fixed and this introduced problems with capture

heterogeneity (since only fish in the sampled segments can be captured). Thus, recapture information was not used outside the JCM reach. However, since the hidden Markov model structure conditions on first capture, we could easily include information about the first captures without violating assumptions required for mark-recapture. Thus, in the unobservable CR, humpback chub could be first captured (i.e., marked) in either April/May (spring) or September/October (fall). Typically, fish from the unobservable CR were captured as part of Humpback Chub Aggregations trips (Van Haverbeke et al. 2018) or as part of NSE or JCM trips in areas outside the rkm 127-129.7, including a reach above the LCR confluence that was systematically monitored by JCM trips from 2012-2016 (rkm 121.9-123.5).

In the LCR, sampling included spring and fall monitoring trips of the lower 13.56 rkm of the LCR. The lower 13.56 km was divided into three sampling reaches: lower (rkm 0 -5), middle (rkm 5-10.5), and upper (rkm 10.5-13.56). Spring trips typically occurred in mid-April and mid-May, exceptions were 2010 (mid-May, early June), 2011 (early May, late May), and 2017 (mid-April, mid-June) when floods or logistical issues caused delays in sampling. During each sampling trip, each reach was divided into three equal subreaches (nine subreaches total), and each subreach was sampled with three passes of hoop nets. The three hoop net passes for each subreach occurred on consecutive days, and each pass consisted of 20 nets set for ~24 hours. Hoop nets were similar to those used in the CR (see above paragraph). For some trips, sampling efforts were shortened by 1-3 days due to logistical issues and(or) floods. Fish handling protocols were similar to CR trips, with the exception that adult humpback chub were systematically checked for ripeness. Antenna detections in the LCR included detections from a stationary multiplexer system (MUX) installed at rkm 1.78 in May 2009. Difficulties of powering the MUX through winter preclude its use in 2009-2011, but detection data in spring of

2012-2018 were used in the model. In spring 2019, antenna detections in the LCR were from seven continuously-operating, shore-based antennas (Marsh and Associates) deployed between rkm 1.3 – 2.1.

Appendix B

Bias of using a hidden Markov model for continuous resight data

B.1 Methods

We simulated eight years of mark-recapture data and then fit a hidden Markov mark-recapture model. Similar to the applied model described in the accompanying paper, the model included five biological states which corresponded with resident, observable Colorado River migrant, unobservable Colorado River migrant, observable Colorado River skipped migrant and unobservable Colorado River skipped migrant. Unlike the applied model, the simulated model only included one demographic state. All parameters with random effects were modeled on the logit-scale, but we present the means of these parameters on the real scale to help with interpretability. For all simulations, we modeled yearly survival and state transition probabilities as random effects with a shared mean and standard deviation set to 0.5. Survival probabilities were also unique to season, which included winter (Oct-Apr) and summer (Apr-Oct). Season-specific mean survival and transition probabilities were modeled as coming from a uniform distribution on the real scale, then logit-transformed. The bounds of these uniform distributions were : 40-100% (winter survival of residents), 90-99% (summer survival of residents), 5-20% (resident to migrant transition), 30-70% (migrant to skipped migrant transition), and 30-70% (skipped migrant to migrant transition). Survival of skipped migrants was set equal to that of migrants and differed according to scenario described below.

We first simulated the states of individual fish, where the simulated population started with 10,000 individuals in the first year. After the first year, abundance was the number of surviving fish from the first year plus an additional recruitment of 1,000 fish each year. Yearly

initial starting probabilities and capture probabilities were modeled as temporally-varying random effects with standard deviation equal to 0.5. For each simulation, mean starting probabilities were randomly selected from a normal distribution with standard deviation set to 1. These means are described on the logit-scale and set to -1 (i.e., 26.9% probability fish is skipped migrant given fall CR capture), -2 (i.e., 11.9% probability fish is skipped migrant given spring CR capture), -1 (i.e., 26.9% probability fish is resident given spring LCR capture), and 1 (i.e, 73.1% probability fish is resident given fall LCR capture). Logit-transformed fall capture probabilities were centered on -1 (i.e., 26.9% for LCR) and -3 (i.e., 4.7% for observable Colorado River). Spring captures were modeled as robust design with four passes, similar to what is described in the applied model of the accompanying paper. The logit-scale mean for each pass-specific capture probability was set to -2, which translates to an across-trip capture probability of ~40% for fish that are available for both spring sampling trips. The detection probability of the multiplexer array differed for each year and was drawn from a uniform distribution (10-70%). The availability parameters corresponded to the probabilities that migrants were available for both spring LCR sampling trips, the first trip only, the second trip only, and not available for capture for either trip. The first three of these availability categories were drawn from a standard normal distribution and transformed using a multinomial logit link. This formulation allows for a wide range of possible availability values. The last availability parameter, or the probability a fish was not available for either spring sampling trip, was calculated by subtraction. The availability of migrants in the LCR in fall was also modeled as a yearly random effect, with mean drawn from a uniform distribution (0.05, 0.3) and standard deviation equal to 0.5.

We ran four different scenarios that were identical except for migrant survival parameters. We ran one scenario where we treated the MUX data as occurring in discrete time. While this assumption is not realistic, it provides a good control for comparing other survival scenarios and we refer to this as the reference scenario. The reference scenario had mean migrant survival probabilities between 45-99% (winter) between 84-99% (summer). The other three survival scenarios treated MUX detection data as continuous and had survival rates for summer and winter drawn from a uniform distribution with bounds 90-99% (high survival scenario), 80-90% (mid survival scenario), and 70-80% (low survival scenario). In these continuous detection scenarios, we changed capture probabilities in the following manner. For fish in the spawning category that died over the winter interval, we randomly chose 2/7 of these fish and exposed them to MUX detection for the following spring sampling. The 2/7 number corresponds to the February and March months in the winter interval (Oct – Apr), and these fish could have been detected on the MUX but died before the spring sampling trips. Note this method assumes that survival within the winter interval is constant. Additionally, we randomly deleted 2/6 (May and June of the May-Oct period) of MUX detections of migrant fish that died over the summer and were detected on the MUX. We ran 50 simulations for each scenario. Each simulation included 3 chains with 500 posterior draws, with first 250 posterior draws acting as burn-in. This resulted in 750 posterior draws for each simulation. For each simulation, we took the mean parameter estimate for each year and estimated bias of the yearly estimates. Since there were 50 simulations, each with 8 years, this led to 400 estimates for each parameter and simulation. Bias was calculated as the estimated value minus the true value.

Simulations were also used to evaluate bias in abundance for the reference and high survival scenarios. For each year in the simulation, state-specific abundances (i.e., abundance of

residents, migrants, and skipped migrants) were calculated. Note that the method used to estimate state-specific abundance must account for state uncertainty and details about the abundance calculation method are provided in Appendix B. Bias was evaluated for total abundance as well as for proportion composition. Total abundance was the summed value for the abundance estimates of residents, migrants, and skipped migrants. This value was estimated for all years in all simulations, for a total of 400 estimates. Bias for total abundance is calculated as relative bias, which was calculated as the estimated value minus the true value divided by the true value. Proportion composition was the proportion of the population that falls into the residents, migrant, and skipped migrant categories. This value was calculated by taking the state-specific abundance and dividing by the total abundance for each category. Due to dependency in proportion among the different years within a simulation, the proportion composition was the mean proportion for all eight years within a simulation. Thus, there were 50 simulations used to assess bias in the proportion composition estimate. For proportion composition, bias is presented as the estimated value minus the true value.

B.2. Results

The reference scenario resulted in no detectable bias in survival or state transition parameters. In contrast, the continuous detection scenarios did show bias, and the magnitude of the bias was always lowest for the high survival scenario, followed by the mid-survival scenario and the low survival scenario (Figure S1, Figure S2). Biases in survival were low compared to biases in state transition parameters. As expected, biases in migrant survival were of higher magnitude than biases in resident survival. For both residents and migrants, there was a seasonal trend in the direction of bias, where the model would over estimate summer survival and

underestimate winter survival. In the worst case (i.e., low survival) scenario, mean bias was 0.00 (resident summer), -0.05 (resident winter), +0.08 (migrant summer), and -0.04 (migrant winter). The high survival scenario is closest to what was observed in our applied example (where seasonal estimates among demographic groups ranged from 89-98%). In the high survival scenario, means for season bias was +0.01 (resident summer), 0.00 (resident winter), +0.01 (migrant summer), and -0.01 (migrant winter). Bias in transition parameters was more problematic. In the low survival scenario, mean biases were +0.08 (resident to migrant), -0.15 (migrant to skipped migrant), and +0.08 (skipped migrant to migrant). In the high survival scenario, mean biases were +0.03 (resident to migrant), -0.02 (migrant to skipped migrant), and +0.03 (skipped migrant to migrant).

For abundance, both median and mean bias were estimated, and the first value reported is always the median and the second value is the mean. For the reference scenario, relative bias in total abundance was negative (-3% & -7%). Biases were as follows for proportions: residents (0.00 & +0.01) migrants (0.00 & -0.01) and skipped migrants (0.00 & 0.00). Bias in total abundance in the high survival scenario was similar to that of the reference scenario (-3% & -5%). For the proportion of abundance, bias was as follows: residents (0.00 & +0.01), migrants (+0.01 & +0.01), and skipped migrants (-0.02 & -0.02).

This simulation exercise was useful for assessing bias in the current model. Simulations indicate that treating continuous resight data as occurring in discrete time does indeed result in bias, but that this bias is minimal when survival is high. While we expected biases in survival, the consistent difference in the directionality of bias (i.e., + or -) across seasons would indicate that annual survival estimates should be less biased than season-specific estimates. The bias in

the state transition parameters was not expected and underlines the importance of running simulation models to help assess bias and interpret model results.

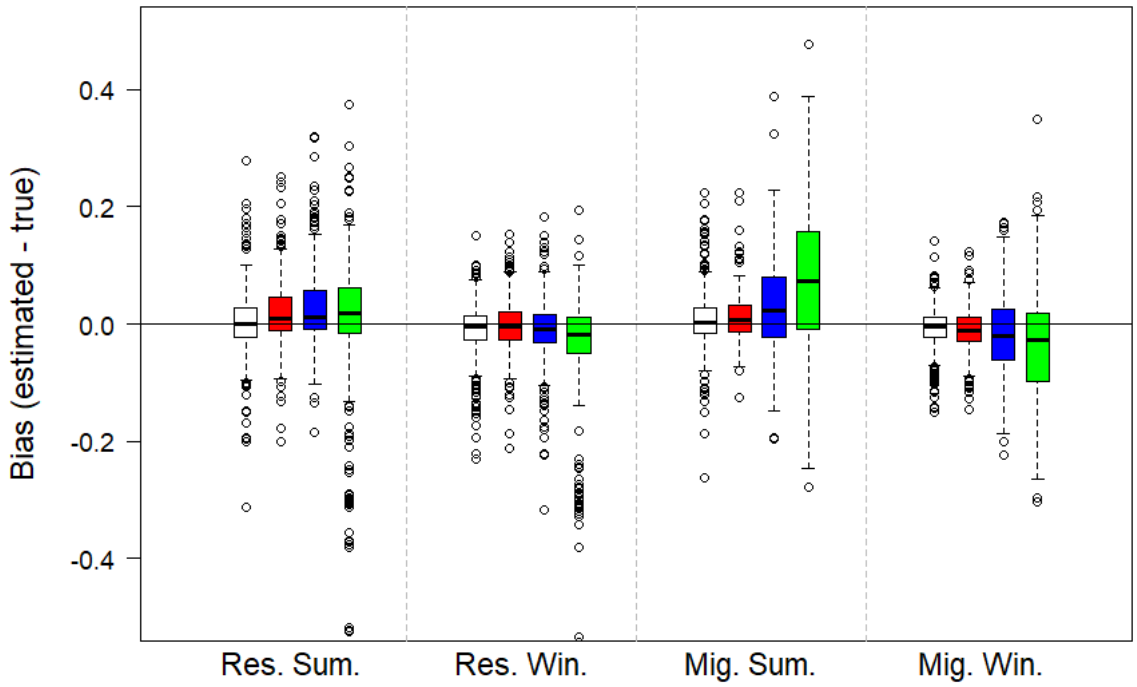

FIGURE B1. Bias in survival probabilities for four different simulation scenarios: reference (white), high survival (red), mid survival (blue), and low survival (green). The boxplots illustrate how these biases differ for two different states, residents (Res.) and migrants (Mig.), and for two different seasons, summer (Sum.) and winter (Win.). Bias is calculated as the estimated value minus the true value. The bold lines in each boxplot correspond to the median, the lower and upper sides of the rectangle are the 25% and 75% quantiles, respectively. The dotted lines extend 1.5 times the interquartile range above and below the 75% and 25% quartiles, resp.

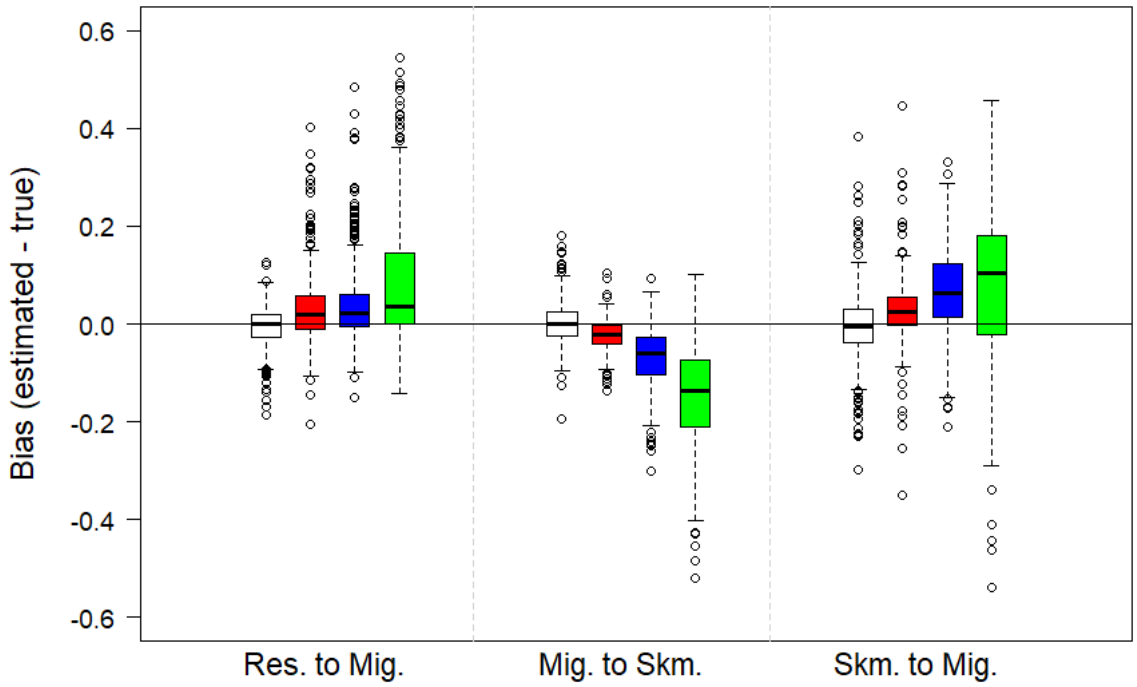

FIGURE B2. Bias in state transition probabilities for four different simulation scenarios: reference (white), high survival (red), mid survival (blue), and low survival (green). The boxplots illustrate how these biases differ for the following state transitions: resident to migrant (Res. to Spa.), migrant to skipped migrant (Mig. to Skm.), and skipped migrant to migrant (Skm. to Mig.). Bias is calculated as the estimated value minus the true value. The bold lines in each boxplot correspond to the median, the lower and upper sides of the rectangle are the 25% and 75% quantiles, respectively. The dotted lines extend 1.5 times the interquartile range above and below the 75% and 25% quartiles, resp.

Appendix C

Estimating state-specific abundances (with state uncertainty)

The state transition matrix ($\boldsymbol{\psi}$), the initial state assignment vector ($\boldsymbol{\pi}$), and the capture probability matrices were reconstructed for each posterior draw of the skipped migration model using parameter estimates from that posterior draw. The next step required obtaining an estimate of catch for each state, and this step was not straight-forward because many of the states were not observable and often fish could not be definitively assigned to a single state. State-specific catch estimates were calculated for each row of the capture history matrix, as described below.

For each unique capture history, matrices were used to calculate conditional likelihoods for each possible state (e.g., Eq 14-17 in main paper), starting at the initial capture occasion for that particular capture history and ending at the last sampling occasion. Specifically, the length of conditional likelihood vector was the number of possible states (in our applied example this was 21), and each element within the conditional likelihood vector corresponded to the probability of the observed capture history for that specific sampling occasion conditional on fish belonging to that particular state. If a fish was physically captured during a capture occasion (with or without antenna detection), the conditional likelihood vector was rescaled (to sum to one) by dividing each element within the vector by the sum of the vector. We refer to the rescaled conditional likelihood vector as the state probability vector. The state probability vector was multiplied by the number of fish with that particular capture probability to estimate the 'catch' of individuals (with that capture history) that belonged to each state. Note that, often, this state-specific catch did not have an integer value. For example, if the state probability vector predicted that for the first interval of a particular capture history there was a 50% chance of fish

being a state 1 and 50% state 2 and only 3 fish had this capture history, this would result in state-specific catch of 1.5 (state 1) and 1.5 (state 2).

State-specific catch estimates were summed across all possible capture histories. Then, abundance was estimated by adding state-specific catch to a random draw from the negative binomial distribution. The parameters for the negative binomial distribution were the number of successes (i.e., the state-specific catch estimate) and the probability of success (i.e., state-specific capture probability). Using random draws from a negative binomial distribution represents one method for estimating abundance in Bayesian models and is a good alternative to data augmentation (King et al. 2016), particularly when capture probabilities are low and the number of animals is high. Mean and 95% credible intervals for state-specific abundance can then be calculated using estimates across all posterior draws. Evaluation of bias for the above-described method in the current study is presented in Appendix B.

Appendix D

Stan code for skipped migration model

Part 1 – R code (data processing – import data here:)

```
chubdat<- read.csv() #load data here
clchubdat<- read.csv() #load data here


#Convert flat file to data format used by model (closed model):
spr_ind<-which(substr(names(chubdat,1,2)== “SP”))
fall_ind<- which(substr(names(chubdat,1,2)== “FA”))

Ntot= dim(chubdat)[1]
Ny= length(spr_ind)
CH_spring<-chubdat[,spr_ind]
CH_fall<-chubdat[,fall_ind]


clchubdat$row_col<-paste(clchubdat$row, clchubdat$col, sep=" ")
urow_col<-unique(clchubdat$row_col)
cCHstartX<-array(0, dim=c(Ntot, Ny-1))
cCHendX<-array(0, dim=c(Ntot, Ny-1))
for(i in 1:length(urow_col)){
        z<-which(clchubdat$row_col==urow_col[i])
        zmin<-min(z)
        zmax<-max(z)
        cCHstartX[clchubdat$row[zmin], clchubdat$col[zmin]]<-zmin
        cCHendX[clchubdat$row[zmax], clchubdat$col[zmax]]<-zmax}


#Create data list for importing into Stan:

Stan.chub.list<-list(
        Ntot= Ntot,
        Ny= Ny,
        freq = chubdat$freq,
        sumf = chubdat$sumf,
        season_release =  chubdat$season_release,
        CH_spring = array(CH_spring,dim=c(Ntot,Ny)),
        CH_fall = array(CH_fall, dim=c(Ntot,Ny-1)),
        flow = c(1.1599,  0.6852, -1.0150, -0.9159,  0.3641,-0.1523,  0.8807, -0.5655,  1.1878,-
1.6288),
        lcr_cap = chubdat$lcr_cap,
```

```
        cr_mux_cap = chubdat$cr_mux_cap,
        Ntot_cl = length(clchubdat$cCHind),
        cCH_ind=clchubdat$cCHind,
        cCH_freq = clchubdat$cCHfreq,
        cCH_start= array(cCHstartX,dim=c(Ntot,Ny-1)),
        cCH_end= array(cCHendX, dim=c(Ntot,Ny-1)),
        cl_ind=chubdat$cl_ind,
        spring_turb=matrix(c(1,0,0,1,0,0,0,0,0,1,
                             0,0,0,0,0,0,0,0,0,0), nrow=2,col=Ny-1, byrow=TRUE),
        fall_lcr_turb=c(1 ,2, 1, 1, 1, 1 ,1, 0 ,0, 0),
        site_ind = c(1,1,2,2),
        size_ind=c(1,2,1,2),
        S_ind=c(1,2,1,2,3,4,3,4,3,4,3,4),
        fall_cr_temp=c(-0.9931, -0.6080,  1.1472, -1.0379, -0.7424,  1.6576,  0.8695,  0.5024,
0.1620, -0.9573),
        ntrip_cr = c(2, 2, 2, 1, 1, 1, 1, 1, 1, 1),
        ntrip_lcr = c(2,2,2,2,2,2,2,2,2,1),
        newtag=chudat$newtag,
        JCM_ind=c(1,1,1,1,1,1,1,1,2,2))
```

#Stan model :

```
data{
	int Ny; // number of years
	int Ntot; // number of unique CHs
	int freq[Ntot];
	int sumf[Ntot];
	int<lower=1, upper=2>  season_release[Ntot];
	int<lower=1, upper=14> CH_spring[Ntot, Ny];
	int<lower=1, upper=10> CH_fall[Ntot, Ny-1];
	int<lower=1, upper=2> lcr_cap[Ntot]; // number of lcr captures in fall for fish 100-199mm TL
	int<lower=1, upper=2> cr_mux_cap[Ntot]; // 1= not captured in cr btwn 100-199mm TL; 2= previously captured in cr 100-
	199mm TL //(therefore must be migrant if first marked in lcr)
	int Ntot_cl;// number of unique secondary ch's for closed periods (for each unique open CH and each year);
	int<lower=1, upper=31> cCH_ind[Ntot_cl]; // indicator for closed CH (1 = 11111 - or detected both passes and Apr & May
	trips & //detected on MUX, see p1_cl for more details)
	int cCH_freq[Ntot_cl]; // number of fish with that particular secondary CH (within the primary CH) in a particular year
	int cCH_start[Ntot, Ny-1]; // indexing for CH_closed_ind and CH_closed_freq - tells the number of unique secondary ch's for
	unique //primary ch (dim1) and year (dim2)
	int cCH_end[Ntot, Ny-1];
	int<lower=0, upper=1> cl_ind[Ntot];// 0 = not observed in spring after marking (excludes spring of marking), 1= observed in
	spring //sometime after marking (and used in closed ch likelihood)
	int<lower=0, upper=1> skip[Ntot,Ny];//index to determine whether or not you can skip the likelihood calculation for the time
	in the //columns (if ch agrees with ch of previous individual)- should hopefully speed things up
	vector[Ny-1] fall_lcr_turb;
	vector[Ny-1] fall_cr_temp;
	vector[Ny-1] spring_turb[2];
	int site_ind[4];// should be 1,1,2,2
	int size_ind[4];//should be 1,2,1,2
	int S_ind[12]; //should be 1,2,1,2,3,4,3,4,3,4,3,4
	real ntrip_cr[Ny-1]; // number of trips in cr in fall
	real ntrip_lcr[Ny-1]; // number of trips in lcr in fall
```

```
        int<lower=0, upper=1> newtag[Ntot]; // 1 = fish given tag at sumf and 0=fish had tag previously
        int JCM_ind[Ny-1]; //1 = sampling confined entirely to JCM reach (2009-2016), 2= sampling outside JCM reach (2017-2018)

        }


parameters{
        vector<lower = 0, upper=1>[12] g; // growth
        vector[8] S_mu[2]; // mean survival
        vector[8] z_S[Ny-1,2]; // survival random effect
        vector[4] S_offset; // survival offset for skipped migrants
        real<lower=0, upper=5> S_sd[4]; // sd for survival random effects
        vector[12] w_mu; // prob of changing migratory status (differs slightly from 'migration prob' described in paper)
        real<lower=0,upper=1> w_sd; // sd of migration status RE
        vector[12] z_w[Ny-1]; // migration status RE
        real<lower=0, upper =1> tau; // prob of being in the uCR given fish is from the CR
        real<lower=0, upper =1> j[8]; // unconditional prob of being female
        vector<lower=0, upper=1>[4] r; // probability of fish being ripe in LCR in spring
        vector[4] p_spring_mu; // mean spring captureof  probabilities
        vector[6] p_fall_mu; // mean fall capture probabilities
        vector<lower=0, upper=5>[2] p_sd; // sd of capture probabilities
        vector[Ny-1] z_p_spring[4]; //RE of spring p-caps
        vector[Ny-1] z_p_fall[4]; // RE of fall p-caps
        real b0[4]; // intercept to determine prob. fish is lcr resident versus migrant at first capture (pi-matrix)
        real b_lcr_cap[4];// how the number of captures between 100-199mm TL in fall in the LCR affects the probability fish is a
        resident at first //marking (pi-matrix) : [1] is for male spring captures, [2] for female spring captures, [3] for male fall captures,
        [4] for female fall captures
        vector[4] a0; // intercept for fall availability (prob migrant is in LCR in fall)
        vector[4] z_a[Ny-1]; //yearly random effect for fall availability
        real<lower=0, upper=5> a_sd; //standard deviation for fall availability
        vector[2] behavior; // behavioral effect (for spring closed model)
        real beta_p_turb; // turbidity effect on LCR captures
        real beta_p_temp; // temperature effect on CR captures
```

```
        vector<lower=0,upper=1>[Ny-1] p_mux; // MUX detection probability
        real<lower=0, upper=5> m_av_sd;  // SD for spring availabilities
        vector[Ny-1] z_av_1[3]; // RE for spring availabilities
        vector[Ny-1] z_av_2[3]; // RE for spring availabilities
        vector[Ny-1] z_av_3[3]; // RE for spring availabilities
        vector[Ny-1] z_av_4[3]; // RE for spring availabilities
        vector[3] m_av_1_mu; //mean for spring availabilities
        vector[3] m_av_2_mu; //mean for spring availabilities
        vector[3] m_av_3_mu; //mean for spring availabilities
        vector[3] m_av_4_mu; //mean for spring availabilities
        vector[11] v_mu; // means for starting probabilities (used in pi-matrix)
        real<lower=0, upper=5> v_sd; //SD for starting probabilities
        vector[Ny-1] z_v[10]; // RE for starting probabilities
        vector[2] b_pi_large; // effect of being large on starting probabilities
        vector<lower=0, upper=1>[4] p_SUB; // submersible antenna detection prob
        real<lower=0, upper=1> tag_loss_rate; // one-time tagloss/mortality rate

        }



transformed parameters {
        matrix[21,21] psi1[Ny-1]; // overwinter transition matrix
        matrix[21,21] psi2[Ny-1]; // oversummer transition matrix
        matrix[14,21] p1_open[Ny-1]; // data model – spring open captures
        matrix[8,21] p2[Ny-1]; // data model -fall captures
        matrix[15,21] p1_cl[Ny]; // data model – spring closed captures
        real<lower=0, upper=1> pi_spring[10,2,2,21,Ny-1];
        real<lower=0, upper=1> pi_fall[10,2,2,21,Ny-1];
        vector[4] a[Ny-1]; //fall availabilities
        real<lower=0, upper=1> S[Ny-1,2,12]; // survival
        real<lower=0, upper=1> w[Ny-1,14]; // movement
```

```
        vector[8] v0[Ny-1]; // intercept term for starting probabilities
        vector<lower=0, upper=1>[13] v[Ny-1]; //starting probabilities
        vector<lower=0, upper=1>[19] p[Ny-1]; // p-caps
        vector<lower=0, upper=1>[6] pc[Ny-1]; // p-stars
        real<lower=0, upper=1> upsm; // unconditional prob of being male given small and not ripe
        real<lower=0, upper=1> upsf; // unconditional prob of being male given small and not ripe
        real<lower=0, upper=1> uplm; // unconditional prob of being male given large and not ripe
        real<lower=0, upper=1> uplf; // unconditional prob of being male given large and not ripe
        vector<lower=0, upper=1>[Ny-1] av[12]; // spring availabilities
        vector[Ny-1] m_av_1[3]; //m-logit transformed availabilities
        vector[Ny-1] m_av_2[3]; //m-logit transformed availabilities
        vector[Ny-1] m_av_3[3]; //m-logit transformed availabilities
        vector[Ny-1] m_av_4[3]; //m-logit transformed availabilities

        //Note: probability of migration is different here from how it's described in the paper
        //Here 'w' is the probability of switching groups (so 'w' for the migrant group is actually one minus the migration probability)
        for(y in 1:(Ny-1)){
                for(i in 1:12) {
                        w[y,i]=inv_logit(w_mu[i] + z_w[y,i]*w_sd);}
                for(k in 13:14){
                        w [ y,k]=0;}
}

        //for capture probabilities, make the p-cap for skipped migrants in the CR in spring an additive offset of that for CR migrants
        for(y in 1:(Ny-1)){
                for(k in 1:2){
                        for(h in 1:8){
                                S[y,k,h] = inv_logit(S_mu[k,h]+z_S[y,k,h]*S_sd[S_ind[h]]);}
                        for(h in 9:12){
                                S[y,k,h] = inv_logit(S_mu[k,h-4]+S_offset[h-8]+z_S[y,k,h-4]*S_sd[S_ind[h]]);}

                        }}
```

```
	//fall p-caps:
	for(y in 1:(Ny-1)){
		p[y,1] = 1-pow(1-inv_logit(p_fall_mu[1] + p_sd[1]*z_p_fall[1,y] + beta_p_turb*fall_lcr_turb[y]),ntrip_lcr[y]);
		p[y,2] = 1-pow(1-inv_logit(p_fall_mu[2] + p_sd[1]*z_p_fall[2,y] + beta_p_turb*fall_lcr_turb[y]),ntrip_lcr[y]);
		p[y,3] = 1-pow(1-inv_logit(p_fall_mu[JCM_ind[y]+2] + p_sd[2]*z_p_fall[3,y] +
beta_p_temp*fall_cr_temp[y]),ntrip_cr[y]);
		p[y,4] = 1-pow(1-inv_logit(p_fall_mu[JCM_ind[y]+4] + p_sd[2]*z_p_fall[4,y] +
beta_p_temp*fall_cr_temp[y]),ntrip_cr[y]);		p[y,5] = inv_logit(p_spring_mu[1] + p_sd[1]*z_p_spring[1,y] +
beta_p_turb*spring_turb[1,y]);//p-cap for small fish in April, pass1
		p[y,6] = inv_logit(p_spring_mu[2] + p_sd[1]*z_p_spring[2,y] + beta_p_turb*spring_turb[1,y]);// p[6] : p-cap large in
April, pass 1
		p[y,7] = inv_logit(p_spring_mu[3] + p_sd[1]*z_p_spring[3,y] + beta_p_turb*spring_turb[2,y]);// p[7] : p-cap small in
May, pass 1
		p[y,8] = inv_logit(p_spring_mu[4] + p_sd[1]*z_p_spring[4,y] + beta_p_turb*spring_turb[2,y]);// p[8] : p-cap large in
May, pass 1
		p[y,9] = 1-pow(1-p[y,5],2);// p[9] : p-cap for small fish in April, passes 2& 3
		p[y,10] = 1-pow(1-p[y,6],2);;// p[10] : p-cap for large in April, passes 2& 3
		p[y,11] = 1-pow(1-p[y,7],2);// p[11] : p-cap for small fish in May, passes 2& 3
		p[y,12] = 1-pow(1-p[y,8],2);// p[12] : p-cap for large fish in May, passes 2& 3
		p[y,13] = inv_logit(logit(p[y,9])+behavior[1]);// p[13] : recap for small fish in April, passes 2& 3
		p[y,14] = inv_logit(logit(p[y,10])+behavior[2]);// p[14] : recap for large in April, passes 2& 3
		p[y,15] = inv_logit(logit(p[y,11])+behavior[1]);// p[15] : recap for small fish in May, passes 2& 3
		p[y,16] = inv_logit(logit(p[y,12])+behavior[2]);// p[16] : recap for large fish in May, passes 2& 3
			}

	//fix MUX detection from 2009-2012 to zero:
	for(y in 1:2){
		p[y,17] = 0;}

	for(y in 3:(Ny-1)){
		p[y,17] = p_mux[y];}
```

```
for(y in 1:7){
        p[y,18]=0;
        p[y,19]=0;}

p[8,18]=p_SUB[1];
p[8,19]=p_SUB[2];
p[9,18]=0;
p[9,19]=0;
p[10,18]=p_SUB[3];
p[10,19]=p_SUB[4];

//fall availability (in lcr) is a function of flow:

for(y in 1:(Ny-1)){

        a[y]=inv_logit(a0  + a_sd*z_a[y]);

        for(i in 1:3){
                m_av_1[i,y]=m_av_1_mu[i]+z_av_1[i,y]*m_av_sd;
                m_av_2[i,y]=m_av_2_mu[i]+z_av_2[i,y]*m_av_sd;
                m_av_3[i,y]=m_av_3_mu[i]+z_av_3[i,y]*m_av_sd;
                m_av_4[i,y]=m_av_4_mu[i]+z_av_4[i,y]*m_av_sd;
                }}

//Note: vectorized
//small female migrants:
av[1] = exp(m_av_1[1])./(1+exp(m_av_1[1])+exp(m_av_1[2])+exp(m_av_1[3]));
av[5] = exp(m_av_1[2])./(1+exp(m_av_1[1])+exp(m_av_1[2])+exp(m_av_1[3]));
av[9] = exp(m_av_1[3])./(1+exp(m_av_1[1])+exp(m_av_1[2])+exp(m_av_1[3]));
//small male migrants:
av[2] = exp(m_av_2[1])./(1+exp(m_av_2[1])+exp(m_av_2[2])+exp(m_av_2[3]));
av[6] = exp(m_av_2[2])./(1+exp(m_av_2[1])+exp(m_av_2[2])+exp(m_av_2[3]));
av[10] = exp(m_av_2[3])./(1+exp(m_av_2[1])+exp(m_av_2[2])+exp(m_av_2[3]));
```

```
//large female migrants:
av[3] = exp(m_av_3[1])./(1+exp(m_av_3[1])+exp(m_av_3[2])+exp(m_av_3[3]));
av[7] = exp(m_av_3[2])./(1+exp(m_av_3[1])+exp(m_av_3[2])+exp(m_av_3[3]));
av[11] =exp(m_av_3[3])./(1+exp(m_av_3[1])+exp(m_av_3[2])+exp(m_av_3[3]));
//large male migrants:
av[4] = exp(m_av_4[1])./(1+exp(m_av_4[1])+exp(m_av_4[2])+exp(m_av_4[3]));
av[8] = exp(m_av_4[2])./(1+exp(m_av_4[1])+exp(m_av_4[2])+exp(m_av_4[3]));
av[12] = exp(m_av_4[3])./(1+exp(m_av_4[1])+exp(m_av_4[2])+exp(m_av_4[3]));


//define 'pc' (prob of being captured at least once during spring sampling):
//these parameters are used as p-caps in the open model
//also, the p-caps of the secondary occasions (closed model) are divided by (1-(1-pc)*(1-p_MUX)) - to condition on fish that
were //detected during spring
for(y in 1:(Ny-1)){
        pc[y,1] = 1-(av[1,y]*(1-p[y,5])*(1-p[y,9])*(1-p[y,7])*(1-p[y,11])+ av[5,y]*(1-p[y,5])*(1-p[y,9])+av[9,y]*(1-
p[y,7])*(1-p[y,11])+(1-av[1,y]-av[5,y]-av[9,y])); //small female migrants
        pc[y,2] = 1-(av[2,y]*(1-p[y,5])*(1-p[y,9])*(1-p[y,7])*(1-p[y,11])+ av[6,y]*(1-p[y,5])*(1-p[y,9])+av[10,y]*(1-
p[y,7])*(1-p[y,11])+(1-av[2,y]-av[6,y]-av[10,y]));//small male migrants
        pc[y,3] = 1-(av[3,y]*(1-p[y,6])*(1-p[y,10])*(1-p[y,8])*(1-p[y,12])+ av[7,y]*(1-p[y,6])*(1-p[y,10])+av[11,y]*(1-
p[y,8])*(1-p[y,12])+(1-av[3,y]-av[7,y]-av[11,y]));//large female migrants
        pc[y,4] = 1-(av[4,y]*(1-p[y,6])*(1-p[y,10])*(1-p[y,8])*(1-p[y,12])+ av[8,y]*(1-p[y,6])*(1-p[y,10])+av[12,y]*(1-
p[y,8])*(1-p[y,12])+(1-av[4,y]-av[8,y]-av[12,y]));//large male migrants
        pc[y,5] = 1- (1-p[y,5])*(1-p[y,9])*(1-p[y,7])*(1-p[y,11]); // small residents
        pc[y,6] = 1- (1-p[y,6])*(1-p[y,10])*(1-p[y,8])*(1-p[y,12]);} // large residents


for(i in 1:21) {for(h in 1:21) {for(y in 1:(Ny-1)) {psi1[y,i,h] = 0;}}}
for(i in 1:21) {for(h in 1:21) {for(y in 1:(Ny-1)) {psi2[y][i,h] = 0;}}}
for(i in 1:14) {for(h in 1:21) {for(y in 1:(Ny-1)) {p1_open[y,i,h] = 0;}}}
for(i in 1:15) {for(h in 1:21) {for(y in 1:(Ny-1)) {p1_cl[y,i,h] = 0;}}}
for(i in 1:8) {for(h in 1:21) {for(y in 1:(Ny-1)) {p2[y,i,h] = 0;}}}
for(i in 1:10) {for(k in 1:2) {for(z in 1:2) {for(h in 1:21) {for(y in 1:(Ny-1)){pi_spring[i,k,z,h,y] = 0;}}}}}
```

```
for(i in 1:10) {for(k in 1:2) {for(z in 1:2) {for(h in 1:21) {for(y in 1:(Ny-1)){pi_fall[i,k,z,h,y] = 0;}}}}}


for(y in 1:(Ny-1)){
        psi1 [y, 1 , 1 ]= S[y,1,1] * (1 - g[1]) * (1 - w[y,1]);
        psi1 [y, 1 , 2 ]= S[y,1,1] * (1 - g[1]) * w[y,1] * tau;
        psi1 [y, 1 , 3 ]= S[y,1,1] * (1 - g[1]) * w[y,1] * (1 - tau);
        psi1 [y, 1 , 11 ]= S[y,1,1] * g[1] * (1 - w[y,7]);
        psi1 [y, 1 , 12 ]= S[y,1,1] * g[1] * w[y,7] * tau;
        psi1 [y, 1 , 13 ]= S[y,1,1] * g[1] * w[y,7] * (1 - tau);
        psi1 [y, 1 , 21 ]= 1 - S[y,1,1];
        psi1 [y, 2 , 2 ]= S[y,1,5] * (1 - g[2]) * (1 - w[y,2]);
        psi1 [y, 2 , 4 ]= S[y,1,5] * (1 - g[2]) * w[y,2];
        psi1 [y, 2 , 12 ]= S[y,1,5] * g[2] * (1 - w[y,8]);
        psi1 [y, 2 , 14 ]= S[y,1,5] * g[2] * w[y,8];
        psi1 [y, 2 , 21 ]= 1 - S[y,1,5];
        psi1 [y, 3 , 3 ]= S[y,1,5] * (1 - g[2]) * (1 - w[y,2]);
        psi1 [y, 3 , 5 ]= S[y,1,5] * (1 - g[2]) * w[y,2];
        psi1 [y, 3 , 13 ]= S[y,1,5] * g[2] * (1 - w[y,8]);
        psi1 [y, 3 , 15 ]= S[y,1,5] * g[2] * w[y,8];
        psi1 [y, 3 , 21 ]= 1 - S[y,1,5];
        psi1 [y, 4 , 2 ]= S[y,1,9] * (1 - g[3]) * w[y,3];
        psi1 [y, 4 , 4 ]= S[y,1,9] * (1 - g[3]) * (1 - w[y,3]);
        psi1 [y, 4 , 12 ]= S[y,1,9] * g[3] * w[y,9];
        psi1 [y, 4 , 14 ]= S[y,1,9] * g[3] * (1 - w[y,9]);
        psi1 [y, 4 , 21 ]= 1 - S[y,1,9];
        psi1 [y, 5 , 3 ]= S[y,1,9] * (1 - g[3]) * w[y,3];
        psi1 [y, 5 , 5 ]= S[y,1,9] * (1 - g[3]) * (1 - w[y,3]);
        psi1 [y, 5 , 13 ]= S[y,1,9] * g[3] * w[y,9];
        psi1 [y, 5 , 15 ]= S[y,1,9] * g[3] * (1 - w[y,9]);
        psi1 [y, 5 , 21 ]= 1 - S[y,1,9];
        psi1 [y, 6 , 6 ]= S[y,1,3] * (1 - g[4]) * (1 - w[y,4]);
        psi1 [y, 6 , 7 ]= S[y,1,3] * (1 - g[4]) * w[y,4] * tau;
```

```
psi1 [y, 6 , 8 ]= S[y,1,3] * (1 - g[4]) * w[y,4] * (1 - tau);
psi1 [y, 6 , 16 ]= S[y,1,3] * g[4] * (1 - w[y,10]);
psi1 [y, 6 , 17 ]= S[y,1,3] * g[4] * w[y,10] * tau;
psi1 [y, 6 , 18 ]= S[y,1,3] * g[4] * w[y,10] * (1 - tau);
psi1 [y, 6 , 21 ]= 1 - S[y,1,3];
psi1 [y, 7 , 7 ]= S[y,1,7] * (1 - g[5]) * (1 - w[y,5]);
psi1 [y, 7 , 9 ]= S[y,1,7] * (1 - g[5]) * w[y,5];
psi1 [y, 7 , 17 ]= S[y,1,7] * g[5] * (1 - w[y,11]);
psi1 [y, 7 , 19 ]= S[y,1,7] * g[5] * w[y,11];
psi1 [y, 7 , 21 ]= 1 - S[y,1,7];
psi1 [y, 8 , 8 ]= S[y,1,7] * (1 - g[5]) * (1 - w[y,5]);
psi1 [y, 8 , 10 ]= S[y,1,7] * (1 - g[5]) * w[y,5];
psi1 [y, 8 , 18 ]= S[y,1,7] * g[5] * (1 - w[y,11]);
psi1 [y, 8 , 20 ]= S[y,1,7] * g[5] * w[y,11];
psi1 [y, 8 , 21 ]= 1 - S[y,1,7];
psi1 [y, 9 , 7 ]= S[y,1,11] * (1 - g[6]) * w[y,6];
psi1 [y, 9 , 9 ]= S[y,1,11] * (1 - g[6]) * (1 - w[y,6]);
psi1 [y, 9 , 17 ]= S[y,1,11] * g[6] * w[y,12];
psi1 [y, 9 , 19 ]= S[y,1,11] * g[6] * (1 - w[y,12]);
psi1 [y, 9 , 21 ]= 1 - S[y,1,11];
psi1 [y, 10 , 8 ]= S[y,1,11] * (1 - g[6]) * w[y,6];
psi1 [y, 10 , 10 ]= S[y,1,11] * (1 - g[6]) * (1 - w[y,6]);
psi1 [y, 10 , 18 ]= S[y,1,11] * g[6] * w[y,12];
psi1 [y, 10 , 20 ]= S[y,1,11] * g[6] * (1 - w[y,12]);
psi1 [y, 10 , 21 ]= 1 - S[y,1,11];
psi1 [y, 11 , 11 ]= S[y,1,2] * (1 - w[y,7]);
psi1 [y, 11 , 12 ]= S[y,1,2] * w[y,7] * tau;
psi1 [y, 11 , 13 ]= S[y,1,2] * w[y,7] * (1 - tau);
psi1 [y, 11 , 21 ]= 1 - S[y,1,2];
psi1 [y, 12 , 12 ]= S[y,1,6] * (1 - w[y,8]);
psi1 [y, 12 , 14 ]= S[y,1,6] * w[y,8];
psi1 [y, 12 , 21 ]= 1 - S[y,1,6];
psi1 [y, 13 , 13 ]= S[y,1,6] * (1 - w[y,8]);
```

```
psi1 [y, 13 , 15 ]= S[y,1,6] * w[y,8];
psi1 [y, 13 , 21 ]= 1 - S[y,1,6];
psi1 [y, 14 , 12 ]= S[y,1,10] * w[y,9];
psi1 [y, 14 , 14 ]= S[y,1,10] * (1 - w[y,9]);
psi1 [y, 14 , 21 ]= 1 - S[y,1,10];
psi1 [y, 15 , 13 ]= S[y,1,10] * w[y,9];
psi1 [y, 15 , 15 ]= S[y,1,10] * (1 - w[y,9]);
psi1 [y, 15 , 21 ]= 1 - S[y,1,10];
psi1 [y, 16 , 16 ]= S[y,1,4] * (1 - w[y,10]);
psi1 [y, 16 , 17 ]= S[y,1,4] * w[y,10] * tau;
psi1 [y, 16 , 18 ]= S[y,1,4] * w[y,10] * (1 - tau);
psi1 [y, 16 , 21 ]= 1 - S[y,1,4];
psi1 [y, 17 , 17 ]= S[y,1,8] * (1 - w[y,11]);
psi1 [y, 17 , 19 ]= S[y,1,8] * w[y,11];
psi1 [y, 17 , 21 ]= 1 - S[y,1,8];
psi1 [y, 18 , 18 ]= S[y,1,8] * (1 - w[y,11]);
psi1 [y, 18 , 20 ]= S[y,1,8] * w[y,11];
psi1 [y, 18 , 21 ]= 1 - S[y,1,8];
psi1 [y, 19 , 17 ]= S[y,1,12] * w[y,12];
psi1 [y, 19 , 19 ]= S[y,1,12] * (1 - w[y,12]);
psi1 [y, 19 , 21 ]= 1 - S[y,1,12];
psi1 [y, 20 , 18 ]= S[y,1,12] * w[y,12];
psi1 [y, 20 , 20 ]= S[y,1,12] * (1 - w[y,12]);
psi1 [y, 20 , 21 ]= 1 - S[y,1,12];
psi1 [y, 21 , 21 ]= 1;



psi2 [y, 1 , 1 ]= S[y,2,1] * (1 - g[7]);
psi2 [y, 1 , 11 ]= S[y,2,1] * g[7];
psi2 [y, 1 , 21 ]= (1 - S[y,2,1]);
psi2 [y, 2 , 2 ]= S[y,2,5] * (1 - w[y,13]) * (1 - g[8]);
psi2 [y, 2 , 3 ]= S[y,2,5] * w[y,13] * (1 - g[8]);
```

```
psi2 [y, 2 , 12 ]= S[y,2,5] * (1 - w[y,13]) * g[8];
psi2 [y, 2 , 13 ]= S[y,2,5] * w[y,13] * g[8];
psi2 [y, 2 , 21 ]= (1 - S[y,2,5]);
psi2 [y, 3 , 2 ]= S[y,2,5] * w[y,14] * (1 - g[8]);
psi2 [y, 3 , 3 ]= S[y,2,5] * (1 - w[y,14]) * (1 - g[8]);
psi2 [y, 3 , 12 ]= S[y,2,5] * w[y,14] * g[8];
psi2 [y, 3 , 13 ]= S[y,2,5] * (1 - w[y,14]) * g[8];
psi2 [y, 3 , 21 ]= (1 - S[y,2,5]);
psi2 [y, 4 , 4 ]= S[y,2,9] * (1 - g[9]) * (1 - w[y,13]);
psi2 [y, 4 , 5 ]= S[y,2,9] * (1 - g[9]) * w[y,13];
psi2 [y, 4 , 14 ]= S[y,2,9] * g[9] * (1 - w[y,13]);
psi2 [y, 4 , 15 ]= S[y,2,9] * g[9] * w[y,13];
psi2 [y, 4 , 21 ]= (1 - S[y,2,9]);
psi2 [y, 5 , 4 ]= S[y,2,9] * (1 - g[9]) * w[y,14];
psi2 [y, 5 , 5 ]= S[y,2,9] * (1 - g[9]) * (1 - w[y,14]);
psi2 [y, 5 , 14 ]= S[y,2,9] * g[9] * w[y,14];
psi2 [y, 5 , 15 ]= S[y,2,9] * g[9] * (1 - w[y,14]);
psi2 [y, 5 , 21 ]= (1 - S[y,2,9]);
psi2 [y, 6 , 6 ]= S[y,2,3] * (1 - g[10]);
psi2 [y, 6 , 16 ]= S[y,2,3] * g[10];
psi2 [y, 6 , 21 ]= (1 - S[y,2,3]);
psi2 [y, 7 , 7 ]= S[y,2,7] * (1 - w[y,13]) * (1 - g[11]);
psi2 [y, 7 , 8 ]= S[y,2,7] * w[y,13] * (1 - g[11]);
psi2 [y, 7 , 17 ]= S[y,2,7] * (1 - w[y,13]) * g[11];
psi2 [y, 7 , 18 ]= S[y,2,7] * w[y,13] * g[11];
psi2 [y, 7 , 21 ]= (1 - S[y,2,7]);
psi2 [y, 8 , 7 ]= S[y,2,7] * w[y,14] * (1 - g[11]);
psi2 [y, 8 , 8 ]= S[y,2,7] * (1 - w[y,14]) * (1 - g[11]);
psi2 [y, 8 , 17 ]= S[y,2,7] * w[y,14] * g[11];
psi2 [y, 8 , 18 ]= S[y,2,7] * (1 - w[y,14]) * g[11];
psi2 [y, 8 , 21 ]= (1 - S[y,2,7]);
psi2 [y, 9 , 9 ]= S[y,2,11] * (1 - g[12]) * (1 - w[y,13]);
psi2 [y, 9 , 10 ]= S[y,2,11] * (1 - g[12]) * w[y,13];
```

```
psi2 [y, 9 , 19 ]= S[y,2,11] * g[12] * (1 - w[y,13]);
psi2 [y, 9 , 20 ]= S[y,2,11] * g[12] * w[y,13];
psi2 [y, 9 , 21 ]= (1 - S[y,2,11]);
psi2 [y, 10 , 9 ]= S[y,2,11] * (1 - g[12]) * w[y,14];
psi2 [y, 10 , 10 ]= S[y,2,11] * (1 - g[12]) * (1 - w[y,14]);
psi2 [y, 10 , 19 ]= S[y,2,11] * g[12] * w[y,14];
psi2 [y, 10 , 20 ]= S[y,2,11] * g[12] * (1 - w[y,14]);
psi2 [y, 10 , 21 ]= (1 - S[y,2,11]);
psi2 [y, 11 , 11 ]= S[y,2,2];
psi2 [y, 11 , 21 ]= (1 - S[y,2,2]);
psi2 [y, 12 , 12 ]= S[y,2,6] * (1 - w[y,13]);
psi2 [y, 12 , 13 ]= S[y,2,6] * w[y,13];
psi2 [y, 12 , 21 ]= (1 - S[y,2,6]);
psi2 [y, 13 , 12 ]= S[y,2,6] * w[y,14];
psi2 [y, 13 , 13 ]= S[y,2,6] * (1 - w[y,14]);
psi2 [y, 13 , 21 ]= (1 - S[y,2,6]);
psi2 [y, 14 , 14 ]= S[y,2,10] * (1 - w[y,13]);
psi2 [y, 14 , 15 ]= S[y,2,10] * w[y,13];
psi2 [y, 14 , 21 ]= (1 - S[y,2,10]);
psi2 [y, 15 , 14 ]= S[y,2,10] * w[y,14];
psi2 [y, 15 , 15 ]= S[y,2,10] * (1 - w[y,14]);
psi2 [y, 15 , 21 ]= (1 - S[y,2,10]);
psi2 [y, 16 , 16 ]= S[y,2,4];
psi2 [y, 16 , 21 ]= (1 - S[y,2,4]);
psi2 [y, 17 , 17 ]= S[y,2,8] * (1 - w[y,13]);
psi2 [y, 17 , 18 ]= S[y,2,8] * w[y,13];
psi2 [y, 17 , 21 ]= (1 - S[y,2,8]);
psi2 [y, 18 , 17 ]= S[y,2,8] * w[y,14];
psi2 [y, 18 , 18 ]= S[y,2,8] * (1 - w[y,14]);
psi2 [y, 18 , 21 ]= (1 - S[y,2,8]);
psi2 [y, 19 , 19 ]= S[y,2,12] * (1 - w[y,13]);
psi2 [y, 19 , 20 ]= S[y,2,12] * w[y,13];
psi2 [y, 19 , 21 ]= (1 - S[y,2,12]);
```

```
        psi2 [y, 20 , 19 ]= S[y,2,12] * w[y,14];
        psi2 [y, 20 , 20 ]= S[y,2,12] * (1 - w[y,14]);
        psi2 [y, 20 , 21 ]= (1 - S[y,2,12]);
        psi2 [y, 21 , 21 ]= 1;
}


    for(y in 1:(Ny-1)){
            p2 [y, 1 , 1 ]= p[y,1];
      p2 [y, 1 , 2 ]= p[y,1] * a[y,1];
      p2 [y, 1 , 3 ]= p[y,1] * a[y,1];
      p2 [y, 1 , 6 ]= p[y,1];
      p2 [y, 1 , 7 ]= p[y,1] * a[y,2];
      p2 [y, 1 , 8 ]= p[y,1] * a[y,2];
      p2 [y, 2 , 11 ]= p[y,2];
      p2 [y, 2 , 12 ]= p[y,2] * a[y,3];
      p2 [y, 2 , 13 ]= p[y,2] * a[y,3];
      p2 [y, 2 , 16 ]= p[y,2];
      p2 [y, 2 , 17 ]= p[y,2] * a[y,4];
      p2 [y, 2 , 18 ]= p[y,2] * a[y,4];
      p2 [y, 3 , 2 ]= p[y,3] * (1 - a[y,1]) * (1 - p[y,18]);
      p2 [y, 3 , 4 ]= p[y,3] * (1 - p[y,18]);
      p2 [y, 3 , 7 ]= p[y,3] * (1 - a[y,2]) * (1 - p[y,18]);
      p2 [y, 3 , 9 ]= p[y,3] * (1 - p[y,18]);
      p2 [y, 4 , 12 ]= p[y,4] * (1 - a[y,3]) * (1 - p[y,19]);
      p2 [y, 4 , 14 ]= p[y,4] * (1 - p[y,19]);
      p2 [y, 4 , 17 ]= p[y,4] * (1 - a[y,4]) * (1 - p[y,19]);
      p2 [y, 4 , 19 ]= p[y,4] * (1 - p[y,19]);
      p2 [y, 5 , 2 ]= p[y,3] * (1 - a[y,1]) * p[y,18];
      p2 [y, 5 , 4 ]= p[y,3] * p[y,18];
      p2 [y, 5 , 7 ]= p[y,3] * (1 - a[y,2]) * p[y,18];
      p2 [y, 5 , 9 ]= p[y,3] * p[y,18];
      p2 [y, 6 , 12 ]= p[y,4] * (1 - a[y,3]) * p[y,19];
```

```
p2 [y, 6 , 14 ]= p[y,4] * p[y,19];
p2 [y, 6 , 17 ]= p[y,4] * (1 - a[y,4]) * p[y,19];
p2 [y, 6 , 19 ]= p[y,4] * p[y,19];
p2 [y, 7 , 2 ]= (1 - p[y,3]) * (1 - a[y,1]) * p[y,18];
p2 [y, 7 , 4 ]= (1 - p[y,3]) * p[y,18];
p2 [y, 7 , 7 ]= (1 - p[y,3]) * (1 - a[y,2]) * p[y,18];
p2 [y, 7 , 9 ]= (1 - p[y,3]) * p[y,18];
p2 [y, 7 , 12 ]= (1 - p[y,4]) * (1 - a[y,3]) * p[y,19];
p2 [y, 7 , 14 ]= (1 - p[y,4]) * p[y,19];
p2 [y, 7 , 17 ]= (1 - p[y,4]) * (1 - a[y,4]) * p[y,19];
p2 [y, 7 , 19 ]= (1 - p[y,4]) * p[y,19];
p2 [y, 8 , 1 ]= (1 - p[y,1]);
p2 [y, 8 , 2 ]= (1 - p[y,3]) * (1 - a[y,1]) * (1 - p[y,18]) + (1 - p[y,1]) * a[y,1];
p2 [y, 8 , 3 ]= 1 - a[y,1] + a[y,1] * (1 - p[y,1]);
p2 [y, 8 , 4 ]= (1 - p[y,3]) * (1 - p[y,18]);
p2 [y, 8 , 5 ]= 1;
p2 [y, 8 , 6 ]= (1 - p[y,1]);
p2 [y, 8 , 7 ]= (1 - p[y,3]) * (1 - a[y,2]) * (1 - p[y,18]) + (1 - p[y,1]) * a[y,2];
p2 [y, 8 , 8 ]= 1 - a[y,2] + a[y,2] * (1 - p[y,1]);
p2 [y, 8 , 9 ]= (1 - p[y,3]) * (1 - p[y,18]);
p2 [y, 8 , 10 ]= 1;
p2 [y, 8 , 11 ]= (1 - p[y,2]);
p2 [y, 8 , 12 ]= (1 - p[y,2]) * a[y,3] + (1 - p[y,4]) * (1 - a[y,3]) * (1 - p[y,19]);
p2 [y, 8 , 13 ]= (1 - a[y,3]) + (1 - p[y,2]) * a[y,3];
p2 [y, 8 , 14 ]= (1 - p[y,4]) * (1 - p[y,19]);
p2 [y, 8 , 15 ]= 1;
p2 [y, 8 , 16 ]= (1 - p[y,2]);
p2 [y, 8 , 17 ]= (1 - p[y,2]) * a[y,4] + (1 - a[y,4]) * (1 - p[y,4]) * (1 - p[y,19]);
p2 [y, 8 , 18 ]= 1 - a[y,4] + (1 - p[y,2]) * a[y,4];
p2 [y, 8 , 19 ]= (1 - p[y,4]) * (1 - p[y,19]);
p2 [y, 8 , 20 ]= 1;
p2 [y, 8 , 21 ]= 1;
```

```
p1_open [y, 1 , 2 ]= r[2] * pc[y,1] * p[y,17];
p1_open [y, 1 , 3 ]= r[2] * pc[y,1] * p[y,17];
p1_open [y, 2 , 7 ]= r[1] * pc[y,2] * p[y,17];
p1_open [y, 2 , 8 ]= r[1] * pc[y,2] * p[y,17];
p1_open [y, 3 , 2 ]= (1 - r[2]) * pc[y,1] * p[y,17];
p1_open [y, 3 , 3 ]= (1 - r[2]) * pc[y,1] * p[y,17];
p1_open [y, 3 , 7 ]= (1 - r[1]) * pc[y,2] * p[y,17];
p1_open [y, 3 , 8 ]= (1 - r[1]) * pc[y,2] * p[y,17];
p1_open [y, 4 , 12 ]= r[4] * pc[y,3] * p[y,17];
p1_open [y, 4 , 13 ]= r[4] * pc[y,3] * p[y,17];
p1_open [y, 5 , 17 ]= r[3] * pc[y,4] * p[y,17];
p1_open [y, 5 , 18 ]= r[3] * pc[y,4] * p[y,17];
p1_open [y, 6 , 12 ]= (1 - r[4]) * pc[y,3] * p[y,17];
p1_open [y, 6 , 13 ]= (1 - r[4]) * pc[y,3] * p[y,17];
p1_open [y, 6 , 17 ]= (1 - r[3]) * pc[y,4] * p[y,17];
p1_open [y, 6 , 18 ]= (1 - r[3]) * pc[y,4] * p[y,17];
p1_open [y, 7 , 2 ]= (1 - pc[y,1]) * p[y,17];
p1_open [y, 7 , 3 ]= (1 - pc[y,1]) * p[y,17];
p1_open [y, 7 , 7 ]= (1 - pc[y,2]) * p[y,17];
p1_open [y, 7 , 8 ]= (1 - pc[y,2]) * p[y,17];
p1_open [y, 7 , 12 ]= (1 - pc[y,3]) * p[y,17];
p1_open [y, 7 , 13 ]= (1 - pc[y,3]) * p[y,17];
p1_open [y, 7 , 17 ]= (1 - pc[y,4]) * p[y,17];
p1_open [y, 7 , 18 ]= (1 - pc[y,4]) * p[y,17];
p1_open [y, 8 , 1 ]= r[2] * pc[y,5];
p1_open [y, 8 , 2 ]= r[2] * pc[y,1] * (1 - p[y,17]);
p1_open [y, 8 , 3 ]= r[2] * pc[y,1] * (1 - p[y,17]);
p1_open [y, 9 , 6 ]= r[1] * pc[y,5];
p1_open [y, 9 , 7 ]= r[1] * pc[y,2] * (1 - p[y,17]);
p1_open [y, 9 , 8 ]= r[1] * pc[y,2] * (1 - p[y,17]);
p1_open [y, 10 , 1 ]= (1 - r[2]) * pc[y,5];
p1_open [y, 10 , 2 ]= (1 - r[2]) * pc[y,1] * (1 - p[y,17]);
```

```
p1_open [y, 10 , 3 ]= (1 - r[2]) * pc[y,1] * (1 - p[y,17]);
p1_open [y, 10 , 6 ]= (1 - r[1]) * pc[y,5];
p1_open [y, 10 , 7 ]= (1 - r[1]) * pc[y,2] * (1 - p[y,17]);
p1_open [y, 10 , 8 ]= (1 - r[1]) * pc[y,2] * (1 - p[y,17]);
p1_open [y, 11 , 11 ]= r[4] * pc[y,6];
p1_open [y, 11 , 12 ]= r[4] * pc[y,3] * (1 - p[y,17]);
p1_open [y, 11 , 13 ]= r[4] * pc[y,3] * (1 - p[y,17]);
p1_open [y, 12 , 16 ]= r[3] * pc[y,6];
p1_open [y, 12 , 17 ]= r[3] * pc[y,4] * (1 - p[y,17]);
p1_open [y, 12 , 18 ]= r[3] * pc[y,4] * (1 - p[y,17]);
p1_open [y, 13 , 11 ]= (1 - r[4]) * pc[y,6];
p1_open [y, 13 , 12 ]= (1 - r[4]) * pc[y,3] * (1 - p[y,17]);
p1_open [y, 13 , 13 ]= (1 - r[4]) * pc[y,3] * (1 - p[y,17]);
p1_open [y, 13 , 16 ]= (1 - r[3]) * pc[y,6];
p1_open [y, 13 , 17 ]= (1 - r[3]) * pc[y,4] * (1 - p[y,17]);
p1_open [y, 13 , 18 ]= (1 - r[3]) * pc[y,4] * (1 - p[y,17]);
p1_open [y, 14 , 1 ]= 1 - pc[y,5];
p1_open [y, 14 , 2 ]= (1 - pc[y,1]) * (1 - p[y,17]);
p1_open [y, 14 , 3 ]= (1 - pc[y,1]) * (1 - p[y,17]);
p1_open [y, 14 , 4 ]= 1;
p1_open [y, 14 , 5 ]= 1;
p1_open [y, 14 , 6 ]= (1 - pc[y,5]);
p1_open [y, 14 , 7 ]= (1 - pc[y,2]) * (1 - p[y,17]);
p1_open [y, 14 , 8 ]= (1 - pc[y,2]) * (1 - p[y,17]);
p1_open [y, 14 , 9 ]= 1;
p1_open [y, 14 , 10 ]= 1;
p1_open [y, 14 , 11 ]= (1 - pc[y,6]);
p1_open [y, 14 , 12 ]= (1 - pc[y,3]) * (1 - p[y,17]);
p1_open [y, 14 , 13 ]= (1 - pc[y,3]) * (1 - p[y,17]);
p1_open [y, 14 , 14 ]= 1;
p1_open [y, 14 , 15 ]= 1;
p1_open [y, 14 , 16 ]= (1 - pc[y,6]);
p1_open [y, 14 , 17 ]= (1 - pc[y,4]) * (1 - p[y,17]);
```

```
    p1_open [y, 14 , 18 ]= (1 - pc[y,4]) * (1 - p[y,17]);
    p1_open [y, 14 , 19 ]= 1;
    p1_open [y, 14 , 20 ]= 1;
    p1_open [y, 14 , 21 ]= 1;

}


for(y in 1:(Ny-1)){
        p1_cl [y, 1 , 1 ]= (p[y,5] * p[y,13] * p[y,7] * p[y,15])/pc[y,5];
    p1_cl [y, 1 , 2 ]= (av[1,y] * p[y,5] * p[y,13] * p[y,7] * p[y,15])/pc[y,1];
    p1_cl [y, 1 , 3 ]= (av[1,y] * p[y,5] * p[y,13] * p[y,7] * p[y,15])/pc[y,1];
    p1_cl [y, 1 , 6 ]= (p[y,5] * p[y,13] * p[y,7] * p[y,15])/pc[y,5];
    p1_cl [y, 1 , 7 ]= (av[2,y] * p[y,5] * p[y,13] * p[y,7] * p[y,15])/pc[y,2];
    p1_cl [y, 1 , 8 ]= (av[2,y] * p[y,5] * p[y,13] * p[y,7] * p[y,15])/pc[y,2];
    p1_cl [y, 1 , 11 ]= (p[y,6] * p[y,14] * p[y,8] * p[y,16])/pc[y,6];
    p1_cl [y, 1 , 12 ]= (av[3,y] * p[y,6] * p[y,14] * p[y,8] * p[y,16])/pc[y,3];
    p1_cl [y, 1 , 13 ]= (av[3,y] * p[y,6] * p[y,14] * p[y,8] * p[y,16])/pc[y,3];
    p1_cl [y, 1 , 16 ]= (p[y,6] * p[y,14] * p[y,8] * p[y,16])/pc[y,6];
    p1_cl [y, 1 , 17 ]= (av[4,y] * p[y,6] * p[y,14] * p[y,8] * p[y,16])/pc[y,4];
    p1_cl [y, 1 , 18 ]= (av[4,y] * p[y,6] * p[y,14] * p[y,8] * p[y,16])/pc[y,4];
    p1_cl [y, 2 , 1 ]= (p[y,5] * p[y,13] * p[y,7] * (1 - p[y,15]))/pc[y,5];
    p1_cl [y, 2 , 2 ]= (av[1,y] * p[y,5] * p[y,13] * p[y,7] * (1 - p[y,15]))/pc[y,1];
    p1_cl [y, 2 , 3 ]= (av[1,y] * p[y,5] * p[y,13] * p[y,7] * (1 - p[y,15]))/pc[y,1];
    p1_cl [y, 2 , 6 ]= (p[y,5] * p[y,13] * p[y,7] * (1 - p[y,15]))/pc[y,5];
    p1_cl [y, 2 , 7 ]= (av[2,y] * p[y,5] * p[y,13] * p[y,7] * (1 - p[y,15]))/pc[y,2];
    p1_cl [y, 2 , 8 ]= (av[2,y] * p[y,5] * p[y,13] * p[y,7] * (1 - p[y,15]))/pc[y,2];
    p1_cl [y, 2 , 11 ]= (p[y,6] * p[y,14] * p[y,8] * (1 - p[y,16]))/pc[y,6];
    p1_cl [y, 2 , 12 ]= (av[3,y] * p[y,6] * p[y,14] * p[y,8] * (1 - p[y,16]))/pc[y,3];
    p1_cl [y, 2 , 13 ]= (av[3,y] * p[y,6] * p[y,14] * p[y,8] * (1 - p[y,16]))/pc[y,3];
    p1_cl [y, 2 , 16 ]= (p[y,6] * p[y,14] * p[y,8] * (1 - p[y,16]))/pc[y,6];
    p1_cl [y, 2 , 17 ]= (av[4,y] * p[y,6] * p[y,14] * p[y,8] * (1 - p[y,16]))/pc[y,4];
    p1_cl [y, 2 , 18 ]= (av[4,y] * p[y,6] * p[y,14] * p[y,8] * (1 - p[y,16]))/pc[y,4];
```

```
p1_cl [y, 3 , 1 ]= (p[y,5] * p[y,13] * (1 - p[y,7]) * p[y,11])/pc[y,5];
p1_cl [y, 3 , 2 ]= (av[1,y] * p[y,5] * p[y,13] * (1 - p[y,7]) * p[y,11])/pc[y,1];
p1_cl [y, 3 , 3 ]= (av[1,y] * p[y,5] * p[y,13] * (1 - p[y,7]) * p[y,11])/pc[y,1];
p1_cl [y, 3 , 6 ]= (p[y,5] * p[y,13] * (1 - p[y,7]) * p[y,11])/pc[y,5];
p1_cl [y, 3 , 7 ]= (av[2,y] * p[y,5] * p[y,13] * (1 - p[y,7]) * p[y,11])/pc[y,2];
p1_cl [y, 3 , 8 ]= (av[2,y] * p[y,5] * p[y,13] * (1 - p[y,7]) * p[y,11])/pc[y,2];
p1_cl [y, 3 , 11 ]= (p[y,6] * p[y,14] * (1 - p[y,8]) * p[y,12])/pc[y,6];
p1_cl [y, 3 , 12 ]= (av[3,y] * p[y,6] * p[y,14] * (1 - p[y,8]) * p[y,12])/pc[y,3];
p1_cl [y, 3 , 13 ]= (av[3,y] * p[y,6] * p[y,14] * (1 - p[y,8]) * p[y,12])/pc[y,3];
p1_cl [y, 3 , 16 ]= (p[y,6] * p[y,14] * (1 - p[y,8]) * p[y,12])/pc[y,6];
p1_cl [y, 3 , 17 ]= (av[4,y] * p[y,6] * p[y,14] * (1 - p[y,8]) * p[y,12])/pc[y,4];
p1_cl [y, 3 , 18 ]= (av[4,y] * p[y,6] * p[y,14] * (1 - p[y,8]) * p[y,12])/pc[y,4];
p1_cl [y, 4 , 1 ]= (p[y,5] * p[y,13] * (1 - p[y,7]) * (1 - p[y,11]))/pc[y,5];
p1_cl [y, 4 , 2 ]= (av[1,y] * p[y,5] * p[y,13] * (1 - p[y,7]) * (1 - p[y,11]) + av[5,y] * p[y,5] * p[y,13])/pc[y,1];
p1_cl [y, 4 , 3 ]= (av[1,y] * p[y,5] * p[y,13] * (1 - p[y,7]) * (1 - p[y,11]) + av[5,y] * p[y,5] * p[y,13])/pc[y,1];
p1_cl [y, 4 , 6 ]= (p[y,5] * p[y,13] * (1 - p[y,7]) * (1 - p[y,11]))/pc[y,5];
p1_cl [y, 4 , 7 ]= (av[2,y] * p[y,5] * p[y,13] * (1 - p[y,7]) * (1 - p[y,11]) + av[6,y] * p[y,5] * p[y,13])/pc[y,2];
p1_cl [y, 4 , 8 ]= (av[2,y] * p[y,5] * p[y,13] * (1 - p[y,7]) * (1 - p[y,11]) + av[6,y] * p[y,5] * p[y,13])/pc[y,2];
p1_cl [y, 4 , 11 ]= (p[y,6] * p[y,14] * (1 - p[y,8]) * (1 - p[y,12]))/pc[y,6];
p1_cl [y, 4 , 12 ]= (av[3,y] * p[y,6] * p[y,14] * (1 - p[y,8]) * (1 - p[y,12]) + av[7,y] * p[y,6] * p[y,14])/pc[y,3];
p1_cl [y, 4 , 13 ]= (av[3,y] * p[y,6] * p[y,14] * (1 - p[y,8]) * (1 - p[y,12]) + av[7,y] * p[y,6] * p[y,14])/pc[y,3];
p1_cl [y, 4 , 16 ]= (p[y,6] * p[y,14] * (1 - p[y,8]) * (1 - p[y,12]))/pc[y,6];
p1_cl [y, 4 , 17 ]= (av[4,y] * p[y,6] * p[y,14] * (1 - p[y,8]) * (1 - p[y,12]) + av[8,y] * p[y,6] * p[y,14])/pc[y,4];
p1_cl [y, 4 , 18 ]= (av[4,y] * p[y,6] * p[y,14] * (1 - p[y,8]) * (1 - p[y,12]) + av[8,y] * p[y,6] * p[y,14])/pc[y,4];
p1_cl [y, 5 , 1 ]= (p[y,5] * (1 - p[y,13]) * p[y,7] * p[y,15])/pc[y,5];
p1_cl [y, 5 , 2 ]= (av[1,y] * p[y,5] * (1 - p[y,13]) * p[y,7] * p[y,15])/pc[y,1];
p1_cl [y, 5 , 3 ]= (av[1,y] * p[y,5] * (1 - p[y,13]) * p[y,7] * p[y,15])/pc[y,1];
p1_cl [y, 5 , 6 ]= (p[y,5] * (1 - p[y,13]) * p[y,7] * p[y,15])/pc[y,5];
p1_cl [y, 5 , 7 ]= (av[2,y] * p[y,5] * (1 - p[y,13]) * p[y,7] * p[y,15])/pc[y,2];
p1_cl [y, 5 , 8 ]= (av[2,y] * p[y,5] * (1 - p[y,13]) * p[y,7] * p[y,15])/pc[y,2];
p1_cl [y, 5 , 11 ]= (p[y,6] * (1 - p[y,14]) * p[y,8] * p[y,16])/pc[y,6];
p1_cl [y, 5 , 12 ]= (av[3,y] * p[y,6] * (1 - p[y,14]) * p[y,8] * p[y,16])/pc[y,3];
p1_cl [y, 5 , 13 ]= (av[3,y] * p[y,6] * (1 - p[y,14]) * p[y,8] * p[y,16])/pc[y,3];
```

```
p1_cl [y, 5 , 16 ]= (p[y,6] * (1 - p[y,14]) * p[y,8] * p[y,16])/pc[y,6];
p1_cl [y, 5 , 17 ]= (av[4,y] * p[y,6] * (1 - p[y,14]) * p[y,8] * p[y,16])/pc[y,4];
p1_cl [y, 5 , 18 ]= (av[4,y] * p[y,6] * (1 - p[y,14]) * p[y,8] * p[y,16])/pc[y,4];
p1_cl [y, 6 , 1 ]= (p[y,5] * (1 - p[y,13]) * p[y,7] * (1 - p[y,15]))/pc[y,5];
p1_cl [y, 6 , 2 ]= (av[1,y] * p[y,5] * (1 - p[y,13]) * p[y,7] * (1 - p[y,15]))/pc[y,1];
p1_cl [y, 6 , 3 ]= (av[1,y] * p[y,5] * (1 - p[y,13]) * p[y,7] * (1 - p[y,15]))/pc[y,1];
p1_cl [y, 6 , 6 ]= (p[y,5] * (1 - p[y,13]) * p[y,7] * (1 - p[y,15]))/pc[y,5];
p1_cl [y, 6 , 7 ]= (av[2,y] * p[y,5] * (1 - p[y,13]) * p[y,7] * (1 - p[y,15]))/pc[y,2];
p1_cl [y, 6 , 8 ]= (av[2,y] * p[y,5] * (1 - p[y,13]) * p[y,7] * (1 - p[y,15]))/pc[y,2];
p1_cl [y, 6 , 11 ]= (p[y,6] * (1 - p[y,14]) * p[y,8] * (1 - p[y,16]))/pc[y,6];
p1_cl [y, 6 , 12 ]= (av[3,y] * p[y,6] * (1 - p[y,14]) * p[y,8] * (1 - p[y,16]))/pc[y,3];
p1_cl [y, 6 , 13 ]= (av[3,y] * p[y,6] * (1 - p[y,14]) * p[y,8] * (1 - p[y,16]))/pc[y,3];
p1_cl [y, 6 , 16 ]= (p[y,6] * (1 - p[y,14]) * p[y,8] * (1 - p[y,16]))/pc[y,6];
p1_cl [y, 6 , 17 ]= (av[4,y] * p[y,6] * (1 - p[y,14]) * p[y,8] * (1 - p[y,16]))/pc[y,4];
p1_cl [y, 6 , 18 ]= (av[4,y] * p[y,6] * (1 - p[y,14]) * p[y,8] * (1 - p[y,16]))/pc[y,4];
p1_cl [y, 7 , 1 ]= (p[y,5] * (1 - p[y,13]) * (1 - p[y,7]) * p[y,11])/pc[y,5];
p1_cl [y, 7 , 2 ]= (av[1,y] * p[y,5] * (1 - p[y,13]) * (1 - p[y,7]) * p[y,11])/pc[y,1];
p1_cl [y, 7 , 3 ]= (av[1,y] * p[y,5] * (1 - p[y,13]) * (1 - p[y,7]) * p[y,11])/pc[y,1];
p1_cl [y, 7 , 6 ]= (p[y,5] * (1 - p[y,13]) * (1 - p[y,7]) * p[y,11])/pc[y,5];
p1_cl [y, 7 , 7 ]= (av[2,y] * p[y,5] * (1 - p[y,13]) * (1 - p[y,7]) * p[y,11])/pc[y,2];
p1_cl [y, 7 , 8 ]= (av[2,y] * p[y,5] * (1 - p[y,13]) * (1 - p[y,7]) * p[y,11])/pc[y,2];
p1_cl [y, 7 , 11 ]= (p[y,6] * (1 - p[y,14]) * (1 - p[y,8]) * p[y,12])/pc[y,6];
p1_cl [y, 7 , 12 ]= (av[3,y] * p[y,6] * (1 - p[y,14]) * (1 - p[y,8]) * p[y,12])/pc[y,3];
p1_cl [y, 7 , 13 ]= (av[3,y] * p[y,6] * (1 - p[y,14]) * (1 - p[y,8]) * p[y,12])/pc[y,3];
p1_cl [y, 7 , 16 ]= (p[y,6] * (1 - p[y,14]) * (1 - p[y,8]) * p[y,12])/pc[y,6];
p1_cl [y, 7 , 17 ]= (av[4,y] * p[y,6] * (1 - p[y,14]) * (1 - p[y,8]) * p[y,12])/pc[y,4];
p1_cl [y, 7 , 18 ]= (av[4,y] * p[y,6] * (1 - p[y,14]) * (1 - p[y,8]) * p[y,12])/pc[y,4];
p1_cl [y, 8 , 1 ]= (p[y,5] * (1 - p[y,13]) * (1 - p[y,7]) * (1 - p[y,11]))/pc[y,5];
p1_cl [y, 8 , 2 ]= (av[1,y] * p[y,5] * (1 - p[y,13]) * (1 - p[y,7]) * (1 - p[y,11]) + av[5,y] * p[y,5] * (1 - p[y,13]))/pc[y,1];
p1_cl [y, 8 , 3 ]= (av[1,y] * p[y,5] * (1 - p[y,13]) * (1 - p[y,7]) * (1 - p[y,11]) + av[5,y] * p[y,5] * (1 - p[y,13]))/pc[y,1];
p1_cl [y, 8 , 6 ]= (p[y,5] * (1 - p[y,13]) * (1 - p[y,7]) * (1 - p[y,11]))/pc[y,5];
p1_cl [y, 8 , 7 ]= (av[2,y] * p[y,5] * (1 - p[y,13]) * (1 - p[y,7]) * (1 - p[y,11]) + av[6,y] * p[y,5] * (1 - p[y,13]))/pc[y,2];
p1_cl [y, 8 , 8 ]= (av[2,y] * p[y,5] * (1 - p[y,13]) * (1 - p[y,7]) * (1 - p[y,11]) + av[6,y] * p[y,5] * (1 - p[y,13]))/pc[y,2];
```

```
p1_cl [y, 8 , 11 ]= (p[y,6] * (1 - p[y,14]) * (1 - p[y,8]) * (1 - p[y,12]))/pc[y,6];
p1_cl [y, 8 , 12 ]= (av[3,y] * p[y,6] * (1 - p[y,14]) * (1 - p[y,8]) * (1 - p[y,12]) + av[7,y] * p[y,6] * (1 - p[y,14]))/pc[y,3];
p1_cl [y, 8 , 13 ]= (av[3,y] * p[y,6] * (1 - p[y,14]) * (1 - p[y,8]) * (1 - p[y,12]) + av[7,y] * p[y,6] * (1 - p[y,14]))/pc[y,3];
p1_cl [y, 8 , 16 ]= (p[y,6] * (1 - p[y,14]) * (1 - p[y,8]) * (1 - p[y,12]))/pc[y,6];
p1_cl [y, 8 , 17 ]= (av[4,y] * p[y,6] * (1 - p[y,14]) * (1 - p[y,8]) * (1 - p[y,12]) + av[8,y] * p[y,6] * (1 - p[y,14]))/pc[y,4];
p1_cl [y, 8 , 18 ]= (av[4,y] * p[y,6] * (1 - p[y,14]) * (1 - p[y,8]) * (1 - p[y,12]) + av[8,y] * p[y,6] * (1 - p[y,14]))/pc[y,4];
p1_cl [y, 9 , 1 ]= ((1 - p[y,5]) * p[y,9] * p[y,7] * p[y,15])/pc[y,5];
p1_cl [y, 9 , 2 ]= (av[1,y] * (1 - p[y,5]) * p[y,9] * p[y,7] * p[y,15])/pc[y,1];
p1_cl [y, 9 , 3 ]= (av[1,y] * (1 - p[y,5]) * p[y,9] * p[y,7] * p[y,15])/pc[y,1];
p1_cl [y, 9 , 6 ]= ((1 - p[y,5]) * p[y,9] * p[y,7] * p[y,15])/pc[y,5];
p1_cl [y, 9 , 7 ]= (av[2,y] * (1 - p[y,5]) * p[y,9] * p[y,7] * p[y,15])/pc[y,2];
p1_cl [y, 9 , 8 ]= (av[2,y] * (1 - p[y,5]) * p[y,9] * p[y,7] * p[y,15])/pc[y,2];
p1_cl [y, 9 , 11 ]= ((1 - p[y,6]) * p[y,10] * p[y,8] * p[y,16])/pc[y,6];
p1_cl [y, 9 , 12 ]= (av[3,y] * (1 - p[y,6]) * p[y,10] * p[y,8] * p[y,16])/pc[y,3];
p1_cl [y, 9 , 13 ]= (av[3,y] * (1 - p[y,6]) * p[y,10] * p[y,8] * p[y,16])/pc[y,3];
p1_cl [y, 9 , 16 ]= ((1 - p[y,6]) * p[y,10] * p[y,8] * p[y,16])/pc[y,6];
p1_cl [y, 9 , 17 ]= (av[4,y] * (1 - p[y,6]) * p[y,10] * p[y,8] * p[y,16])/pc[y,4];
p1_cl [y, 9 , 18 ]= (av[4,y] * (1 - p[y,6]) * p[y,10] * p[y,8] * p[y,16])/pc[y,4];
p1_cl [y, 10 , 1 ]= ((1 - p[y,5]) * p[y,9] * p[y,7] * (1 - p[y,15]))/pc[y,5];
p1_cl [y, 10 , 2 ]= (av[1,y] * (1 - p[y,5]) * p[y,9] * p[y,7] * (1 - p[y,15]))/pc[y,1];
p1_cl [y, 10 , 3 ]= (av[1,y] * (1 - p[y,5]) * p[y,9] * p[y,7] * (1 - p[y,15]))/pc[y,1];
p1_cl [y, 10 , 6 ]= ((1 - p[y,5]) * p[y,9] * p[y,7] * (1 - p[y,15]))/pc[y,5];
p1_cl [y, 10 , 7 ]= (av[2,y] * (1 - p[y,5]) * p[y,9] * p[y,7] * (1 - p[y,15]))/pc[y,2];
p1_cl [y, 10 , 8 ]= (av[2,y] * (1 - p[y,5]) * p[y,9] * p[y,7] * (1 - p[y,15]))/pc[y,2];
p1_cl [y, 10 , 11 ]= ((1 - p[y,6]) * p[y,10] * p[y,8] * (1 - p[y,16]))/pc[y,6];
p1_cl [y, 10 , 12 ]= (av[3,y] * (1 - p[y,6]) * p[y,10] * p[y,8] * (1 - p[y,16]))/pc[y,3];
p1_cl [y, 10 , 13 ]= (av[3,y] * (1 - p[y,6]) * p[y,10] * p[y,8] * (1 - p[y,16]))/pc[y,3];
p1_cl [y, 10 , 16 ]= ((1 - p[y,6]) * p[y,10] * p[y,8] * (1 - p[y,16]))/pc[y,6];
p1_cl [y, 10 , 17 ]= (av[4,y] * (1 - p[y,6]) * p[y,10] * p[y,8] * (1 - p[y,16]))/pc[y,4];
p1_cl [y, 10 , 18 ]= (av[4,y] * (1 - p[y,6]) * p[y,10] * p[y,8] * (1 - p[y,16]))/pc[y,4];
p1_cl [y, 11 , 1 ]= ((1 - p[y,5]) * p[y,9] * (1 - p[y,7]) * p[y,11])/pc[y,5];
p1_cl [y, 11 , 2 ]= (av[1,y] * (1 - p[y,5]) * p[y,9] * (1 - p[y,7]) * p[y,11])/pc[y,1];
p1_cl [y, 11 , 3 ]= (av[1,y] * (1 - p[y,5]) * p[y,9] * (1 - p[y,7]) * p[y,11])/pc[y,1];
```

```
p1_cl [y, 11 , 6 ]= ((1 - p[y,5]) * p[y,9] * (1 - p[y,7]) * p[y,11])/pc[y,5];
p1_cl [y, 11 , 7 ]= (av[2,y] * (1 - p[y,5]) * p[y,9] * (1 - p[y,7]) * p[y,11])/pc[y,2];
p1_cl [y, 11 , 8 ]= (av[2,y] * (1 - p[y,5]) * p[y,9] * (1 - p[y,7]) * p[y,11])/pc[y,2];
p1_cl [y, 11 , 11 ]= ((1 - p[y,6]) * p[y,10] * (1 - p[y,8]) * p[y,12])/pc[y,6];
p1_cl [y, 11 , 12 ]= (av[3,y] * (1 - p[y,6]) * p[y,10] * (1 - p[y,8]) * p[y,12])/pc[y,3];
p1_cl [y, 11 , 13 ]= (av[3,y] * (1 - p[y,6]) * p[y,10] * (1 - p[y,8]) * p[y,12])/pc[y,3];
p1_cl [y, 11 , 16 ]= ((1 - p[y,6]) * p[y,10] * (1 - p[y,8]) * p[y,12])/pc[y,6];
p1_cl [y, 11 , 17 ]= (av[4,y] * (1 - p[y,6]) * p[y,10] * (1 - p[y,8]) * p[y,12])/pc[y,4];
p1_cl [y, 11 , 18 ]= (av[4,y] * (1 - p[y,6]) * p[y,10] * (1 - p[y,8]) * p[y,12])/pc[y,4];
p1_cl [y, 12 , 1 ]= ((1 - p[y,5]) * p[y,9] * (1 - p[y,7]) * (1 - p[y,11]))/pc[y,5];
p1_cl [y, 12 , 2 ]= (av[1,y] * (1 - p[y,5]) * p[y,9] * (1 - p[y,7]) * (1 - p[y,11]) + av[5,y] * (1 - p[y,5]) * p[y,9])/pc[y,1];
p1_cl [y, 12 , 3 ]= (av[1,y] * (1 - p[y,5]) * p[y,9] * (1 - p[y,7]) * (1 - p[y,11]) + av[5,y] * (1 - p[y,5]) * p[y,9])/pc[y,1];
p1_cl [y, 12 , 6 ]= ((1 - p[y,5]) * p[y,9] * (1 - p[y,7]) * (1 - p[y,11]))/pc[y,5];
p1_cl [y, 12 , 7 ]= (av[2,y] * (1 - p[y,5]) * p[y,9] * (1 - p[y,7]) * (1 - p[y,11]) + av[6,y] * (1 - p[y,5]) * p[y,9])/pc[y,2];
p1_cl [y, 12 , 8 ]= (av[2,y] * (1 - p[y,5]) * p[y,9] * (1 - p[y,7]) * (1 - p[y,11]) + av[6,y] * (1 - p[y,5]) * p[y,9])/pc[y,2];
p1_cl [y, 12 , 11 ]= ((1 - p[y,6]) * p[y,10] * (1 - p[y,8]) * (1 - p[y,12]))/pc[y,6];
p1_cl [y, 12 , 12 ]= (av[3,y] * (1 - p[y,6]) * p[y,10] * (1 - p[y,8]) * (1 - p[y,12]) + av[7,y] * (1 - p[y,6]) * p[y,10])/pc[y,3];
p1_cl [y, 12 , 13 ]= (av[3,y] * (1 - p[y,6]) * p[y,10] * (1 - p[y,8]) * (1 - p[y,12]) + av[7,y] * (1 - p[y,6]) * p[y,10])/pc[y,3];
p1_cl [y, 12 , 16 ]= ((1 - p[y,6]) * p[y,10] * (1 - p[y,8]) * (1 - p[y,12]))/pc[y,6];
p1_cl [y, 12 , 17 ]= (av[4,y] * (1 - p[y,6]) * p[y,10] * (1 - p[y,8]) * (1 - p[y,12]) + av[8,y] * (1 - p[y,6]) * p[y,10])/pc[y,4];
p1_cl [y, 12 , 18 ]= (av[4,y] * (1 - p[y,6]) * p[y,10] * (1 - p[y,8]) * (1 - p[y,12]) + av[8,y] * (1 - p[y,6]) * p[y,10])/pc[y,4];
p1_cl [y, 13 , 1 ]= ((1 - p[y,5]) * (1 - p[y,9]) * p[y,7] * p[y,15])/pc[y,5];
p1_cl [y, 13 , 2 ]= (av[1,y] * (1 - p[y,5]) * (1 - p[y,9]) * p[y,7] * p[y,15] + av[9,y] * p[y,7] * p[y,15])/pc[y,1];
p1_cl [y, 13 , 3 ]= (av[1,y] * (1 - p[y,5]) * (1 - p[y,9]) * p[y,7] * p[y,15] + av[9,y] * p[y,7] * p[y,15])/pc[y,1];
p1_cl [y, 13 , 6 ]= ((1 - p[y,5]) * (1 - p[y,9]) * p[y,7] * p[y,15])/pc[y,5];
p1_cl [y, 13 , 7 ]= (av[2,y] * (1 - p[y,5]) * (1 - p[y,9]) * p[y,7] * p[y,15] + av[10,y] * p[y,7] * p[y,15])/pc[y,2];
p1_cl [y, 13 , 8 ]= (av[2,y] * (1 - p[y,5]) * (1 - p[y,9]) * p[y,7] * p[y,15] + av[10,y] * p[y,7] * p[y,15])/pc[y,2];
p1_cl [y, 13 , 11 ]= ((1 - p[y,6]) * (1 - p[y,10]) * p[y,8] * p[y,16])/pc[y,6];
p1_cl [y, 13 , 12 ]= (av[3,y] * (1 - p[y,6]) * (1 - p[y,10]) * p[y,8] * p[y,16] + av[11,y] * p[y,8] * p[y,16])/pc[y,3];
p1_cl [y, 13 , 13 ]= (av[3,y] * (1 - p[y,6]) * (1 - p[y,10]) * p[y,8] * p[y,16] + av[11,y] * p[y,8] * p[y,16])/pc[y,3];
p1_cl [y, 13 , 16 ]= ((1 - p[y,6]) * (1 - p[y,10]) * p[y,8] * p[y,16])/pc[y,6];
p1_cl [y, 13 , 17 ]= (av[4,y] * (1 - p[y,6]) * (1 - p[y,10]) * p[y,8] * p[y,16] + av[12,y] * p[y,8] * p[y,16])/pc[y,4];
p1_cl [y, 13 , 18 ]= (av[4,y] * (1 - p[y,6]) * (1 - p[y,10]) * p[y,8] * p[y,16] + av[12,y] * p[y,8] * p[y,16])/pc[y,4];
```

```
    p1_cl [y, 14 , 1 ]= ((1 - p[y,5]) * (1 - p[y,9]) * p[y,7] * (1 - p[y,15]))/pc[y,5];
    p1_cl [y, 14 , 2 ]= (av[1,y] * (1 - p[y,5]) * (1 - p[y,9]) * p[y,7] * (1 - p[y,15]) + av[9,y] * p[y,7] * (1 - p[y,15]))/pc[y,1];
    p1_cl [y, 14 , 3 ]= (av[1,y] * (1 - p[y,5]) * (1 - p[y,9]) * p[y,7] * (1 - p[y,15]) + av[9,y] * p[y,7] * (1 - p[y,15]))/pc[y,1];
    p1_cl [y, 14 , 6 ]= ((1 - p[y,5]) * (1 - p[y,9]) * p[y,7] * (1 - p[y,15]))/pc[y,5];
    p1_cl [y, 14 , 7 ]= (av[2,y] * (1 - p[y,5]) * (1 - p[y,9]) * p[y,7] * (1 - p[y,15]) + av[10,y] * p[y,7] * (1 - p[y,15]))/pc[y,2];
    p1_cl [y, 14 , 8 ]= (av[2,y] * (1 - p[y,5]) * (1 - p[y,9]) * p[y,7] * (1 - p[y,15]) + av[10,y] * p[y,7] * (1 - p[y,15]))/pc[y,2];
    p1_cl [y, 14 , 11 ]= ((1 - p[y,6]) * (1 - p[y,10]) * p[y,8] * (1 - p[y,16]))/pc[y,6];
    p1_cl [y, 14 , 12 ]= (av[3,y] * (1 - p[y,6]) * (1 - p[y,10]) * p[y,8] * (1 - p[y,16]) + av[11,y] * p[y,8] * (1 - p[y,16]))/pc[y,3];
    p1_cl [y, 14 , 13 ]= (av[3,y] * (1 - p[y,6]) * (1 - p[y,10]) * p[y,8] * (1 - p[y,16]) + av[11,y] * p[y,8] * (1 - p[y,16]))/pc[y,3];
    p1_cl [y, 14 , 16 ]= ((1 - p[y,6]) * (1 - p[y,10]) * p[y,8] * (1 - p[y,16]))/pc[y,6];
    p1_cl [y, 14 , 17 ]= (av[4,y] * (1 - p[y,6]) * (1 - p[y,10]) * p[y,8] * (1 - p[y,16]) + av[12,y] * p[y,8] * (1 - p[y,16]))/pc[y,4];
    p1_cl [y, 14 , 18 ]= (av[4,y] * (1 - p[y,6]) * (1 - p[y,10]) * p[y,8] * (1 - p[y,16]) + av[12,y] * p[y,8] * (1 - p[y,16]))/pc[y,4];
    p1_cl [y, 15 , 1 ]= ((1 - p[y,5]) * (1 - p[y,9]) * (1 - p[y,7]) * p[y,11])/pc[y,5];
    p1_cl [y, 15 , 2 ]= (av[1,y] * (1 - p[y,5]) * (1 - p[y,9]) * (1 - p[y,7]) * p[y,11] + av[9,y] * (1 - p[y,7]) * p[y,11])/pc[y,1];
    p1_cl [y, 15 , 3 ]= (av[1,y] * (1 - p[y,5]) * (1 - p[y,9]) * (1 - p[y,7]) * p[y,11] + av[9,y] * (1 - p[y,7]) * p[y,11])/pc[y,1];
    p1_cl [y, 15 , 6 ]= ((1 - p[y,5]) * (1 - p[y,9]) * (1 - p[y,7]) * p[y,11])/pc[y,5];
    p1_cl [y, 15 , 7 ]= (av[2,y] * (1 - p[y,5]) * (1 - p[y,9]) * (1 - p[y,7]) * p[y,11] + av[10,y] * (1 - p[y,7]) * p[y,11])/pc[y,2];
    p1_cl [y, 15 , 8 ]= (av[2,y] * (1 - p[y,5]) * (1 - p[y,9]) * (1 - p[y,7]) * p[y,11] + av[10,y] * (1 - p[y,7]) * p[y,11])/pc[y,2];
    p1_cl [y, 15 , 11 ]= ((1 - p[y,6]) * (1 - p[y,10]) * (1 - p[y,8]) * p[y,12])/pc[y,6];
    p1_cl [y, 15 , 12 ]= (av[3,y] * (1 - p[y,6]) * (1 - p[y,10]) * (1 - p[y,8]) * p[y,12] + av[11,y] * (1 - p[y,8]) * p[y,12])/pc[y,3];
    p1_cl [y, 15 , 13 ]= (av[3,y] * (1 - p[y,6]) * (1 - p[y,10]) * (1 - p[y,8]) * p[y,12] + av[11,y] * (1 - p[y,8]) * p[y,12])/pc[y,3];
    p1_cl [y, 15 , 16 ]= ((1 - p[y,6]) * (1 - p[y,10]) * (1 - p[y,8]) * p[y,12])/pc[y,6];
    p1_cl [y, 15 , 17 ]= (av[4,y] * (1 - p[y,6]) * (1 - p[y,10]) * (1 - p[y,8]) * p[y,12] + av[12,y] * (1 - p[y,8]) * p[y,12])/pc[y,4];
    p1_cl [y, 15 , 18 ]= (av[4,y] * (1 - p[y,6]) * (1 - p[y,10]) * (1 - p[y,8]) * p[y,12] + av[12,y] * (1 - p[y,8]) * p[y,12])/pc[y,4];

}


//use this to fill out pi-matrix:

//if fish is small not ripe:
        upsm = ((1-j[1])*(1-r[1]))/(j[1]*(1-r[2])+(1-j[1])*(1-r[1]));// unconditional probability of being male given not ripe
        upsf = 1-upsm;//unconditional prob of being female given not ripe
```

```
//if fish is large not ripe:
        uplm = ((1-j[2])*(1-r[3]))/(j[2]*(1-r[4])+(1-j[2])*(1-r[3]));// unconditional probability of being male given not ripe
        uplf = 1-uplm;//unconditional prob of being female given not ripe


//indexing for both pi_spring and pi_fall are as follows:
//where dim = [,,1,,]:
        // here detections in LCR (1-6) could be resident or migrant
        // detection in CR (7-10) could be migrant or skipped migrant
// 1 = small ripe female captured in LCR - no MUX detection - no previous cr capture 100-199mm TL
// 2 = small ripe male captured in LCR - no MUX detection - no previous cr capture 100-199mm TL
// 3 = small nonripe fish captured in LCR - no MUX detection - no previous cr capture 100-199mm TL
// 4 = large ripe female captured in LCR - no MUX detection - no previous cr capture 100-199mm TL
// 5 = large ripe male captured in LCR - no MUX detection - no previous cr capture 100-199mm TL
// 6 = large nonripe fish captured in LCR - no MUX detection - no previous cr capture 100-199mm TL
// 7 = small fish captured in oCR - no MUX detection
// 8 = large fish captured in oCR - no MUX detection
// 9 = small fish captured in uCR - no MUX detection
// 10 = large fish captured in uCR - no MUX detection

//where dim =[,,2,,]
        //here these fish are all migrants
// 1 = small ripe female captured in LCR - MUX detection OR previous cr capture 100-199mm TL
// 2 = small ripe male captured in LCR - MUX detection OR previous cr capture 100-199mm TL
// 3 = small nonripe fish captured in LCR - MUX detection OR previous cr capture 100-199mm TL
// 4 = large ripe female captured in LCR - MUX detection OR previous cr capture 100-199mm TL
// 5 = large ripe male captured in LCR - MUX detection OR previous cr capture 100-199mm TL
// 6 = large nonripe fish captured in LCR - MUX detection OR previous cr capture 100-199mm TL
// 7 = small fish captured in oCR -  MUX detection
// 8 = large fish captured in oCR -  MUX detection
// 9 = small fish captured in uCR -  MUX detection
// 10 = large fish captured in uCR -  MUX detection
```

```
//Fill-in v's:
        //v[1] = prob small male is migrant (not resident) given spring capture in LCR = include yearly RE and info about
        previous //capture (see above)
        //v[2] = v[1] (assume sex doesn't affect this)
        //v[3] = prob large male is migrant (not resident) given spring capture in LCR = include yearly RE and info about
        previous capture //(see above)
        //v[4] = v[4] (assume sex doesn't affect this)

        //v[5] = prob small male is a skipped migrant (not migrant) given CR fall capture = yearly RE
        //v[6] = prob small female is a skipped migrant (not migrant) given CR fall capture = yearly RE
        //v[7] = additive offset of v[5]
        //v[8] = additive offset of v[6]

        //v[9] = prob small male is migrant (not resident) given fall capture in LCR = include yearly RE and info about
        previous capture //(see above)
        //v[10] =
        //v[11] = prob large male is migrant (not resident) given fall capture in LCR = include yearly RE and info about
        previous capture //(see above)
        //v[12] =

        //v[13] = prob small male is skipped migrant (not migrant) given spring capture in CR = constant (this only pertains to
48 fish)
        //v[14] = v[13]
        //v[15] = v[13]
        //v[16] = v[13]

for(y in 1:(Ny-1)){
        v[y,13] = inv_logit(v_mu[11]);

        v[y,5] =inv_logit(v_mu[1] + v_sd*z_v[1,y]);
        v[y,6] =inv_logit(v_mu[2] + v_sd*z_v[2,y]);
        v[y,7] =inv_logit(logit(v[y,5])+b_pi_large[1]);
```

```
v[y,8] =inv_logit(logit(v[y,6])+b_pi_large[2]);

v0[y,1] = v_mu[3] + v_sd*z_v[3,y]; // will become v[1]
v0[y,2] = v_mu[4] + v_sd*z_v[4,y]; // will become v[2]
v0[y,3] = v_mu[5] + v_sd*z_v[5,y]; // will become v[3]
v0[y,4] = v_mu[6] + v_sd*z_v[6,y]; //will become v[4]
v0[y,5] = v_mu[7] + v_sd*z_v[7,y]; //will become v[9]
v0[y,6] = v_mu[8] + v_sd*z_v[8,y]; //will become v[10]
v0[y,7] = v_mu[9] + v_sd*z_v[9,y]; //will become v[11]
v0[y,8] = v_mu[10] + v_sd*z_v[10,y]; //will become v[12]


for(k in 1:2){

//spring captures in observeable CR: - here fish are not observed on MUX
pi_spring[7,k,1,2,y]=j[3]*(1-v[y,13]); // prob small fish captured in cr is small female migrant
pi_spring[7,k,1,4,y]=j[3]*v[y,13]; // prob small fish captured in cr is small female skipped migrant
pi_spring[7,k,1,7,y]=(1-j[3])*(1-v[y,13]); // prob small fish captured in cr is small male migrant
pi_spring[7,k,1,9,y]=(1-j[3])*v[y,13]; // prob small fish captured in cr is small male skipped migrant
pi_spring[8,k,1,12,y]=j[4]*(1-v[y,13]); // prob large fish captured in cr is large female migrant
pi_spring[8,k,1,14,y]=j[4]*v[y,13]; // prob large fish captured in cr is large female skipped migrant
pi_spring[8,k,1,17,y]=(1-j[4])*(1-v[y,13]); // prob large fish captured in cr is large male migrant
pi_spring[8,k,1,19,y]=(1-j[4])*v[y,13]; // prob large fish captured in cr is large male skipped migrant

//spring captures in observeable CR: w/ MUX detection
pi_spring[7,k,2,2,y]=j[3]; // prob small fish captured in cr is small female migrant
pi_spring[7,k,2,7,y]=(1-j[3]); // prob small fish captured in cr is small male migrant
pi_spring[8,k,2,12,y]=j[4]; // prob large fish captured in cr is large female migrant
pi_spring[8,k,2,17,y]=(1-j[4]); // prob large fish captured in cr is large male migrant


//spring captures in unobserveable CR: - not observed on MUX
pi_spring[9,k,1,3,y]=j[3]*(1-v[y,13]); // prob small fish captured in cr in spring is small female migrant
```

```
pi_spring[9,k,1,5,y]=j[3]*v[y,13]; // prob small fish captured in cr in spring is small female skipped migrant
pi_spring[9,k,1,8,y]=(1-j[3])*(1-v[y,13]); // prob small fish captured in cr in spring is small male migrant
pi_spring[9,k,1,10,y]=(1-j[3])*v[y,13]; // prob small fish captured in cr in spring is small male skipped migrant
pi_spring[10,k,1,13,y]=j[4]*(1-v[y,13]); // prob large fish captured in cr in spring is large female migrant
pi_spring[10,k,1,15,y]=j[4]*v[y,13]; // prob large fish captured in cr in spring is large female skipped migrant
pi_spring[10,k,1,18,y]=(1-j[4])*(1-v[y,13]); // prob large fish captured in cr in spring is large male migrant
pi_spring[10,k,1,20,y]=(1-j[4])*v[y,13]; // prob large fish captured in cr in spring is large male skipped migrant

//spring captures in unobserveable CR: - observed on MUX
pi_spring[9,k,2,3,y]=j[3]; // prob small fish captured in cr in spring is small female migrant
pi_spring[9,k,2,8,y]=(1-j[3]); // prob small fish captured in cr in spring is small male migrant
pi_spring[10,k,2,13,y]=j[4]; // prob large fish captured in cr in spring is large female migrant
pi_spring[10,k,2,18,y]=(1-j[4]); // prob large fish captured in cr in spring is large male migrant


//fall captures in observeable CR -with no previous spring MUX detection
pi_fall[7,k,1,2,y]=j[5]*(1-v[y,6]); // prob small fish captured in cr is small female migrant
pi_fall[7,k,1,4,y]=j[5]*v[y,6]; // prob small fish captured in cr is small female skipped migrant
pi_fall[7,k,1,7,y]=(1-j[5])*(1-v[y,5]); // prob small fish captured in cr is small male migrant
pi_fall[7,k,1,9,y]=(1-j[5])*v[y,5]; // prob small fish captured in cr is small male skipped migrant
pi_fall[8,k,1,12,y]=j[6]*(1-v[y,8]); // prob large fish captured in cr is large female migrant
pi_fall[8,k,1,14,y]=j[6]*v[y,8]; // prob large fish captured in cr is large female skipped migrant
pi_fall[8,k,1,17,y]=(1-j[6])*(1-v[y,7]); // prob large fish captured in cr is large male migrant
pi_fall[8,k,1,19,y]=(1-j[6])*v[y,7]; // prob large fish captured in cr is large male skipped migrant

//fall captures in observeable CR -with previous spring MUX detection
pi_fall[7,k,2,2,y]=j[5]; // prob small fish captured in cr is small female migrant
pi_fall[7,k,2,7,y]=(1-j[5]); // prob small fish captured in cr is small male migrant
pi_fall[8,k,2,12,y]=j[6]; // prob large fish captured in cr is large female migrant
pi_fall[8,k,2,17,y]=(1-j[6]); // prob large fish captured in cr is large male migrant


//fall captures in unobserveable CR - no previous MUX detection:
```

```
pi_fall[9,k,1,3,y]=j[5]*(1-v[y,6]); // prob small fish captured in cr is small female migrant
pi_fall[9,k,1,5,y]=j[5]*v[y,6]; // prob small fish captured in cr is small female skipped migrant
pi_fall[9,k,1,8,y]=(1-j[5])*(1-v[y,5]); // prob small fish captured in cr is small male migrant
pi_fall[9,k,1,10,y]=(1-j[5])*v[y,5]; // prob small fish captured in cr is small male skipped migrant
pi_fall[10,k,1,13,y]=j[6]*(1-v[y,8]); // prob large fish captured in cr is large female migrant
pi_fall[10,k,1,15,y]=j[6]*v[y,8]; // prob large fish captured in cr is large female skipped migrant
pi_fall[10,k,1,18,y]=(1-j[6])*(1-v[y,7]); // prob large fish captured in cr is large male migrant
pi_fall[10,k,1,20,y]=(1-j[6])*v[y,7];// prob large fish captured in cr is large male skipped migrant

//fall captures in unobserveable CR - previous MUX detection:
pi_fall[9,k,2,3,y]=j[5]; // prob small fish captured in cr is small female migrant
pi_fall[9,k,2,8,y]=(1-j[5]); // prob small fish captured in cr is small male migrant
pi_fall[10,k,2,13,y]=j[6]; // prob large fish captured in cr is large female migrant
pi_fall[10,k,2,18,y]=(1-j[6]); // prob large fish captured in cr is large male migrant


//for lcr captures, prob a fish is resident is dependent on whether fish had previous lcr capture and the presence of a cr capture
100-//199mm TL
//specifically, if a fish is captured in the cr between 100-199, it cannot be a resident
//also, the for fish never previously captured in the cr between 100-199, the prob of being an lcr resident is a function of hte
number of //times its captured in the lcr in fall btwn 100-199

//note that you are constantly over-writing v[1-4] and v[9-12] - as these are functions of the number of lcr captures
for(h in 1:2){
    v[y,h]=inv_logit(v0[y,h] + b_lcr_cap[1]*(k-1));}
for(h in 3:4){
    v[y,h]=inv_logit(v0[y,h] + b_lcr_cap[2]*(k-1));}
for(h in 9:10){
    v[y,h]=inv_logit(v0[y,h-4] + b_lcr_cap[3]*(k-1));}
for(h in 11:12){
    v[y,h]=inv_logit(v0[y,h-4] + b_lcr_cap[4]*(k-1));}

//spring lcr captures - never captured in cr and not detected on MUX
```

```
//if fish is captured as small ripe female:
pi_spring[1,k,1,1,y] = (1-v[y,2]); //prob small fish is resident
pi_spring[1,k,1,2,y] = v[y,2]*tau; //prob small fish is oCR migrant
pi_spring[1,k,1,3,y] = v[y,2]*(1-tau); // prob fish is uCR migrant
//if fish is small ripe male:
pi_spring[2,k,1,6,y] = (1-v[y,1]); //prob small fish is resident
pi_spring[2,k,1,7,y] = v[y,1]*tau;//prob small fish is oCR migrant
pi_spring[2,k,1,8,y] = v[y,1]*(1-tau); // prob fish is uCR migrant

//spring lcr captures -  captured in cr btwn 100-199mm TL or detected on MUX current spring
//if fish is captured as small ripe female:
//pi_spring[1,k,2,1] = 0; //prob small fish is resident
pi_spring[1,k,2,2,y] = tau; //prob small fish is oCR migrant
pi_spring[1,k,2,3,y] = (1-tau); // prob fish is uCR migrant
//if fish is small ripe male:
//pi_spring[2,k,2,6] = 0; //prob small fish is resident
pi_spring[2,k,2,7,y] = tau;//prob small fish is oCR migrant
pi_spring[2,k,2,8,y] = (1-tau); // prob fish is uCR migrant

for(i in 1:2){
        pi_spring[3,k,i,1,y] = pi_spring[1,k,i,1,y]*upsf; //prob small fish is resident
        pi_spring[3,k,i,2,y] = pi_spring[1,k,i,2,y]*upsf; //prob small fish is resident
        pi_spring[3,k,i,3,y] = pi_spring[1,k,i,3,y]*upsf;//prob small fish is oCR migrant
        pi_spring[3,k,i,6,y] = pi_spring[2,k,i,6,y]*upsm; // prob fish is uCR migrant
        pi_spring[3,k,i,7,y] = pi_spring[2,k,i,7,y]*upsm;//prob small fish is oCR migrant
        pi_spring[3,k,i,8,y] = pi_spring[2,k,i,8,y]*upsm; }// prob fish is uCR migrant

//spring lcr captures - never captured in cr and not detected on MUX during current spring:
//if fish is captured as large ripe female:
pi_spring[4,k,1,11,y] = (1-v[y,4]); //prob small fish is resident
pi_spring[4,k,1,12,y] = v[y,4]*tau; //prob small fish is oCR spawne r
pi_spring[4,k,1,13,y] = v[y,4]*(1-tau); // prob fish is uCR migrant
//if fish is small ripe male:
```

```
pi_spring[5,k,1,16,y] = (1-v[y,3]); //prob small fish is resident
pi_spring[5,k,1,17,y] = v[y,3]*tau;//prob small fish is oCR migrant
pi_spring[5,k,1,18,y] = v[y,3]*(1-tau); // prob fish is uCR migrant

//spring lcr captures - captured in CR btwn 100-199mm TL or detected on MUX
//if fish is captured as large ripe female:
//pi_spring[4,k,2,11,y] = 0; //prob small fish is resident
pi_spring[4,k,2,12,y] = tau; //prob small fish is oCR spawne r
pi_spring[4,k,2,13,y] = (1-tau); // prob fish is uCR migrant
//if fish is small ripe male:
//pi_spring[5,k,2,16,y] = 0; //prob small fish is resident
pi_spring[5,k,2,17,y] = tau;//prob small fish is oCR migrant
pi_spring[5,k,2,18,y] = (1-tau); // prob fish is uCR migrant

//for non-ripe fish in spring:
for(i in 1:2){
        pi_spring[6,k,i,11,y] = pi_spring[4,k,i,11,y]*uplf; //prob small fish is female resident
        pi_spring[6,k,i,12,y] = pi_spring[4,k,i,12,y]*uplf; //prob small fish is female oCR migrant
        pi_spring[6,k,i,13,y] = pi_spring[4,k,i,13,y]*uplf;//prob small fish is female uCR migrant
        pi_spring[6,k,i,16,y] = pi_spring[5,k,i,16,y]*uplm; // prob fish is male resident
        pi_spring[6,k,i,17,y] = pi_spring[5,k,i,17,y]*uplm;//prob small fish is male oCR migrant
        pi_spring[6,k,i,18,y] = pi_spring[5,k,i,18,y]*uplm;} // prob fish is male uCR migrant

//fall lcr captures - fish never captured in cr and not detected on MUX spring previous:
//ripe small female:
pi_fall[1,k,1,1,y]=(1-v[y,10]);
pi_fall[1,k,1,2,y]=v[y,10]*tau;
pi_fall[1,k,1,3,y]=v[y,10]*(1-tau);
//ripe fall male:
pi_fall[2,k,1,6,y]=(1-v[y,9]);
pi_fall[2,k,1,7,y]=v[y,9]*tau;
pi_fall[2,k,1,8,y]=v[y,9]*(1-tau);
```

```
//fall lcr captures - fish captured in cr 100-199mm TL or detected on MUX spring previous:
//ripe small female:
//pi_fall[1,k,2,1,y]=0; // can't be resident
pi_fall[1,k,2,2,y]=tau;
pi_fall[1,k,2,3,y]=(1-tau);
//ripe fall male:
//pi_fall[2,k,2,6,y]=0;// can't be resident
pi_fall[2,k,2,7,y]=tau;
pi_fall[2,k,2,8,y]=(1-tau);

//small not ripe:
for(i in 1:2){
        pi_fall[3,k,i,1,y] = j[7]*pi_fall[1,k,i,1,y];
        pi_fall[3,k,i,2,y] = j[7]*pi_fall[1,k,i,2,y];
        pi_fall[3,k,i,3,y] = j[7]*pi_fall[1,k,i,3,y];
        pi_fall[3,k,i,6,y] = (1-j[7])*pi_fall[2,k,i,6,y];
        pi_fall[3,k,i,7,y] = (1-j[7])*pi_fall[2,k,i,7,y];
        pi_fall[3,k,i,8,y] = (1-j[7])*pi_fall[2,k,i,8,y];}


//ripe large female -never captured in cr and not detected on MUX spring previous:
pi_fall[4,k,1,11,y]=(1-v[y,12]);
pi_fall[4,k,1,12,y]=v[y,12]*tau;
pi_fall[4,k,1,13,y]=v[y,12]*(1-tau);
//ripe large male:
pi_fall[5,k,1,16,y]=(1-v[y,11]);
pi_fall[5,k,1,17,y]=v[y,11]*tau;
pi_fall[5,k,1,18,y]=v[y,11]*(1-tau);

//ripe large female -captured in cr btwn 100-199mm TL or detected on MUX spring previous:
//pi_fall[4,k,2,11]=0;// can't be resident
pi_fall[4,k,2,12,y]=tau;
pi_fall[4,k,2,13,y]=(1-tau);
```

```
		//ripe large male:
		//pi_fall[5,k,2,16]=0; // can't be resident
		pi_fall[5,k,2,17,y]=tau;
		pi_fall[5,k,2,18,y]=(1-tau);


		//large not ripe:
		for(i in 1:2){
			pi_fall[6,k,i,11,y] = j[8]*pi_fall[4,k,i,11,y];
			pi_fall[6,k,i,12,y] = j[8]*pi_fall[4,k,i,12,y];
			pi_fall[6,k,i,13,y] = j[8]*pi_fall[4,k,i,13,y];
			pi_fall[6,k,i,16,y] = (1-j[8])*pi_fall[5,k,i,16,y];
			pi_fall[6,k,i,17,y] = (1-j[8])*pi_fall[5,k,i,17,y];
			pi_fall[6,k,i,18,y] = (1-j[8])*pi_fall[5,k,i,18,y];}}}



	}


model{

	vector[Ntot] lprob; //likelihood from open model (spring & fall)
	vector[Ntot_cl] lprob_cl; // likelihood from closed model (spring)
	real pvect[Ny,21,2];
	real pvect_cl[21];
	real spvect_cl[21];
	real temp[21];
	real temp2[21];
	real sum_pvect;

	m_av_1_mu~normal(-0.5,1);
	m_av_2_mu~normal(-0.5,1);
```

```
m_av_3_mu~normal(-0.5,1);
m_av_4_mu~normal(-0.5,1);

for(i in 1:3){
        z_av_1[i]~normal(0,1);
        z_av_2[i]~normal(0,1);
        z_av_3[i]~normal(0,1);
        z_av_4[i]~normal(0,1);
        }

for(i in 1:(Ny-1)) {z_a[i] ~normal(0,1);
                    z_w[i] ~normal(0,1);
        for(k in 1:2){
                z_S[i,k]~normal(0,1);}}

for(k in 1:2){
        S_mu[k]~ normal(0,2);}


S_offset ~ normal(0,2);
w_mu~ normal(0,2);

for(i in 1:4){z_p_spring[i]~normal(0,1);
            z_p_fall[i]~normal(0,1);}
for(i in 1:10){z_v[i]~normal(0,1);}

behavior~normal(0,2);
a0~normal(0,2);
b0~normal(0,2);
b_lcr_cap~normal(0,2);
p_spring_mu~normal(0,2);
p_fall_mu~normal(0,2);
beta_p_turb~normal(0,2);
```

```
beta_p_temp~normal(0,2);
b_pi_large~normal(0,2);
v_mu~normal(0,2);

for(h in 1:Ntot){
	if(season_release[h]==1){

	for (i in 1:21){
		pvect[sumf[h],i,1]=(1-
newtag[h]*tag_loss_rate)*pi_spring[CH_spring[h,sumf[h]],lcr_cap[h],cr_mux_cap[h],i,sumf[h]] ;}
	pvect[sumf[h],21,1]=newtag[h]*tag_loss_rate ;

	//open model:
	if(sumf[h]<Ny) {
		for (t in sumf[h]:(Ny-1)) {
			for (i in 1:21) {
				for (z in 1:21) {
					temp[z] = pvect[t, z,1] * psi2[t,z, i] * p2[t, CH_fall[h, t], i];}
				pvect[t, i,2] = sum(temp); }
			for (i in 1:21) {
				for (z in 1:21) {
					temp[z] = pvect[t, z,2] * psi1[t,z, i] * p1_open[t, CH_spring[h, t+1], i];}
				pvect[t+1, i,1] = sum(temp); }
				}
			}

		lprob[h]=freq[h]*log(sum(pvect[Ny,,1]));

	//closed model:
	if(cl_ind[h]==1){
		for (t in sumf[h]:(Ny-1)) {
			if(cCH_start[h,t]!=0){
				sum_pvect = sum(pvect[t+1,,1]);
```

```
                        //scale pvect so it sums to 1:
                        for(i in 1:21){
                                spvect_cl[i] = pvect[t+1,i,1]/sum_pvect;}
                        for(z in cCH_start[h,t]:cCH_end[h,t]){
                                for(k in 1:21){
                                        pvect_cl[k] = spvect_cl[k] * p1_cl[t,cCH_ind[z],k];}
                                lprob_cl[z] = cCH_freq[z]*log(sum(pvect_cl));}}}}}



        if(season_release[h]==2){

        for (i in 1:21){
                pvect[sumf[h],i,2]=(1-newtag[h]*tag_loss_rate)*pi_fall[CH_fall[h,sumf[h]],lcr_cap[h], cr_mux_cap[h],i,
sumf[h]];}
        pvect[sumf[h],21,2]=newtag[h]*tag_loss_rate;

        for (i in 1:21) {
                for (z in 1:21) {
                        temp[z] = pvect[sumf[h], z,2] * psi1[sumf[h],z, i] * p1_open[sumf[h], CH_spring[h, sumf[h]+1], i];}
                        pvect[sumf[h]+1, i,1] = sum(temp); }

        if(sumf[h]<(Ny-1)) {
                for (t in (sumf[h] + 1):(Ny-1)) {
                        for (i in 1:21) {
                                for (z in 1:21) {
                                        temp[z] = pvect[t, z,1] * psi2[t,z, i] * p2[t, CH_fall[h, t], i];}
                                pvect[t, i,2] = sum(temp); }
                        for (i in 1:21) {
                                for (z in 1:21) {
                                        temp[z] = pvect[t, z,2] * psi1[t,z, i] * p1_open[t, CH_spring[h, t+1], i];}
                                pvect[t+1, i,1] = sum(temp); }
                                }
```

```
                    }

        lprob[h]=freq[h]*log(sum(pvect[Ny,,1]));

if(cl_ind[h]==1){
        for (t in sumf[h]:(Ny-1)) {
                if(cCH_start[h,t]!=0){
                        sum_pvect = sum(pvect[t+1,,1]);
                        //scale pvect so it sums to 1:
                        for(i in 1:21){
                                spvect_cl[i] = pvect[t+1,i,1]/sum_pvect;}
                        for(z in cCH_start[h,t]:cCH_end[h,t]){
                                for(k in 1:21){
                                        pvect_cl[k] = spvect_cl[k] * p1_cl[t,cCH_ind[z],k];}
                                lprob_cl[z] = cCH_freq[z]*log(sum(pvect_cl));}}}}}


        target+= (sum(lprob) + sum(lprob_cl));}
```

Appendix E. Code for including PIT antenna detections into abundance estimates

```
#Closed model simulation
#Produce a capture history 'Y' based on 3 days of sampling
#Y[,c(1,3,5)] correspond to physical capture on days 1-3
#Y[,c(2,4,6)] correspond to antenna detection on days 1-3
#tag refers to whether or not fish was tagged prior to start of the study (0=no; 1=yes)

sim<-function(pact,pdet,pm){
        y<-matrix(0,nrow=1000,ncol=6)
        tag<-rbinom(1000,1,pm)
        y[,1]<-rbinom(1000,1,pact)
        y[,3]<-rbinom(1000,1,pact)
        y[,5]<-rbinom(1000,1,pact)
        t1<-ifelse(rowSums(cbind(tag,y[,1]))>0,1,0)
        t2<-ifelse(rowSums(cbind(tag,y[,1],y[,3]))>0,1,0)
        y[,2]<-rbinom(1000,1,pdet*tag)
        y[,4]<-rbinom(1000,1,pdet*t1)
        y[,6]<-rbinom(1000,1,pdet*t2)
        Y<-subset(y,rowSums(y)>0)
        tag<-subset(tag,rowSums(y)>0)
        return(list(Y=Y,tag=tag))}

#Function for combinations - for y trials and x successes y!/((x-y)!*x!)
lcombo.fun<-function(x,y){
        if(x==0 | x==y){out<-1}
        if(x !=0 & x!=y){out<-exp(sum(log(1:y))-(sum(log(1:x))+sum(log(1:(y-x)))))}
        out}

#First model : fit model to data without antenna detections (reference)
lik_m1<-function(par, data){
 data$Y->Y
 data$tag->tag
 pstar<-par[1]
 Y2<-Y[which(apply(Y[,c(1,3,5)],1,sum)>0),]
 if(pstar>0){
        p1<-1-(1-pstar)^(1/3)
        ll<-numeric()
        for (i in 1:length(Y2[,1])){
                C1<-sum(Y2[i,c(1,3,5)])
```

```
            ll[i]=log(lcombo.fun(C1,3))+C1*log(p1)+(3-C1)*log(1-p1)-log(pstar)}
        sum(-1*ll)} else{10000000}}


#Second model - keep track of gear specific capture
lik_m2<-function(par, data){
 data$Y->Y
 data$tag->tag
 pstar_notag<-par[1]
 pstar_tag<-par[2]
 if(pstar_tag>pstar_notag & pstar_tag>0 & pstar_notag>0){
        p1<-1-(1-pstar_notag)^(1/3)
        p2<-1-(1-pstar_tag)^(1/3)/(1-p1)
        ll<-numeric()
        for (i in 1:length(Y[,1])){
            C1<-sum(Y[i,c(1,3,5)])
            if (tag[i]==1) {
                C2<-sum(Y[i,c(2,4,6)])
                ll[i]=log(lcombo.fun(C1,3))+log(lcombo.fun(C2,3))+C1*log(p1)+(3-C1)*log(1-p1)+C2*log(p2)+(3-C2)*log(1-p2)-
log(pstar_tag)} else {
                if (Y[i,1]==1) {
                    C2<-sum(Y[i,c(4,6)])
                    ll[i]=log(lcombo.fun(C1-1,2))+log(lcombo.fun(C2,2))+C1*log(p1)+(3-C1)*log(1-p1)+C2*log(p2)+(2-C2)*log(1-
p2)-log(pstar_notag)} else {
                    if (Y[i,3]==1) {
                        C2<-Y[i,c(6)]
                        # ditto here.
                        ll[i]=C1*log(p1)+(3-C1)*log(1-p1)+C2*log(p2)+(1-C2)*log(1-p2)-log(pstar_notag)} else {
                            ll[i]=C1*log(p1)+(3-C1)*log(1-p1)-log(pstar_notag)}}}}
            sum(-1*ll)} else{10000000}}


#Horovitz-Thompson estimator for one group
```

```
HTest_1<-function(catch,p,V){
        catch*((1+3*V/(p^2)+(V^2)/(p^4))*(1-p)/(p^2)+(catch-1)*V/(p^4))
        }

#Horovitz-Thompson estimator for two groups (includes covariance)
#Use this when calculating abundance separately for marked and unmarked fish:
HTest_2<-function(catch,pest,vcov.mat){ #assumes p's and catch are in same order
        if (length(catch)!=length(vcov.mat[,1])|length(catch)!=length(vcov.mat[1,])|length(pest)!=length(catch)) (return("ERROR - lengths don't
match!")) else {
                Nstates<-length(catch)
                temp<-numeric()
                temp2<-numeric()
                for (j in 1:Nstates){
                        temp[j]<-(1+3*vcov.mat[j,j]/(pest[j]^2)+(vcov.mat[j,j]^2)/(pest[j]^4))*(1-pest[j])/(pest[j]^2)
                        temp3<-numeric()
                        for (k in 1:Nstates){
                                temp3[k]<-ifelse(j==k,catch[k]-1,catch[k])*vcov.mat[j,k]/((pest[j]^2)*(pest[k]^2))
                                }
                        temp2[j]<-temp[j]+sum(temp3)
                        }
                out<-sum(catch*temp2)
        return(out)
        }}



#Run simulation
#Output includes two matrices (N & N_sd) which correspond to N and sd(N) estimates for each model
#For N & N_sd:
#First row  - model 1- don't use antenna detections
#Second row - model 2- use gear-specific p-caps but estimate abundance only for physical captures
#Third row - model 2- use gear-specific p-caps and estimate abundance separately for marked and unmarked fish

sim.fun<-function(pact, pdet, pm,s) {
```

```
N<-matrix(NA,nrow=100,ncol=3)
N_sd<-matrix(NA,nrow=100,ncol=3)
tt<-list()

for (i in 1:100){
        set.seed(i)
        tt[[i]]<-sim(pact, pdet, pm)
        Y<-tt[[i]]$Y
        tag<-tt[[i]]$tag
        catch<-sum(findInterval(apply(tt[[i]]$Y[,c(1,3,5)],1,sum),1)) #physical captures only

        tm1<-optim(0.4,lik_m1,data=list(Y=Y, tag=tag),method="BFGS",hessian=TRUE)
        if(tm1$convergence==0){
                N[i,1]<-catch/tm1$par[1]
                V<-diag(solve(tm1$hessian))
                v1<-HTest_1(catch,tm1$par[1],V[1])
                N_sd[i,1]<-sqrt(v1)}

        tm2<-optim(c(0.4,0.5),lik_m2,data=list(Y=Y, tag=tag),method="BFGS",hessian=TRUE)
        if(tm2$convergence==0){
                N[i,2]<-catch/tm2$par[1]
                V<-diag(solve(tm2$hessian))
                v1<-HTest_1(catch,tm2$par[1],V[1])
                N_sd[i,2]<-sqrt(v1)
                #Get abundance separately for marked and unmarked groups:
                catch_all<-c(length(which(tt[[i]]$tag==0)),length(which(tt[[i]]$tag==1)))
                N[i,3]<-(catch_all[1]/tm2$par[1]) +  (catch_all[2]/tm2$par[2])
                vcv<-solve(tm2$hessian)
                N_sd[i,3]<-sqrt(HTest_2(catch_all, tm2$par, vcv))}


list(N=N, N_sd=N_sd)
```

```
        }
#Store results in 5d array:
#dim 1 = 1-1000 = simulation id
#dim 2 = 1-6 = model id
#dim 3 = 1-5 = proportion marked (pm = 0.1, 0.2, 0.3, 0.4, 0.5)
#dim 4 = 1-2 = probability of physical capture (pact = 0.1, 0.2)
#dim 5 = 1-2 = probability of antenna detection (pdet = 0.3, 0.6)


N_res = array(NA, dim=c(100,3,5,2,2))
N_sd_res = array(NA, dim=c(100,3,5,2,2))

upm<-1:5*0.1 #proportion marked
upact<-c(0.1,0.2) #capture probability for each pass
updet<-c(0.2,0.6) #antenna detection probability for each pass

for(b in 1:5){
        for(j in 1:2) {
                for(k in 1:2){
                        out<-sim.fun(upact[j], updet[k], upm[b])
                        N_res[,,b,j,k] = out$N
                        N_sd_res[,,b,j,k] = out$N_sd}}}
```

```
#Open model simulation

#Simulate data:
Nocc<-8 #Number of occasions
Nint<-Nocc-1 #Number of intervals
Nstart<-c(2000,1000,2000) #Starting N in each size state
Nadd<-2000 #Number of fish recruited to smallest size state after each occasion
```

```
#Matrix of capture probabilities and antenna detection probabilities
pcap<-array(NA, dim=c(3,Nocc))
pant<-array(NA, dim=c(3,Nocc))

pcap[1,]<-rep(0.3,Nocc)
pcap[2,]<-rep(0.2,Nocc)
pcap[3,]<-rep(0.1,Nocc)

pant[1,]<-rep(0.3,Nocc)
pant[2,]<-rep(0.4,Nocc)
pant[3,]<-rep(0.5,Nocc)

#Function to simulate data, output includes:
# 'sumCH' : a CH matrix that includes antenna detections and physical captures
# 'freq' : a vector describing the number of fish with that particular capture history (where freq[i] corresponds to sumCH[i,])
# 'sumf' : a vector describing the first capture occasion for each capture history (where sumf[i] corresponds to sumCH[i,])
# 'trueN' : a matrix showing the number of fish in each state at each time (to compare estimated value to true value)


sim.dat<-function(seed.i,Nocc,Nstart, Nadd, pcap, pant, stocked){

        Nint<-Nocc-1

        set.seed(seed.i)
        #Growth transition probabilities
        g<-array(NA, dim=c(2,Nint))
        g[1,]<-0.5
        g[2,]<-0.2
        #Survival probabilities
        S<-array(NA, dim=c(3,Nint))
        S[1,]<-0.6
        S[2,]<-0.8
        S[3,]<-0.9
```

```
#Populate state transition matrix
psi<-array(NA,dim=c(4,4, Nint))

for(t in 1:Nint){
        psi[1,1,t]<-S[1,t]*(1-g[1,t])
        psi[1,2,t]<-S[1,t]*g[1,t]
        psi[1,3,t]<-0
        psi[1,4,t]<-1-S[1,t]

        psi[2,1,t]<-0
        psi[2,2,t]<-S[2,t]*(1-g[2,t])
        psi[2,3,t]<-S[2,t]*g[2,t]
        psi[2,4,t]<-1-S[2,t]

        psi[3,1,t]<-0
        psi[3,2,t]<-0
        psi[3,3,t]<-S[3,t]
        psi[3,4,t]<-1-S[3,t]

        psi[4,1,t]<-0
        psi[4,2,t]<-0
        psi[4,3,t]<-0
        psi[4,4,t]<-1}

Ntot<-sum(Nstart)+Nadd*(Nint-1)
Ncum<-cumsum(c(sum(Nstart),rep(Nadd,Nint-1)))

#First simulate true state (1= small; 2=midsize; 3=large, 4 = dead)
true.state<-array(NA, dim=c(Ntot, Nocc))
#Create vector for when fish is first alive
fa<-rep(1,sum(Nstart))
for(y in 2:Nint){fa<-c(fa, rep(y, Nadd))}
```

```
true.state[1:Nstart[1],1]<-1
true.state[(Nstart[1]+1):(Nstart[1]+Nstart[2]),1]<-2
true.state[(Nstart[1]+Nstart[2]+1):(Nstart[1]+Nstart[2]+Nstart[3]),1]<-3

for(y in 1:Nint){
        for(j in 1:sum(Nstart)){
                true.state[j,y+1]<-findInterval(runif(1),cumsum(psi[true.state[j,y],,y]))+1}}

        for(y in 2:Nint){
                true.state[(Ncum[y-1]+1):Ncum[y],y]<-1}

        for(j in (sum(Nstart)+1):Ntot){
                for(y in fa[j]:Nint){
                        true.state[j,y+1]<-findInterval(runif(1),cumsum(psi[true.state[j,y],,y]))+1}}

        0->true.state[is.na(true.state)]
        0->true.state[true.state==4]



#Simulate capture process:
CHcap<-array(0,dim=c(Ntot, Nocc))

if(stocked == FALSE) {
        for(y in 1:Nocc){
                for(j in 1:Ntot){
                        if(true.state[j,y]!=0){
                                CHcap[j,y]<-true.state[j,y]*rbinom(1,1,pcap[true.state[j,y],y])}}}}

if(stocked == TRUE) {
        for(j in 1:Ntot){
                CHcap[j,fa[j]]<-true.state[j,fa[j]]
                if(fa[j]!=Nocc){
                        for(y in (fa[j]+1):Nocc){
```

```
                        if(true.state[j,y]!=0){
                                CHcap[j,y]<-true.state[j,y]*rbinom(1,1,pcap[true.state[j,y],y])}}}}}

#Based on capture history, create mark_mat to indicate whether or not fish is marked during each occasion (0= no; 1=yes)
        mark_mat<-array(0, dim=c(Ntot,Nocc))

        for(j in 1:Ntot){
                for(y in 2:Nocc){
                        if(mark_mat[j,y-1]==0 & CHcap[j,y-1]!=0) {
                                mark_mat[j,y:Nocc]<-1}}}

#Create antenna detection history:
        CHant<-array(0,dim=c(Ntot, Nocc))
        for(y in 2:Nocc){
                for(j in 1:Ntot){
                        if(true.state[j,y]!=0 & mark_mat[j,y-1]==1){
                                CHant[j,y]<-rbinom(1,1,pant[true.state[j,y],y])}}}

        #Create CH that includes antenna detections and physical captures:
        #Key as follows:
        #1 - physical capture only (size 1)
        #2 - physical capture only (size 2)
        #3 - physical capture only (size 3)
        #4 - physical capture with antenna (size 1)
        #5 - physical capture with antenna (size 2)
        #6 - physical capture with antenna (size 3)
        #7 - antenna detection only
        #8 - unobserved

        CH<-CHcap
        for(y in 1:Nocc){
                for(j in 1:Ntot){
                        if(CHant[j,y]!=0 & CHcap[j,y]!=0){
                                CH[j,y]<-CHcap[j,y]+3}
```

```
                    if(CHant[j,y]!=0 & CHcap[j,y]==0){
                        CH[j,y]<-7}}}

#Get true abundance:
trueN<-apply(true.state,2,table)

#Combine similar rows (i.e., make summarized capture history):
tCH<-table(apply(CH,1,paste,collapse=""))
sumCH<-array(NA, dim=c(length(tCH),Nocc))
for(i in 1:length(tCH)){
        for(j in 1:Nocc){
                sumCH[i,j]<-as.numeric(substr(names(tCH)[i],j,j))}}
freq<-as.vector(tCH)

delete<-which(apply(sumCH,1,sum)==0)
if(length(delete>0)){
        sumCH<-sumCH[-delete,]
        freq<-freq[-delete]}

wmin<-function(x){min(which(x!=0))}
sumf<-apply(sumCH,1,wmin)

delete<-which(sumf==Nocc)
if(length(delete>0)){
        sumCH<-sumCH[-delete,]
        freq<-freq[-delete]
        sumf<-sumf[-delete]}

8->sumCH[sumCH==0]

list(sumCH=sumCH, freq=freq,sumf=sumf,trueN=trueN)}


#############
```

```
#Function to calculate physical catch from summarized CH:
catch.fun<-function(sumCH, sumf,freq){
        catch<-array(0, dim=c(dim(sumCH)[1],3,dim(sumCH)[2],2))
        for(i in 1:dim(sumCH)[1]){
                catch[i,sumCH[i,sumf[i]],sumf[i],1]<-freq[i]
                for(j in (sumf[i]+1):dim(sumCH)[2]){
                        if(sumCH[i,j] <7){
                                s<-ifelse(sumCH[i,j]>3,sumCH[i,j]-3,sumCH[i,j])
                                catch[i,s,j,2]<-freq[i]}}}
        apply(catch,c(2,3,4),sum)}


#Function to convert CH to exclude antenna detections:  (to get E1 estimator):
getCH.noantfun<-function(sumCH){
        1->sumCH[which(sumCH==4)]
        2->sumCH[which(sumCH==5)]
        3->sumCH[which(sumCH==6)]
        4->sumCH[which(sumCH>6)]
        #Note (sumf) and Nch and freq should be the same as first capture must always be a physical capture
        #If code is slow, could combine redundant rows in noant sumCH
        sumCH}

#Store output
dat.list<-list()
out<-list() #store stan output for models with antenna detections
out_noant<-list() #store stan output for models without antenna detections
N_E3<-list() #Mean N
N_E2<-list() #Mean N
N_E1<-list() #Mean N
sdN_E3<-list() #sd N
sdN_E2<-list() #sd N
sdN_E1<-list() #sd N
qN_E3<-list() #95% credible interval for N
qN_E2<-list()#95% credible interval for N
```

```
qN_E1<-list()#95% credible interval for N

require("rstan")
rstan_options(auto_write = TRUE)
options(mc.cores = parallel::detectCores())


for(k in 1:100){

	#Simulate data:
	dat.list[[k]]<-sim.dat(k,Nocc,Nstart, Nadd, pcap, pant, stocked=FALSE)
	dat.list[[k]]$catch<-catch.fun(dat.list[[k]]$sumCH, dat.list[[k]]$sumf, dat.list[[k]]$freq)

	#Fit model with antenna detections:
	out[[k]]<-stan(".\\multistate_3sizes_GQ.stan",open_progress=TRUE,data=list(Nch=dim(dat.list[[k]]$sumCH)[1],
Nocc=8,Nint=7,sumCH=dat.list[[k]]$sumCH, sumf=dat.list[[k]]$sumf, freq=dat.list[[k]]$freq, phys_catch=dat.list[[k]]$catch,
tot_phys_catch=apply(dat.list[[k]]$catch,c(1,2),sum)), par=c("pant","pcap","Sdot","gdot","N_E3","N_E2","N_newmark","N_prevmark"),
chains=1, iter=10)
	N_E3post<-extract(out[[k]],"N_E3")[[1]]
	N_E2post<-extract(out[[k]],"N_E2")[[1]]
	N_E3[[k]]<-apply(N_E3post,c(2,3),mean)
	sdN_E3[[k]]<-apply(N_E3post,c(2,3),sd)
	qN_E3[[k]]<-apply(N_E3post,c(2,3),quantile,c(0.025,0.975))
	N_E2[[k]]<-apply(N_E2post,c(2,3),mean)
	sdN_E2[[k]]<-apply(N_E2post,c(2,3),sd)
	qN_E2[[k]]<-apply(N_E2post,c(2,3),quantile,c(0.025,0.975))

	#Fit model without antenna detections:
	out_noant[[k]]<-stan(".\\multistate_3sizes_noant_GQ.stan",open_progress=TRUE,data=list(Nch=dim(dat.list[[k]]$sumCH)[1],
Nocc=8,Nint=7,sumCH=getCH.noantfun(dat.list[[k]]$sumCH), sumf=dat.list[[k]]$sumf, freq=dat.list[[k]]$freq, phys_catch=dat.list[[k]]$catch,
tot_phys_catch=apply(dat.list[[k]]$catch,c(1,2),sum)), par=c("pcap","Sdot","gdot","N_E1"), chains=1, iter=10)
	N_E1post<-extract(out_noant[[k]],"N_E1")[[1]]
	N_E1[[k]]<-apply(N_E1post,c(2,3),mean)
	sdN_E1[[k]]<-apply(N_E1post,c(2,3),sd)
```

```
qN_E1[[k]]<-apply(N_E1post,c(2,3),quantile,c(0.025,0.975))

}
```

```
//Stan code for models with antennas in open model simulation:
// saved as .stan file 'multistate_3sizes_GQ.stan'

data{

 int Nocc; // number of occasions
 int Nch; // number of rows in sumCH
 int Nint; // number of intervals (Nocc-1)
 int<lower=1, upper=7> sumf[Nch]; //vector that indexes first capture for each row of sumCH
 int<lower=1, upper=8> sumCH[Nch,Nocc] ; // capture history that includes both physical captures and antenna detections
 int freq[Nch]; //freq[i] is the number of fish with the capture history denoted in sumCH[i,]
 int phys_catch[3,Nocc,2]; //dim1 = size class, dim2=capture occasion, dim3=either newly marked (1) or previously marked (2)
 int tot_phys_catch[3,Nocc]; //sum across dim 3 of phys_catch so that it includes both newly and previously marked individuals (to get E2)

}

parameters{
  vector<lower=0, upper=1>[3] Sdot;
  vector<lower=0, upper=1>[2] gdot;
  vector<lower=0.0001, upper=1>[Nint] pcap[3]; // pcap for each size and occasion is independent
  vector<lower=0.0001, upper=1>[Nint] pant[3];  // pant for each size and occasion is independent
  }
```

```
transformed parameters{
  simplex[4] psi[4,Nint];
  simplex[8] pmat[4,Nint];
  vector<lower=0, upper=1>[Nint] S[3];
  vector<lower=0, upper=1>[Nint] g[2];

        for(y in 1:Nint){
                for(k in 1:3){
                        S[k,y]=Sdot[k];}
                for(k in 1:2){
                        g[k,y]=gdot[k];}}


        for(t in 1:Nint){
                psi[1,t,1]=S[1,t]*(1-g[1,t]);
                psi[1,t,2]=S[1,t]*g[1,t];
                psi[1,t,3]=0;
                psi[1,t,4]=1-S[1,t];

                psi[2,t,1]=0;
                psi[2,t,2]=S[2,t]*(1-g[2,t]);
                psi[2,t,3]=S[2,t]*g[2,t];
                psi[2,t,4]=1-S[2,t];

                psi[3,t,1]=0;
                psi[3,t,2]=0;
                psi[3,t,3]=S[3,t];
                psi[3,t,4]=1-S[3,t];

                psi[4,t,1]=0;
                psi[4,t,2]=0;
                psi[4,t,3]=0;
                psi[4,t,4]=1;}
```

```
for(y in 1:Nint){
        for(k in 1:4){
                for(j in 1:8){
                        pmat[k,y,j]=0;}}}

//rows correspond to size state (1-3) or dead (4)
//column 1 = physically captured in small state (no antenna detection)
//column 2 = physically captured in midsize state (no antenna detection)
//column 3 = physically captured in large state (no antenna detection)
//column 4 = physically captured in small state (with antenna detection)
//column 5 = physically captured in midsize state (with antenna detection)
//column 6 = physically captured in large state (with antenna detection)
//column 7 = only detected on antennas (no capture)
//column 8 = unobserved (not captured and not detected on antennas)

for(y in 1:Nint){
        pmat[1,y,1] = pcap[1,y]*(1-pant[1,y]);
        pmat[1,y,4] = pcap[1,y]*pant[1,y];
        pmat[1,y,7] = (1-pcap[1,y])*pant[1,y];
        pmat[1,y,8] = (1-pcap[1,y])*(1-pant[1,y]);

        pmat[2,y,2] = pcap[2,y]*(1-pant[2,y]);
        pmat[2,y,5] = pcap[2,y]*pant[2,y];
        pmat[2,y,7] = (1-pcap[2,y])*pant[2,y];
        pmat[2,y,8] = (1-pcap[2,y])*(1-pant[2,y]);

        pmat[3,y,3] = pcap[3,y]*(1-pant[3,y]);
        pmat[3,y,6] = pcap[3,y]*pant[3,y];
        pmat[3,y,7] = (1-pcap[3,y])*pant[3,y];
        pmat[3,y,8] = (1-pcap[3,y])*(1-pant[3,y]);

        pmat[4,y,8]=1;}}
```

```
model{
  vector[Nocc] pvect[4];
  vector[4] temp;

        for(j in 1:Nch){
                for(k in 1:4) {
                        pvect[k,sumf[j]] = (sumCH[j,sumf[j]] ==k);}

                for(y in (sumf[j]+1):Nocc){
                        for(k in 1:4){
                                for(h in 1:4){
                                        temp[h] = pvect[h,y-1]*psi[h,y-1,k];}
                                pvect[k,y] = sum(temp)*pmat[k,y-1,sumCH[j,y]];}}

                target+=freq[j]*log(sum(pvect[,Nocc]));}}

generated quantities{
        vector[Nocc] pvect[Nch,4]; //array of likelihood (same as pvect in model statement except it is saved for each unique CH)
        //Catch values and catch estimates:
        vector[Nocc] ant_only_catch[Nch,3]; //matrix of state-probability vectors estimate catch in each size class for antenna-only detections
        vector[Nocc] add_catch[3]; //sum of 'ant_only_catch' across all unique CH to get total catch for each state and occasion
        vector[Nint] tot_prev_catch[3]; //for previously-marked fish, sum of physical catch and antenna-only detection catch
        //Abundance estimates:
        vector[Nint] N_newmark[3]; //estimated N for newly marked fish
        vector[Nint] N_prevmark[3]; //estimated N for previously marked fish
        vector[Nint] N_E3[3]; // sum N for new marks and previous marks to get E3
        vector[Nint] N_E2[3];
        //These values are constantly overwritten:
        real<lower=0, upper=1> pstar;
        real scale_par;
        real scale_par2;
        vector[4] temp;
        vector<lower=0,upper=1>[3] spvect; //rescaled 'pvect' to be a probability
```

```
//Need to first fill catch with zeros:
for(j in 1:Nch){
	for(s in 1:3){
		for(y in 1:Nocc){
			ant_only_catch[j,s,y]=0;}}}

//Get state likelihoods:
for(j in 1:Nch){
	for(k in 1:4) {
		pvect[j,k,sumf[j]] = (sumCH[j,sumf[j]] ==k);}
	for(y in (sumf[j]+1):Nocc){
		for(k in 1:4){
			for(h in 1:4){
				temp[h] = pvect[j,h,y-1]*psi[h,y-1,k];}
			pvect[j,k,y] = sum(temp)*pmat[k,y-1,sumCH[j,y]];
		//for antenna-only detections, rescale to probability and fill ant_only_catch
		if(sumCH[j,y]==7){
			for(s in 1:3){
				spvect[s]=pvect[j,s,y]/sum(pvect[j,1:3,y]);
				ant_only_catch[j,s,y]=freq[j]*spvect[s];}}}}}

//Can't estimate N for first occasion in open model (fix to zero):
for(s in 1:3){
	N_newmark[s,1]=0;
	N_prevmark[s,1]=0;
	N_E3[s,1]=0;
	N_E2[s,1]=0;
	}

for(s in 1:3){
	for(y in 2:(Nocc-1)){
		//Get E2:
		scale_par = pcap[s,y-1]/(1-pcap[s,y-1]);
```

```
N_E2[s,y]= neg_binomial_rng(tot_phys_catch[s,y],scale_par)+tot_phys_catch[s,y];

//Get E3:
//N for newly marked:
N_newmark[s,y]= neg_binomial_rng(phys_catch[s,y,1],scale_par)+phys_catch[s,y,1];
//N for previously marked:
add_catch[s,y] = sum(ant_only_catch[,s,y]);
pstar=1-(1-pcap[s,y-1])*(1-pant[s,y-1]);
scale_par2 = pstar/(1-pstar);
tot_prev_catch[s,y] = phys_catch[s,y,2]+add_catch[s,y];
N_prevmark[s,y]= neg_binomial_rng(tot_prev_catch[s,y],scale_par2)+tot_prev_catch[s,y];
N_E3[s,y]=N_newmark[s,y]+N_prevmark[s,y];

}}}
```

```
##########################################################################################################################
##########################################################################################################################
##########################################################################################################################
##########################################################################################################################
```

```
//model without antenna for open simulation
// saved as .stan file 'multistate_3sizes_noant_GQ.stan'

data{

 int Nocc; //number of occasions
 int Nch; //number of rows in sumCH
 int Nint; //number of intervals (Nocc-1)
 int<lower=1, upper=7> sumf[Nch]; // first capture occasion for each row of sumCH
 int<lower=1, upper=4> sumCH[Nch,Nocc] ; //capture history matrix (no antenna detections)
 int freq[Nch]; // number of fish with the capture history depicted in corresponding row of sumCH
```

```
 int tot_phys_catch[3,Nocc]; //sum across dim 3 of phys_catch so that it includes both newly and previously marked individuals (to get E2)

}

parameters{
  vector<lower=0, upper=1>[3] Sdot;
  vector<lower=0, upper=1>[2] gdot;
  vector<lower=0.0001, upper=1>[Nint] pcap[3];
  }


transformed parameters{
  simplex[4] psi[4,Nint];
  simplex[4] pmat[4,Nint];
  vector<lower=0, upper=1>[Nint] S[3];
  vector<lower=0, upper=1>[Nint] g[2];

        for(y in 1:Nint){
                for(k in 1:3){
                        S[k,y]=Sdot[k];}
                for(k in 1:2){
                        g[k,y]=gdot[k];}}

        //Fill out state transition matrix:
        for(t in 1:Nint){
                psi[1,t,1]=S[1,t]*(1-g[1,t]);
                psi[1,t,2]=S[1,t]*g[1,t];
                psi[1,t,3]=0;
                psi[1,t,4]=1-S[1,t];

                psi[2,t,1]=0;
                psi[2,t,2]=S[2,t]*(1-g[2,t]);
                psi[2,t,3]=S[2,t]*g[2,t];
                psi[2,t,4]=1-S[2,t];
```

```
        psi[3,t,1]=0;
        psi[3,t,2]=0;
        psi[3,t,3]=S[3,t];
        psi[3,t,4]=1-S[3,t];

        psi[4,t,1]=0;
        psi[4,t,2]=0;
        psi[4,t,3]=0;
        psi[4,t,4]=1;}

//Fill pmat with zeros (will overwrite some of these values below):
for(y in 1:Nint){
        for(k in 1:4){
                for(j in 1:4){
                        pmat[k,y,j]=0;}}}

//rows correspond to size state (1-3) or dead (4)
//column 1 = physically captured in small state
//column 2 = physically captured in midsize state
//column 3 = physically captured in large state
//column 4 = unobserved (not captured)

for(y in 1:Nint){
        pmat[1,y,1] = pcap[1,y];
        pmat[1,y,4] = (1-pcap[1,y]);

        pmat[2,y,2] = pcap[2,y];
        pmat[2,y,4] = (1-pcap[2,y]);

        pmat[3,y,3] = pcap[3,y];
        pmat[3,y,4] = (1-pcap[3,y]);

        pmat[4,y,4]=1;}}
```

```
model{
  vector[Nocc] pvect[4];
  vector[4] temp;

        for(j in 1:Nch){
                for(k in 1:4) {
                        pvect[k,sumf[j]] = (sumCH[j,sumf[j]] ==k);}

                for(y in (sumf[j]+1):Nocc){
                        for(k in 1:4){
                                for(h in 1:4){
                                        temp[h] = pvect[h,y-1]*psi[h,y-1,k];}
                                pvect[k,y] = sum(temp)*pmat[k,y-1,sumCH[j,y]];}}

                target+=freq[j]*log(sum(pvect[,Nocc]));}}

generated quantities{

        real scale_par;
        vector[Nint] N_E1[3];

        for(s in 1:3){
                N_E1[s,1]=0;
                }

        for(s in 1:3){
                for(y in 2:(Nocc-1)){
                        //N for newly marked:
                        scale_par = pcap[s,y-1]/(1-pcap[s,y-1]);
                        N_E1[s,y]= neg_binomial_rng(tot_phys_catch[s,y],scale_par)+tot_phys_catch[s,y];

                        }}}
```

```
#########################################################################################################################
#########################################################################################################################
#########################################################################################################################
#########################################################################################################################

//Applied example (humpback chub in LCR aggregation)

lcr_chub<-read.csv("C:\\Users\\mdzul\\Documents\\N_antenna\\Manuscript\\Data Release\\lcr_chub.csv")


sumCH<-array(unlist(lcr_chub[,1:36]),dim=c(dim(lcr_chub)[1],36))
newtag<-lcr_chub$newtag
suml<-lcr_chub$suml
sumFR<-lcr_chub$sumFR

wmin<-function(x){min(which(x!=14))}
sumf<-apply(sumCH,1,wmin)

#Intervals where LCR was sampled:
LCRs<- c(2,3,5,6,8,9,11,12,13,14,15,16,17,18,19,20,21,22,23,24,25,26,27,28,29,30,31,32,35)
#Intervals where LCR was sampled:
CRs<-c(1,2,4,5,7,8,9,10,11,12,13,14,15,16,17,18,19,20,21,22,23,24,25,26,27,28,29,30,31,32,34,35)
#Index for season:
season<-c(rep(1:3,11),1,2)
#Trip type for CR (accounts for the effect of different sampling protocols)
tt<-c(rep(1,6),rep(2,12),rep(3,14))
#Number of trips for each LCR sampling event:
ntrip_lcr<-c(2,2,2,2,2,2,2,2,1,2,2,1,2,2,1,2,2,1,2,2,1,2,2,1,1,2,1,2,2)

#Temperature covariate for CR capture probability (standardized):
stemp_wtrip<-c(0.1438,0.2566,-0.1868,0.1479,0.5055,1.7142,-1.0621,-0.5309,-0.3356,-1.8465,-0.6845,-0.1271,-1.3494,0.9806,1.8305,-1.5703,-
0.0806,1.2967,-1.6025,0.5085,1.0741,-1.2003,0.3145,0.85,-0.6802,0.0233,0.0492,-1.1373,0.6542,1.8748,0.0946,0.0748)
#Temperature covariate for CR growth probability (standardized):
```

```
stemp<-c(0.0976,0.6089,-1.4581,-0.3852,0.4271,-1.5583,-0.42,2.1254,-0.2678,-0.1034,0.1232,-1.7563,-0.7392,0.0359,-1.3926,0.1912,1.9616,-
0.0428,-0.5383,1.3222,-0.4711,-0.3278,1.3704,-0.3594,-0.2387,1.1071,-0.4849,-0.0824,0.7795,-1.2516,-0.3525,2.3356,-0.6772,-0.1669,0.5886)
#Turbidity covariate for LCR capture probability (0= LCR was mostly bluewater during trips; 1=LCR was mostly brownwater during trips):
turb<-c(0,0,0,0,0,0,1,1,0,1,0,0,1,0,0,0,0,0,0,0,0,0,0,0,1,0,0,0)

#Catch for method 3 (dim 1 = state (size and location), dim 2 = year, dim 3 = (1 = unmarked, 2 = marked)
catch_met3<-
array(c(272,416,174,127,228,124,91,26,105,182,257,181,342,159,88,50,192,280,62,56,177,98,71,62,484,825,265,45,172,31,19,19,152,182,63,26,
117,29,22,10,63,174,141,58,301,60,20,16,313,332,150,53,480,154,19,5,306,642,133,47,222,146,28,12,204,360,186,46,94,40,38,19,25,194,77,33,
46,39,40,12,198,139,101,36,36,18,17,13,996,1140,141,48,61,2,8,7,42,152,113,66,56,28,10,9,28,149,289,175,148,104,41,36,76,132,159,115,132,1
11,83,64,151,406,330,146,25,59,26,18,43,139,152,85,15,25,41,33,24,143,272,181,21,20,28,43,80,168,350,206,57,61,17,17,50,304,241,236,42,66,
13,14,39,317,376,200,24,20,27,54,12,131,223,189,9,20,38,17,7,115,285,194,7,19,21,43,26,75,238,219,3,0,9,8),dim=c(8,12,2))
#Just sum across marked and unmarked fish to get total catch:
catch_met2<-apply(catch_met3, c(1,2),sum)


chubSSdata<-list(NsumCH=dim(sumCH)[1], Nocc=36, Nint=35, Ny=12, sumCH=array(as.vector(sumCH), dim=c(dim(sumCH)[1],36)),
                 sumf=sumf, suml=suml,season=season, sumFR=sumFR, LCRs=LCRs, nLCRs=length(LCRs), CRs=CRs, nCRs=length(CRs),
                 catch_met3=array(catch_met3,dim=dim(catch_met3)), catch_met2=array(catch_met2,dim=dim(catch_met2)),
                 fall_ind=seq(2,35, by=3),stemp_wtrip=stemp_wtrip, stemp=stemp,turb=turb,tt=tt,ntrip_lcr=ntrip_lcr,
                 newtag=newtag, ind_year=c(rep(1,8),2,2,2,2), ind_int=c(rep(1,23),rep(2,12)))

params<-c("s","g","m","mu_ls","mu_lg_CR","mu_lg_LCR","beta_g_temp","mu_lm","sd_ls","sd_lg","sd_lm","tau","p_lcr","p_cr","N_E3",
"N_E2", "N_adult_tot_E3","alpha", "p_ant_par", "N_newmarks_E3","N_prevmarks_E3", "beta_g_temp","beta_p_temp","beta_p_turb")

require("rstan")
rstan_options(auto_write = TRUE)
options(mc.cores = parallel::detectCores())

## Call Stan from R
out<- stan("C:\\users\\mdzul\\Documents\\MD code with 2020\\TEST.stan", data = chubSSdata, pars = params, chains = 1, iter = 10)


//////////////////
```

```
//Stan code:

data {
        int<lower=1> NsumCH;
        int Nocc; //number of occasions
        int Nint; //number of intervals (Nocc-1)
        int Ny; //number of years
        int<lower=1,upper=14> sumCH[NsumCH, Nocc];
        int<lower=1,upper=35> sumf[NsumCH];
        int<lower=2,upper=36> suml[NsumCH];
        int<lower=1,upper=3> season[Nint];
        int<lower=1> sumFR[NsumCH];
        int nLCRs;
        int<lower=1> LCRs[nLCRs];
        int nCRs;
        int<lower=1> CRs [nCRs];
        int catch_met2[8,Ny];//physical catch only
        int catch_met3[8,Ny,2]; //also physical catch only, but [,,1] is newly marked and [,,2] is previously marked
        int fall_ind[Ny];
        int<lower=0, upper=1> newtag[NsumCH];
        int ind_year[Ny];//indicates whether tau2[1] or tau2[2] should be used for abundance estimation
        int ind_int[Nint];//indicates whether tau2[1] or tau2[2] should be used interval (for movement matrix)
        vector[Nint] stemp; //standardized temp in CR (for growth)
        vector[nCRs] stemp_wtrip; //temp within trip (for p-cap in CR)
        vector [nLCRs] turb; //either 0 (bluewater) or 1 (brownwater)
        int tt[nCRs]; // either 1 (NSE : 2 trips per interval, JCM 2012-2016), 2: old 4B - more effort per spatial area, or 3: new 4B: larger reach,
less effort per RM
        int<lower=1, upper=2> ntrip_lcr[nLCRs];//the number of lcr trips for each interval
        }

parameters {
        real<lower = -8, upper = 8> mu_ls[8]; // hyperprior on 3 month survivals for small and large chub in LCR and CR
        real <lower=0,upper =5> sd_ls; // hyperprior on 3 month survivals for small and large chub in LCR and CR
        real <lower=0,upper=1> tau; // proportion of CR adults residing in observable location
```

```
        vector<lower = -8, upper = 8> [3] mu_lg_LCR [3]; // hyperprior on seasonal growth for LCR
        vector<lower = -8, upper = 8> [3] mu_lg_CR; // hyperprior on growth in CR (season excluded in favor of a temperature effect)
        vector<lower = -8, upper = 8> [8] mu_lm [3]; // hyperprior on seasonal movement rates for 2 sizes and locations
        vector <lower=0,upper=5>[2] sd_lg ; // hyperprior on seasonal growth for two rivers
        real <lower=0,upper =5> sd_lm ; // hyperprior on seasonal movement rates for 2 sizes and locations
        vector [8] z_ls [Nint];
        vector [8] z_lm [Nint];
        vector [6] z_lg [Nint]; //
        real<lower=0,upper=1> alpha;//probability fish in uCR is actually in the new expanded 4B reach
        real<lower=0, upper=1> p_ant_par[9,4]; // antenna detection probabilities for 3 size classes
        vector[3] beta_g_temp;
        real<lower=0, upper=5> p_lcr_sd;
        real<lower=0, upper=5> p_cr_sd;
        vector[4] beta_p_turb;//size-specific turbidity effect in LCR
        vector[4] beta_p_temp;//size-specific temperature effect in CR
        vector[4] p_lcr_mu;
        vector[4] p_cr_mu[3];//means for p-cap in CR are centered on size and trip type (tt)
        vector[4] z_p_lcr[nLCRs];
        vector[4] z_p_cr[nCRs];

        }

transformed parameters {
        vector <lower=0,upper=1> [8] s [Nint]; // survival for all intervals, 2 locations, and 2 size classes
        vector <lower=0,upper=1> [6] g [Nint]; // growth for all intervals and 2 size classes
        vector <lower=0,upper=1> [8] m [Nint]; // movement for all intervals, 2 locations, and 2 size classes
        simplex[13] tr[13,Nint];
        simplex[14] p[13,Nint];
        vector [8] ls [Nint]; // logit survival for all intervals, 2 locations, and 2 size classes
        vector [6] lg [Nint]; // logit growth for all intervals and 2 size classes
        vector [8] lm [Nint]; // logit movement for all intervals, 2 locations, and 2 size classes
        real<lower=0, upper=1> tau2[2];
        real p_ant[Nint,4];
        vector<lower=0,upper=1> [4] p_lcr [Nint]; // recapture probability in LCR for two size classes
```

```
vector<lower=0,upper=1> [4] p_cr[Nint]; // recapture probability in CR for two size classes


for (j in 1:8){for(i in 1:Nint){ls[i,j]=mu_ls[j]+z_ls[i,j]*sd_ls;}}
for (j in 1:8){for(i in 1:Nint){lm[i,j]=mu_lm[season[i],j]+z_lm[i,j]*sd_lm;}}
for (j in 1:3){for(i in 1:Nint){lg[i,j]=mu_lg_LCR[season[i],j]+z_lg[i,j]*sd_lg[1];}}
for (j in 4:6){for(i in 1:Nint){lg[i,j]=mu_lg_CR[j-3]+beta_g_temp[j-3]*stemp[i]+z_lg[i,j]*sd_lg[2];}}


for (j in 1:6) g[,j]=inv_logit(lg[,j]);
for (j in 1:8) m[,j]=inv_logit(lm[,j]);
for (j in 1:8){
        for (i in 1:Nint){
                s[i,j]=(inv_logit(ls[i,j]))^(season[i]>2 ? 2 : 1);
                }};

tau2[1]=tau;
tau2[2]=tau + (1-tau)*alpha;

//fill in tr with zero's (will over write later):
for(i in 1:Nint){
        for(j in 1:13){
                for(k in 1:13){
                        tr[j,i,k]=0;}}}

//2009-2016 - reach old 4B (smaller) -use tau2[1]
//2017+ - reach new 4B (larger) -use tau2[2]

for (i in 1:Nint){
        tr[1,i,1]=s[i,1]*(1-g[i,1])*(1-m[i,1]);
        tr[1,i,2]=s[i,1]*g[i,1]*(1-m[i,2]);
        tr[1,i,3]=0;
        tr[1,i,4]=0;
        tr[1,i,5]=s[i,1]*(1-g[i,1])*m[i,1]*tau2[ind_int[i]];
```

```
tr[1,i,6]=s[i,1]*g[i,1]*m[i,2]*tau2[ind_int[i]];
tr[1,i,7]=0;
tr[1,i,8]=0;
tr[1,i,9]=s[i,1]*(1-g[i,1])*m[i,1]*(1-tau2[ind_int[i]]);
tr[1,i,10]=s[i,1]*g[i,1]*m[i,2]*(1-tau2[ind_int[i]]);
tr[1,i,11]=0;
tr[1,i,12]=0;
tr[1,i,13]=1-s[i,1];

tr[2,i,1]=0;
tr[2,i,2]=s[i,2]*(1-g[i,2])*(1-m[i,2]);
tr[2,i,3]=s[i,2]*g[i,2]*(1-m[i,3]);
tr[2,i,4]=0;
tr[2,i,5]=0;
tr[2,i,6]=s[i,2]*(1-g[i,2])*m[i,2]*tau2[ind_int[i]];
tr[2,i,7]=s[i,2]*g[i,2]*m[i,3]*tau2[ind_int[i]];
tr[2,i,8]=0;
tr[2,i,9]=0;
tr[2,i,10]=s[i,2]*(1-g[i,2])*m[i,2]*(1-tau2[ind_int[i]]);
tr[2,i,11]=s[i,2]*g[i,2]*m[i,3]*(1-tau2[ind_int[i]]);
tr[2,i,12]=0;
tr[2,i,13]=1-s[i,2];

tr[3,i,1]=0;
tr[3,i,2]=0;
tr[3,i,3]=s[i,3]*(1-g[i,3])*(1-m[i,3]);
tr[3,i,4]=s[i,3]*g[i,3]*(1-m[i,4]);
tr[3,i,5]=0;
tr[3,i,6]=0;
tr[3,i,7]=s[i,3]*(1-g[i,3])*m[i,3]*tau2[ind_int[i]];
tr[3,i,8]=s[i,3]*g[i,3]*m[i,4]*tau2[ind_int[i]];
tr[3,i,9]=0;
tr[3,i,10]=0;
tr[3,i,11]=s[i,3]*(1-g[i,3])*m[i,3]*(1-tau2[ind_int[i]]);
```

```
tr[3,i,12]=s[i,3]*g[i,3]*m[i,4]*(1-tau2[ind_int[i]]);
tr[3,i,13]=1-s[i,3];

tr[4,i,1]=0;
tr[4,i,2]=0;
tr[4,i,3]=0;
tr[4,i,4]=s[i,4]*(1-m[i,4]);
tr[4,i,5]=0;
tr[4,i,6]=0;
tr[4,i,7]=0;
tr[4,i,8]=s[i,4]*m[i,4]*tau2[ind_int[i]];
tr[4,i,9]=0;
tr[4,i,10]=0;
tr[4,i,11]=0;
tr[4,i,12]=s[i,4]*m[i,4]*(1-tau2[ind_int[i]]);
tr[4,i,13]=1-s[i,4];

//States 5-8 - observeable CR:

tr[5,i,1]=s[i,5]*(1-g[i,4])*m[i,5];
tr[5,i,2]=s[i,5]*g[i,4]*m[i,6];
tr[5,i,3]=0;
tr[5,i,4]=0;
tr[5,i,5]=s[i,5]*(1-g[i,4])*(1-m[i,5]);
tr[5,i,6]=s[i,5]*g[i,4]*(1-m[i,6]);
tr[5,i,7]=0;
tr[5,i,8]=0;
tr[5,i,9]=0;
tr[5,i,10]=0;
tr[5,i,11]=0;
tr[5,i,12]=0;
tr[5,i,13]=1-s[i,5];

tr[6,i,1]=0;
```

```
tr[6,i,2]=s[i,6]*(1-g[i,5])*m[i,6];
tr[6,i,3]=s[i,6]*g[i,5]*m[i,7];
tr[6,i,4]=0;
tr[6,i,5]=0;
tr[6,i,6]=s[i,6]*(1-g[i,5])*(1-m[i,6]);
tr[6,i,7]=s[i,6]*g[i,5]*(1-m[i,7]);
tr[6,i,8]=0;
tr[6,i,9]=0;
tr[6,i,10]=0;
tr[6,i,11]=0;
tr[6,i,12]=0;
tr[6,i,13]=1-s[i,6];

tr[7,i,1]=0;
tr[7,i,2]=0;
tr[7,i,3]=s[i,7]*(1-g[i,6])*m[i,7];
tr[7,i,4]=s[i,7]*g[i,6]*m[i,8];
tr[7,i,5]=0;
tr[7,i,6]=0;
tr[7,i,7]=s[i,7]*(1-g[i,6])*(1-m[i,7]);
tr[7,i,8]=s[i,7]*g[i,6]*(1-m[i,8]);
tr[7,i,9]=0;
tr[7,i,10]=0;
tr[7,i,11]=0;
tr[7,i,12]=0;
tr[7,i,13]=1-s[i,7];

tr[8,i,1]=0;
tr[8,i,2]=0;
tr[8,i,3]=0;
tr[8,i,4]=s[i,8]*m[i,8];
tr[8,i,5]=0;
tr[8,i,6]=0;
tr[8,i,7]=0;
```

```
tr[8,i,8]=s[i,8]*(1-m[i,8]);
tr[8,i,9]=0;
tr[8,i,10]=0;
tr[8,i,11]=0;
tr[8,i,12]=0;
tr[8,i,13]=1-s[i,8];

//States 9-12 - CR unobserveable

tr[9,i,1]=s[i,5]*(1-g[i,4])*m[i,5];
tr[9,i,2]=s[i,5]*g[i,4]*m[i,6];
tr[9,i,3]=0;
tr[9,i,4]=0;
tr[9,i,5]=0;
tr[9,i,6]=0;
tr[9,i,7]=0;
tr[9,i,8]=0;
tr[9,i,9]=s[i,5]*(1-g[i,4])*(1-m[i,5]);
tr[9,i,10]=s[i,5]*g[i,4]*(1-m[i,6]);
tr[9,i,11]=0;
tr[9,i,12]=0;
tr[9,i,13]=1-s[i,5];

tr[10,i,1]=0;
tr[10,i,2]=s[i,6]*(1-g[i,5])*m[i,6];
tr[10,i,3]=s[i,6]*g[i,5]*m[i,7];
tr[10,i,4]=0;
tr[10,i,5]=0;
tr[10,i,6]=0;
tr[10,i,7]=0;
tr[10,i,8]=0;
tr[10,i,9]=0;
tr[10,i,10]=s[i,6]*(1-g[i,5])*(1-m[i,6]);
tr[10,i,11]=s[i,6]*g[i,5]*(1-m[i,7]);
```

```
tr[10,i,12]=0;
tr[10,i,13]=1-s[i,6];

tr[11,i,1]=0;
tr[11,i,2]=0;
tr[11,i,3]=s[i,7]*(1-g[i,6])*m[i,7];
tr[11,i,4]=s[i,7]*g[i,6]*m[i,8];
tr[11,i,5]=0;
tr[11,i,6]=0;
tr[11,i,7]=0;
tr[11,i,8]=0;
tr[11,i,9]=0;
tr[11,i,10]=0;
tr[11,i,11]=s[i,7]*(1-g[i,6])*(1-m[i,7]);
tr[11,i,12]=s[i,7]*g[i,6]*(1-m[i,8]);
tr[11,i,13]=1-s[i,7];

tr[12,i,1]=0;
tr[12,i,2]=0;
tr[12,i,3]=0;
tr[12,i,4]=s[i,8]*m[i,8];
tr[12,i,5]=0;
tr[12,i,6]=0;
tr[12,i,7]=0;
tr[12,i,8]=0;
tr[12,i,9]=0;
tr[12,i,10]=0;
tr[12,i,11]=0;
tr[12,i,12]=s[i,8]*(1-m[i,8]);
tr[12,i,13]=1-s[i,8];


for (j in 1:12){
        tr[13,i,j]=0;
```

```
            }
tr[13,i,13]=1;
}


//in spring 2017, reach 4B was expanded:
tr[1,24,1]=s[24,1]*(1-g[24,1])*(1-m[24,1]);
tr[1,24,2]=s[24,1]*g[24,1]*(1-m[24,2]);
tr[1,24,3]=0;
tr[1,24,4]=0;
tr[1,24,5]=s[24,1]*(1-g[24,1])*m[24,1]*tau2[2];
tr[1,24,6]=s[24,1]*g[24,1]*m[24,2]*tau2[2];
tr[1,24,7]=0;
tr[1,24,8]=0;
tr[1,24,9]=s[24,1]*(1-g[24,1])*m[24,1]*(1-tau2[2]);
tr[1,24,10]=s[24,1]*g[24,1]*m[24,2]*(1-tau2[2]);
tr[1,24,11]=0;
tr[1,24,12]=0;
tr[1,24,13]=1-s[24,1];

tr[2,24,1]=0;
tr[2,24,2]=s[24,2]*(1-g[24,2])*(1-m[24,2]);
tr[2,24,3]=s[24,2]*g[24,2]*(1-m[24,3]);
tr[2,24,4]=0;
tr[2,24,5]=0;
tr[2,24,6]=s[24,2]*(1-g[24,2])*m[24,2]*tau2[2];
tr[2,24,7]=s[24,2]*g[24,2]*m[24,3]*tau2[2];
tr[2,24,8]=0;
tr[2,24,9]=0;
tr[2,24,10]=s[24,2]*(1-g[24,2])*m[24,2]*(1-tau2[2]);
tr[2,24,11]=s[24,2]*g[24,2]*m[24,3]*(1-tau2[2]);
tr[2,24,12]=0;
tr[2,24,13]=1-s[24,2];
```

```
tr[3,24,1]=0;
tr[3,24,2]=0;
tr[3,24,3]=s[24,3]*(1-g[24,3])*(1-m[24,3]);
tr[3,24,4]=s[24,3]*g[24,3]*(1-m[24,4]);
tr[3,24,5]=0;
tr[3,24,6]=0;
tr[3,24,7]=s[24,3]*(1-g[24,3])*m[24,3]*tau2[2];
tr[3,24,8]=s[24,3]*g[24,3]*m[24,4]*tau2[2];
tr[3,24,9]=0;
tr[3,24,10]=0;
tr[3,24,11]=s[24,3]*(1-g[24,3])*m[24,3]*(1-tau2[2]);
tr[3,24,12]=s[24,3]*g[24,3]*m[24,4]*(1-tau2[2]);
tr[3,24,13]=1-s[24,3];

tr[4,24,1]=0;
tr[4,24,2]=0;
tr[4,24,3]=0;
tr[4,24,4]=s[24,4]*(1-m[24,4]);
tr[4,24,5]=0;
tr[4,24,6]=0;
tr[4,24,7]=0;
tr[4,24,8]=s[24,4]*m[24,4]*tau2[2];
tr[4,24,9]=0;
tr[4,24,10]=0;
tr[4,24,11]=0;
tr[4,24,12]=s[24,4]*m[24,4]*(1-tau2[2]);
tr[4,24,13]=1-s[24,4];

//States 4-6 - observeable CR:

tr[5,24,1]=s[24,5]*(1-g[24,4])*m[24,5];
tr[5,24,2]=s[24,5]*g[24,4]*m[24,6];
tr[5,24,3]=0;
tr[5,24,4]=0;
```

```
tr[5,24,5]=s[24,5]*(1-g[24,4])*(1-m[24,5]);
tr[5,24,6]=s[24,5]*g[24,4]*(1-m[24,6]);
tr[5,24,7]=0;
tr[5,24,8]=0;
tr[5,24,9]=0;
tr[5,24,10]=0;
tr[5,24,11]=0;
tr[5,24,12]=0;
tr[5,24,13]=1-s[24,5];

tr[6,24,1]=0;
tr[6,24,2]=s[24,6]*(1-g[24,5])*m[24,6];
tr[6,24,3]=s[24,6]*g[24,5]*m[24,7];
tr[6,24,4]=0;
tr[6,24,5]=0;
tr[6,24,6]=s[24,6]*(1-g[24,5])*(1-m[24,6]);
tr[6,24,7]=s[24,6]*g[24,5]*(1-m[24,7]);
tr[6,24,8]=0;
tr[6,24,9]=0;
tr[6,24,10]=0;
tr[6,24,11]=0;
tr[6,24,12]=0;
tr[6,24,13]=1-s[24,6];

tr[7,24,1]=0;
tr[7,24,2]=0;
tr[7,24,3]=s[24,7]*(1-g[24,6])*m[24,7];
tr[7,24,4]=s[24,7]*g[24,6]*m[24,8];
tr[7,24,5]=0;
tr[7,24,6]=0;
tr[7,24,7]=s[24,7]*(1-g[24,6])*(1-m[24,7]);
tr[7,24,8]=s[24,7]*g[24,6]*(1-m[24,8]);
tr[7,24,9]=0;
tr[7,24,10]=0;
```

```
tr[7,24,11]=0;
tr[7,24,12]=0;
tr[7,24,13]=1-s[24,7];

tr[8,24,1]=0;
tr[8,24,2]=0;
tr[8,24,3]=0;
tr[8,24,4]=s[24,8]*m[24,8];
tr[8,24,5]=0;
tr[8,24,6]=0;
tr[8,24,7]=0;
tr[8,24,8]=s[24,8]*(1-m[24,8]);
tr[8,24,9]=0;
tr[8,24,10]=0;
tr[8,24,11]=0;
tr[8,24,12]=0;
tr[8,24,13]=1-s[24,8];


//States 7-9 - CR unobserveable

tr[9,24,1]=s[24,5]*(1-g[24,4])*m[24,5];
tr[9,24,2]=s[24,5]*g[24,4]*m[24,6];
tr[9,24,3]=0;
tr[9,24,4]=0;
tr[9,24,5]=s[24,5]*(1-g[24,4])*(1-m[24,5])*alpha;
tr[9,24,6]=s[24,5]*g[24,4]*(1-m[24,6])*alpha;
tr[9,24,7]=0;
tr[9,24,8]=0;
tr[9,24,9]=s[24,5]*(1-g[24,4])*(1-m[24,5])*(1-alpha);
tr[9,24,10]=s[24,5]*g[24,4]*(1-m[24,6])*(1-alpha);
tr[9,24,11]=0;
tr[9,24,12]=0;
tr[9,24,13]=1-s[24,5];
```

```
tr[10,24,1]=0;
tr[10,24,2]=s[24,6]*(1-g[24,5])*m[24,6];
tr[10,24,3]=s[24,6]*g[24,5]*m[24,7];
tr[10,24,4]=0;
tr[10,24,5]=0;
tr[10,24,6]=s[24,6]*(1-g[24,5])*(1-m[24,6])*alpha;
tr[10,24,7]=s[24,6]*g[24,5]*(1-m[24,7])*alpha;
tr[10,24,8]=0;
tr[10,24,9]=0;
tr[10,24,10]=s[24,6]*(1-g[24,5])*(1-m[24,6])*(1-alpha);
tr[10,24,11]=s[24,6]*g[24,5]*(1-m[24,7])*(1-alpha);
tr[10,24,12]=0;
tr[10,24,13]=1-s[24,6];

tr[11,24,1]=0;
tr[11,24,2]=0;
tr[11,24,3]=s[24,7]*(1-g[24,6])*m[24,7];
tr[11,24,4]=s[24,7]*g[24,6]*m[24,8];
tr[11,24,5]=0;
tr[11,24,6]=0;
tr[11,24,7]=s[24,7]*(1-g[24,6])*(1-m[24,7])*alpha;
tr[11,24,8]=s[24,7]*g[24,6]*(1-m[24,8])*alpha;
tr[11,24,9]=0;
tr[11,24,10]=0;
tr[11,24,11]=s[24,7]*(1-g[24,6])*(1-m[24,7])*(1-alpha);
tr[11,24,12]=s[24,7]*g[24,6]*(1-m[24,8])*(1-alpha);
tr[11,24,13]=1-s[24,7];

tr[12,24,1]=0;
tr[12,24,2]=0;
tr[12,24,3]=0;
tr[12,24,4]=s[24,8]*m[24,8];
tr[12,24,5]=0;
```

```
        tr[12,24,6]=0;
        tr[12,24,7]=0;
        tr[12,24,8]=s[24,8]*(1-m[24,8])*alpha;
        tr[12,24,9]=0;
        tr[12,24,10]=0;
        tr[12,24,11]=0;
        tr[12,24,12]=s[24,8]*(1-m[24,8])*(1-alpha);
        tr[12,24,13]=1-s[24,8];


for (i in 1:Nint){
        for(j in 1:13){
                for(k in 1:14){p[j,i,k]=0;}
                p[j,i,14]=1;}}

//p-matrix = columns 1,2,3,4 = prob of being captured in the LCR for each size class
//p-matrix = columns 5,6,7,8 = prob of being captured in the CR for each size class (and not detected by at antennas)
//p-matrix = columns 9,10,11,12 = prob of being captured and detected by antennas
//p-matrix = columns 13 = prob of being detected by the antennas but not captured
//p-matrix = column 14 = prob of being unobserved


//fill with zeros (overwrite below)
for(j in 1:4){
        for (i in 1:Nint){
                p_lcr[i,j]=0;}
        //fill-in for when LCR was actually sampled:
        for (i in 1:nLCRs){
                p_lcr[LCRs[i],j]=1-pow(1-inv_logit(p_lcr_mu[j]+beta_p_turb[j]*turb[i]+p_lcr_sd*z_p_lcr[i,j]),ntrip_lcr[i]);}
                }

//fill in p-matrix for LCR states:
for (i in 1:nLCRs){
        p[1,LCRs[i],1]=p_lcr[LCRs[i],1];
```

```
		p[2,LCRs[i],2]=p_lcr[LCRs[i],2];
		p[3,LCRs[i],3]=p_lcr[LCRs[i],3];
		p[4,LCRs[i],4]=p_lcr[LCRs[i],4];
		p[1,LCRs[i],14]=1-p_lcr[LCRs[i],1];
		p[2,LCRs[i],14]=1-p_lcr[LCRs[i],2];
		p[3,LCRs[i],14]=1-p_lcr[LCRs[i],3];
		p[4,LCRs[i],14]=1-p_lcr[LCRs[i],4];

		}


//fill with zeros:
for(j in 1:4) {
		for(i in 1:Nint) {
			p_cr[i,j]=0;}
		//overwrite for when CR was actually sampled:
		for(i in 1:nCRs) {
			p_cr[CRs[i],j] = inv_logit(p_cr_mu[tt[i],j]+beta_p_temp[j]*stemp_wtrip[i]+p_cr_sd*z_p_cr[i,j]);}
		}


//antennas only deployed during trips 24, 28-30 (correponds with p 23, 27-29)
for(j in 1:4) {
		for(i in 1:22) {
			p_ant[i,j]=0;}
		p_ant[23,j]=p_ant_par[1,j];
		for(i in 24:26) {
			p_ant[i,j]=0;}
		for(i in 27:32) {
			p_ant[i,j]=p_ant_par[i-25,j];}
		for(i in 34:35) {
			p_ant[i,j]=p_ant_par[i-26,j];}

		}
```

```
        //fill-in p-matrix for CR states:
        for (i in 1:nCRs){
                p[5,CRs[i],5]=p_cr[CRs[i],1] * (1-p_ant[CRs[i],1]);
                p[6,CRs[i],6]=p_cr[CRs[i],2] * (1-p_ant[CRs[i],2]);
                p[7,CRs[i],7]=p_cr[CRs[i],3] * (1-p_ant[CRs[i],3]);
                p[8,CRs[i],8]=p_cr[CRs[i],4] * (1-p_ant[CRs[i],4]);
                p[5,CRs[i],9]=p_cr[CRs[i],1] * p_ant[CRs[i],1];
                p[6,CRs[i],10]=p_cr[CRs[i],2] * p_ant[CRs[i],2];
                p[7,CRs[i],11]=p_cr[CRs[i],3] * p_ant[CRs[i],3];
                p[8,CRs[i],12]=p_cr[CRs[i],4] * p_ant[CRs[i],4];
                p[5,CRs[i],13]=(1-p_cr[CRs[i],1]) * p_ant[CRs[i],1];
                p[6,CRs[i],13]=(1-p_cr[CRs[i],2]) * p_ant[CRs[i],2];
                p[7,CRs[i],13]=(1-p_cr[CRs[i],3]) * p_ant[CRs[i],3];
                p[8,CRs[i],13]=(1-p_cr[CRs[i],4]) * p_ant[CRs[i],4];
                p[5,CRs[i],14]=(1-p_cr[CRs[i],1])*(1-p_ant[CRs[i],1]);
                p[6,CRs[i],14]=(1-p_cr[CRs[i],2])*(1-p_ant[CRs[i],2]);
                p[7,CRs[i],14]=(1-p_cr[CRs[i],3])*(1-p_ant[CRs[i],3]);
                p[8,CRs[i],14]=(1-p_cr[CRs[i],4])*(1-p_ant[CRs[i],4]);

                }

                }

model {
        real temp[13];
        vector[13] pz[Nocc];

        for(i in 1:Nint){z_ls[i]~normal(0,1);
                        z_lg[i]~normal(0,1);
                        z_lm[i]~normal(0,1);}


        mu_ls~normal(0,2);
```

```
        mu_lg_CR~normal(0,2);
        beta_g_temp~normal(0,2);
        beta_p_turb~normal(0,2);
        beta_p_temp~normal(0,2);
        p_lcr_mu~normal(0,2);

        for(i in 1:nCRs){
                z_p_cr[i]~normal(0,1);}

        for(i in 1:nLCRs){
                z_p_lcr[i]~normal(0,1);}

        for(i in 1:3){mu_lm[i]~normal(0,2);
                    mu_lg_LCR[i]~normal(0,2);
                    p_cr_mu[i]~normal(0,2);}

        for (k in 1:NsumCH) {
                for (j in 1:12){
                        pz[sumf[k], j] = (j == sumCH[k, sumf[k]])*(1-newtag[k]*0.03); }
                        pz[sumf[k], 13] = newtag[k]*0.03;
    for (t in (sumf[k] + 1):suml[k]) {
                for (i in 1:13) {
                        for (j in 1:13) {
                                temp[j] = pz[t - 1, j] * tr[j, t - 1, i] * p[i, t - 1, sumCH[k, t]];}
                        pz[t, i] = sum(temp);
                                }
                        }
          target+=(sumFR[k]*log(sum(pz[suml[k]])));
                }
                        }



generated quantities{
```

```
vector[13] pz[NsumCH,Nocc];
simplex[8] spz;
vector[13] ant_only_catch[NsumCH,Nocc];
vector[Ny] prev_mark_catch[8];
vector[13] temp;

real ptrans;
real<lower=0> scale_par;
real<lower=0> scale_par2;
real<lower=0, upper=1> pstar;
int N_E2[8,Ny];
int N_newmarks_E3[8,Ny];
vector[Ny] N_prevmarks_E3[8];
vector[Ny] N_E3[8];
vector[Ny] N_adult_tot_E3;


for(k in 1:NsumCH){
        for(t in 1:Nocc){
                for (j in 1:8) {
                        ant_only_catch[k,t,j] =0;}}}

for (k in 1:NsumCH) {
        for (j in 1:12){
                pz[k,sumf[k], j] = (j == sumCH[k, sumf[k]])*(1-newtag[k]*0.03); }
        pz[k,sumf[k], 13] = newtag[k]*0.03;
        for (t in (sumf[k] + 1):suml[k]) {
                for (i in 1:13) {
                        for (j in 1:13) {
                                temp[j] = pz[k,t - 1, j] * tr[j, t - 1, i] * p[i, t - 1, sumCH[k, t]];}
                        pz[k,t, i] = sum(temp); }
                if(sumCH[k,t]==13){
```

```
                    for (j in 1:8) {
                        spz[j] = pz[k,t,j]/sum(pz[k,t,1:8]);
                        ant_only_catch[k,t,j] = sumFR[k]*spz[j];}}}}

for(t in 1:Ny){
    for (j in 1:8) {
        prev_mark_catch[j,t] = sum(ant_only_catch[1:NsumCH,fall_ind[t]+1,j])+catch_met3[j,t,2];}}

//for LCR adults - no need to include tau in calculation:
for (i in 1:4){
    for(t in 1:Ny){
        //Note: for subadults in CR do not multiply by tau (since you want abundance of subadults in the JCM reach only):
        scale_par=p_lcr[fall_ind[t],i]/(1-p_lcr[fall_ind[t],i]);
        N_E2[i,t]=neg_binomial_rng(catch_met2[i,t],scale_par)+catch_met2[i,t];
        N_E3[i,t]=N_E2[i,t]; }// no antenna detections in LCR so E2 & E3 are similar
    }

//for CR subadults (don't want to include tau as we only want abundance in old 4B site):
//need to divide p-matrix by (1-ant) because capture history '4' indicates CR capture without antenna capture
//Note: in the catch data, you can still include fish captured and detected by antenna as well as fish captured and not detected on the
//antenna
for(k in 5:6){
    for(t in 1:Ny){
        scale_par=p_cr[fall_ind[t],k-4]/(1-p_cr[fall_ind[t],k-4]);
        N_E2[k,t]=neg_binomial_rng(catch_met2[k,t],scale_par)+catch_met2[k,t];
        pstar = 1-(1-p_cr[fall_ind[t],k-4])*(1-p_ant[fall_ind[t],k-4]);
        scale_par2=pstar/(1-pstar);
        N_newmarks_E3[k,t]=neg_binomial_rng(catch_met3[k,t,1],scale_par)+catch_met3[k,t,1];
        N_prevmarks_E3[k,t]=neg_binomial_rng(prev_mark_catch[k,t],scale_par2)+prev_mark_catch[k,t];
        N_E3[k,t]=N_newmarks_E3[k,t]+N_prevmarks_E3[k,t];
        }}

//for CR adults
//want system-wide abundance -so we divide by tau (note two different taus - one for 2009-2016 one for 2017-2018
```

```
        //need to divide p-matrix by (1-ant) because capture histories '5 & 6' indicates CR capture without antenna capture
        //Note: in the catch data, you can still include fish captured and detected by antenna as well as fish captured and not detected on the
antenna
        for (k in 7:8){
                for(t in 1:Ny){
                        ptrans=p_cr[fall_ind[t],k-4]*tau2[ind_year[t]];
                        scale_par=ptrans/(1-ptrans);
                        N_E2[k,t]=neg_binomial_rng(catch_met2[k,t],scale_par)+catch_met2[k,t];
                        pstar = (1-(1-p_cr[fall_ind[t],k-4])*(1-p_ant[fall_ind[t],k-4]))*tau2[ind_year[t]];
                        scale_par2=pstar/(1-pstar);
                        N_newmarks_E3[k,t]=neg_binomial_rng(catch_met3[k,t,1],scale_par)+catch_met3[k,t,1];
                        N_prevmarks_E3[k,t]=neg_binomial_rng(prev_mark_catch[k,t],scale_par2)+prev_mark_catch[k,t];
                        N_E3[k,t]=N_newmarks_E3[k,t]+N_prevmarks_E3[k,t];}}

        //N_tot is for adults only (exclude subadults):
        for(t in 1:Ny){N_adult_tot_E3[t]= N_E3[3,t]+N_E3[4,t]+N_E3[7,t]+N_E3[8,t];}

        }
```

##
##
##
##

#Applied example (humpback chub in western Grand Canyon): Model with temporary emigration (TE)
#R code:

#Applied example (humpback chub in western Grand Canyon): Model with temporary emigration (TE)
#R code:

```
setwd("C://users//mdzul//Documents//N_antenna//Manuscript//Data Release")
west_chub<-read.csv(".//west_chub.csv")
sumCH<-west_chub[,1:10]
freq<-west_chub$freq

#Get first release occasion:
wmin<-function(x){min(which(x!=12))}
sumf<-apply(sumCH,1,wmin)

#Temperature effect for growth (standardized)
stemp<-c(0.3185,-1.4299,0.5128,0.5179,0.1438,-1.8781,0.0848,1.2331,0.4971)
#Temperature effect for capture probability (standardized)
stemp_wtrip<-c(-0.942,-0.2309,0.9128,0.2915,-1.414,-0.9539,1.0711,1.4339,-0.1685)

#catch:
catch_met3<-
array(c(0,156,191,349,1,45,67,42,6,61,0,115,76,183,4,66,98,412,65,68,0,31,17,118,28,21,34,108,158,83,0,62,35,34,12,4,31,97,110,28,0,37,30,40,
32,5,47,22,59,22,0,0,0,0,0,0,0,0,0,0,0,0,0,0,0,0,0,0,0,0,0,0,0,3,3,8,15,7,16,31,59,48,0,9,3,9,3,1,5,23,44,20,0,4,6,5,11,3,6,4,17,7),dim=c(10,5,2))

dat.list<-list(ch=sumCH, sumf=sumf, fr=freq,I=c(1,7,2,1,2,7,2,1,2), stemp=stemp, stemp_wtrip=stemp_wtrip,
Nch=dim(sumCH)[1],Nint=dim(sumCH)[2]-1, Nocc=dim(sumCH)[2],catch_met3=array(catch_met3,dim=dim(catch_met3)),7, Nant_int=7,
ant_ind=c(1:3,5:7,9))

pars<-
c("s","g","mu_lm","sc4_OFFSET","sc5_OFFSET","m","sd_lm","mu_ls","sd_ls","mu_lg","sd_lg","p_cap","p_ant","pcap_mu","pcap_sd","beta_gt
emp","beta_ptemp")

require("rstan")
rstan_options(auto_write = TRUE)
options(mc.cores = parallel::detectCores())

out <- stan("C:\\users\\mdzul\\Documents\\N_antenna\\Manuscript\\Data Release\\west_chub_test.stan", data = dat.list, pars = pars, chains = 1, iter
= 10)
```

```
//////////////////
//Stan model code:

data {
        int Nocc;
        int Nint;
        int Nant_int; // number of occasions when antennas were deployed
        int<lower=1> Nch;
        int<lower=1> sumf [Nch];
        int<lower=1> fr [Nch];
        int<lower=1> I [Nint];  // number of months between sampling occasions
        int<lower=1> ch [Nch,Nocc];
        int<lower=0> catch_met3 [Nocc,5,2];//for 3rd dimension (1= physical catch of unmarked, 2 = physical catch of marked)
        vector[Nint] stemp; // standardized temperature (between trips – for growth estimation)
        vector[Nint] stemp_wtrip; // standardized temperature (within trips – for pcap estimation)
        int<lower=1> ant_ind[Nant_int];//indicator to show which trips had antennas deployed

        }

parameters {
        real mu_ls[5]; //state-specific mean survival
        real <lower=0, upper=5> sd_ls; //variance in survival random effects (constant across size)
        real mu_lg[4]; //state-specific mean growth
        real <lower=0, upper=5> sd_lg; //variance in growth random effects (constant across size)
        vector[5] beta_gtemp; //temperature effect on growth (size-specific)
        vector [5] z_ls [Nint]; //survival random effects
        vector [4] z_lg [Nint]; //growth random effects
        vector [2] z_lm [Nint]; //movement random effects
        vector <lower=0,upper=1> [5] p_ant_par [Nant_int]; // antenna detection probabilities
        vector[5] pcap_mu; //mean physical capture probabilities (size-specific)
        real<lower=0, upper=5> pcap_sd; // variance in physical capture probabilities (constant)
        vector[5] beta_ptemp; // temperature effect on capture probabilities (size-specific)
        vector[5] zp_cap [Nint]; //random effects on capture probabilities
        vector[2] mu_lm; // mean movement (1st value = prob of emigration, 2nd value = prob of immigration)
```

```
        vector[2] sc4_OFFSET; // effect of small adult on movement (additive model)
        vector[2] sc5_OFFSET; // effect of large adult on movement (additive model)
        real <lower=0, upper=5> sd_lm; // standard deviation of movement
                }


transformed parameters {
        vector <lower=0,upper=1> [5] s [Nint];
        vector <lower=0,upper=1> [4] g [Nint];
        vector <lower=0,upper=1> [10] m [Nint];
        simplex[11] tr[11,Nint];
        simplex[12] pmat[11,Nint];
        vector <lower=0,upper=1> [5] p_cap [Nint];
        vector <lower=0,upper=1> [5] p_ant [Nint];

        //tr 1-5 is the observable JCM-west for sc 1-5
        //tr 6-10 is the unobservable JCM-west for sc 1-5
        //tr 11 is dead

        for (j in 1:10){
                for (i in 1:Nint){
                        m[i,j]=0;}};

        //TE (obs to unobs) for size classes 3,4,5 only:
        for (i in 1:Nint){
                m[i,3]=inv_logit(mu_lm[1]+sd_lm*z_lm[i,1]);
                m[i,4]=inv_logit(mu_lm[1]+sc4_OFFSET[1]+sd_lm*z_lm[i,1]);
                m[i,5]=inv_logit(mu_lm[1]+sc5_OFFSET[1]+sd_lm*z_lm[i,1]);}
        //TE (unobs to obs) for size classes 3,4,5 only:
        for (i in 2:Nint){
                m[i,8]=inv_logit(mu_lm[2] +sd_lm*z_lm[i,2]);
                m[i,9]=inv_logit(mu_lm[2]+sc4_OFFSET[2]+sd_lm*z_lm[i,2]);
                m[i,10]=inv_logit(mu_lm[2]+sc5_OFFSET[2]+sd_lm*z_lm[i,2]);}
```

```
for (j in 1:5){
        for (i in 1:Nint){
                s[i,j]=inv_logit(mu_ls[j]+sd_ls*z_ls[i,j])^(I[i]);
                }};

for (j in 1:4){
        for (i in 1:Nint){
                g[i,j]=1-(1-inv_logit(mu_lg[j]+beta_gtemp[j]*stemp[i]+sd_lg*z_lg[i,j])^(I[i]));
                }};

//Fill state transition matrix with zero's: (will overwrite)
for(i in 1:Nint){
        for(j in 1:11){
                for(k in 1:11){
                        tr[j,i,k]=0;}}}

//state transition matrix 'tr' indexing:
//row 1 = juvenile fish in sampling area
//row 2 = small subadult in sampling area
//row 3 = large subadult in sampling area
//row 4 = small adult in sampling area
//row 5 = large adult in sampling area
//row 6 = juvenile outside sampling area
//row 7 = small subadult outside sampling area
//row 8 = large subadult outside sampling area
//row 9 = small adult outside sampling area
//row 10 = large adult outside sampling area
//row 11 = dead

for (i in 1:Nint){
        for (j in 1:4){
                tr[j,i,j]=s[i,j]*(1-g[i,j])*(1-m[i,j]);
                tr[j,i,(j+1)]=s[i,j]*g[i,j]*(1-m[i,j+1]);
```

```
                tr[j,i,j+5]=s[i,j]*(1-g[i,j])*m[i,j];
                tr[j,i,(j+6)]=s[i,j]*g[i,j]*m[i,j+1];
                }
        tr[5,i,5]=s[i,5]*(1-m[i,5]);
        tr[5,i,10]=s[i,5]*m[i,5];
        for (j in 6:9){
                tr[j,i,j]=s[i,j-5]*(1-g[i,j-5])*(1-m[i,j]);
                tr[j,i,(j+1)]=s[i,j-5]*g[i,j-5]*(1-m[i,j+1]);
                tr[j,i,j-5]=s[i,j-5]*(1-g[i,j-5])*m[i,j];
                tr[j,i,(j-4)]=s[i,j-5]*g[i,j-5]*m[i,j+1];
                }
        tr[10,i,5]=s[i,5]*m[i,10];
        tr[10,i,10]=s[i,5]*(1-m[i,10]);

        for (j in 1:10){
                tr[j,i,11]=1-sum(tr[j,i,1:10]);
                }

        tr[11,i,11]=1;}

for (i in 1:Nint){
        for (j in 1:5){
                p_cap[i,j]=inv_logit(pcap_mu[j]+beta_ptemp[j]*stemp_wtrip[i]+zp_cap[i,j]*pcap_sd);}}


for (i in 1:Nint){
        for (j in 1:5){
                p_ant[i,j]=0;}}

for (i in 1:Nant_int){
        for (j in 1:5){
                p_ant[ant_ind[i],j]=p_ant_par[i,j];}}

for (i in 1:Nint){
```

```
                for (j in 1:11){
                        for (k in 1:12){
                                pmat[j,i,k]=0;}}}

        //detection probability matrix
        //columns 1-5 (physical capture only)
        //columns 6-10 (physical capture and antenna detection)
        //column 11 : antenna detection only
        //column 12 : unobserved

        for (i in 1:Nint){
                for (j in 1:5){
                        pmat[j,i,j]=p_cap[i,j]*(1-p_ant[i,j]);
                        pmat[j,i,(j+5)]=p_cap[i,j]*p_ant[i,j];
                        pmat[j,i,11]=p_ant[i,j]*(1-p_cap[i,j]);
                        pmat[j,i,12]=1-sum(pmat[j,i,1:11]);
                        }
                for (j in 6:11){
                        pmat[j,i,12]=1;}
                }}

model {
        real temp[11];
        vector[11] pz[Nint+1];

        mu_ls~normal(0,2);
        mu_lg~normal(0,2);
        mu_lm~normal(0,2);
        beta_gtemp~normal(0,2);
        beta_ptemp~normal(0,2);
        pcap_mu~normal(0,2);
        sc4_OFFSET~normal(0,2);
        sc5_OFFSET~normal(0,2);
```

```
        for (j in 1:Nint){z_ls[j]~normal(0,1);
                          zp_cap[j]~normal(0,1);
                             z_lg[j]~normal(0,1);
                             z_lm[j]~normal(0,1);}

        for (k in 1:Nch) {
        for (j in 1:11){
                             pz[sumf[k], j] = (j == ch[k, sumf[k]]);  }
        for (t in (sumf[k] + 1):(Nint+1)) {
                             for (i in 1:11) {
                                      for (j in 1:11)
                                               temp[j] = pz[t - 1, j] * tr[j, t - 1, i] * pmat[i, t - 1 ,ch[k, t]];
                                      pz[t, i] = sum(temp);
                                      }}
                    target+=(fr[k]*log(sum(pz[Nint+1,])));
                    }
        }

generated quantities{

        //to get state probability vector
        vector[11] temp;
        vector[11] pvect[Nch,Nocc]; //array of likelihood (same as pvect in model statement except it is saved for each unique CH)
        simplex[5] spvect;
        vector[5] ant_only_catch[Nch,Nocc]; //matrix of state-probability vectors estimate catch in each size class for antenna-only detections
        vector[5] tot_prev_catch[Nocc]; //for previously-marked fish, sum of physical catch and antenna-only detection catch

        //for negative binomial step:
        real<lower=0> scale_par;
        real<lower=0> scale_par2;
        real<lower=0,upper=1> pstar;
        real<lower=0,upper=1> pstar2;
        int N_newmarks[Nint,5];
        vector[5] N_prevmarks[Nint];
```

```
vector[5] N_E3[Nint];


//fill with zeros (will get overwritten)
for (k in 1:Nch) {
for(t in 1:Nocc){
                    for (j in 1:11){
                              pvect[k,t,j]=0;}
                    for (j in 1:5){
                              ant_only_catch[k,t,j]=0;}}}

//get state probability vectors:
for (k in 1:Nch) {
          for (j in 1:11){
                    pvect[k,sumf[k], j] = (j == ch[k, sumf[k]]);  }
for (t in (sumf[k] + 1):(Nint+1)) {
                    for (i in 1:11) {
                              for (j in 1:11) {
                                        temp[j] = pvect[k,t - 1, j] * tr[j, t - 1, i] * pmat[i, t - 1 ,ch[k, t]];}
                              pvect[k,t, i] = sum(temp);
                              }
                    //for capture histories that are antenna-detection only:
                    if(ch[k,t] == 11){
                              for(j in 1:5){
                                        spvect[j] = pvect[k,t,j]/sum(pvect[k,t,1:5]);
                                        ant_only_catch[k,t,j]=(fr[k]*spvect[j]); }
                                        }
          }}

for(j in 1:5){
          for(t in 1:Nocc){
                    tot_prev_catch[t,j] = sum(ant_only_catch[1:Nch,t,j])+catch_met3[t,j,2];}}

//Can't get N or U for first occasion – fill with zero:
```

```
    for(j in 1:5){
        N_E3[1,j]=0;
        N_newmarks[1,j]=0;
        N_prevmarks[1,j]=0;}

    for(t in 2:Nint){
        for(j in 3:5){
            pstar = p_cap[t-1,j];
            scale_par = pstar/(1-pstar);
            N_newmarks[t,j] = neg_binomial_rng(catch_met3[t,j,1], scale_par)+catch_met3[t,j,1];
            pstar2 = 1-(1-p_cap[t-1,j])*(1-p_ant[t-1,j]);
            scale_par2 = pstar2/(1-pstar2);
            N_prevmarks[t,j] = neg_binomial_rng(tot_prev_catch[t,j], scale_par2) +tot_prev_catch[t,j];
            N_E3[t,j] = N_prevmarks[t,j] + N_newmarks[t,j];
}}}
```

Appendix F. Closed models to estimate abundance of age-0 humpback chub in summer and fall

We present two separate analyses that estimate abundance of age-0 humpback chub in summer (i.e., late June or early July) and fall (i.e., mid-September). Although the general sampling protocol remained consistent across all years of the study, the marking protocol changed multiple times due to changes in the types of marks given and the minimum sizes for marking (see main paper). Both summer and fall analyses used the package "rjags" (Plummer 2016) to run JAGS (Plummer 2003) using the statistical program R (R Core Development Team 2020). For both analyses, there was mark-recapture information from within-trips (i.e. from the 2-3 passes) and for the fall analysis there was additional information about fish recaptured between-trips (e.g., from fish marked in September then recaptured in October). We included a 3% one-time tag loss for both VIE and PIT tags (Ward et al. 2008), as well as an additional 3% monthly tag loss for VIE tags (Yackulic et al. 2014).

SUMMER SAMPLING METHODS

Between 2013 and 2019, USGS visited the lower 13.56 km of the LCR in late June for a ten day sampling effort to estimate abundances of age-0 humpback chub before the onset of outmigration to the Colorado River. In 2020, sampling occurred but was restricted to the lower 3.2km of the LCR due to COVID-19 restrictions. These efforts utilized hoop nets, seines, and dip nets, to capture fish. Sampling included three teams that sampled fifteen reaches two times per trip (i.e., two passes), with four days between sampling the two passes of the same reach. Each day, biologists would deploy 10-15 hoop nets in a sampling reach and return the following morning to check for fish (haul A). Hoop nets were reset in their same location, and biologists

spent mid-day sampling fish using seines and dip nets. Then, hoop nets would be checked a second time in late afternoon and pulled from the water (haul B). Biologists would then hike to a new sampling reach to set hoop nets which would be checked the following morning. This corresponded to a total of four hoop net hauls per reach (two hauls for pass 1 and two hauls for pass 2). Upon capture, humpback chub 40-99mm TL (2013-2016) or 40-79mm TL(2017-2020) were given two marks using visual implant elastomer (VIE). One VIE mark was specific to the trip and gear type, where fish captured in hoop nets were given a different mark from fish captured with a different gear type (i.e., dip nets or seines). The second VIE mark was specific to size strata (40-59mm TL, 60-79mm TL, and 80-99mm TL). We did not use the size mark in our analyses, however. Humpback chub larger than the maximum VIE size were marked with passive integrated transponder (PIT) tags.

FALL SAMPLING METHODS

Between 2000 and 2020, USFWS conducted two trips each fall into the lower 13.56 km of the LCR to estimate abundances of humpback chub via biannual closed mark-recapture studies (see Van Haverbeke et al. 2013 for detailed methods). The one exception was 2018, when only one trip was conducted in mid-September. In other years, these two trips typically occurred in mid-September and mid-October, which correspond to the marking trip and recapture trip, respectively. These efforts utilized hoop nets (0.5 - 0.6 m diameter, 1.0 m length, 6-mm [1/4”] mesh, with a single 0.1-m throat, Memphis Net and Twine, Memphis, TN) as gear type. Generally, each marking event and each recapture event was 10 days in length and incorporated at least a two week time span in between mark and recapture trips to allow for mixing of fish to occur. Also, each trip corresponded to three passes of nine adjacent

subreaches, though in some years only two passes occurred on some subreaches due to logistical issues. With a few exceptions, ~180 hoop nets were deployed and spread under a stratified sampling regime in the lower 13.56 km of the LCR during each trip. Each hoop net was deployed for three 24-hr periods, resulting in ~540 24-hr hoop net sets being deployed during each trip. The protocol strove for a uniform sampling regime among trips across years. Exceptions were five trips during 2001 and 2002 when nets were set for four 24-hour periods rather than three and were baited with Aquamax Grower 600 for Carnivorous Species (Purina Mills, Inc., Brentwood, MO). Minor variation also occurred because logistics occasionally resulted in slightly shortened trips (e.g., spring 2006, and fall 2011, 2013, 2014 mark trips). Prior to data analysis, all data from fourth passes were discarded in order to standardize across trips.

SUMMER ABUNDANCE ESTIMATION – BAYESIAN MODELING

We assumed all fish <100 mm during the summer trip were part of that season's age-0 cohort. Note that, to stay consistent with parameterization in JAGS, throughout the Methods section parameters of the normal distribution are presented as mean (μ) and precision (τ), where τ is the inverse of the variance. We used an additive model structure to estimate abundance in each subreach in each year, as this structure helped us estimate total abundance in 2020, a year when only partial sampling occurred. Abundances of humpback chub between 40-99mm total length (N_{over40}) were modeled as a function of a year effect (μ_y), a subreach effect (η_s), and an error term ($\varepsilon_{y,s}$) which was given a normal prior with precision τ_ε. The precision parameters were

converted to a standard deviations which received a uniform priors (0-10).

$$\ln\left(N_{over40,y,s}\right) = \mu_y + \eta_s + \varepsilon_{y,s}$$

$$\varepsilon_{y,s} \sim Normal(0, \tau_\varepsilon)$$

$$\mu_y \sim Normal\ (0,0.01)$$

$$\eta_s \sim Normal\ (0, \tau_s)$$

To estimate capture probabilities, we divide the population into three groups: unmarked fish, fish with marks from dip nets or seines, and fish with marks from hoop nets. Catch of fish in these three groups were modeled separately, with the relative numbers of fish in each group being updated with each pass and haul. For the unmarked population, unmarked catch during year *y*, subreach *s*, pass *x,* and haul *h* was fit to a binomial distribution with the number of trials equal to the size of the unmarked population and probabilities related to pass-specific capture probabilities (*p*). For the fish marked with seines and dip nets, we assumed no behavioral effects for capture by hoop net and therefore modeled this group as a binomial distribution with capture probabilities equal to the unmarked group. For fish with hoop net marks, we assumed a same-day behavioral effect that pertained to fish captured during haul B but that the four days in between pass 1 and pass 2 was enough to erase any behavioral response. Accordingly, fish with hoop nets marks for pass 1 haul B were recaptured with probability $c_{y,s,x=1,h=2}$, which was an additive offset of $p_{y,s,1,2}$. However, fish captured during pass 2 haul A were recaptured with probability $p_{y,s,2,1}$. Because the fish captured during pass 2 haul B could have either been marked during pass 1 (in which case they would not have a behavioral response) or pass 2 haul A (in which case they would have a behavioral response), we estimated the expected number of

recaptures for pass 2 haul B as a mixture of recaps from pass 1 $\left(predR_{pass\ 1,y,s}\right)$ and pass 2 haul A $\left(predR_{pass\ 2,y,s}\right)$ as follows:

$$predR_{pass\ 1,y,s} = \sum_{h=1}^{2} \mathrm{M}_{y,s,x=1,h}\, p_{y,s,x=2,h=2}$$

$$predR_{pass\ 2,y,s} = \mathrm{M}_{y,s,x=2,h=1}\ \ c_{y,s,x=2,h=2}$$

$$predR_{tot,y,s} = predR_{pass\ 1,y,s} + predR_{pass\ 2,y,s}$$

$$\mathrm{R}_{y,s,x=2,h=2} \sim Poisson\ \ (predR_{tot,y,s})$$

Where $\mathrm{M}_{y,s,x,h}$ is the total number of fish marked with hoop net marks in year *y* subreach *s* pass *x* and haul *h* and $\mathrm{R}_{y,s,x=2,h=2}$ is the number of fish recaptured with hoop net marks during pass 2 haul B.

Capture probabilities *p* were logit-transformed and modeled as a random effect centered on a year-specific and camp-specific mean ($\alpha_{y,c}$), a turbidity offset β_T , an afternoon offset for haul B (β_A), and with precision (τ_p). The turbidity offset was based on a dummy variable for turbidity (*T*) that represented whether the mean flow during the trip was above (*T*=1) or equal (*T*=0) to LCR baseflow (Stone 2010), and the afternoon offset was 0 when *h* = 1 and 1 when *h* = 2. Capture probabilites were first calculated on the scale of hoop nets (*i*), then adjusted for the number of hoop nets (*n_hoop*):

$$logit\left(i_{y,s,x,h}\right) = \alpha_{y,c} + \beta_T T_{y,s,x,h} + \beta_A A_{y,s,x,h} + \varepsilon_{y,s,x,h}$$

$$p_{y,s,x,h} = 1 - (1 - i_{y,s,x,h})^{n\_hoop}$$

We assumed that recaptures for haul B exhibited a behavioral response, and this was modeled as the sum of the capture probability for unmarked fish (above) and a behavioral response (δ).

$$logit(j_{y,s,x,h}) = logit(i_{y,s,x,h}) + \delta$$

$$c_{y,s,x,h} = 1 - (1 - j_{y,s,x,h})^{n\_hoop}$$

Lastly, some proportion of age-0 fish were not included in the mark-recapture model above because they were less than 40mm total length. To correct for this, we modeled the number of fish less than 40mm total length from a binomial distribution with probability equal to the proportion of the population that was less than 40mm TL (κ) and trials equal to the total number of humpback chub less than 100mm TL that were captured in dip nets or seines during year *y* subreach *s* and pass *x*. We then divided the number over 40mm TL ($N_{over40,y,s}$) by the proportion that was over 40mm TL ($1-\kappa_{y,s}$) to get abundance ($N_{y,s}$) and summed across all subreaches to get total abundance in year *y*, which was used in the integrated population model to evaluate age-0 humpback chub population dynamics in the accompanying paper.

We ran three independent chains and included 1000 burn-in iterations. We thinned by 200 and kept 1000 posterior draws to estimate credible intervals for model parameters. For all parameters that represented root nodes, we used a normal distribution with parameters ($\mu = 0$ and $\tau = 0.25$) for logit-transformed parameters (e.g. behavioral effects, capture probabilities), a normal distribution with parameters ($\mu = 0$ and $\tau = 0.01$) for log-transformed abundance parameters, and a uniform distribution between 0 and 10 for the standard deviations of random effects.. We used the criteria of $\hat{R}$ <1.1 (Gelman et al. 2014) to determine convergence.

FALL ABUNDANCE ESTIMATION – BAYESIAN MODELING

We first review some key differences between the summer and fall analyses. The fall abundance analysis differed from the summer analysis because only hoop nets were used to sample fish (i.e.,no dip nets or seines) and also there were three hoop net passes that all occurred on consecutive days. For these reasons, the capture process for all within-trip captures always includes a behavioral response. Because the fall analysis includes two trips per year (unlike the summer analysis which only includes one trip), we model across-trip recaptures between the first and second trips and assume that the population is closed during this interval and that across-trip recaptures do not exhibit a behavioral response. Violation of the closure assumption should not bias estimates under scenarios where only additions (i.e. births/immigration) or losses (i.e. deaths/emigration) are occurring in the population (Kendall 1999), though the population estimate obtained will only refer to one time period. In our application, the population estimates pertain to that of the first trip (i.e. the September trip) because we assume that only population losses occur between trips. In addition, the fall analyses differ from the summer because in some years age-0 fish were not marked (2000 – 2009), and so we are reliant on capture probabilities in 2010-2020 to inform capture probabilities from 2000-2009. Lastly, the age-0 population is larger during fall analysis and more likely to be marked with a PIT tag, so we include PIT tagged fish in the fall analysis as well as fish given VIE marks.

For the fall analysis, in years without marked fish (2000-2009), only catch data were available, where catch data correspond to the number of fish captured per pass per trip. We assumed all fish <100 mm during the first fall trip were part of that season's age-0 cohort. To help account for growth the first and second trips, we adjusted the bounds of our subset on total length. To do this, we first estimated mean growth between the two trips and added this to our

upper and lower bounds. For example, we expanded our subset to include all fish < ~106 mm in October after it was estimated that 6 mm was the mean growth between September and October.

Similar to the summer analysis, year- and subreach-specific abundances were modeled as with a lognormal prior. However, unlike the summer analysis, no information was shared across years or subreaches. For trips with mark-recapture (2010-2020), catch of marked and unmarked fish were modeled similar to the summer analysis (with some differences described earlier). For years where fish were not marked (2000-2009), it was not possible to keep track of marked and unmarked groups separately. Catch (C) for pass 1 was composed entirely of new captures, and the number of 'unmarked' fish (*U*) after pass 1 was computed for later calculations:

$$\mathrm{C}_{y,t,s,x=1} \sim binomial\left(p_{y,t,s,x=1}, N_{y,s}\right)$$

$$U_{y,t,s,x=1} = N_{y,s} - \mathrm{C}_{y,t,s,x=1}$$

Note that we introduce subscript *t* for trip and exclude subscript *h* for haul because haul is synonymous with pass for these data. Unlike pass 1, pass 2 catch and pass 3 catch were modeled as a mixtures of newly and previously captured individuals. For example, we predicted the number of previously captured fish (*predM*) that were recaptured during pass 2 and the number of fish that were newly captured (*predU*) during pass 2. Predicted catch (*predC*) was then the sum of the predicted number of marked and unmarked fish, and this number was compared to the observed catch using a Poisson distribution.

$$predM_{y,t,s,x=2} = \mathrm{C}_{y,t,s,x=1} c_{y,t,s,2}$$

$$predU_{y,t,s,x=2} = U_{y,t,s,x=1} p_{y,t,s,x=2}$$

$$predC_{y,t,s,x=2} = predU_{y,t,s,x=2} + predM_{y,t,s,x=2}$$

$$\mathrm{C}_{y,t,s,x=2} \sim Poisson\ (predC_{y,t,s,x=2})$$

Similar to the summer analysis, capture probabilities were logit-transformed and modeled as the sum of a trip-specific mean, turbidity offset, and error term but did not include the afternoon effect. Capture probability was first calculated on the scale of hoop nets (*i*), then adjusted for the number of hoop nets (*n_hoop*). The behavioral response for within-trip recaptures was modeled as the sum of the capture probability for unmarked fish (above), a trip-specific offset (δ_t), and a month-specific turbidity interaction (ρ_m).

We ran three independent chains and included 5000 burn-in iterations. We thinned by 100 and kept 5000 posterior draws to estimate credible intervals for model parameters. Priors were similar to those used in the summer analysis. We ran 3 chains with 100,000 simulations (after 5000 burn-in iterations), and thinned by every 100^{th} posterior draw.

Appendix G. Time series comparison of juvenile, subadult, and adult humpback chub abundances

We used the multistate model of humpback chub that spawn in the Little Colorado River (described in Chapter 2) to obtain abundances of small subadults (100-149mm total length [TL]), large subadults (150-199mm TL), and adults (>199mm TL) from 2009-2020. We compare these abundance estimates to those of juvenile humpback chub (<100mm TL) in the observable Colorado River study site, as estimated by the multistate outmigration model described in the main paper. Comparing these time series illustrates how the large pulse of outmigrating juveniles in 2011 and 2012 led to lagged increases in subadults and adults. Specifically, small subadult abundances were generally increasing from 2012-2016, large subadult abundances increased ~2014-2016, and adult abundances increased ~2016-2018. The subsequent decline in juvenile abundances from 2014-2019 can also be tracked by lagged decreases in abundances of subadults, where small subadult abundances declined ~2017-2019 and large subadult abundances declined ~2018-2020. It is possible that adults declined slightly in 2019-2020. Collectively, these time series illustrate that trends in juvenile abundances often lead to lagged responses in population growth of adults.

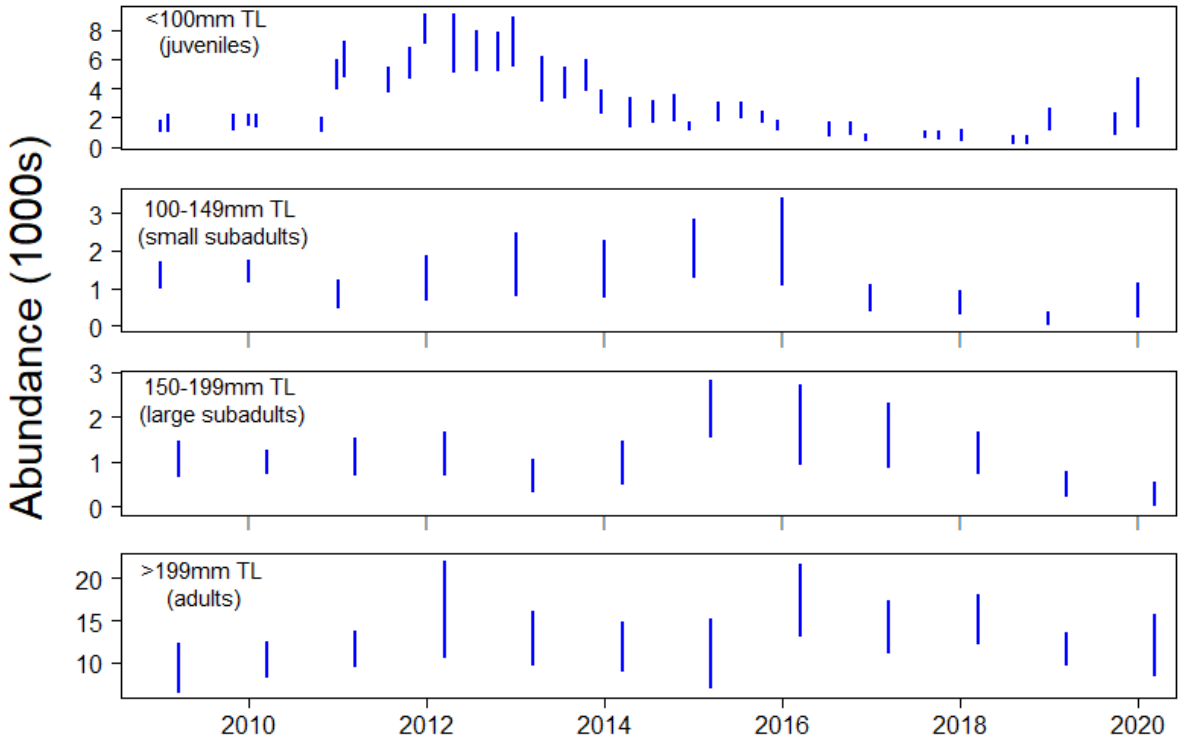

FIGURE G1. Graph of abundances of humpback chub juveniles, small subadults, large subadults, and adults from 2009-2020. Estimates of juveniles and subadults are both for the observable Colorado River study site, located 127-129.7 km downstream of Glen Canyon Dam, whereas adult estimates pertain to all adults that spawn in the Little Colorado River.